Effect of processing on muscle structure and protein digestibility *in vitro*

A thesis presented in partial fulfilment of the requirements for the degree of

Doctor of Philosophy

in

Food Technology

at Massey University, Palmerston North, New Zealand

Chian Feng Ming

2021

Abstract

The objective of this thesis was to investigate the effect of processing on meat protein properties, muscle structure and *in vitro* protein digestibility of beef. Meat processing techniques including pulsed electric field (PEF), shockwave (SW) processing, exogenous enzyme (actinidin) treatment, and sous vide (SV) cooking were explored, either alone or in combination, in this project. This thesis also aimed to study the diffusion of enzymes (actinidin from kiwifruit and pepsin in the gastric juice) into the meat.

The first experiment investigated the effect of PEF processing alone on the ultrastructure and *in vitro* protein digestibility of bovine *Longissimus thoracis*, a tender meat cut (**Chapter 3**). It was observed that the moisture content of the PEF-treated samples (specific energy of 48 ± 5 kJ/kg and 178 ± 11 kJ/kg) was significantly lower ($p < 0.05$) by 1.3 to 4.6 %, compared to the untreated samples. The pH, colour, and protein thermal profile of the PEF-treated muscles remained unchanged. Pulsed electric field treatment caused the weakening of the Z-disk and I-band junctions and sarcomere elongation (25 to 38 % longer) of the muscles. The treatment improved *in vitro* meat protein digestibility by at least 18 %. In this thesis, the protein digestibility was determined in terms of the ninhydrin-reactive amino nitrogen released during simulated oral-gastro-small intestinal digestion. An enhanced proteolysis of the PEF-treated meat proteins (such as α-actinin and β-actinin subunit) during simulated digestion was also observed using sodium dodecyl sulfate-polyacrylamide gel electrophoresis (SDS-PAGE). The improvement in protein digestibility of the PEF-treated meat was supported by more severe disruption of Z-disks and I-bands observed in PEF-treated samples, at the end of simulated digestion.

In the second experiment, PEF treatment (specific energy of 99 ± 5 kJ/kg) was applied to bovine *Deep* and *Superficial pectoral* muscles in conjunction with SV cooking (60 °C for

24 h) (**Chapter 4**). This muscle cut was tested as it is a tough cut and requires slow cooking. There was no significant difference detected in the specific activities of the sarcoplasmic cathepsins present in the cytosol between the control and PEF-treated samples, both before and after cooking. In addition, similar micro- and ultrastructures were observed between the control SV-cooked and PEF-treated SV-cooked *pectoral* muscles. The combined PEF-SV treatment increased the *in vitro* protein digestibility of the *pectoral* muscles by approximately 29 %. An improvement in proteolysis of the treated meat proteins (e.g. myosin heavy chains and C-protein) during simulated digestion was also observed using SDS-PAGE. More damaged muscle micro- and ultrastructures were detected in PEF-treated SV-cooked muscles at the end of *in vitro* oral-gastro-small intestinal digestion, showing its enhanced proteolysis compared to the control cooked meat.

Next, the effect of SW processing and subsequent SV cooking on meat protein properties, muscle structure and *in vitro* protein digestibility of bovine *Deep* and *Superficial pectoral* muscles were investigated (**Chapter 5 and 6**). Shockwave processing (11 kJ/pulse) alone decreased the enthalpy and thermal denaturation temperature of the collagen ($p < 0.05$) when compared to the raw control, studied using a differential scanning calorimeter. The purge loss, pH, colour, and the protein gel electrophoresis profile of the SW-treated raw muscles remained unaffected. Shockwave processing led to the disorganisation of the sarcomere structure and also modified the protein secondary structure of the myofibres. After subsequent SV cooking (60 ℃ for 12 h), more severe muscle fibre coagulation and denaturation were observed in the SW-treated cooked meat compared to the cooked control. An increase in cook loss and a decrease in the Warner-Bratzler shear force were detected in the SW-treated SV-cooked meat compared to the control cooked meat ($p < 0.05$). The *in vitro* protein digestibility of the SW-treated SV-cooked meat was improved

by approximately 22 %, with an enhanced proteolysis observed via SDS-PAGE, compared to the control SV-cooked meat. These results were supported by the observation of more destruction of the micro- and ultrastructures of SW-treated cooked muscles, observed at the end of the simulated digestion.

The effect of the kiwifruit enzyme actinidin on muscle microstructure was studied using Picro-Sirius Red staining (**Chapter 7**). Meat samples were subjected to two different conditions, simulating meat marination (pH 5.6) and gastric digestion in humans (pH 3). Actinidin was found to have a greater proteolytic effect on the myofibrillar proteins than the connective tissue under both conditions. When compared with pepsin under simulated gastric conditions, actinidin had a weaker proteolytic effect on the connective tissue of cooked meats. Nevertheless, incubating the cooked meat in a solution containing both actinidin and pepsin resulted in more severe muscle structure degradation, when compared to muscles incubated in a single enzyme system. Thus, the co-ingestion of kiwifruit and meat could promote protein digestion of meat in the stomach. In addition, both actinidin and pepsin were successfully located at the edges of the muscle cells and in the endomysium using immunohistofluorescence imaging. The observations suggest that the incubation solutions penetrate into the muscle through the extracellular matrix to the intracellular matrix, enabling the proteases to access their substrates.

Overall, the present work demonstrated that there were strong interactions between processing, muscle protein properties and structure, and *in vitro* protein digestibility of the meat. Processing induces changes in meat protein properties and muscle structure, which in turn affects the digestion characteristics of muscle-based foods.

Acknowledgements

My PhD journey at Massey University has been a rewarding, challenging and amazing experience. I am very blessed to have an awesome and inspiring supervisory team, who have provided constant support and encouragement throughout my entire doctoral journey. Thank you very much to my primary supervisor, Dr. Lovedeep Kaur, for giving me a chance to take up this PhD project and always making time for me when I face problems. I am grateful for your guidance, patience, and encouragement. Thank you to Dr. Mike Boland, my project co-supervisor, for your meaningful discussion, prompt feedback and constructive advice. You have inspired me to be a better writer and researcher. I would like to express gratitude to my co-supervisor, Dr. Thierry Astruc, for your guidance and insightful advices. It has been a fruitful experience for me to learn so much from your expertise in muscle structure research. Many thanks to Thierry and his family for their warm welcome and hospitality during my stay in Clermont Ferrand. I am also grateful to Dr. Suzanne Hodgkinson, for her co-supervision, mentoring, discussion, and valuable feedback.

I am grateful to the Riddet Institute, the Centre of Research Excellence, for funding this research project, providing travel grants for conferences and collaborative work, both locally and internationally, as well as granting me the Overseas Placement Award to complete part of my PhD research in French National Research Institute for Agriculture, Food and the Environment (INRAE), for five months. This overseas placement at INRAE is one of the greatest experiences of my PhD journey. I would like to express my sincere gratitude to INRAE for hosting me and providing me with French lessons. A big thanks to Dr. Thierry Astruc, Mr. Olivier Loison, Ms. Annie Vénien, Dr. Pattama Supaphon, Ms.

Francoise Lassalas, and other staff of INRAE, for giving me a fantastic and memorable experience in France. Merci beaucoup!

I would also like to express my deepest gratitude to the staff of the German Institute for Food Technology (DIL), especially Dr. Kemal Aganovic and Ms. Anna-Sophie Stübler, for hosting me and providing constant support and help for the shockwave project. I would like to thank the staff of the Department of Food Science of the University of Otago, particularly Professor Indrawati Oey, Dr. Sze Ying Leong, Dr. Amali Alahakoon and Mr. Ian Ross, for hosting me there during the pulsed electric field study. I also want to thank the Food Industry Enabling Technologies programme (FIET), funded by the New Zealand Ministry of Business, Innovation and Employment (MBIE) for supporting this PhD research. I would also like to express gratitude to visiting interns, Ms. Meryem El Haddioui, Mr. Abhilash Borah, and Ms. June Seah Xin Hui, for their assistance in the standardisation of the cathepsins activity assays.

I am also thankful to all the laboratory managers and staff members, to Mr. Steve Glasgow, Mrs. Michelle Tamehana, Mr. Garry Radford, Mr. Warwick Johnson, Mrs. Anne-Marie Jackson, Ms. Kylie Evans and Dr. Haoran Wang from the School of Food and Advanced Technology, Ms. Maggie Zou, Dr. Peter Zhu, and Mr. Jian Cui from the Riddet Institute, and Mr. Chris Hall and Ms. Janiene Gilliland from the Food Innovation team, for their kind help and lab training. I am grateful to Dr. Matthew Savoian, Ms. Jordan Taylor, Ms. Niki Minards from the Manawatu Microscopy and Imaging Centre (MMIC), Dr. Matthew Perrott, Ms. Saritha Gils, Ms. Evelyn Lupton and Ms. Petru Daniels from the Histology lab (School of Veterinary Science, Massey University), and Ms. Claire Szczepaniak from the CICS laboratory (Clermont Ferrand University, France), for their assistance in microscopy analysis. I would like to show my appreciation for the help and support

provided by the IT and administrative staff from both Massey School of Food and Advanced Technology and the Riddet Institute, thanks Mr. Matt Levin, Mr. Tim O'Dea, Mr. Peter Jeffery, Ms. Yvonne Parkes, Ms. Pip Littlejohn, the late Mrs. Fliss Stibbards, Ms. Christine Ramsay, Ms. Lee-Anne Hannan, Mrs. Miria Busby, Ms. Eteta Trueman, Ms. Ansley Te Hiwi, Ms. Terri Palmer, Ms. Hannah Hutchinson, Dr. Sarah Golding, Mr. John Henley-King, Ms. Meg Wedlock and Ms. Angela Gemmell.

Thank you to my mentors, Professor Jeya Henry, Dr. Lara Matia-Merino and Associate Professor Kelvin Goh, for your guidance and be role models in my research journey. Lara, I really enjoy your BodyStep class which is fun and keeps me physically and mentally fit. Thanks Mrs. Heather McClean for your care and words of encouragement. Thank you to my friends in New Zealand, Cai ling, Wani, Matthew, Teck Ann, Anynda, Chih-Chieh, Wang Che, Jie Hong, Claudia, Marina, Jessie, Boning, Navdeep, Mana 85 fellows, postgraduate students from office C1.136, Nutri-sprinky girls, SIT-Massey students, and many more, for sharing fun and great moments with me while I am away from home.

A big thank you to my partner, Blake, for his help in proof-reading my writing. I am very blessed to have met you, Bas, and your family, who are always there supporting and encouraging me. Last but not least, I want to thank my family, especially my parents back in Malaysia, for their care, support and unconditional love. I appreciate my siblings for taking care of the family when I am away from home.

Table of contents

List of figures

List of tables

List of abbreviations

2D-PAGE	Two-dimensional (non-reducing / reducing) sodium dodecyl sulfate–polyacrylamide gel electrophoresis
*a**	Redness
ADP	Adenosine diphosphate
Ag/Ab	Antigen-antibody
AMP	Adenosine monophosphate
ANOVA	Analysis of variance
ATR	Attenuated total reflection
ATP	Adenosine triphosphate
*b**	Yellowness
BaF_2	Barium fluoride
CaF_2	Calcium fluoride
CHAPS	3-[(3-Cholamidopropyl) dimethylammonio]-1-propanesulfonate
CP	Creatine phosphate
CSA	Cross-sectional area
Cy3	Cyanine dye
DIAAS	Digestible indispensable amino acid score
DSC	Differential scanning calorimetry
DTT	Dithiothreitol
ECSA	Extracellular space area
EDTA	Ethylenediaminetetraacetic acid
FDA	Food and Drug Administration
FT-IR	Fourier – transform infrared
FU	Fluorescence unit
GRAS	Generally Recognized as Safe
HCl	Hydrochloric acid
HPLC	High performance liquid chromatography

IgG	Immunoglobulin G
IR	Infrared
l	Optical path length
*L**	Lightness
M	Molar
MALDI-TOF-MS	Matrix-assisted laser desorption/ionisation time of flight mass spectrometry
MHC	Myosin heavy chains
MLC	Myosin light chains
MW	Molecular weight
NIPALS	Non-linear Iterative Projections by Alternating Least-Squares
OPA	O-phthalaldehyde
PC	Principal component
PCA	Principal component analysis
PEF	Pulsed electric field
pHu	Ultimate pH
PSR	Picro-Sirius Red
PVDF	Polyvinylidene fluoride
SDS	Sodium dodecyl sulfate
SDS-PAGE	Sodium dodecyl sulfate–polyacrylamide gel electrophoresis
SEM	Scanning electron microscopy
SGF	Simulated gastric fluid
SIF	Simulated intestinal fluid
SSF	Simulated salivary fluid
SV	Sous vide
SW	Shockwave
TCA	Trichloroacetic acid
TD-NMR	Time domain-nuclear magnetic resonance
TEM	Transmission electron microscopy

TPA	Texture profile analysis
V	Volume
WB	Warner-Bratzler
Wt	Weight
Z-L-Lys-ONp	N-α-carbobenzoxy-L-lysine-P-nitrophenyl ester
α-NH_2	Primary amino groups
Δε	Extinction coefficient

List of publications and conference proceedings

Peer reviewed journal articles

- **Chian, F. M.**, Kaur, L., Oey, I., Astruc, T., Hodgkinson, S., & Boland, M. (2019). Effect of pulsed electric fields (PEF) on the ultrastructure and *in vitro* protein digestibility of bovine *Longissimus thoracis*. *LWT, 103*, 253-259. https://doi.org/10.1016/j.lwt.2019.01.005

- **Chian, F. M.**, Kaur, L., Oey, I., Astruc, T., Hodgkinson, S., & Boland, M. (2021). Effects of pulsed electric field processing and sous vide cooking on muscle structure and *in vitro* protein digestibility of beef brisket. *Foods*, *10*(3), 512. https://doi.org/10.3390/foods10030512

- **Chian, F. M.**, Kaur, L., Astruc, T., Vénien, A., Stübler, A.-S., Aganovic, K., Loison, O., Hodgkinson, S., & Boland, M. (2021). Shockwave processing of beef brisket in conjunction with sous vide cooking: Effects on protein structural characteristics and muscle microstructure. *Food Chemistry*, *343*, 128500. https://doi.org/10.1016/j.foodchem.2020.128500

- **Chian, F. M**., Kaur, L., Astruc, T., Vénien, A., Loison, O., Stubler, A. S., Aganovic, K., Hodgkinson, S., & Boland, M. Shockwave processing and sous vide cooking of beef brisket: Effects on meat physicochemical properties, texture and protein digestibility *in vitro*. (In submission).

Book chapter

- Boland, M., Kaur, L., **Chian, F. M**., & Astruc, T. (2019). Muscle proteins. In L. Melton, F. Shahidi, & P. Varelis (Eds.), *Encyclopedia of food chemistry* (pp. 164-179). Academic Press. https://doi.org/10.1016/B978-0-08-100596-5.21602-8

Conference proceedings and presentations

- **Chian, F. M.**, Kaur, L., Astruc, T., Vénien, A., Loison, O., Stubler, A. S., Aganovic, K., Hodgkinson, S., & Boland, M. (2019, 1st-3rd October). *Shockwave processing and sous vide cooking improve sensorial and nutritional qualities of beef.* [Poster presentation]. 5th International Conference on Food Structures, Digestion and Health, Rotorua, New Zealand.

- **Chian, F. M**., Kaur, L., Astruc, T., Vénien, A., Loison, O., Stubler, A. S., Aganovic, K., Hodgkinson, S., & Boland, M. (2019, 2nd-4th July). *Effect of shockwave processing and sous vide cooking on beef brisket structure and protein digestibility in vitro.* [Oral presentation]. New Zealand Institute of Food Science and Technology Conference 2019, Christchurch, New Zealand.

- **Chian, F. M.**, Kaur, L., Astruc, T., Vénien, A., Loison, O., Stübler, A.-S., Aganovic, K., Hodgkinson, S., & Boland, M. (2018, 12th-17th August). *The effect of shockwave processing on muscle protein structure and digestibility in vitro.* [Paper & oral presentation]. 64th International Congress of Meat Science and Technology, Melbourne, Australia.

- **Chian, F. M**., Kaur, L., Astruc, T., Vénien, A., Loison, O., Stubler, A. S., Aganovic, K., Hodgkinson, S., & Boland, M. (2018, 10th-12th July). *The effect of shockwave processing on muscle protein structure and digestibility in vitro.* [Oral presentation]. Riddet Institute Student Colloquium 2018, Wellington, New Zealand.

- **Chian, F. M**., Kaur, L., Astruc, T., Vénien, A., Loison, O., Stubler, A. S., Aganovic, K., Hodgkinson, S., & Boland, M. (2018, 11th-12th June). *The effect of shockwave processing on muscle protein structure and digestibility in vitro.* [Poster & oral presentation]. Food Industry Enabling Technologies Symposium 2018, Palmerston North, New Zealand.

- **Chian, F.M**., Kaur, L., Astruc, T., Oey, I., Hodgkinson, S., & Boland, M. (2017, 14th-28th September). *Pulsed electric field processing improves the in vitro protein digestibility of bovine Longissimus dorsi muscle.* [Poster presentation]. 2nd World Congress On Electroporation, Norfolk, VA, USA.

- Kaur, L., **Chian, F.M**., Zhu, X., Astruc, T., Oey, I., & Boland, MJ. (2017). Improving protein digestibility and texture of beef meat with novel processing technologies. In D. Troy, C. McDonnell, L. Hinds, & J. Kerry (Eds.) *63rd International Congress of Meat Science and Technology. Nurturing locally, growing globally.* (pp. 676 - 677). Wageningen Academic Publishers.

- **Chian, F.M**., Kaur, L., Astruc, T., Oey, I., Hodgkinson, S., & Boland, M. (2017, 4th-6th July). *The effect of pulsed electric field on bovine muscle protein digestibility in vitro.* [Poster presentation]. New Zealand Institute of Food Science and Technology Conference 2017, Nelson, New Zealand.

- **Chian, F.M**., Kaur, L., Astruc, T., Oey, I., Hodgkinson, S., & Boland, M. (2017, 14th-15th June). *The effect of pulsed electric field (PEF) on meat microstructure and protein digestibility in vitro.* [Oral presentation]. Food Industry Enabling Technologies Symposium 2017, Palmerston North, New Zealand.

- **Chian, F.M**., Kaur, L., Astruc, T., & Boland, M. (2016, 31st October – 2nd November). *Effect of processing on muscle protein structure and digestibility in vitro.* [Oral Presentation]. Riddet Institute Student Colloquium 2016, Palmerston North, New Zealand.

- **Chian, F.M**., Kaur, L., Astruc, T., & Boland, M. (2016, 21st-22nd July). *Effect of processing on muscle protein structure and digestibility in vitro.* [Oral presentation]. Food Industry Enabling Technologies Symposium 2016, Palmerston North, New Zealand.

Awards

- Second Best Oral Presentation at the 64th International Congress of Meat Science and Technology (ICOMST), Melbourne, Australia, awarded by Meat Science.

- Travel Grant (2018), Riddet Institute, New Zealand, to attend the 64th International Congress of Meat Science and Technology (ICOMST), Melbourne, Australia.

- Overseas Placement Award (2017), Riddet Institute, New Zealand, to conduct research at French National Institute for Agriculture, Food, and Environment (INRAE), France, for five months.

- Doctoral scholarship (2016 – 2019), Riddet Institute, New Zealand, to complete the PhD in Food Technology at the Massey University, New Zealand.

Chapter 1 Introduction

Global meat consumption has doubled over the past 20 years to reach 360 million tonnes in 2018 and is projected to increase over the coming years due to growing population and rising incomes (Sanchez-Sabate & Sabate, 2019; Whitnall & Pitts, 2019). As one of the major global red meat exporters, New Zealand has exported $ 9.4 billion of sheep meat, beef, and co-products for the year ending June 2020, achieving a 7 % increment compared to the year ending June 2019 (Meat Industry Association, 2020). The volume of beef exports has risen by 2 % to 3.8 thousand tonnes and the value has grown by 15 % to $ 3.8 billion, contributing significantly to the economy of the country. In order to continue to be competitive in the global market, the industry has been trying to capture increased market value by matching the customer needs and demands. In general, a consumer's purchasing decision is made primarily based on the appearance and organoleptic properties of the food products (Troy & Kerry, 2010). However, as there is an increasing awareness of the link between food, health and nutrition, consumers are demanding products that contain high-value animal protein (Hung et al., 2016; Kraus, 2015). To meet consumer demands, novel processing techniques have been explored and used extensively by the food industry to create high quality, safe and nutritious products without compromising their 'fresh-like' product characteristics (Troy et al., 2016). For example, sous vide (SV) cooking (Vaudagna et al., 2002), pulsed electric field (PEF) processing (Alahakoon et al., 2018b), shockwave (SW) processing (Bolumar et al., 2014), and exogenous enzyme technology such as the use of actinidin (Zhu, Kaur, Staincliffe, et al., 2018) have been explored to improve the organoleptic properties of meat by meat tenderisation.

In the process of designing appetising and wholesome foods, it is important to recognise the relationship between the manufacturing process, food structure and human physiology. In general, protein is not fully digested before entering the large intestine. The true ileal protein digestibility values for most of the dietary proteins (animal- and plant-based) in humans were found to be between 84 and 96 % (Mariotti, 2017; Tomé, 2013; Yao et al., 2016). It has been reported that around 3 to 18 g of protein can reach the colon of a person per day, including both undigested dietary proteins and non-dietary endogenous proteins excreted by the human body (Chacko & Cummings, 1988; Cummings & Macfarlane, 1991; Muir & Yeow, 2000). The amount of undigested protein entering the colon depends on the daily dietary protein intake and the protein digestibility of the ingested foods. Daily dietary protein intake varies between individuals, but the protein digestibility of some foods could be improved through food processing (Carmody & Wrangham, 2009; Yao et al., 2016).

Food processing alters the physical and chemical properties of food, which ultimately affects its digestive characteristics (Kong & Singh, 2008). For example, cooking meat at a temperature between 70 and 75 °C improves the protein digestion rate as the treatment changes the meat structure, which enhances the accessibility of pepsin during digestion (Bax et al., 2012). Hodgkinson et al. (2018) also found that boiled (97 – 99 %) and pan-fried (97 – 99 %) beef topside had a significantly higher digestible indispensable amino acid score (DIAAS) than roasted (91 %) or grilled meat (80 %) in growing pigs. Digestible indispensable amino acid score is determined based on the true ileal digestibility of the indispensable amino acids. Meat with improved protein digestibility and digestion rate results in a steep elevation in postprandial aminoacidemia, providing a rapid amino acids supply for protein anabolism (Boirie et al., 1997; Rémond et al., 2007). This is beneficial for sports nutrition and in the elderly, where it can combat sarcopenia.

Rapid protein digestion also reduces the possibility of generation of toxic nitrogenous metabolites from undigested proteins entering the large intestine (Attene-Ramos et al., 2010; Hughes et al., 2008).

The interaction between food consumption and human physiology depends on the food composition, properties and structure, along with the pattern and time of consumption (Sensoy, 2014). Understanding the interaction between the food matrix, structure, and the human digestive system will underpin the rational development of novel muscle-based foods with enhanced nutritional value through the use of different processing methods. Hence, the main aim of this study is to investigate the effects of different processing techniques, alone or in combination, on meat proteins (molecular size and thermal stability), muscle structure (molecular, micro- and ultrastructures) and *in vitro* protein digestibility. Meat processing techniques such as PEF, shockwave (SW) processing and SV cooking are explored in this project. The findings will provide an insight into how different processing techniques affect the meat proteins and structure, which in turn influences the digestion characteristics of muscle-based foods. In addition, the thesis aims to develop a method to understand the diffusion of enzymes, such as actinidin from kiwifruit, and pepsin in the gastric juice, into meat, using advanced microscopy techniques.

This thesis consists of eight chapters and the outline of the thesis with research questions and project objectives, is presented in **Figure 1-1**. In brief:

Chapter 1 describes the background and outlines the objectives and main framework of the research project.

Chapter 2 is a literature review of the fundamental knowledge of muscle proteins and the effects of different processing methods on muscle structure and protein digestibility.

Some methodologies used to investigate muscle structure and protein digestibility are also discussed.

Chapter 3 discusses the effect of PEF treatment alone on the physicochemical properties, protein thermal profile, muscle structure and *in vitro* protein digestibility of beef *Longissimus thoracis*.

Chapter 4 describes the effects of PEF in combination with SV cooking on the muscle structure and *in vitro* protein digestibility of beef *Deep* and *Superficial pectoral* muscles. The effect of PEF on the activities of lysosomal enzymes was also investigated, before and after SV cooking.

Chapter 5 characterises the effects of SW processing, alone and in combination with SV cooking, on the protein thermal profile, protein structural characteristics and muscle microstructure of beef *Deep* and *Superficial pectoral* muscles.

Chapter 6 investigates the effects of SW processing in conjunction with SV cooking on the physicochemical properties, texture and *in vitro* digestibility of beef *Deep* and *Superficial pectoral* muscles.

Chapter 7 examines the effect of exogenous enzyme actinidin present in the kiwifruit extract, on the structure of both raw and SV-cooked beef *Deep* and *Superficial pectoral* muscles. The effects of a combined actinidin-pepsin system on meat structure during simulated gastric digestion were also discussed. A protocol for the localisation of the enzymes actinidin and pepsin in meat was also developed using immunohistofluorescence approach.

Chapter 8 concludes all the research findings and provides recommendations and directions for future work.

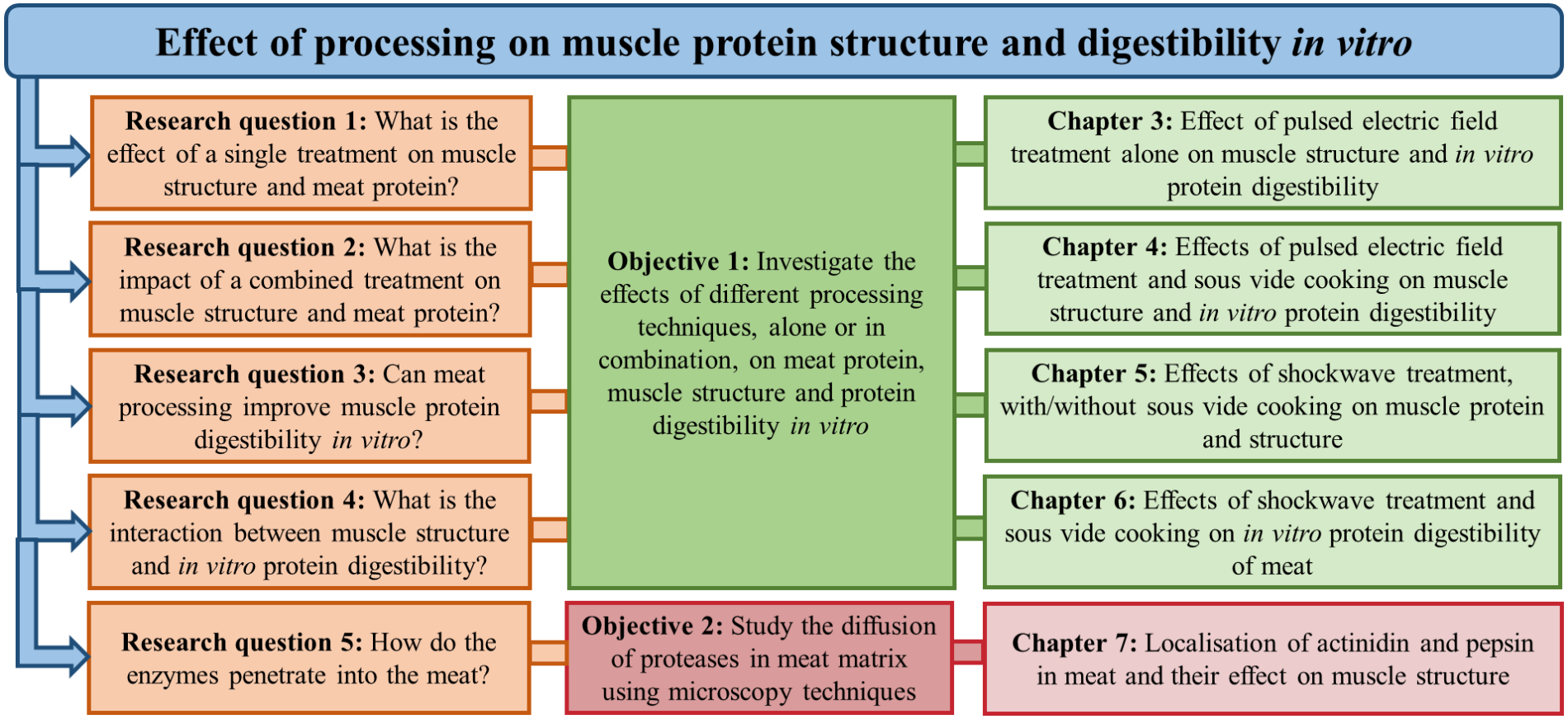

Figure 1-1. An overview of the thesis structure with research questions and project objectives.

Chapter 2 [1]Literature review

This literature review aims to provide a comprehensive summary of the existing literature on muscle structure and protein digestibility, and how these are influenced by processing. Fundamental information on muscle composition and chemistry, and the principles of different processing techniques are presented in this section. Various methodologies to examine muscle structure and digestibility are also reviewed.

2.1 Muscle structure and composition

Meat is derived from skeletal muscles that have undergone a series of biochemical reactions following the slaughter of animals (Strasburg et al., 2008). Skeletal muscles consist of multinucleated muscle fibres made up of bundles of elongated myofibrils in a parallel configuration (**Figure 2-1**) (Gault, 1992; Strasburg et al., 2008). A muscle fibre is ensheathed by a fine connective tissue layer network embedded in a proteoglycan matrix (the endomysium), which contains blood capillaries and nerves for muscle function. Each muscle fibre is composed of dozens of myofibrils and is enclosed by the muscle plasma membrane, called the sarcolemma, which is made up of a phospholipid bilayer with embedded proteins, glycoproteins and glycolipids. The myofibrils are bathed in sarcoplasm containing several nuclei, sarcoplasmic reticulum, Golgi apparatus, mitochondria, lysosomes, glycogen granules, enzymes and other soluble constituents, that are vital for muscle functionality. The sarcoplasmic reticulum acts as a calcium ion reservoir for muscle contraction. Bundles of muscle fibres are organised into fascicles that are encased in another layer of connective tissue containing larger blood vessels, nerves, and others (e.g. adipocytes and fibroblasts), called the perimysium. Several fascicles are assembled into a whole muscle by an outer layer of connective tissue sheaths known as the epimysium, which extends into tendons to join muscles and bones together.

[1]Part of this chapter has been published as Boland, M., Kaur, L., **Chian, F. M.**, & Astruc, T. (2019). Muscle proteins. In L. Melton, F. Shahidi, & P. Varelis (Eds.), *Encyclopedia of food chemistry* (pp. 164-179). Academic Press. https://doi.org/10.1016/B978-0-08-100596-5.21602-8

Regardless of the animal species, myofibrils in muscle fibres consist of longitudinal myofilaments comprising thick and thin filaments (Strasburg et al., 2008; Tortora & Derrickson, 2013). Thick filaments are made up of myosin molecules while thin filaments are composed of actin, tropomyosin and troponin. Alternating light isotropic (I-band) and dark anisotropic (A-band) bands are seen on myofibrils under polarised light microscopy. Longitudinal sections of muscle fibres observed by transmission electron microscopy (TEM) show that each I-band is separated into two by a dark and narrow line called the Z-disk. The region between two Z-disks is known as a sarcomere, which is the repeating longitudinal contractile functional unit of a myofibril. A sarcomere comprises an I-band, consisting purely of thin filaments, an A-band containing alternatively overlapping thin and thick filaments, a H-zone that is in the centre region of A-band where the thin filaments are absent and a M-line that is in the middle of the H-zone. When a muscle contracts, the Z-disks shift closer together due to shortening of the I-band, and the length of the sarcomere is decreased (Gault, 1992).

Skeletal muscle proteins can be classified into myofibrillar (50 to 60 %), sarcoplasmic (30 %) and stromal (10 % to 20 %) proteins, based on their solubility at varying salt concentrations (Strasburg et al., 2008). The myofibrillar proteins, which are soluble at high salt concentrations (> 0.3 M), consist of contractile, structural and regulatory proteins (**Figure 2-2**). The sarcoplasmic proteins can be solubilised in low ionic strength (< 0.3 mM) and are located in the sarcoplasm surrounding the myofibrils. The sarcoplasmic proteins include the oxidative enzymes (e.g. cytochromes), the haem pigments (e.g. myoglobin), the glycolytic enzymes (e.g. glyceraldehyde phosphate dehydrogenase), the mitochondrial oxidative enzymes (e.g. succinate dehydrogenase), the lysosomal enzymes (e.g. cathepsins), the nucleoproteins (e.g. e.g. ribosomes) and others, which are involved in various tissue functions (Pearson & Gillett, 2012; Pearson & Young,

1989; Smith, 2000; Strasburg et al., 2008). Stromal proteins are relatively insoluble in salt solutions and constitute connective tissue, which provides mechanical support and protection to the muscle in the form of tendon, epimysium, perimysium and endomysium (Gault, 1992; Strasburg et al., 2008). Connective tissue contains different types of cells, including fibroblasts, macrophages, lymphoid cells, mast cells and eosinophils and is mainly composed of collagen (90 %) along with other fibrous proteins including elastin, laminin and fibronectin, and proteoglycans (Chagnot et al., 2012; Voermans et al., 2008).

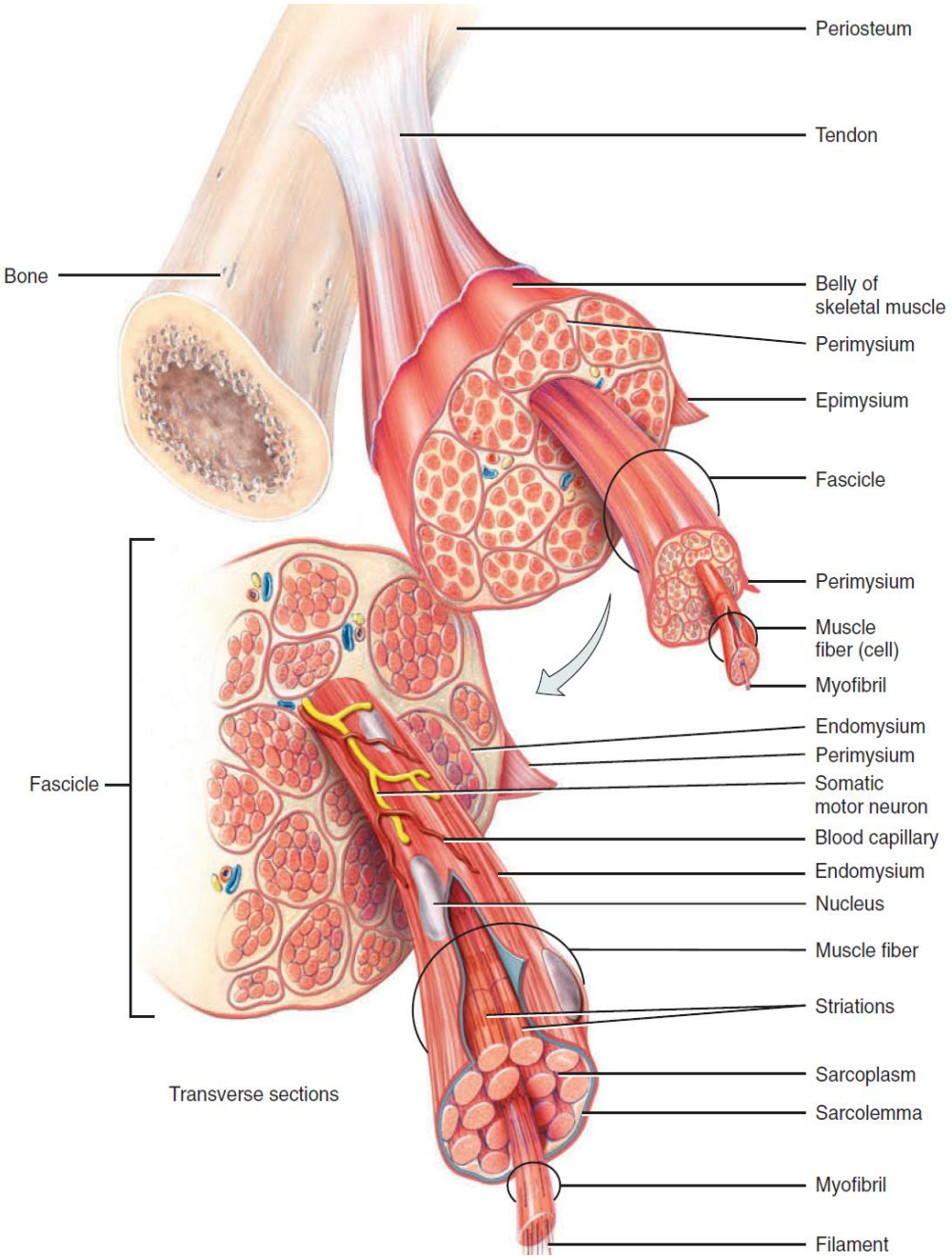

Figure 2-1.Structure of skeletal muscle.
From Tortora & Derrickson, Principles of Anatomy & Physiology, 14th Edition. Copyright © 2014, 2012, 2009, 2006, 2003, 2000. © Gerard J. Tortora, L.L.C., Bryan Derrickson, John Wiley & Sons, Inc. Reprinted by permission from John Wiley & Sons, Inc.

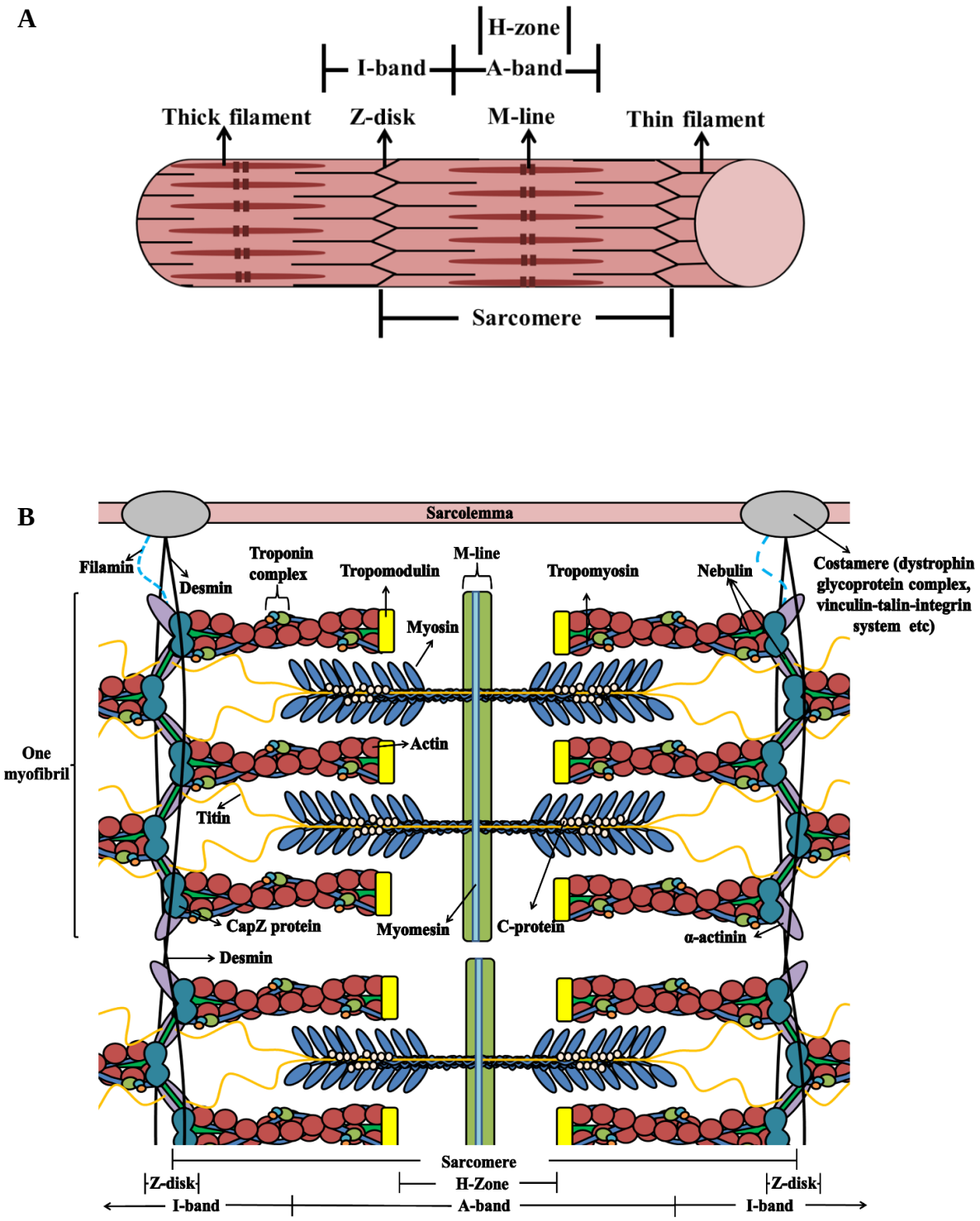

Figure 2-2. (A) Basic functional unit of a myofibril and (B) the arrangement of filaments within a sarcomere.

Reproduced from Boland et al. (2019) with permission from Elsevier Books.

2.2 Myofibrillar proteins

2.2.1 Contractile proteins

Myosin (molecular weight, MW of 520 kDa) is a filamentous protein that forms the thick filaments of muscle cells (Gault, 1992; Strasburg et al., 2008). It is the principal protein of the A-band. A myosin molecule has a quaternary structure consisting of six subunits, which include two myosin heavy chains (MHC), two essential myosin light chains (MLC1) and two regulatory myosin light chains (MLC2), with MW of approximately 220 kDa, 23 kDa and 20 kDa correspondingly (Clark et al., 2002; Swartz et al., 2009). Individual MHC forms a globular head domain at the N-terminal, which is bound to a pair of MLC (MLC1 and MLC2) (Strasburg et al., 2008). An α-helix rod is formed at the C-terminal of each MHC and the α-helix rods from two MHC intertwine to form an α-helix coiled rod. Myosin molecules originate from the M-line, orientated symmetrically and pointing their head domains away from both sides of M-line.

Actin is the building block of thin filaments and is present in two forms namely globular actin (G-actin) and filamentous actin (F-actin) (Gault, 1992; Strasburg et al., 2008). F-actin is formed by the polymerisation of G-actin (MW of 42kDa) into double-stranded, coiled filaments. F-actin is bound to tropomyosin and troponin, forming thin filaments that are originated at the Z-disk and extended in the direction toward the M-line.

During muscle contraction, actin binds myosin to form actomyosin cross-bridges, which activate the myosin ATPase, leading to the pulling of thin filaments by myosin toward the M-line, resulting in shortening of the sarcomere (Lawrie, 2006). The binding of actin and myosin is regulated by tropomyosin and troponin.

2.2.2 Regulatory proteins

Tropomyosin and troponin are two main proteins that regulate muscle contraction and relaxation (Choi & Kim, 2009; Zot & Potter, 1987). They prevent the activation of actomyosin ATPase in the absence of calcium ions by interacting with actin filaments to block the myosin binding site. Tropomyosin is a long, coiled protein (MW of 65 kDa) that comprises two α-helix polypeptide subunits, called α- and β-tropomyosin. Tropomyosin molecules bind head-to-tail along the F-actin filament. Each tropomyosin molecule is attached to a troponin complex (MW of 80 kDa) which is made up of troponin C (MW of 18 kDa), troponin I (MW of 21 kDa) and troponin T (MW of 31 kDa) (**Figure 2-3**). Each type of troponin serves a different function in the muscle: troponin C acts as the calcium binding site, troponin T connects troponin complex to tropomyosin while troponin I inhibits actomyosin ATPase activity when it is bound to actin (Lehman & Craig, 2008). At high calcium ion concentrations, calcium ions bind to troponin C, which initiates a conformation change in the tropomyosin-troponin complex, dislocating troponin I, allowing the action of actomyosin ATPase for muscle contraction.

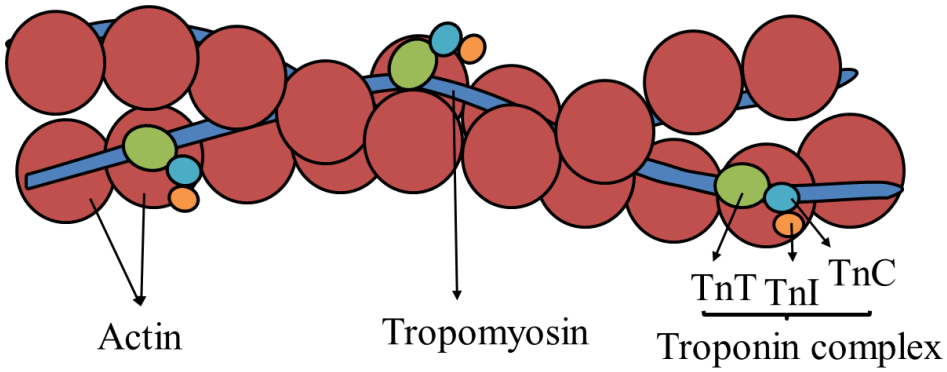

Figure 2-3. A schematic diagram of a thin filament comprising actin, tropomyosin and troponin complex troponin T (TnT), troponin I (TnI) and troponin C (TnC).
Reproduced from Boland et al. (2019) with permission from Elsevier Books.

2.2.3 Structural proteins

The structural proteins comprise titin, nebulin, α-actinin, β-actinin, tropomodulin, desmin, filamin, C-protein, H-protein and myomesin, which control the fillamentous structure and integrity of myofibrils (Obinata et al., 1981) (**Table 2-1**).

Table 2-1. List of structural proteins present in the myofibrils.

Structural proteins	Descriptions
[1]**Titin/connectin** (MW: 4200 kDa)	- Anchors from the Z-disk to the M-line - Provides elasticity to the sarcomere
[2]**Nebulin** (MW: 800 kDa)	- Attached to the Z-disk and extends to the end of the thin filaments - Regulates the length of thin filaments
[3]**α-Actinin** (MW: 95 kDa)	- Major constituent of the Z-disk which attaches actin to the Z-disk - Interacts with actin and titin which strengthen the Z-disk
[3]**β-actinin/CapZ protein** ➢ α-subunit (MW: 37/36 kDa) ➢ β-subunit (MW: 34/32 kDa)	- Binds α-actinin in the Z-disk - Prevents network formation between actin filaments
[4]**Tropomodulin** (MW: of 40 kDa)	- Binds tropomyosin and actin - Controls the length of thin filaments
[5]**Desmin** (MW: 55 kDa) & **filamin** (MW :300 kDa)	- Localised at the border of the Z-disk - Links the Z-disk to the sarcolemma and stabilises muscle structure
[6]**C-protein** (MW: 140 kDa) & **H-protein** (MW: 58 kDa)	- Myosin-binding proteins found in A-band of thick filaments - Contribute to the alignment and stabilisation of thick filaments - C-protein inhibits the elongation of titin filaments in the A-band
[7]**Myomesin** (MW: 185 kDa)	- Major protein in the M-line - Responsible for the binding of titin and myosin

[1]Labeit and Kolmerer (1995) & Tskhovrebova and Trinick (2003); [2]McElhinny et al. (2003) & Strasburg et al. (2008); [3]Obinata et al. (1981) and Strasburg et al. (2008); [4]Clark et al. (2002); [5]Capetanaki et al. (1997) & vanderVen et al. (2000); [6]Koretz et al. (1993) & Xiong (1997); [7]Strasburg et al. (2008)
MW represents molecular weight.

2.3 Sarcoplasmic proteins

2.3.1 Cathepsins

Cathepsins are lysosomal enzymes which are active at an acidic pH, and are released postmortem in the sarcoplasm (Geesink & Veiseth, 2008). Among the family of cathepsins, cysteine cathepsin B, H and L and aspartic cathepsin D are the most abundant in muscles. Cathepsin B has optimum activity at pH 5.5 to 6.5 and is unstable at pH 7. It breaks down MHC, troponin T, troponin I, tropomyosin (Bechet et al., 2005), intact myofibrils and collagen (Koohmaraie, 1988). Cathepsin H has an optimum pH range of 5.5 to 6.5 (Huff-Lonergan, 2014). It degrades myosin but is unable to hydrolyse intact myofibrils (Ouali et al., 1987). In contrast, cathepsin L acts optimally at pH 5 but remains stable at neutral pH, retaining approximately 30 % of its maximum activity (Geesink & Veiseth, 2008). It hydrolyses the majority of the myofibrillar proteins (except troponin C and tropomyosin) (Matsukura et al., 1981) and collagen (Agarwal, 1990). Cathepsin D has an optimum activity at pH 3 to 5 and is inactive at neutral pH (Bohley & Seglen, 1992). The proteolytic activity of cysteine cathepsins and cathepsin D can be inhibited by cystatins (Geesink & Veiseth, 2008) and pepstatin (Bohley & Seglen, 1992), respectively.

2.3.2 Calpains

Calpains are calcium-activated, cysteine proteases which have maximum activity at neutral pH (Sentandreu et al., 2002). There are two types of calpain responsible for postmortem proteolysis, which are ubiquitous µ-calpain and m-calpain (Raynaud et al., 2005; Strasburg et al., 2008). The calcium concentrations for the activation of both µ-calpain and m-calpain are in the range of micromolar and millimolar level correspondingly (Camou et al., 2007). *In vivo*, calpains degrade myofibrillar proteins during protein turnover for muscle growth (Goll et al., 2008; Huang & Forsberg, 1998).

They are found and act mostly in the Z-disks. Calpastatin is the natural inhibitor of μ-calpain and m-calpain.

2.3.3 Myoglobin

Myoglobin is a haem protein that acts as an oxygen carrier in muscle cells and is responsible for the colour of both raw and cooked meat (Claus, 2007; Suman & Joseph, 2014). Four forms of myoglobin exist in the muscle, including deoxymyoglobin (purplish red), oxymyoglobin (cherry red), metmyoglobin (brown) and carboxymyoglobin (cherry red) (**Figure 2-4**) (Suman & Joseph, 2013). The colour of the muscle depends on the ratio of these forms of myoglobin (Baldwin, 2012). Cooking of meat results in denaturation of myoglobin, causing the oxidation of haem which induces a change in meat colour. For example, the denaturation of metmyoglobin produces ferrihemochrome which gives cooked meat a dull brownish appearance (King & Whyte, 2006)

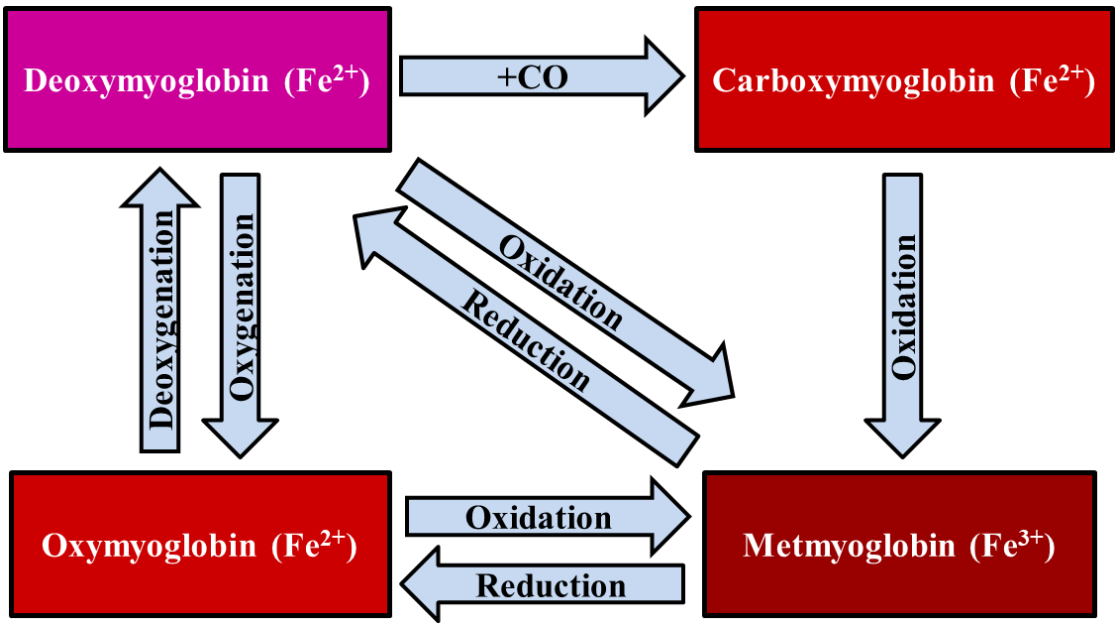

Figure 2-4. Interconversion of myoglobin redox forms in fresh meats.
Reproduced from Boland et al. (2019) with permission from Elsevier Books.

2.4 Stromal proteins

2.4.1 Collagen

Collagen is the predominant stromal protein existing in skeletal muscles that is synthesised by fibroblasts (Bailey & Light, 1989; Duance et al., 1977; Gault, 1992). There are four major classes of collagen based on their aggregation characteristics: striated and fibrous (Types I, II, III, V and XI); non-fibrous and network forming (Type IV); microfibrillar or filamentous (Type VI), and lastly fibril-associated collagen (Type VII) (Bailey, 1991). The basic structure of collagen consists of three polypeptide alpha chains with -Gly-X-Y- repeating units, where X and Y are commonly proline and hydroxyproline respectively, that coil to create a triple helix structure, forming tropocollagen that is about 280 nm in length and 1.4 nm to 1.5 nm in diameter (Astruc, 2014a; Bailey & Light, 1989; Gault, 1992; Strasburg et al., 2008). Tropocollagen molecules are polymerised into collagen fibres via covalent intermolecular cross-links, by the formation of aldehydes through oxidative deamination of lysine or hydroxylysine residues. These divalent, reducible cross-linkages offer substantial tensile strength to collagen fibres. As the collagen fibres age, these cross-linkages interact to form mature trivalent, non-reducible, more heat-stable cross-links, which further enhances their stability and mechanical strength.

Collagen has been linked to the toughness of muscle-based foods, and its content and extent of cross-linking differ among different animal species, age, muscle function, exercise and treatment with growth promoter (Strasburg et al., 2008). Bailey and Light (1989), McCormick (1999) and Purslow (2005) reported an increase in meat toughness as the animal aged due to an increase in collagen cross-linking and a decrease in collagen solubility (Taylor, 2004). It was also found that the tender meat cut, bovine *Longissimus*

dorsi, contains only half to two thirds of the total collagen content and hydroxylysylpyridinoline cross-links of that found in the tougher cut, *Biceps femoris* (McCormick, 1999). Various studies have been done to improve the meat quality by partial solubilisation of collagen in tough meat cuts such as *Semitendinosus* (Christensen, Bertram, et al., 2011; Christensen, Ertbjerg, et al., 2011; Combes et al., 2004; Sullivan & Calkins, 2010).

2.4.2 Elastin

Elastin is a minor constituent of connective tissue that offers elasticity to the blood vessels and ligaments in the muscles, but it could contribute to meat toughness (Debelle & Alix, 1999). Elastin is an insoluble, hydrophobic, heat-stable and cross-linked protein fibre that behaves in a highly elastic manner in the presence of water. Elastin fibre is characterised by the cross-linking of two amino acids, namely desmosine and isodesmosine, which are responsible for its extremely insoluble characteristic (Lawrie, 2006). Both desmosine and isodesmosine are formed by the condensation of the intermediate products from oxidative deamination of lysine side-chains (Anwar, 1990).

2.5 Postmortem changes in muscles

The death of animals results in postmortem biochemical, physicochemical and structural changes in muscles (Bendall, 1973; Greaser, 1986; Lawrie, 1992). The major biochemical events that happen during the conversion of muscle to meat are postmortem glycolysis and proteolysis. As blood circulation ceases, the supply of oxygen and nutrients is stopped (Honikel, 2014b; Strasburg et al., 2008). However, muscle homoeostasis is still being maintained by anoxic regeneration of adenosine triphosphate (ATP). Energy is released from the degradation of ATP into adenosine diphosphate (ADP) and inorganic phosphate.

This is accompanied by the production of hydrogen ions which accumulate in the cells, leading to a pH fall in the muscle. Adenosine triphosphate is regenerated by the following three main reactions: 1) conversion of creatine phosphate (CP) into creatine via the phosphorylation of ADP, 2) conversion of ADP into ATP and adenosine monophosphate (AMP) by myokinase, and 3) degradation of glycogen into lactic acid through the anaerobic glycolysis pathway.

When glycogen is fully depleted, ATP re-synthesis is interrupted, glycolysis reaction stops and the pH usually stabilises at around 5.5, which is known as the ultimate pH (pHu). The pHu of meat depends on the animal species, muscle types and pre-slaughter stress (Honikel, 2014a). Sometimes, glycolysis stops even in the presence of residual glycogen (Immonen & Puolanne, 2000). This was deduced to be due to the pH inhibition of glycolytic enzymes and/or the unavailability of AMP, a positive cofactor of glycogenolytic enzymes. The pHu is near to the isoelectric point of the myofibrillar proteins (Huff-Lonergan & Lonergan, 2005). This causes the shrinkage of myofibrils, which results in the exudation of intermyofilament water into the sarcoplasm, followed by extracellular spaces and finally out of the muscle (Offer & Trinick, 1983; Pearce et al., 2011). As the CP and glycogen stores in the muscles are depleted, there is a shortage of ATP to keep the contractile proteins actin and myosin apart, leading to the formation of the actomyosin bond (Hopkins, 2014). This muscle stiffening process is described as rigor mortis. This process lasts up to 12 h in red meat and 2 h in poultry.

After rigor mortis, the muscle enters the ageing process (Strasburg et al., 2008). At this stage, muscle proteins increase in extensibility as a result of proteolysis. This process degrades some structural myofibrillar proteins, predominantly along the Z-disks (Listrat et al., 2016; Taylor, Geesink, et al., 1995) and to a lesser extent the connective tissue

(Nishimura et al., 1995; Taylor, 2004), which tenderises the meat. Degradation of the Z-disks (Suzuki et al., 1982), desmin (Wheeler & Koohmaraie, 1994), titin (Koohmaraie, 1994), nebulin (Huff-Lonergan et al., 1995) and troponin T (Wheeler & Koohmaraie, 1994) have been observed in the postmortem muscle.

The postmortem decrease of energy supply causes the release of calcium ions from the sarcoplasmic reticulum and mitochondria, which triggers the calcium-activated μ-calpains and m-calpains, especially at pH 6 where glycolysis is yet to be completed (Gault, 1992). During postmortem ageing, troponin T, titin, nebulin, C-protein, desmin and filamin are hydrolysed by calpains whereas the principal contractile proteins, such as myosin and actin, are unaffected (Huff-Lonergan et al., 1996; Koohmaraie, 1988). It has been concluded that postmortem muscle tenderisation is due mainly to the action of μ-calpain and to a lesser extent the action of m-calpain (Goll et al., 2003; Koohmaraie & Geesink, 2006).

In addition, the cell membrane of the lysosomes is weakened as the pH falls below 6, which releases cathepsins that attack predominantly the contractile proteins and less significantly the connective tissue. It has been reported that elevated temperature and electrical stimulation accelerate the pH decline in the muscles, which promotes the release of cathepsins from the lysosomes and eventually facilitates muscle tenderisation (Dutson et al., 1980; Geesink & Veiseth, 2008; Moeller et al., 1977). However, as Cathepsin D is active at a pH range from 3 to 5, it has a relatively less important role in muscle tenderisation than other cathepsins at a postmortem pH of 5.5 (Mikami et al., 1987).

Apart from the calpains and the cathepsin system, caspases, which are cysteine aspartic-specific proteases, have recently received attention in regard to postmortem proteolysis and tenderisation (Cramer et al., 2018; Huang et al., 2018; Kemp et al., 2010; Ouali et al.,

2013; Ouali et al., 2006). Caspases are involved in the initial mechanisms of apoptosis or programmed cell death, which are activated by the release of cytochrome c from the mitochondrial membrane to the cytoplasm (Green & Reed, 1998). Apoptosis has been identified as the first proteolytic system involved in the degradation of structural proteins including actin, troponin T, troponin I, MLC and desmin, postmortem chronologically (Becila et al., 2010; Kemp & Parr, 2008). Cramer et al. (2018) discovered a significantly lower cytochrome c level and more intact desmin and troponin T during ageing in callipyge lamb loins than normal lamb loins, suggesting a weaker apoptosis activity in the former which resulted in meat toughness. Callipyge lambs have a genetic mutation which results in muscular hypertrophy of the loins and hindquarters, and are usually tougher than the normal, non-mutated lambs. Another endogenous protease system, proteasomes, which perform ubiquitin-mediated proteolysis in both the cytosol and the cell nucleus, have a major role in the intracellular protein degradation (Goll et al., 2008; Lee et al., 2010). However, the role of the proteasomes in postmortem meat tenderisation is not well understood. Studies have shown that purified proteasome is capable of hydrolysing myofibrillar proteins, but the degradation pattern and ultrastructural changes differ from typical postmortem ageing (Geesink & Veiseth, 2008; Koohmaraie, 1992; Taylor, Tassy, et al., 1995). Instead, the ultrastructural changes in myofibrils incubated with purified proteasomes resembles those observed in high pH meat and postmortem slow-twitch muscles, showing the possible involvement of proteasomes in meat tenderisation (Sentandreu et al., 2002). Liu, Du, et al. (2016) discovered that sheep *Longissimus lumborum* muscles injected with proteasome inhibitor had a less damaged muscle ultrastructure after 48 h of injection, suggesting that proteasomes might contribute to postmortem meat tenderisation. Dutaud et al. (2006) have also observed 30 to 48 % of intact proteasomes in meat after storage at 0 to 4 ℃ for 16 days and proposed that

proteasomes might have better proteolytic potential than μ-calpain during ageing. Other proteolytic systems such as metalloproteases, thrombin or plasmin may also be involved in the postmortem degradation of muscle tissue.

Ageing improves meat tenderness and may last for a couple of days for poultry, pork and lamb and about two weeks for beef. Meat tenderness has been reported to be a function of the intramuscular connective tissue content and cross-linking, as well as the formation of actomyosin complex in the muscles (Baldwin, 2012). High collagen content and low heat-induced collagen solubility contribute to connective tissue toughness while the overlapping of myosin and actin filaments during rigor mortis causes actomyosin toughness. It has been reported that the myofibrils in pork *Longissimus dorsi* aged for eight days were more fragmented and had smaller particle size distribution than the unaged meat (Lametsch et al., 2007).

2.6 Nutritional characteristics of muscle-based foods

Muscle-based food is an excellent source of nutrients. It provides micronutrients such as iron, selenium and vitamin B12, which are either absent or possess poor bioavailability in plant-based foods (Biesalski, 2005). The compositions of lean tissue in muscle-based foods are tabulated in **Table 2-2** (Foegeding et al., 1996; Strasburg et al., 2008). About 17 to 23 % of lean muscle is made up of protein which contains all the essential amino acids required on a daily basis for muscle growth and health maintenance. The most abundant amino acid in meat is glutamine (16.5 %), followed by arginine, alanine and aspartic acid (Williams, 2007). Consuming meat with plant-based foods, such as cereals and legumes, compensates for the lower levels of lysine (cereals) as well as methionine and cysteine (legumes) in the diet (Bodwell & Anderson, 1986). The lipid content and composition vary considerably among different animal species and muscle types, as well

as the fatty acid profile of the animal feed. In contrast, carbohydrate is relatively scarce in meat because glycogen is converted to lactate during the postmortem process. Muscle-based foods are rich in some water-soluble vitamins, such as vitamin B_1, B_2, B_3, B_6 and B_{12} and are relatively deficient in vitamins C, D, E and K. They contain a significant amount of highly bioavailable haem iron due to their higher myoglobin content, especially red meat (Buzała et al., 2015). Other constituents include minerals, such as potassium, phosphorus and magnesium.

Table 2-2. Composition of lean muscle tissues in general (raw).

Species	Proximate composition (%)			
	Water	**Protein**	**Lipid**	**Ash**
Beef[a,b,c]	70 - 73	20 - 23	3 - 8	1
Pork[b,c]	68 - 70	19 - 20	9 - 11	1.4
Chicken[b,c]	73.7	20 - 23	4.7	1
Lamb[a,b,c]	73	20-22	5 - 6	1.6
Cod (lean fish)[b,c]	81.2	17.6	0.3	1.2
Salmon (fatty fish)[b,c]	64	20 - 22	13 - 15	1.3

Reproduced from Boland et al. (2019) with permission from Elsevier Books.
[a]Williams (2007)
[b]Strasburg et al. (2008)
[c]Foegeding et al. (1996)

2.7 Human digestive system and protein digestion

The human digestive system is a tubular structure extending from the mouth to the anus which is responsible for food digestion and absorption (Boland, 2016; Tortora & Derrickson, 2013). The system breaks down ingested food into smaller molecules that are available to be taken up and assimilated into the body cells. Digestion involves both mechanical and chemical actions. After ingestion, food is mixed with saliva (near neutral pH), comminuted into smaller particles by the teeth and forms a bolus. A bolus usually consists of food particles that are between 1 to 3 mm, and is transferred to the stomach by the tongue and smooth muscle of pharynx and oesophagus (Jalabert-Malbos et al., 2007; Tortora & Derrickson, 2013). Salivary amylase is secreted by the salivary glands

in the mouth to break down carbohydrates, such as starches and disaccharides, into smaller molecules, and continues to act on its substrates in the stomach until its inactivation by gastric acid.

The entrance of a bolus to the stomach triggers the secretion of gastric juice by the gastric glands (Tortora & Derrickson, 2013). The bolus mixes with gastric juice and its particle size is reduced slightly due to the effect of peristaltic movement, forming chyme. Gastric juice contains hydrochloric acid, pepsinogen, gastric lipase, gastrin, some intrinsic factors, electrolytes and other organic substances. Hydrochloric acid in the gastric juice partially denatures food proteins and activates the proteolytic enzyme pepsin, that is secreted by the gastric chief cells. Pepsin is an endopeptidase, which initiates protein digestion by cleaving peptide bonds located at the interior of the protein chain, producing polypeptide fragments with high molecular weight. Pepsin has an optimum activity at pH 2 and is inactivated at pH 8 and above (Piper & Fenton, 1965). During the fasting state, the pH in the stomach is around 2 or below. The ingestion of food leads to a rise in the pH to 5 or more, depending on the buffering capacity of the food. Due to constant secretion of hydrochloric acid, the pH in the stomach decreases slowly to fasting pH, which favours the proteolytic action of pepsins (Minekus et al., 2014). Pepsins cleave peptide bonds adjacent to phenylalanine, tryptophan and tyrosine residues (Blanco & Blanco, 2017). Peptic digestion of protein results in the formation of polypeptides and oligopeptides, with negligible release of free amino acids (Erickson & Kim, 1990). Gastric lipase, which has an optimum activity at pH 5 to 6, has little activity in the acidic environment of the adult stomach. Hence, the majority of the digestion of triglycerides occurs in the small intestine by pancreatic lipase with the aid of bile. The gastric emptying process starts when the particle size of chyme is less than 1 to 2 mm, allowing it to pass through the

pyloric sphincter into the first section of the small intestine, the duodenum (Singh et al., 2015).

Pancreatic and intestinal juices, and bile secreted into the small intestine further break down the partially-digested carbohydrates, proteins and lipids present in the chyme from the stomach (Smith & Morton, 2010). Protein and peptide fragments in the small intestine are hydrolysed by trypsin, chymotrypsin, carboxypeptidase and elastase in the pancreatic juice, and other peptidases, such as aminopeptidases, oligopeptidase, di- and tripeptidases, present in the microvilli brush border membranes or the cytosol of the absorptive cells. Pancreatic juice contains bicarbonate that neutralises the pH of the chyme, creating a favourable environment for these enzymes. The endopeptidases, which include trypsin, chymotrypsin and elastase, cleave the peptide bonds forming smaller peptides from large polypeptides (Erickson & Kim, 1990). Trypsin cleaves peptide bonds on the carboxyl terminal of basic amino acids (lysine and arginine). Chymotrypsin hydrolyses peptide bonds on the carboxyl aromatic amino acids (tyrosine, tryptophan and phenylalanine). Elastase breaks down elastin and break the peptide bonds in polypeptides with aliphatic amino acid residues (alanine, leucine, glycine, valine and isoleucine) on the carboxyl terminal. The exopeptidases include carboxypeptidases A and B, and peptidases present in microvilli. Carboxypeptidases cleave single amino acids from the carboxyl terminal while aminopeptidases cleave single amino acids from the amino terminal ends of peptides (Smith & Morton, 2010). The hydrolysis products produced by the endopeptidases are ideal substrates for the carboxypeptidases (Gray & Cooper, 1971). Carboxypeptidase A has high specificity for the peptide bonds with neutral amino acid at the carboxyl terminal, such as the aromatic and aliphatic amino acids at the carboxyl terminal of peptides produced by the actions of chymotrypsin and elastase. Carboxypeptidase B favours the peptide bonds with basic amino acid at the carboxyl

terminal, such as the peptides produced by the action of trypsin. The hydrolysed fragments produced by the pancreatic enzymes, mainly oligopeptides with two to eight amino acid residues (~70 %) and some free amino acids (~30 %). The oligopeptides are further broken down into single amino acid, dipeptides and tripeptides by peptidases in the brush border membrane. The dipeptides and tripeptides enter the absorptive cells of the microvilli via hydrogen-dependent secondary active transport, which are further degraded into amino acids by cytosolic tri- and dipeptidases. The amino acids enter the absorptive cells of the microvilli through active transport or sodium-dependent secondary active transport and then being transported into the blood stream through passive diffusion (e.g. hydrophobic amino acids such as tryptophan), facilitated diffusion or active transport (e.g. all free amino acids). The rate of protein digestion and the absorption of dietary amino acids are believed to have an impact on postprandial protein deposition (Boirie et al., 1997; Dangin et al., 2001). Various studies have suggested that proteins that are digested at a faster rate have an enhanced postprandial protein gain especially in the elderly (Boirie et al., 1997; Dangin et al., 2003).

Unlike fat, which is almost digested completely in ileum, protein tends to enter the colon without complete digestion (Jørgensen et al., 2000). Undigested chyme enters the large intestine where it is fermented by the microflora present in the lumen. The amount of undigested proteinaceous substances reaching the human large intestine has been reported to range from 3 to 18 g per day (Cummings & Macfarlane, 1991; Cummings & Macfarlane, 1997; Muir & Yeow, 2000). There are approximately 3 g of non-dietary endogenous proteins such as glycoproteins and mucinous proteins that enter the large intestine daily (Chacko & Cummings, 1988). In addition to daily dietary protein intake, the amount of undigested dietary protein reaching the large intestine is affected by the protein digestibility of the ingested foods. The protein digestibility is largely dependent

on the source and processing history of foods (Yao et al., 2016). High protein digestibility reduces the amount of undigested proteinaceous substance entering the colon. Several studies have found that the true ileal digestibility of dietary protein in humans to range from 84 to 96 % (Mariotti, 2017; Tomé, 2013; Yao et al., 2016). The true ileal digestibility of animal proteins such as eggs, meat, and milk were 91 to 96 %, 90 to 94 % and 95 to 96 %, respectively. Plant proteins were found to have a slightly wider and lower true ileal digestibility range, which was between 84 and 92 %. Rapeseed protein (84 %) had a lower ileal digestibility while soy protein isolate (91.5 %), pea protein isolate (89.5 to 91.5 %), legumes (e.g. soy beans and kidney beans; 89 to 92 %) and oats (90 %) had higher ileal digestibility. Nevertheless, the protein digestibility from both animal and plant sources could be improved or reduced by processing, depending on the processing methods, conditions and severity (Kaur et al., 2016; Li et al., 2017; Sa et al., 2019; van Lieshout et al., 2020).

These undigested proteins are metabolised by colonic microflora either via proteolysis or a fermentation process. Fermentation of protein generates nitrogenous metabolites such as ammonia, amines, N-nitroso, phenolic, cresolic and indolic compounds (Macfarlane, Cummings, et al., 1986). These products may cause long term detrimental effects on colonic heath, such as colorectal cancer and inflammatory bowel disease, depending on the balance between the rate of toxic metabolite generation, detoxification and excretion from the large intestine (Yao et al., 2016). For example, ammonia has been reported to adversely affect the epithelial barrier and colonocyte lifespan (Hughes et al., 2008; Lin & Visek, 1991). Three to ten hours after reaching the large intestine, chyme is solidified forming faeces (Tortora & Derrickson, 2013). Faeces are stored in the rectum before excretion via the anus.

Other than the enzymatic action of digestive proteases, Astruc (2014b) reported the physiochemical environment in the gastrointestinal tract also plays an important role in the food digestion process. Subjecting raw bovine *Semitendinosus* muscle to simulated gastric digestion at pH 1.8, both with and without the addition of pepsin, resulted in the swelling of muscle cells and collagen fibres, which is consistent with the findings by Kaur et al. (2016), Rao et al. (1989) and Bailey and Light (1989). He suggested that the acidic pH partially denatures muscle proteins, which aids the access of digestive enzymes to the substrates. As excessive protein aggregation caused by thermal unfolding of proteins may reduce protein degradation by digestive enzymes (Gatellier & Sante-Lhoutellier, 2009; Santé-Lhoutellier et al., 2008), the acid-induced denaturation and swelling of muscle cells may limit the penetration of digestive juices into the core of the food (Astruc, 2014b). Moreover, he reported that pepsin digestion of meat in the stomach mainly disrupts the Z-disks while subsequent trypsin and chymotrypsin digestion in the small intestine degrades the sarcomere. The structure weakened during postmortem ageing is also more susceptible to hydrolysis by digestive enzymes.

2.8 Processing techniques and their effects on muscle protein structure and consequence on digestibility

Meat processing impacts the physical and chemical properties of the product by the action of mechanical forces, heat or the addition of salts and additives (Lewis, 1992). For instance, meat tenderisation through electrical stimulation, ultrasonic waves, blade tenderization and pressure treatment have been reported to modify the muscle structure and protein profile (Hopkins, 2014). These processes may decrease the overlapping of actin and myosin, cause physical damage to the sarcomere and connective tissue, or improve proteolysis rates through the activation of calpains by release of calcium ions

and/or lysosomal proteases such as cathepsins, after membrane disruption. These structural changes are likely to influence the accessibility of digestive enzymes to their substrates, and thus affect the product digestibility in the gastro-intestinal tract (Astruc, 2014b). For instance, high pressure processing has been reported to alter muscle structure and enhance *in vitro* protein digestibility of beef (Kaur et al., 2016). Many innovative meat processing technologies have been explored in recent decades. It is valuable for the meat industry to have a better understanding of how these technologies affect muscle structure and protein digestibility of meat as there is increasing demand for products that contain high-value animal protein (Hung et al., 2016; Kraus, 2015). The technologies focused on in this section are pulsed electric field (PEF) processing, hydrodynamic shockwave (SW) processing, sous vide (SV) cooking, and exogenous enzyme processing.

2.8.1 Pulsed Electric field (PEF)

Pulsed electric field is a non-thermal process used in food and bioengineering applications since the 1960s (Toepfl et al., 2007a). This technology involves applying an electric field, in the form of short wave pulses, to food placed between two electrodes (O'Dowd et al., 2013). Pulsed electric field leads to electroporation of cell membrane when the induced transmembrane potential goes beyond a critical value of 1 Volt, causing permanent or temporary pore formation and cell disintegration (McDonnell et al., 2014; Toepfl et al., 2007a). In the past, this treatment has been applied mainly for the purpose of food preservation in milk, eggs, juices and other liquid foods (Castro et al., 1993; Toepfl et al., 2007b). High intensity PEF, normally 20 to 80 kV/cm, effectively inactivates microbes with minimal detrimental effect on the food properties (Leadley & Williams, 2006). Recently, there has been an increasing interest in non-preservative applications of PEF, which modifies food properties leading to an enhancement of overall product quality.

Low intensity PEF applications, such as juice pressing and extraction, meat tenderisation and curing, fruit and vegetable dehydration and others have been studied (Gachovska et al., 2006; Mhemdi et al., 2012; O'Dowd et al., 2013; Puértolas et al., 2012).

Low intensity PEF treatment has been reported to induce changes in the structure of myofibrillar-based foods, which could potentially improve their texture and functional properties (Arroyo, Eslami, et al., 2015). The effect of PEF on meat depends on both the processing parameters and the properties of meat samples (dielectric properties, meat types, pre- and post-slaughtering process) (Alahakoon et al., 2016; Toepfl et al., 2007a). Pulsed electric field treatment performed at an appropriate electric field strength, pulse frequency and or specific energy are required in creating large permanent pores in meat tissues, causing structural modification and eventually affecting functional properties of meat. Excessive electric field strength (1.7 to 2 kV/cm) led to cooking effect on the edges of raw meat (Faridnia et al., 2015). Application of electric pulses perpendicular to the muscle fibre direction maximises the electroporation effect while achieving optimum electric field strength (Alahakoon et al., 2016).

2.8.1.1 Effect of PEF processing on muscle protein profile, structure and digestibility

Low intensity PEF has been reported to cause structural changes in the muscles (**Table 2-3**) but their protein profile was largely unaffected (Faridnia et al., 2014; Gudmundsson & Hafsteinsson, 2001). Hence, it was suggested that the impact of low intensity PEF treatment on muscle structure was mainly the result of electroporation of cell membrane but not protein denaturation. However, increased proteolysis of troponin T and desmin were observed in PEF-treated meat during ageing (Suwandy et al., 2015a; Suwandy et al., 2015b).

Troponin T is the substrate of cathepsin L and calpains while desmin is the substrate of calpains (Huff-Lonergan, 2014). Hence, the enhanced proteolysis is speculated to be due to the release of calcium ions by electroporation, leading to early activation of calpains, and/or the action of lysosomal enzymes released due to the permeabilisation of muscle cells by PEF (Alahakoon et al., 2016; Bhat et al., 2018b). Recent studies have discovered improved calpain activity in PEF-treated beef *Semimembranosus* (0.36 kV/cm, 90 Hz and 0.60 kV/cm, 20 Hz) (Bhat, Morton, et al., 2019a) and cold-boned venison *Longissimus dorsi* (2.5 kV, 50 Hz and 10 kV, 90 Hz) (Bhat, Morton, Mason, Mungure, et al., 2019), along with increased degradation of troponin T during ageing. However, there is no information available on the effect of PEF on lysosomal proteases such as cathepsins in meat.

Scanning electron micrograph of the PEF-treated beef *Longissimus thoracis* muscles showed that the treated muscles were porous, which led to a higher moisture loss from the treated cuts than the control untreated meat during storage (Faridnia et al., 2014). The size of the muscle cells of the PEF-treated beef, chicken and salmon was smaller than their untreated counterparts, which may due to greater water losses after the treatment (Gudmundsson & Hafsteinsson, 2001; O'Dowd et al., 2013). Furthermore, gap formation (Gudmundsson & Hafsteinsson, 2001), fragmentation of myofibrils (O'Dowd et al., 2013) and elongated muscle bundles (Khan et al., 2017) were observed in PEF-treated meat samples. The extent of myofibrillar degradation along the Z-disks of PEF-treated beef *Biceps femoris* was observed to be to a greater than in untreated muscles during the ageing process, indicating accelerated postmortem proteolysis (Faridnia et al., 2016).

To date, limited low intensity PEF treatment studies have been conducted to investigate the effect of PEF on individual meat components for meat tenderisation. Alahakoon et al.

(2017) observed porous surface structure of the PEF-treated connective tissue isolated from beef *Deep pectoralis* muscle, under scanning electron microscope. A significantly decreased denaturation temperature and increased heat solubility of the PEF-treated connective tissue isolate were also detected. These observations suggest the use of PEF could reduce the cooking time of collagen-rich meat.

The effect of PEF on muscle protein digestibility has only received attention in recent years and is not well studied. *In vitro* protein digestibility of raw cold-boned bovine *Bicep femoris* (10 kV, 20 Hz, 20 µs) (Bhat et al., 2018c) and cold-boned deer *Longissimus dorsi* (10 kV, 90 Hz) (Bhat, Morton, Mason, Bekhit, et al., 2019) was found to improve with increased free individual amino acids measured at the end of digestion using a high performance liquid chromatography (HPLC) method. In another study, *in vitro* protein digestibility of PEF-treated (10 kV, 20 Hz, 20 µs) water bath-cooked (core temperature of 75 ℃) bovine *Semimembranosus* was improved while no significant difference was observed in the free individual amino acids released (Bhat, Morton, Mason, Jayawardena, et al., 2019). Conversely, Alahakoon et al. (2019) did not detect any improvement in protein digestibility of PEF-treated (0.7 and 1.5 KV/cm, specific energy of 90 to 100 kJ/kg) SV-cooked (60 ℃ for 12 h or 24 h) beef brisket. Current research to understand the effect of PEF on meat digestibility is limited, and if the structural changes induced by PEF influence meat breakdown during digestion requires further research.

Table 2-3. Summary of the effects of low intensity PEF on muscle structure.

Types of meat	Processing parameters	Structural changes	References
Chicken	1.36 kV/cm, 40 pulses	Reduction in muscle cell size without visible gapping between muscle fibres	Gudmundsson and Hafsteinsson (2001)
Salmon	1.36 kV/cm, 40 pulses	Leakage of collagen into extracellular spaces with visible gapping between muscle fibres	
Lumpfish roes	12 kV/cm, 12 pulses	Roes remain intact and unaffected	
Bovine *Longissimus thoracis*	0.2 to 0.6 kV/cm, 1 to 50 Hz, 20 µs	Increase in porosity of muscle tissue	Faridnia et al. (2014)
Frozen-thawed Bovine *Semitendinosus*	1.4 kV/cm, 50 Hz, 20 µs, 250 kJ/kg	Jagged edges in sarcomere; Separation of myofibrils from the Z-disks; Rupture of the Z-disk and I-band junction	Faridnia et al. (2015)
Bovine *Semitendinosus*	1.1 to 2.8 kV/cm, 5 to 200 Hz, 152 to 300 pulses, 12.7 to 226 kJ/kg	More fragmented myofibrils; Reduction in muscle fibre diameter and volume	O'Dowd et al. (2013)
Bovine *Biceps femoris*	1.7 to 2.0 kV/cm, 50 Hz, 185 kJ/kg	More ruptured myofibrils along the Z-disks and more porous structure	Faridnia et al. (2016)
Beef *Longissimus lumborum*	2.5 kV, 200 Hz, 20 µs	Formation of gaps between elongated muscle bundles	Khan et al. (2017)
Connective tissue isolate (bovine *Deep pectoralis*)	1.0 and 1.5 kV/cm, 50 and 100 kJ/kg, 50 Hz, 20 µs	Porous structure of the isolated connective tissue observed under scanning electron microscope	Alahakoon et al. (2017)

2.8.1.2 Effect of PEF processing on meat quality

The colour of meat has been reported to remain unaffected by the low-intensity PEF treatment (Arroyo, Lascorz, et al., 2015; Faridnia et al., 2014; Suwandy et al., 2015c). However, higher intensity and or repeated PEF treatment resulted in elevated temperature of the samples leading to increased myoglobin oxidation and eventually may have negatively affected the colour of meat (Alahakoon et al., 2016; O'Dowd et al., 2013). Khan et al. (2017) reported a significantly higher lightness (L^* value) and lower redness

(*a** value) in high-intensity PEF-treated bovine *Longissimus lumborum* (10 kV, 200 Hz, 20 µs). Pulsed electric field treatment has been reported to increase the purge loss of meat, which could be due to the structural changes induced by the processing (Arroyo, Lascorz, et al., 2015; Faridnia et al., 2016). The reported effect of PEF on the cook loss in the current literature is not unanimous, due to different cooking methods and rates as well as the end-point temperature of the meat (Alahakoon et al., 2016). Low intensity PEF treatment has been reported to have no adverse impact on the lipid oxidation of meat (Arroyo, Eslami, et al., 2015; McDonnell et al., 2014). However, Khan et al. (2017) observed a higher lipid oxidation in beef *Longissimus lumborum* treated with high PEF intensity (10 kV, 200 Hz, 20 µs) when compared to the samples treated with lower PEF intensity (2.5 kV, , 200 Hz, 20 µs). Increased lipid oxidation has also been found in frozen-thawed PEF-treated muscles (Alahakoon et al., 2016). Faridnia et al. (2015) suggested that PEF processing renders frozen-thawed muscles to lipid oxidation during storage due to the exposure of fatty acids to pro-oxidant released from muscle cells after the freezing-thawing process. Research on the effect of low intensity PEF treatment on the protein oxidation of meat is scarce.

The effects of PEF on muscle texture reported in the literature is also contradictory and vary due to the variation in experimental setup, such as processing parameters, sample preparation prior to PEF treatment, handling of animals pre- and post-slaughtering and muscle types (Alahakoon et al., 2016). Bekhit, van de Ven, et al. (2014) observed improved tenderness in PEF-treated cold boned beef *Longissimus lumborum* (0.31 to 0.56 kV/cm, 20, 50 and 90 Hz) (19.5 % shear force reduction) and S*emimembranosus* (0.27 to 0.56 kV/cm, 20, 50 and 90 Hz) (4.1 to 19.1 % shear force reduction) muscles. Shear force is the amount of force required to slice through a piece of meat (Williams, 2008). Suwandy et al. (2015a) reported improved tenderness (up to 21.6 % shear force reduction)

in PEF-treated hot boned S*emimembranosus* (0.31 to 0.56 kV/cm, 20, 50 and 90 Hz). Pulsed electric field treatment also effectively tenderised frozen-thawed beef Semitendinosus (1.4 kV/cm, 50 Hz, 20 µs) (20.13 % shear force reduction) as discovered by Faridnia et al. (2015). Conversely, there was no change in the texture of PEF-treated bovine *Longissimus thoracis* (0.2 to 0.6 kV/cm, 1 to 50 Hz, 20 µs) (Faridnia et al., 2014). The shear force of beef *Semitendinosus* was also reported to be unaffected by PEF (1.9 kV/cm, 65 Hz, 20 µs, pulse number of 250), although there was an increase in myofibrillar fragmentation (O'Dowd et al., 2013).

2.8.2 Hydrodynamic shockwave (SW) processing

Hydrodynamic SW processing is a novel technology that generates a SW up to 1 GPa which travels through water in fractions of a millisecond (Bolumar et al., 2014; Hopkins, 2014). In food applications, SW processing can be performed as a batch process through an explosive approach or as a continuous process by the electrical discharge method. The early SW processing work was mainly done based on the use of explosives, which raised problems concerning the operators' safety and the potential contamination of food with explosive chemical residues (Bolumar & Toepfl, 2016; Long, 1993; Solomon et al., 1997). This led to the development of SW equipment operated by an underwater electric discharge, which is more suitable to be transformed for industry use (Long, 2000). The electric discharge approach allows an automated continuous process for improved throughput in addition to better control of hydrodynamic pressure intensity by manipulating electrical voltage and pulse number (Bolumar et al., 2013; Bolumar & Toepfl, 2016).

A SW process can be set up by sealing meat in an impermeable bag and placing it in a water-filled container (Hopkins, 2014). As meat is high in moisture, the SW travels from

the surrounding water to the meat sample, reflects from the walls of the container and intersect, producing an extremely high pressure that is able to cause physical disruption of meat. Shockwave processing has been reported to be effective in tenderising meat by altering sarcomere structure (Zuckerman & Solomon, 1998). The structural disruption may facilitate the penetration and proteolytic action of endogenous enzymes during maturation.

2.8.2.1 Effect of SW processing on muscle protein profile, structure and digestibility

The effect of SW processing on protein profile is debatable. Bolumar et al. (2014) and Schilling et al. (2002) have reported that there was no distinct difference in the myofibrillar and sarcoplasmic proteins between the control and explosive or electrical SW-treated meat. Marriott et al. (2001) observed no changes in collagen solubility of the explosive SW-treated bovine *Longissimus lumborum*. However, in other studies, it was revealed that explosive SW-treated muscle has higher solubility of myofibrillar proteins (beef strip loins) (Bowker, Fahrenholz, Paroczay, & Solomon, 2008), increased collagen solubility (beef top rounds) (Eastridge et al., 2005), exhibited changes in the profile of sarcoplasmic proteins and decreased solubility of sarcoplasmic proteins (beef strip loins) (Bowker, Fahrenholz, Paroczay, & Solomon, 2008). Spanier and Fahrenholz (2005) observed the actin and myosin in the explosive SW-treated meat changed significantly, which was deduced to be due to the breakdown of C-protein resulting in loss of structural integrity. A decrease in troponin T band intensity and more intense troponin T degradation product band (30 kDa) was observed in explosive SW-treated beef strip loins during ageing, indicating their enhanced proteolysis (Bowker, Fahrenholz, Paroczay, Eastridge, et al., 2008).

The effect of SW processing on the structure of muscle-based foods is summarised in **Table 2-4**. Shockwave treatment led to increased endomysium spaces between muscle fibres (Bolumar et al., 2014), myofibrillar fragmentation alongside the Z-disks (Bolumar et al., 2014; Zuckerman & Solomon, 1998) and the destruction of collagen fibrils of the endomysium (Zuckerman et al., 2013). Hopkins (2014) stated that the physical disruption of muscles may have led to the release of endogenous proteases or their activators, thus enhancing the tenderization effect. However, Bolumar et al. (2014) did not observe any changes in the cathepsin and peptidase activities of electrical SW-treated beef loins. The authors suggested that the tenderisation effect of SW treatment is due to the enhanced enzymatic contact and the disruption of muscle structure. Bowker, Fahrenholz, Paroczay, Eastridge, et al. (2008) also proposed that SW processing altered myofibrillar structure which facilitated the action of endogenous proteases during the ageing process. No studies were found in the literature which determine the effect of SW processing on muscle protein digestibility.

Table 2-4. Summary of the effects of shockwave processing on muscle structure.

Types of meat	Processing parameters	Structural changes	References
Bovine *Semitendinosus*	150 g explosive (plastic container), 35.6 cm between explosive and meat; 450 g explosive (stainless steel container), 61.0 cm between explosive and meat; ~100 MPa on the meat surface	Disruption of collagen fibril network of the endomysium	Zuckerman et al. (2013)
Bovine *Longissimus dorsi*	100 g of explosive (~60 to 70 MPa), 30.5 cm between explosive and meat	Myofibrillar fragmentation along Z-disks; Increment in intramyofibrillar spaces	Zuckerman and Solomon (1998)
Bovine *Longissimus lumborum*	1.8 kV/cm, 11664 J/pulse, single pulse, 20 cm between meat and electrical spark source	Disruption of muscle fibres structure; Increment in endomysium spaces; Alteration of collagen fibril network in endomysium	Bolumar et al. (2014)

2.8.2.2 Effect of SW processing on meat quality

The appearance of SW-treated meat remained uninfluenced when a pressure of approximately 100 MPa was applied (Bowker et al., 2016). However, a slight difference in shape was observed, depending on the orientation of meat fibres and the direction of the shockwave pressure front. Hydrodynamic pressure treatment had no effect on the colour (Claus et al., 2001a; Moeller et al., 1999; Solomon et al., 1997) and drip loss (Bolumar & Toepfl, 2016; Moeller et al., 1999) of the treated muscles. Mixed effects of SW processing on cook loss has been reported, depending on the cooking method, cooking rate and the end-point temperature of meat (Claus et al., 2001a, 2001b; Marriott et al., 2001; Moeller et al., 1999). No research has been reported on the effect of shockwave processing on lipid and protein oxidation of meat.

Shockwave processing research has focused on meat tenderisation, primarily for red meats (Bolumar et al., 2013; Bowker, Liu, et al., 2010; Solomon et al., 1997). Shockwave processing of bovine *Longissimus dorsi, Semimembranosus, and Biceps femoris* muscles lowered Warner-Bratzler (WB) shear force by 10 to 70 %, depending on the processing parameters and muscle types (Bolumar et al., 2014; Solomon et al., 1997; Spanier et al., 2005). Shear resistance of beef loin also decreased by 10 to 50 % after explosive SW treatment (Spanier & Romanowski, 2000). Other than red meat, the tenderness of poultry *pectoralis* was improved by 12 to 42 % by both explosive and electrical SW treatment (Bowker, Callahan, et al., 2010; Claus et al., 2001a, 2001b). The texture variation within meat cuts was also reduced. Hopkins (2014) reported that SW processing decreased the toughness of cuts high in connective tissue by up to 70 %, even when the cuts that had undergone cold-induced shortening after storage. These cuts were stored 1.5 h after slaughter at a temperature of 2 to 4 °C for a day. The extent of tenderness improvement

was associated with the initial tenderness, handling of animal post-slaughter, postmortem time and processing conditions of the SW treatment (Bolumar et al., 2013). In general, the tenderising effect of the electrical SW treatment was less intense than the explosive SW treatment, with only 10 to 30 % decrease in toughness observed across beef, pork, turkey and chicken meats.

2.8.3 Sous vide (SV) cooking

Thermal processing has been widely adopted alone, or in combination with other processing techniques in the food industry (Troy et al., 2016). Conventional thermal processing such as roasting applies high heat to food which causes overheating of the product surface, leading to undesirable product quality (Chen et al., 2012). Sous vide is a cooking method that has been used in the restaurants and food catering services where food is cooked under vacuum at a precise and controlled temperature, usually in a water bath (Baldwin, 2012; Schellekens, 1996). Cooking under vacuum results in uniform and efficient heat transfer from water to food, overcoming the drawback of uneven heating encountered in the conventional cooking process. Volatile compounds and moisture in food can be better retained. Due to microbiological safety considerations, a minimum meat cooking temperature of 60 °C is recommended by the government authority in some countries (Purslow, 2018).

2.8.3.1 Effect of SV cooking on muscle protein profile, structure and digestibility

During the cooking process, heat denatures proteins leading to several physical changes in the muscles. The effect of cooking on muscle protein largely depends on the cooking time and temperature as well as the heating rate (Suriaatmaja, 2013). The myofibrillar proteins, mostly myosin and actin, shrink during heating, causing the contraction of muscle fibres (Baldwin, 2012). When meat is subjected to 40 to 60 °C, muscle fibres

shrink transversely which causes the widening of the gap between them (Palka & Daun, 1999; Tornberg, 2005). As the temperature further increase, muscle fibres shrink longitudinally and water held between thick and thin filaments is expelled. Myosin starts to denature from 40 to 50 ℃ while titin and actin begin to denature from 60 ℃ and 70 to 80 ℃, respectively (Bejerholm et al., 2014).

The sarcoplasmic proteins start to aggregate and gel when heated at 40 to 60 ℃ (Baldwin, 2012). At SV cooking temperature range, some of the endogenous proteases remain active (Laakkonen, Sherbon, et al., 1970; Laakkonen, Wellington, et al., 1970). At 55 ℃, cathepsins B and L were found to be active up to 24 h of cooking whereas both μ- and m-calpains were inactivated within 10 min (Ertbjerg et al., 2012). Myoglobin starts to denature at temperature between 55 and 65 ℃ and the denaturation process usually ends by 75 or 80 ℃ (King & Whyte, 2006).

In general, connective tissue such as collagen denature and shrink at around 60 ℃ and more intensely over 65 ℃ (Baldwin, 2012). This leads to the formation of water-soluble random coiled gelatine due to the destruction of triple helix structure of collagen, which decreases the adhesion between muscle fibres. The gelatinisation of collagen usually occurs at above 75 ℃, but can also be achieved at a lower temperature during extended moist cooking (e.g. braising) (Bejerholm et al., 2014). Roldan et al. (2013) observed that in SV-cooked lamb *Longissimus dorsi* at 70 ℃, connective tissue was denatured and there was gel formation which filled the gaps between muscle fibres. Differential scanning calorimetry (DSC) analysis done by Christensen et al. (2013) showed that prolonged heating at elevated temperature (53 ℃ for 19.5 h) resulted in diminishing of myosin and collagen peaks of bull *Semitendinosus* in the thermograph, indicating the denaturation of these proteins after low temperature long time cooking. Although meat proteins were

heated at temperature lower than the reported thermal denaturation temperature, prolonged heating still resulted in proteins thermal denaturation (Bertola et al., 1994; Zielbauer et al., 2016). However, it was found that the collagen in intramuscular connective tissue consisted of thermally-liable and -stable fractions (Latorre et al., 2019; Purslow, 2018). The latter remained undenatured after heating at 60 ℃ for 24 h, which requires further research exploring mechanisms to degrade this fraction for meat tenderisation. Elastin remained heat-stable at 100 ℃ (Taylor, 2004). The structural changes in muscles during heat treatment are summarised in **Table 2-5.**

Table 2-5. Summary of the effect of thermal processing on muscle structure.

Types of meat	Processing parameters	Structural changes	References
Bovine *Pectoralis*	60 ℃ to 80 ℃; 15 to 60 min; cook vide, SV and atmospheric pressure cooking	Granular structure formed at 70 ℃; Less compact myofibre-sarcoplama structure observed in sous vide-cooked meat	García-Segovia et al. (2007)
Ovine *Longissimus dorsi*	60 ℃, 70 ℃, 80 ℃; 6, 12 and 24 h	Granulation and gelation of connective tissue at 60 ℃ and 70 ℃ respectively; Denser structure of meat cooked at 70 ℃ than 60 ℃ and 80 ℃; Visible gaps between muscle fibres in meat cooked at 60 ℃ and 80 ℃	Roldan et al. (2013)
Pork cheek	60 ℃ and 80 ℃; 5 and 12 h	Incomplete collagen fibre denaturation at 60 ℃; Complete collagen denaturation at 80 ℃	Del Pulgar et al. (2012)
Porcine *Longissimus dorsi*	53 ℃, 55 ℃, 57 ℃ and 59 ℃; 3 and 20 h	Reduction in muscle fibre diameter as cooking temperature and time increased	Christensen, Bertram, et al. (2011)
Bovine *Rectus abdominis*	100 ℃ for 15 to 60 min; 270 ℃ for 1 min	Lateral shrinkage, gap formation, granulation of myofibrils as well as detachment of myofibril from sarcolemma observed in all heated muscle; High temperature short time cooking caused severe gapping between muscle bundles	Astruc et al. (2010)
Bovine *Semitendinosus*	Internal temperature: 50 ℃, 60 ℃, 70 ℃, 80 ℃, 90 ℃, 100 ℃ and 121 ℃	Granulation of perimysium and sarcolemma started at 60 ℃; Gradual compression of muscle transversely when heated at 80 to 121 ℃	Palka (1999)
Bovine *Semitendinosus*	Internal temperature: 50 ℃, 60 ℃, 70 ℃, 80 ℃, 90 ℃, 100 ℃ and 121 ℃	Granulation when cooked at 70 to 100 ℃; Clear gap between fibres and endomysial tubes when cooked at 50 ℃; More compact structure as cooking temperature increased, especially at 100 ℃ and 121 ℃; Decreased muscle fibre diameter when heated at 60 to 121 ℃; Gradual decrease in sarcomere length when cooked at 50 to 121 ℃	Palka and Daun (1999)

Several studies have been conducted to examine the effect of heating on muscle protein digestibility. In most of the literature, protein digestibility was found to be affected by heating temperature and time, where protein digestibility decreased as heating temperature and time increased (**Table 2-6**) (Astruc, 2014b; Kaur et al., 2014; Oberli et al., 2015). These were explained by different extent of protein structure modification at different cooking temperatures. At lower heating temperature, meat protein is denatured and substrate cleavage sites are exposed, which favours the enzymatic action of digestive proteases. As the temperature further increases, the degree of protein denaturation increases and the exposure of hydrophobic residues leads to the formation of aggregates that hinder the contact of digestive enzyme to the cleavage sites. Hence, optimum cooking temperature and time should be explored in order to prepare meat products that are delicious, safe and yet nutritious. In contrast, Bax, Buffiere, et al. (2013) discovered that cooking temperature did not affect the overall protein digestibility but protein digestibility rate *in vivo*. Prodhan et al. (2020) reported that different cooking temperature and time did not affect the postprandial plasma amino acid concentrations in healthy adults.

Table 2-6. Summary of the effect of thermal processing on the protein digestibility of different muscles.

Types pf meat	Processing parameters	Comments on protein digestibility	References
Beef	90 ℃ for 30 min; 55 ℃ for 5 min	High temperature long time cooking reduced the true ileal protein digestibility of human subjects	Oberli et al. (2015)
Bovine *Longissimus dorsi*	100 ℃ for 10 and 30 min	Decrease in protein digestibility when meat was cooked especially for prolonged time, in terms of ninhydrin free amino nitrogen released during *in vitro* gastro-small intestinal digestion	Kaur et al. (2014)
Meat (not specified)	60 ℃ and 90 ℃	Decrease in peptides released (measured via spectrophotometric at 280 nm) during *in vitro* gastro-small intestinal digestion in the following order: raw meat > cooked meat at 60 ℃ > cooked meat at 90 ℃	Astruc (2014b)
Bovine *Longissimus dorsi*	Internal temperature: 60 ℃, 75 ℃ and 95 ℃ for 30 min	Protein true ileal digestibility was unaffected by cooking temperature *in* mini pigs.	Bax, Buffiere, et al. (2013)
Bovine *Semitendinosus*	Control: core temperature of 75 ℃; SV-cooked at 60 ℃ for 4.5 h and 10 h	Significantly higher free amino acids released from the sous vide-cooked meat after 180 min of *in vitro* gastro-small intestinal digestion	Bhat et al. (2020)
Beef rump steaks	Cooking of beef: Pan frying at 240 ℃ for 5 min; sous vide cooking at 80 ℃ for 6 h	No significant difference was observed in the postprandial plasma amino acid concentrations in adults consuming steak cooked by different methods	Prodhan et al. (2020)

Wen, Zhou, Li, et al. (2015), Filgueras et al. (2011) and Santé-Lhoutellier et al. (2008) observed that pepsin acted differently on meat cooked at different temperatures and times, which in turn affected the rate of protein digestibility. Cooking of meat induced protein oxidation which may reduce the accessibility of pepsins to their substrates. Aromatic amino acid residues are very susceptible to the attack of reactive oxygen species, resulting in the formation of peptide with α-ketoacyl derivatives on the N-terminal (Berlett & Stadtman, 1997). As pepsins cleave peptide bonds adjacent to aromatic amino acids, the

peptides with α-ketoacyl derivatives formed due to oxidation might block the access of pepsins, resulting in impaired digestibility. In addition, oxidation may also alter the protein tertiary structure, influencing proteolytic activity of pepsins. However, it was found that partial oxidation of proteins might enhance the cleavage of peptide bonds by proteases (Dean et al., 1997). Findings of the effect of cooking temperature and time on the rates of proteolysis by digestive enzymes are consolidated in **Table 2-7**.

The protein digestion kinetics of different muscles can also be evaluated through advanced microscopy techniques. When beef *Semitendinosus* cooked at 60 ℃ for 45 min was subjected to *in vitro* digestion, disruption of the A-bands, the I-bands and the Z-disks was observed after gastric digestion (Astruc, 2014b). Furthermore, there were swollen muscle cells and fading of extracellular space spotted at the peripheral of the sample, which might reduce the diffusion rate of the digestive juices into the sample as the transport of the solution mainly occurs in the extracellular space of the muscle. When the digested muscles were observed under fluorescence microscopy, the fluorescence intensity detected from the edge of the sample was lower than the core due to the swelling of the muscle cells and the degradation of the myofibrillar proteins. It was also observed that digestive enzymes acted randomly on raw bovine *Semitendinosus* whilst they acted from the edges towards the centre of cooked meat during *in vitro* digestion (Kaur et al., 2014). This showed that heating modifies myofibrillar structure which affects diffusion of digestive juices and enzymes into the meat substrate.

Table 2-7. Summary of the effect of thermal processing on the protein digestion rate of different muscles.

Types of meat	Processing parameters	Comments on protein digestibility rate	References
Bovine *Rectus abdominis*	100 ℃ for 5, 15, 30, and 45 min; 270 ℃ for 1 min	Decreased pepsin proteolysis rate of meat after cooking; No significant difference was observed in the pancreatic proteolysis rate between raw and cooked meats; The overall in *vitro* protein digestion rate was unaffected in fast cooked meat (100 ℃ for 5 min and 270 ℃ for 1 min) when compared to raw meat	Santé-Lhoutellier et al. (2008)
Porcine *Longissimus dorsi*	Internal temperature: 60 ℃, 65 ℃, 70 ℃ and 100 ℃	Decrease in *in vitro* peptic digestion rate as meat was cooked at 60 ℃; Rate was further decreased as temperature increased from 70 to 100 ℃; Decreased pancreatic proteolysis rate significantly only when meat was cooked at 100 ℃	Wen, Zhou, Li, et al. (2015)
Porcine *Longissimus dorsi*	70 ℃, 100 ℃ and 140 ℃ for 30 min	*In vitro* gastric proteolysis rate increased when meat was cooked at 70 ℃ and decreased as meat was cooked at increasing temperature of 100 ℃ and 140 ℃; Cooking at 70 ℃, 100 ℃ and 140 ℃ increased protein digestion rate in small intestine	Bax et al. (2012)
Rhea *Gastrocnemius pars*	100 ℃ for 30 min	Decreased gastric but increased small intestinal digestibility rate *in vitro* in cooked meat	Filgueras et al. (2011)
Bovine *Longissimus dorsi*	Internal temperature: 60 ℃, 75 ℃ and 95 ℃ for 30 min	Fastest ileal digestion rate in mini pigs for meat cooked at 75 ℃ for 30 min	Bax, Buffiere, et al. (2013)

2.8.3.2 Effect of SV cooking on meat quality

During the cooking process, deoxymyoglobin, metmyoglobin and oxymyoglobin undergo oxygenation, oxidation and reduction reactions, and the ratio between them determines the colour of final product (Liu & Chen, 2001). The colour of the cooked meat also depends on the rate in achieving the designated core temperature and the duration it is held at that temperature. Cooked meat tends to be redder when the rate of heating is faster and paler when it is held at specific temperature longer (Baldwin, 2012). Higher

cooking temperature results in more protein denaturation and aggregation, leading to an increase in light scattering (Christensen, Ertbjerg, et al., 2011).

Cooking results in heat denaturation of muscle protein which causes shrinkage of muscle fibres and the formation of gaps between myofibrils, leading to water redistribution and eventually water expulsion from the muscle (Palka & Daun, 1999; Straadt et al., 2007). As the water-binding proteins myosin and actin are denatured during cooking, muscle fibres lose their water holding capacity which causes water expulsion (Offer & Knight, 1988). A recent study conducted by Liu, Arner, et al. (2016) postulates that the gel formation of the sarcoplasmic proteins during the cooking process creates a network around myofibrils which binds water, preventing water release from the muscle. Many studies have shown the effect of different cooking temperature and time combinations on the cook loss of meat (Del Pulgar et al., 2012; García-Segovia et al., 2007; Palka & Daun, 1999). Cook loss has been reported to be more dependent on the cooking temperature and it does not necessarily increase during prolonged cooking (Warner et al., 2017).

Cooking induces the formation of reactive oxygen species, accelerating the protein oxidation in meats (Soladoye et al., 2015) The common signs of protein oxidation, such as the increased surface hydrophobicity and tryptophan degradation, protein aggregation, loss of thiol groups, increased carbonylation, and Schiff base generation, have been observed in heat-treated muscles (Gatellier et al., 2010; Mitra et al., 2018; Santé-Lhoutellier et al., 2008). The extent of protein oxidation is affected by both the cooking temperature and time. Higher cooking temperature and longer cooking time have been reported to increase the protein oxidation in porcine muscles (Mitra et al., 2018). Lipid oxidation plays a major role not only in the formation of the desirable flavour compounds during cooking of meat but is also responsible for the deterioration in meat product quality

during storage due the formation of rancid and off-flavours (Lorenzo & Domínguez, 2014). Although an increment in the total volatile compounds in meat was detected by Dominguez et al. (2014) after cooking, lower intensity of the desirable flavour compounds was observed by Christensen et al. (2012) in the low temperature-long time-cooked meat as the volatile compounds are usually generated at higher temperatures. Limited off-flavour as a result of lipid oxidation, was detected in the SV-cooked roast beef (59 or 62 ℃ for 5 h) stored in intact vacuum packages at 2 or 10 ℃ for 34 days (Hansen et al., 1995).

Improved tenderness of sous vide-cooked meat has been reported in various studies (Christensen, Ertbjerg, et al., 2011; Christensen et al., 2013; Christensen et al., 2000; García-Segovia et al., 2007; Suriaatmaja, 2013). The temperature of SV cooking should be set where it is high enough for collagen solubilisation and microbiological inactivation, yet has minimum myofibrillar shrinkage, to achieve optimum tenderisation action (Ruiz et al., 2013). When a tough meat cut is cooked at a temperature between 55 to 60 ℃ for 24 h, the tenderness is improved as the collagen is converted to gelatine and the myofibrillar proteins are hydrolysed by the endogenous enzymes which are yet to be denatured at this temperature (Bouton & Harris, 1981; Tornberg, 2005). During the cooking process, meat toughness increases at cooking temperatures between 40 ℃ and 50 ℃, decreases between 50 ℃ and 65 ℃, and increases again when the temperature exceeds 65 ℃ and continues to increase up to 80 ℃ (Baldwin, 2012; Tornberg, 2005) (**Figure 2-5**). The initial toughening might be due to the denaturation of myosin (Bejerholm et al., 2014). The improvement in meat tenderness at cooking temperature between 50 to 65 ℃ has been proposed to be due partial denaturation, shrinkage and solubilisation of collagen along with the formation of a gel from the sarcoplasmic proteins which filled the channels between fibre bundles, resulting in a decrease in elastic modulus

that requires lesser tensile stress to fracture the meat (Christensen et al., 2000; Tornberg, 2005). The denaturation and shrinkage of myofibrillar proteins, especially titin and actin, results in an increase in toughness when meat continues to be cooked at 65 to 80 ℃. It is recommended to SV cook beef, pork or lamb meat at temperatures between 58 ℃ and 63 ℃ for 10 to 48 h to achieve a tender product (Roldan et al., 2013).

Recently, multi-stage SV cooking has been explored for meat tenderisation. Uttaro et al. (2019) reported that the multi-stage SV cooking of beef at 39 ℃ for 1 h, followed by 49 ℃ for 1 h and 59 ℃ for a further 4 h resulted in a shear force reduction of bovine *Supraspinatus* (22.8 % reduction) and *Rectus femoris* (25.1 % reduction) muscles when compared to muscles cooked at 59 ℃ for 22 min (core temperature of 70 ℃) in a water bath. A study has been conducted by Ismail et al. (2019) to investigate the effect of single- and two-stage SV cooking at different temperatures for either 6 or 12 h. The WB shear force of the bovine *Semitendinosus* muscles were significantly affected by temperatures, cooking times, and the interaction between temperatures and cooking times. Meat samples which had undergone two-stage (45 ℃ + 60 ℃) SV cooking for 6 h had the lowest WB shear force when compared to other SV-cooked muscles, both single- and two-stage, at higher temperatures for longer times. In addition, two-stage (45 ℃ + 60 ℃) SV cooking of beef for 6 h also better retained the redness of the muscles and reduced cook loss.

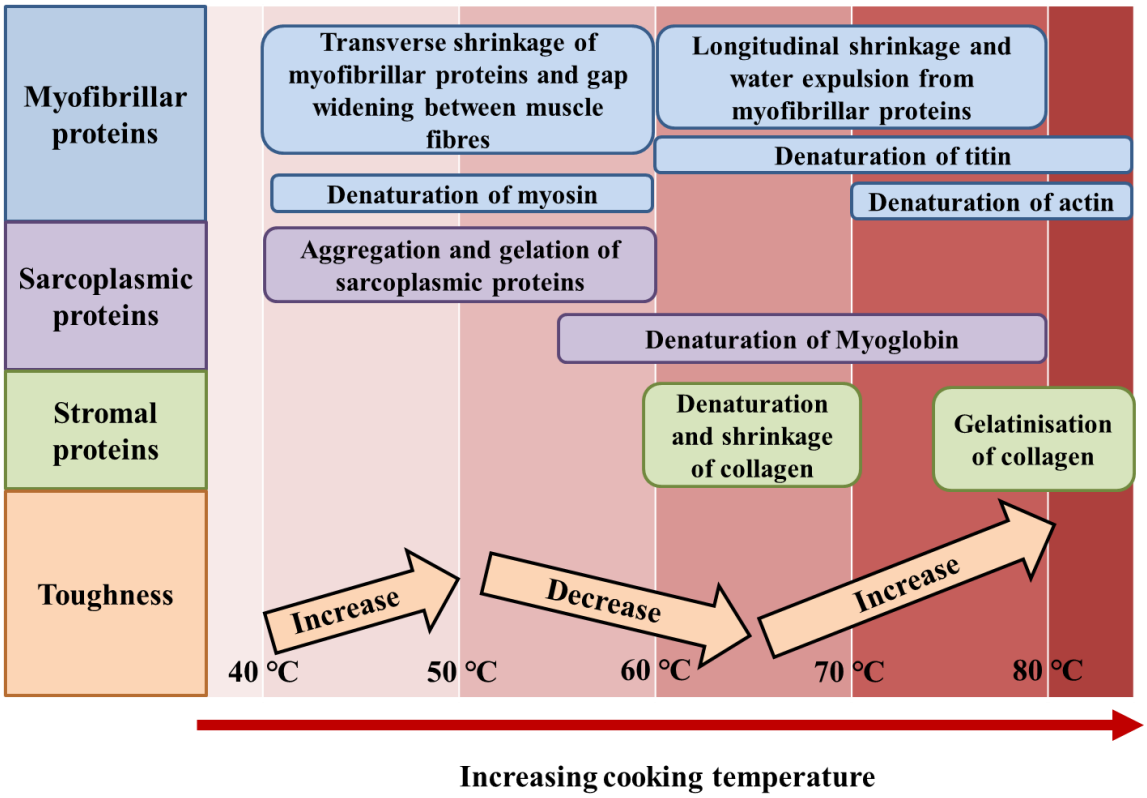

Figure 2-5. Schematic diagram showing the effect of different cooking temperatures on muscle proteins thermal stability and meat toughness.

2.8.4 Exogenous enzyme processing

Exogenous proteases have been applied in meat tenderisation for centuries (Sullivan & Calkins, 2010). The proteases papain (from papaya), ficin (from fig), bromelain (from pineapple), *Aspergillus oryzae* and *Bacillus subtilis* are approved as Generally Recognized as Safe (GRAS) food additives by the United States Food and Drug Administration (FDA). These enzymes have shown their abilities in improving actomyosin toughness and background toughness by hydrolysing myofibrillar proteins and connective tissue, respectively (Ashie et al., 2002; Ha et al., 2012; Ha et al., 2013; Miyada & Tappel, 1956). However, these enzymes have wide substrate specificity and they tend to break down most of the major bonds (peptide, amide, ester and thiol ester bonds) present in meat proteins (Bekhit, Hopkins, et al., 2014; Huff-Lonergan, 2014). Their excessive proteolytic action has the tendency of causing over-tenderisation leading

to mushy meat texture (Ashie et al., 2002; McKeith et al., 1994; Weir et al., 1958). This has led to the exploration of other enzyme alternatives such as actinidin (from kiwifruit), whose tenderising action is milder and more controlled (Aminlari et al., 2009; Christensen et al., 2009; Lewis & Luh, 1988).

Actinidin is a cysteine protease found in kiwifruit, which contains a free sulfhydryl group essential for its proteolytic activity (Baker, 1976; McDowall, 1970). Actinidin has a wide substrate specificity and it hydrolyses peptide bonds presented in proteins, simple esters and amides (Boland, 2013). It has a broader active pH range (pH 3 to 8) than other sulfhydryl proteases including papain, ficin and bromelain, and has a lower inactivation temperature of 60 °C (Boland, 2013; Huff-Lonergan, 2014; McDowall, 1970; Payne, 2009). *Actinidia deliciosa* cv. 'Hayward' (green kiwifruit) and *Actinidia chinenis* cv. 'SunGold' (gold kiwifruit) are two of the main commercial varieties where the former has approximately eight times higher proteolytic enzyme activity than the latter (Chao, 2016).

2.8.4.1 Effect of actinidin treatment on muscle protein profile, structure and digestibility

Application of actinidin on meat causes the degradation of myofibrillar proteins and solubilisation of connective tissue. Actinidin has an optimum pH from 3.0 to 4.5 for all myofibrillar proteins in addition to its ability to selectively hydrolyse MHC into fragments with smaller molecular mass at pH 5.5 to 8.0 (Nishiyama, 2007). Han et al. (2009) observed the formation of new peptides (with MW of 75 kDa, 28 to 32 kDa and 20 kDa) in the myofibrillar proteins extracted from kiwifruit juice-injected lamb *Longissimus dorsi*, demonstrating the breakdown of muscle protein. Ha et al. (2012) also reported the actinidin has an exceptional hydrolysis effect on the myofibrillar proteins compared to other commercial plant derived enzymes. Wada et al. (2004) discovered the

formation of collagen subunit α- and β-chain by incubating cattle Achilles tendon with commercial actinidin at both acidic (pH 3.3) and alkaline (pH 6.0) condition at 20 ℃, showing its ability in solubilising collagen without heating. Mostafaie et al. (2008) discovered that actinidin hydrolysed purified type I and II collagen at neutral and alkaline conditions at 37 ℃. Nevertheless, Toohey et al. (2011) proposed that actinidin prefers to act on myofibrillar proteins rather than stromal proteins based on their observation in the improvement of shear force but not compression force in bovine *Semimembranosus* treated with actinidin extract.

Actinidin treatment caused structural changes in meat. Zhu, Kaur, Staincliffe, et al. (2018) detected a significant destruction of muscles along the Z-disks and elongated sarcomeres with extended A-bands in actinidin-injected raw beef brisket. Endomysium damage, more desmin degradation and more heat-soluble collagen were observed in actinidin-treated porcine *Biceps femoris* muscles compared with the untreated muscles (Christensen et al., 2009).

The application of kiwifruit extract or actinidin has shown positive effects on meat protein digestibility. Zhu, Kaur, Staincliffe, et al. (2018) reported enhanced initial muscle protein degradation of actinidin-treated (5 % of 3 mg/ml commercial actinidin extract) SV-cooked (70 ℃ for 30 min) beef brisket under simulated gastric digestion. Other studies have shown the enhancement of meat digestion in the stomach by dietary actinidin (Kaur et al., 2010a, 2010b; Montoya et al., 2014; Rutherfurd et al., 2011), but the mechanisms of its action are still unclear.

2.8.4.2 Effect of actinidin treatment on meat quality

The application of kiwifruit juice and actinidin has been found to be effective in meat tenderisation. The shear force of actinidin-injected (5 % of 3 mg/ml commercial actinidin

solution) beef brisket SV-cooked at 70 ℃ for 30 min was significantly lower than the control water-injected meat, with no impact on the meat colour and cook loss (Zhu, Kaur, Staincliffe, et al., 2018). Kiwifruit juice infusion of lamb *Longissimus dorsi* muscles and hind legs has been reported to slow down the lipid oxidation during 21-day ageing and subsequent six-day of display when compared to the control (Bekhit et al., 2007). Pooona et al. (2019) also observed lower lipid oxidation products in the kiwifruit juice-marinated spent hen meat when compared to the control during storage. Both studies suggested that the lower the extent of lipid oxidation in kiwifruit juice-treated meat could be due to the presence of natural antioxidants in the kiwifruit juice. No information on the effect of actinidin treatment on protein oxidation of meats is available in the literature. Lamb *Longissimus dorsi* muscles injected with green kiwifruit juice pre-rigor were significantly lower in shear force than non-injected control after six days of infusion due to degradation of myofibrillar proteins in the former (Han et al., 2009). There was a 10 % decrease in shear force of beef after incubation with actinidin at 37 ℃ for two hours (Aminlari et al., 2009). It was also found that after two days of actinidin injections, treated porcine *Biceps femoris* had similar WB shear force as control untreated muscles stored for five or nine days (Christensen et al., 2009). Actinidin injection (0.5 mg/100 g muscle) of pork and rabbit *Longissimus* muscles, incubation for 3 h at room temperature, followed by cooking at 75 ℃ for 30 min, resulted in more than 50 % shear force reduction of the muscles (Zhang et al., 2017).

2.9 Characterisation of muscle protein structure and digestibility

2.9.1 Digestion Models

In order to observe and understand the fate and dynamics of food being broken down in the gastro-intestinal tract, several models have been developed to simulate digestion

process, executed either *in vivo* or *in vitro* (Astruc, 2014b; Dyer & Grosvenor, 2014). *In vivo* models are the gold standard and are considered more precise and accurate systems involving either animal or human clinical studies. However, the process is time consuming, expensive, complex and must be conducted ethically. Hence it is often performed at the final stage of the studies to validate the observations or hypotheses from *in vitro* models. In contrast, *in vitro* models are more commonly being adopted as they are relatively inexpensive, rapid and simple. The current models vary in the composition of the simulated digestive fluids, the physiological conditions and the residence time during digestion. Simulated digestion can be performed either in a simple static model or a more complex dynamic model, focusing either on one or multiple compartments of the digestive tracts.

In vitro digestion has been utilised to determine the digestibility of macronutrients such as carbohydrates, proteins and fats as well as the accessibility of materials in a delivery system (Hur et al., 2011; Minekus et al., 2014). There are different models described in the literature which differ across different research groups. The source and activity of digestive enzymes, the formulation of simulated digestive juices, the ratio of food to digestive enzymes, the physiological conditions, and the time of digestion often vary in various studies. These variations lead to difficulty in comparison of the results among different studies.

A static *in vitro* digestion is a system where the ratio of tested food to simulated digestive juices and enzymes, as well the physiological environment such as pH and ionic strength remain constant throughout the study (Minekus et al., 2014). In order to provide a guideline on setting up a static *in vitro* digestion model, an internationally agreed protocol was proposed by INFOGEST, an international network joined by scientists working on

food digestion, which outlined the experimental parameters and conditions that most closely mimic human physiology and is applicable to various research topics (Mackie & Rigby, 2015; Minekus et al., 2014). The protocol is made up of three major phases, namely oral, gastric and intestinal digestion. Each of these digestion phases is conducted with the addition of simulated digestive juices of different compositions, as depicted in **Table 2-8**.

Table 2-8. Recommended concentrations of electrolytes for use in simulated digestive juices based on human *in vivo* data, as suggested by Minekus et al. (2014).

Components	Concentration (mmol/L)		
	Simulated salivary fluid (SSF)	Simulated gastric fluid (SGF)	Simulated intestinal fluid (SIF)
K^+	18.8	7.8	7.6
Na^+	13.6	72.2	123.4
Cl^-	19.5	70.2	55.5
$H_2PO_4^-$	3.7	0.9	0.8
HCO_3^-, CO_3^{2-}	13.7	25.5	85
Mg^{2+}	0.15	0.1	0.33
NH_4^+	0.12	1.0	-
Ca^{2+}	1.5	0.15	0.6

The proposed sample to simulated digestive fluid ratio, enzyme activity, simulated physiological environment and digestion time are illustrated in **Figure 2-6**. The summarised protocols for oral processing, gastric digestion and small-intestinal digestion for solid foods are as follows. Solid food is first chopped into smaller particles and is mixed with simulated salivary fluid (SSF) (1:1) to create a thin pasty bolus. A mastication experiment conducted by Jalabert-Malbos et al. (2007) found the mean particle size of cooked meat and ham were near to 1.5 mm with some exceeding 4 mm and bolus particle size was generally less than 2 mm before swallowing. To initiate oral digestion, salivary α-amylase (75 U/mL in final mixture) is added and the pH is maintained at 7. Incubation time of 2 min is recommended for food that contains carbohydrates that are hydrolysable by α-amylase. After that, the food bolus is mixed with simulated gastric fluid (SGF) (1:1)

followed by the addition of pepsin (2000 U/mL in final mixture) and pH adjustment to 3 to commerce gastric digestion. Unlike most of the reports (Escudero et al., 2010; Kaur et al., 2014; Wen, Zhou, Song, et al., 2015), pH 3 is recommended after taking into account the secretion of hydrochloric acid, the buffering effect of ingested food and the active pH for pepsin (pH 2 to 4). Based on the first static *in vitro* digestion protocol (INFOGEST method 1.0), gastric lipase was not added due to the unavailability of a commercial gastric lipase that has comparable properties to human gastric lipase (Minekus et al., 2014). However, in the latest protocol published in year 2019 (INFOGEST 2.0 method), rabbit gastric extract which contains both gastric pepsin and gastric lipase in a ratio that resembles human gastric fluid was introduced to the protocol (Brodkorb et al., 2019). The duration of gastric digestion varies between individuals as well the nature of the ingested food and two hours were suggested to cater for a wide range of foods. After two hours of gastric digestion, simulated intestinal fluid (SIF) is added into the chyme mixture (1:1) and the pH is adjusted to 7. This pH is recommended based on a combination effect of the initial pH in the duodenum, the secretion of bicarbonate, the gastric emptying rate as well as the nature of the meals ingested. Finally, pancreatin (based on trypsin activity of 100 U/mL in final mixture) and bile salt (10 mM in final mixture) are added and the sample is digested for a further two hours. The whole process is carried out at 37 °C. Both simulated gastric and small intestinal digestion models employ either a stirrer, a shaker or an impeller to ensure good mixing of digestive enzymes and substrates and to achieve and maintain constant digestion pH during each steps of the digestion. However, these agitation methods do not reflect the mechanical action *in vivo*. Digests are taken out at designated time of interest and are suggested to be either snap frozen in liquid nitrogen or have protease inhibitor added to them before snap freezing to prevent further enzymatic

hydrolysis. It has also been advised to conduct the simulated digestion in individual tubes or reactors for different designated time points.

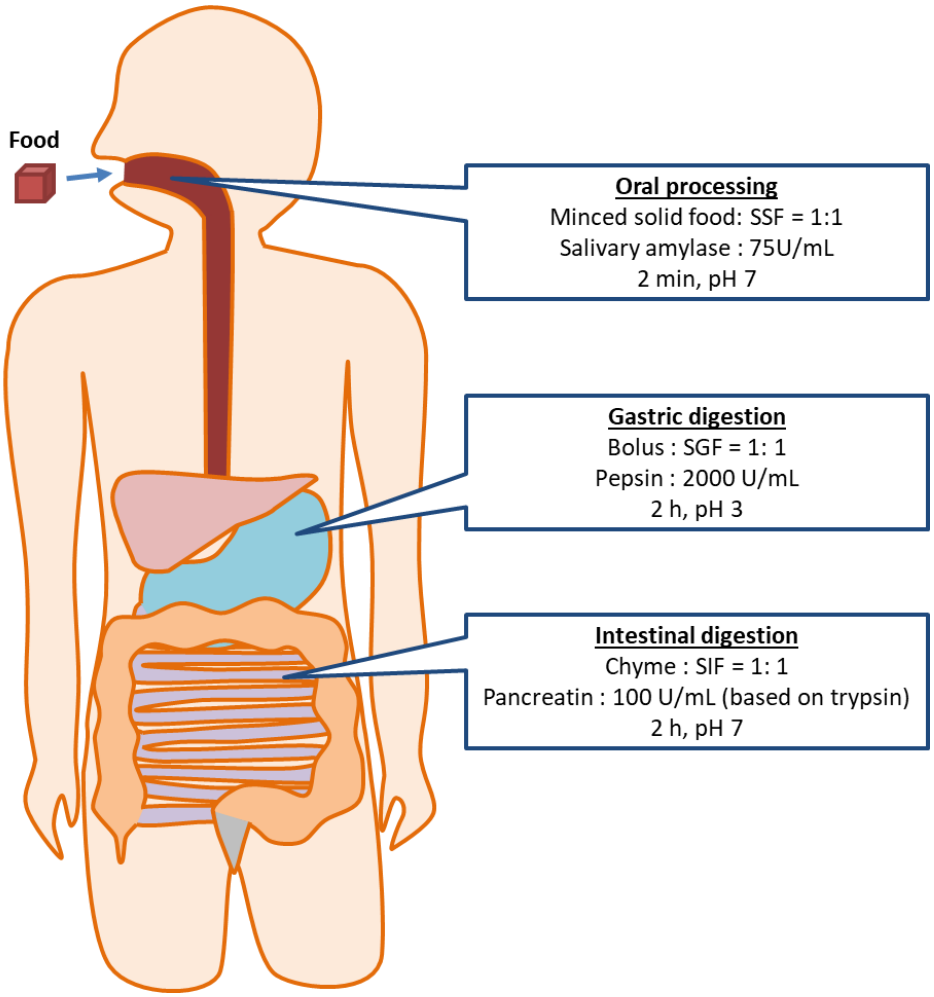

Figure 2-6. Simulated gastro-small intestinal digestion conditions consolidated by Minekus et al. (2014) and Mackie and Rigby (2015).

Although the INFOGEST consensus paper proposes a protocol that is close to human physiological conditions, amendments are still necessary to appropriately fit the current research objectives and questions. For instance, the suggested digestive enzyme concentration might be too high to study the dynamics of food hydrolysis over time. Johnston and Coon (1979) reported a decrease in pepsin concentration increases the test sensitivity during protein digestion. Distinct differences in protein digestibility were detected in animal proteins digested in a lower pepsin concentration (0.002 %) but not in a high pepsin concentration (0.2 %). Different digestive enzyme concentrations for

muscle-based foods digestion in the literature are summarised in **Table 2-9**. Most of the studies adopted 2.5 to 10 U/mg, 6.6 U/mg, 0.05 to 0.33 U/mg and 0.01 to 0.04 USP/mg meat protein as enzyme concentrations of pepsin, trypsin, chymotrypsin and pancreatin, respectively.

Table 2-9. Summary of digestive enzyme activities and digestion times for gastric and small intestinal phases of *in vitro* methods to study meat digestion from the literature.

Digestive enzyme concentrations and digestion duration		References
Gastric phase	**Intestinal phase**	
Pepsin: 8 U/mg protein **1 h*	Pancreatin: 0.04 USP /mg protein **2 h*	Kaur et al. (2016); Kaur et al. (2014)
Pepsin: 2.5 U/mg protein **2 h*	Pancreatin: 0.01 USP /mg protein **2 h*	Kapsokefalou and Miller (1991); Argyri et al. (2009)
Pepsin: 5 U/mg protein **1 h*	Trypsin: 6.6 U/mg protein α-chymotrypsin: 0.33 U/mg protein **0.5 h*	Santé-Lhoutellier et al. (2008); Filgueras et al. (2011)
Pepsin: 5 U/mg protein **1 h*	Trypsin: 5 U/mg protein α-chymotrypsin: 0.05 U/mg protein **1 h*	Liu and Xiong (2000)
Pepsin: 8 U/mg meat **2 h*	Trypsin: 20 U/mg meat **2 h*	Wen, Zhou, Song, et al. (2015)
Pepsin: 10 U/mg protein ** 1.5 to 2 h*	Trypsin: 6.55 U/mg protein α-chymotrypsin: 0.33 U/mg protein **4 h*	Bax, Sayd, et al. (2013); Bax et al. (2012)
Pepsin: 10 U/mg protein **0.5 h*	Trypsin: 2.5 U/mg protein α-chymotrypsin: 1 U/mg protein **0.5 h*	Sun et al. (2011)
Pepsin: 25 U/mg protein **2 h*	Trypsin: 6.55 U/mg protein α-chymotrypsin: 0.33 U/mg protein **2 h 10 min*	Gatellier and Sante-Lhoutellier (2009)
Pepsin: 330 U/mg protein **1 h*	Trypsin: 200 U/mg protein α-chymotrypsin: 40 U/mg protein **4 h*	Huang et al. (2010)

*digestion time

2.9.2 Characterisation of muscle protein digestibility

Throughout digestion, food breaks down into components with varying MW (Dyer & Grosvenor, 2014). The products generated during protein digestion largely depend on the structural properties of food, including protein solubility and accessibility of digestive

enzymes. These resultant components can be analysed and evaluated using polyacrylamide gel electrophoresis (Kaur et al., 2016; Liu & Xiong, 2000) and chemical analyses such as ninhydrin-reactive amino nitrogen test (Kaur et al., 2016; Kaur et al., 2014) and O-phthalaldehyde (OPA) assay (Yi et al., 2016).

Sodium dodecyl sulfate polyacrylamide gel electrophoresis (SDS-PAGE) has been broadly used in muscle protein analysis. Tricine SDS-PAGE is efficient for the separation of low MW proteins or fragmented peptides produced from enzymatic hydrolysis with high resolution (Haider et al., 2012). Prior to electrophoresis, the meat protein extract is first dissolved in sodium dodecyl sulfate (SDS) to break down protein to polypeptide subunit level, with the addition of β-mercaptoethanol to create reducing conditions and is boiled for 5 min (Greaser, 2008; Toldra & Reig, 2004). Electrophoresis is run by loading the protein extract at the top of either a homogeneous acrylamide gel or a concentration-gradient gel (usually 5 to 15 % polyacrylamide) or a pH-gradient gel. When a current is applied to the gel, proteins present in the sample are separated by migrating through the gel at different speeds, based on their molecular size. Proteins with small molecular size move faster than those with larger molecular size. The gel is often stained with Coomassie Blue after the electrophoresis and protein quantification is done by scanning the gel using a densitometer. The concentration of protein loaded into the gels affects the intensity of each protein band and hence care has to be taken during sample preparation and loading. It is recommended to run a standard on the same gel to serve as a control or perform direct sample comparison between each other. Tricine SDS-PAGE is very useful for separating peptides present in meat digest, ranging from 1 to 30 kDa, for further analysis using mass spectrometry (Toldra et al., 2008).

The degree of hydrolysis of meat protein in the digests can be determined by quantification of the level of free amino nitrogen using a ninhydrin assay (Chalabi et al., 2014). Ninhydrin reacts with primary amino groups (α-NH_2) to form a purple chromophore, known as Ruhemann's purple, when heated to boiling (Friedman, 2004; Work & Rurdon, 1981). The resultant coloured mixture is then measured at the absorption band of 570 nm using a spectrophotometer. A calibration curve has to be prepared using an amino acid as standard. The assay is capable of detecting the amino acids and peptides as most of the peptides have α-NH_2 after the cleavage of peptide bonds, except peptides with N-terminal proline or N-terminal hydroxyproline groups. However, this assay is not recommended for samples containing ammonia or primary amines as they readily react with ninhydrin to form Ruhemann's purple.

The degree of proteolysis can also be determined using an o-phthalaldehyde (OPA) fluorometric assay (Church et al., 1985; Rutherfurd, 2010). O-phthalaldehyde reacts with the primary amines in amino acids, peptides, and proteins, at the presence of thiol groups, forming OPA-amine product which is highly fluorescent (excitation wavelength of 350 nm; emission wavelength of 450 nm). This assay is not suitable for samples rich in proline, cysteine, and lysine. Proline and cysteine have poor reactivity with OPA, resulting in underestimation. In contrast, OPA can interfere with the side chains of lysine, leading to overestimation.

2.9.3 Characterisation of muscle structure

Microscopy and imaging techniques have been used to evaluate food structure. Among them, optical microscopy and electron microscopy are the most common techniques practised in the food industry and research (Kaláb et al., 1995; Pospiech et al., 2011). Other special techniques including confocal laser scanning microscopy, atomic force

microscopy, and others are adopted. These techniques enable the detection and characterisation of individual components in food (Sifre et al., 2013).

Optical microscopy such as a bright field microscopy and fluorescence microscopy is the oldest and the most versatile technique used in food microstructure analysis (Kaláb et al., 1995; Quiles et al., 2008). When observing a sample under a bright field microscope, a light source is transmitted through the condenser, the sample specimen, and the objective, forming a magnified image which is then further magnified by the eyepiece. In general, dyes and stains are used to enhance the image contrast especially in muscle cells (Gunning, 2013). As muscle cells are composed of water enclosed within a phospholipid bilayer, relatively similar refractive index of muscle cell and water renders them difficult to observe clearly under light microscope.

Electron microscopes such as transmission electron microscopes (TEM) and scanning electron microscopes (SEM) have been used to examine meat ultrastructure (Astruc et al., 2010; Bolumar et al., 2014; Kaur et al., 2016; Macfarlane, McKenzie, et al., 1986) due to their higher magnification properties (Pospiech et al., 2011). In fact, the operating principle of electron microscope is similar to a transmitted light microscope. An electron microscope creates images by generating a beam of electrons using an electron gun without the use of light (Groves & Parker, 2013).

In TEM, the electron beam generated is focused by electrostatic and electromagnetic lenses and are directed through the column of microscope to a very thinly cut specimen and are finally transmitted through the specimen to produce an image on a phosphorescent screen (Groves & Parker, 2013; Quiles et al., 2008). Generally, the sample preparation of TEM involves primary chemical fixation, washing, dehydration, resin embedding and ultra-thin sectioning (70 to 100 nm) using an ultra-microtome, which is very tedious and

time consuming. Staining using heavy metal stains such as osmium tetroxide, uranyl acetate and lead citrate is typically performed to bind the components and to produce good image contrast. Samples are usually fixed in glutaraldehyde, a primary chemical fixative with improved fixation rate, followed by post fixation in osmium tetroxide. This technique is very useful in characterising the banding of muscle fibres.

Histological staining is a microscopy technique practised in the assessment of the structure of animals and plants by observing the stained section under light or electron microscope (Alturkistani et al., 2015). This technique has been used extensively in forensic, autopsy, diagnosis and medical studies traditionally. Recently, food scientists have adopted histological staining in examining the structure and the individual components in muscle-based foods (Astruc, 2014b; Dubost et al., 2013; Kaur et al., 2016). For instance, toluidine blue and haematoxylin-eosin staining are the basic staining methods used in meat sample analysis, which stain the meat in blue and red respectively (Pospiech et al., 2011). Picro-Sirius red staining has been used to localise collagen in muscle (Flint & Pickering, 1984; Lattouf et al., 2014). Cryofixation of muscle sample in liquid nitrogen (−196 ℃) or chilled isopentane (−160 ℃) is normally performed prior to cryosectioning (**Figure 2-7**) (Astruc et al., 2010; Kaur et al., 2016; Realini et al., 2013).

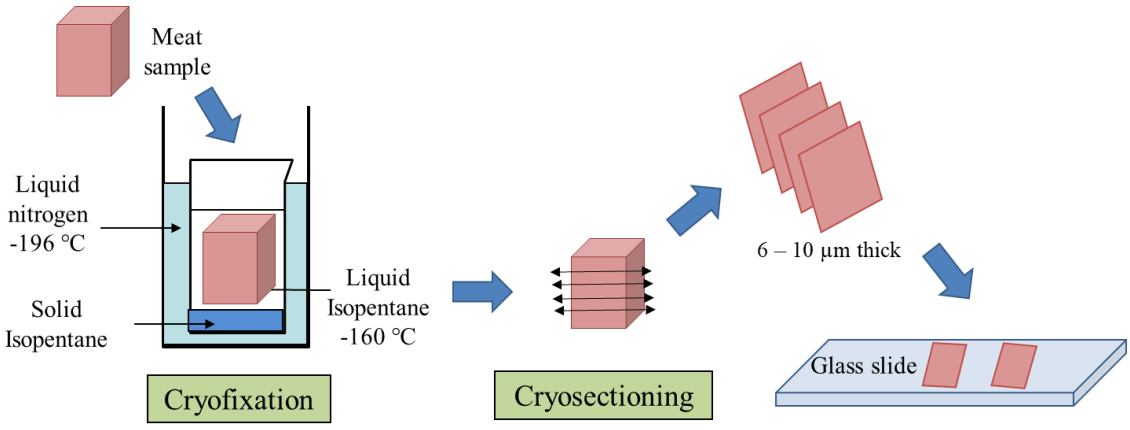

Figure 2-7. Schematic diagram showing the process of cryofixation and cryosectioning.

Recently, the combination of microscopy techniques with spectroscopy, such as Fourier-transform infrared (FT-IR) has been reported to study the chemical composition of microscopic domains in food (Wellner, 2013). This imaging technique creates a hyperspectral data cube which is made up of spectra obtained at multiple points in a grid pattern overlaid on the sample section. It has been used to study beef and pork muscle tissue treated using different processing methods such as cooking, salting and ageing (Böcker et al., 2007; Kirschner et al., 2004).

Fourier-transform infrared microspectroscopy is set up by connecting an infrared microscope to an FT-IR spectrometer (Wellner, 2013; You & Cheng, 2014). There are three main modes that are available to perform FT-IR microspectrometry, which are the transmission, reflection, and attenuated total reflection (ATR) modes. When performing FT-IR microspectroscopy, IR light is passed through apertures into a Michelson interferometer which modulates and directs IR light to the microscope optics that is focused onto the sample. The transmitted or reflected IR light is then collected into the IR detector and the measured intensity is converted into a single beam spectrum with a fast Fourier transform. The resultant spectrum is the ratio between two single beam spectra of sample and blank (without sample). Polar groups, such as hydroxyl group and carbonyl group, have strong IR absorption. As such, dry sample sections are preferable when water is not of interest in the analysis. Sample drying prevents strong water absorption during the analysis, enabling a more accurate and precise characterisation of proteins, carbohydrates and lipids in the food samples. It is suggested that high moisture content samples are cut to 5 to 10 μm thick to aid in sample drying before the analysis. Dry cutting or cryosectioning are also recommended. As infrared absorbs signal from glass, the sections have to be mounted on slides made of CaF_2 or BaF_2 crystals, which are IR-transparent, when using transmission mode. Paraffin or polyethylene glycol for

sample fixing or embedding should be avoided to prevent overlapping of the band of these materials and the samples.

Microscopic techniques provide both qualitative and quantitative description of the food structure (Pospiech et al., 2011). Images created can be analysed using a computer program by identifying the selected component of interest and measuring the area of the selected section. It is recommended to conduct structural analysis using different methods to validate the accuracy of the results as the structure of the samples might be altered during sample preparation (Kaláb et al., 1995).

2.9.4 Characterisation of the diffusion of enzymes into meat matrix

In order to assess the penetration of the digestive enzymes into muscle during digestion, Astruc (2014b) adopted immunohistofluorescence techniques to identify the presence and spatial distribution of pepsin in digested meat samples. In short, the digested sample was treated with a primary antibody, pepsin antibody, washed, followed by depositing a secondary antibody containing a fluorescent marker onto the samples. The antigen-antibody (Ag/Ab) complex formed was observed under a fluorescence microscope. They detected that pepsin was mainly found in perimysium and endomysium and concluded that digestive juices first diffused through the extracellular spaces and subsequently into intracellular spaces of the muscle. However, there might be some inaccuracy in the observation as the fluorescent signal may be corrupted by the collagen autofluorescence and some non-specific interactions of the antibodies induced by the muscle structure modified by acidic digestive juices. In addition, the activity of the pepsin located in the digested sample is yet to be verified. The method could potentially be utilised to locate the exogenous enzymes used for meat tenderisation in the meat matrix, such as actinidin.

2.10 Gaps in the literature

The literature survey has provided a good insight into the effect of different processing techniques on meat structure. However, there are gaps in the current literature which require further investigation. Firstly, little information is available on the effect of different meat processing technologies, alone or in combination, on muscle protein digestibility. For instance, no studies have been performed on the protein digestibility of SW-treated meat. Limited studies on the protein digestibility of PEF-treated meat have been reported which focused mostly on biochemical approaches (Alahakoon et al., 2019; Bhat, Morton, et al., 2019b; Bhat, Morton, Mason, Jayawardena, et al., 2019). Information on other aspects such as the structural changes in meat during digestion is not available. The relationship between process-modified muscle structure and protein digestibility is underexplored. In addition, limited research has been done to investigate the action of proteases on muscle structure (Astruc, 2014b). The action and diffusion of enzymes such as exogenous enzymes (e.g. actinidin) used for meat tenderisation on meat microstructure are not well understood. Lastly, it is speculated that the enhanced proteolysis of PEF-treated meat during ageing is due to the early activation of calpains, and/or the action of lysosomal enzymes released due to the permeabilisation of muscle cells by PEF (Alahakoon et al., 2016; Bhat et al., 2018a). The former has been verified in recent studies by Bhat, Morton, Mason, Mungure, et al. (2019) and Bhat, Morton, et al. (2019a) but no information is available on the effect of PEF on lysosomal proteases such as cathepsins in meat. Thus, further studies are needed to investigate these gaps.

Chapter 3 [2]Effect of pulsed electric fields (PEF) on the ultrastructure and *in vitro* protein digestibility of bovine *Longissimus thoracis*

3.1 Introduction

Pulsed electric field processing is a food processing technique that involves applying short electric pulses to food products (Toepfl et al., 2007a). This process causes electroporation of the cell membrane when the induced transmembrane potential exceeds a critical value of 1 Volt. Pulsed electric field treatment has been applied with a high intensity for food preservation (20 to 80 kV/cm) (Castro et al., 1993; Toepfl et al., 2007b) and with a lower-intensity for non-preservative applications, such as meat tenderisation (O'Dowd et al., 2013). Low-intensity PEF treatment causes a modification of food structure, which could improve the texture and functional properties of meat (Arroyo, Eslami, et al., 2015). For instance, PEF has been reported to improve the tenderness of cold-boned bovine *Longissimus lumborum* muscles (0.31 to 0.56 kV/cm, 20, 50 and 90 Hz) (Suwandy et al., 2015d) and frozen-thawed beef *Semitendinosus* muscles (1.4 kV/cm, 50 Hz, 20 µs) (Faridnia et al., 2015).

As discussed in section **2.8.1.1**, low-intensity PEF treatment induces changes in the structure of myofibrillar foods. Pulsed electric field-treated muscles have been found to be more porous and smaller in cell size than control untreated meat (Faridnia et al., 2014; Gudmundsson & Hafsteinsson, 2001). Gap formation and fragmentation of myofibrils were detected in PEF-treated samples (Gudmundsson & Hafsteinsson, 2001; O'Dowd et al., 2013). These changes in the physical properties of meat post-PEF processing may affect the accessibility of digestive enzymes which in turn influence the protein digestibility of meat (Astruc, 2014b; Carmody & Wrangham, 2009). However, to date, there is little information in the literature on how PEF treatment affects the protein

[2]This chapter has been published as **Chian, F. M.**, Kaur, L., Oey, I., Astruc, T., Hodgkinson, S., & Boland, M. (2019). Effect of pulsed electric fields (PEF) on the ultrastructure and *in vitro* protein digestibility of bovine *Longissimus thoracis*. *LWT, 103*, 253-259. https://doi.org/10.1016/j.lwt.2019.01.005

digestibility, especially in regards to meat structure. Although PEF treatment has been reported to improve the *in vitro* protein digestibility of raw cold-boned bovine *Bicep femoris* (Bhat et al., 2018c) and deer *Longissimus dorsi* (Bhat, Morton, Mason, Bekhit, et al., 2019), no information on the structural changes in meat during simulated digestion has been provided. Investigation of the structural changes induced by processing and subsequent simulated digestion will provide some understanding on the accessibility of digestive enzymes to the PEF-treated meat.

This experiment aims to investigate the effect of low-intensity PEF treatment on the protein digestibility of beef muscle using an *in vitro* digestion model. The ultrastructure of beef muscles was also examined after PEF processing and after subsequent simulated digestion process. As this chapter is focusing on PEF treatment alone (with no further processing such as cooking), ribeye scotch fillet was chosen as the muscle cut for investigation. Tender beef cuts, such as the ribeye scotch fillet, are low in connective tissue and are normally used in raw beef dishes such as beef carpaccio and beef tartare (Bronfen, 2019).

3.2 Materials and methods

3.2.1 Pulsed electric field treatment of bovine *Longissimus thoracis* muscles

Two days postmortem Hereford heifer (< 18 months old) whole ribeye scotch fillets (*Longissimus thoracis*) were obtained from a local butcher (The Mad Butcher, Dunedin, New Zealand). Conductivities of the fillets were 6 ± 3 mS/cm, measured at five different positions using a handheld meat conductometer (LF-STAR, R. Mathäus, Nobitz, Germany). Pulsed electric field treatment was carried out on meat cut of about 65 g based on the method of Alahakoon et al. (2018a) using a pilot scale PEF system (Elcrack-HVP 5, DIL, Quakenbruck, Germany) with a batch-mode configuration. The samples were

placed in the treatment chamber in such a way that the muscle fibre direction was perpendicular to the electric current applied during the treatment, as stated in most of the literature (Arroyo & Lyng, 2017). The treatment was performed using an electric field strength of 1.00 to 1.25 kV/cm at two different pulse numbers of 500 and 2000 (hereafter referred to as PN500 and PN2000 respectively) to create specific energies of 48 ± 5 kJ/kg and 178 ± 11 kJ/kg respectively, at a constant pulse width of 20 µs and a frequency of 50 Hz. During the treatment, pulse shape (square wave bipolar) was observed on-line with an oscilloscope (Model UT2025C, Uni-Trend Group Ltd., Hong Kong, China). The processing parameters were chosen after studying the PEF experiments on meat tenderisation application in the literature (Alahakoon et al., 2017; Faridnia et al., 2014; Faridnia et al., 2016). The specific input energy of the treatment was calculated using equation below:

Specific energy input (kJ/kg) = pulse number x pulse energy/sample weight --**Eq. (3-1)**

The sampling of the control (thereafter referred to as C500 and C2000 respectively) and PEF-treated samples of the meat cut is illustrated in **Figure 3-1**. The samples were vacuum-packed and were stored at -20 ℃ for further analysis.

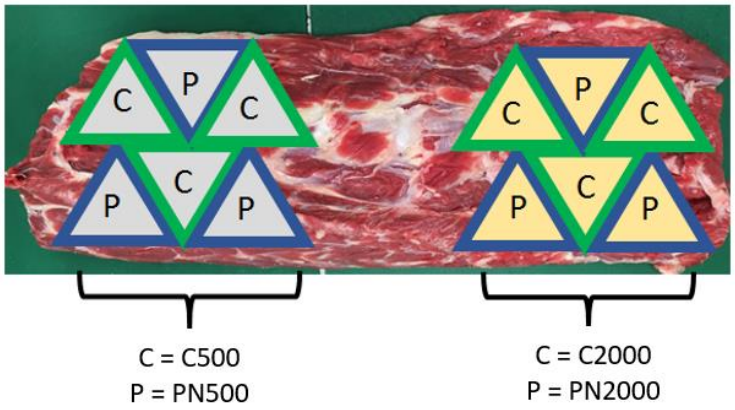

Figure 3-1. Meat sampling position of the PEF-treated samples (P) with different pulse numbers (left: pulse number 500 (PN500); right: pulse number 2000 (PN2000)) and their control untreated counterpart (C) (left: C500; right: C2000) on the meat cut *Longissimus thoracis*.
The sampling was conducted by assigning the control and PEF-treated meat adjacent to each other to prevent inconsistency results due to inhomogeneity of meat. The meat was cut into triangular pieces (6 cm in height, 4 cm in width, and 6 cm in length) of about 65 g for PEF processing.

3.2.2 pH, moisture content and colour measurements

The frozen samples were thawed at 4 ℃ for 16 h before the analysis. The pH of the control and PEF-treated meat were measured as described by Faridnia et al. (2014) with some modifications using a pH meter (S20 SevenEasy™, Mettler-Toledo Limited, New Zealand) at 25 ℃. The measurement was performed after homogenising 5 g of the sample with 50 mL of Milli-Q water at 20500 rpm for 30 s using an overhead homogeniser (DIAX 600, Heidolph Instrument, Germany). The moisture content of the samples was determined using the AOAC method 950.46 by drying approximately 2 g of finely chopped samples in an oven at 102 ℃ for 16 h (Lawrence, 2010). The moisture content was calculated by subtracting the total weight of sample and drying dish before and after drying. The drying dishes were cooled in desiccator before weighing. The pH and moisture content analyses were performed in triplicate. The colour of the samples was measured at 12 different individual measurement points using a handheld Chroma meter (CR200, Konica Minolta, Tokyo, Japan) with a 'D-65' light source and 10 ° observer setting (Brewer et al., 2006). Prior to the measurement, the samples were allowed to bloom at 4 ℃ for approximately 30 min. The average value of L^* (black-white), a^* (red-

green), *b** (blue-yellow) for each sample was determined from 12 individual measurements on the surface of each individual triangular-shaped sample.

3.2.3 Differential Scanning Calorimetry (DSC)

The protein thermal profiles of the samples were determined using the method of Torrescano et al. (2003) with minor modifications of sample weight and heating temperature range. The analysis was conducted using a differential scanning calorimeter (Q2000, TA instruments, New Castle, DE, USA) by heating both the samples (approximately 20 mg of minced samples) and reference empty pans from 20 to 100 ℃ at a rate of 2 ℃/min. The thermal curves were analysed using the associated software (TA Universal Analysis, TA Instruments, New Castle, DE, USA). DSC measurements were done in triplicate.

3.2.4 Protein digestibility

3.2.4.1 In vitro digestion

The *in vitro* digestion protocol was modified based on the method described by Kaur et al. (2016) and Minekus et al. (2014). The protein concentration of the digestive enzymes was set based on the findings of the literature review as discussed in section **2.9.1**. Four grams of samples (approximately 140 mg of nitrogen) were chopped into pieces of about 2 mm. Simulated oral processing was initiated by mixing the chopped samples with 4 mL of simulated salivary fluid (SSF) containing α-amylase (10025, Sigma-Aldrich, Saint Louis, MO, USA) (75 U/mL activity in the final mixture) for 2 min at pH 7 ± 0.1. Next, 16 mL of simulated gastric fluid (SGF) containing pepsin (P7125, Sigma-Aldrich, Saint Louis, MO, USA) (2.5 U/mg protein of meat) was added to the simulated bolus and the pH was adjusted to 3.0 ± 0.1 using 6 M hydrochloride acid (HCl) to mimic human gastric digestion. Five glass balls (3 - 5 mm) were used for sample maceration in each digestion

reactor. After an hour of gastric digestion, small intestinal digestion was initiated by adding 21 mL of simulated intestinal fluid (SIF) with pancreatin (4 x USP, P1750, Sigma-Aldrich, Saint Louis, MO, USA) (enzyme: substrate = 1: 100) and 3 mL of bile extract (10 mM in final mixture) (B8631, Sigma-Aldrich, Saint Louis, MO, USA) into the reactor. The digestion was carried out for a further 120 min at pH 7.0 ± 0.1, adjusting using 1 M sodium hydroxide. The simulated digestion was carried out at 37 ℃. Samplings were conducted at 0, 30 and 60 min of gastric digestion (cumulative digestion time of 2, 32 and 62 min) and further 60 and 120 min of small intestinal digestion (cumulative digestion time of 122 and 182 min). After sampling, the digests were immersed immediately in an ice bath to stop the enzyme activity and the samples were stored at -20 ℃ for further analysis. The information of the digestive enzyme types and concentrations, as well as the sampling time points in each digestion phase (oral, gastric and small intestinal phase) is summarised in **Table 3-1**.

Table 3-1. Digestive enzyme types and concentrations, digestion duration and sampling time points for each digestion phase (oral, gastric and small intestinal) for the *in vitro* digestion of the control untreated (C500 and C2000) and PEF-treated samples ((PN500, 48 ± 5 kJ/kg) and (PN2000, 178 ± 11 kJ/kg)) using an electric field strength of 1.00 to 1.25 kV/cm.

Digestion phase	Enzyme types	Enzyme concentrations	Digestion duration (min)	Cumulative digestion time (min)	Sampling time (min) based on cumulative digestion time
Oral (pH 7 ± 0.1)	α-amylase	75 U /mL bolus	2	2	No
Gastric (pH 3 ± 0.1)	Pepsin	2.5 U/mg meat protein	60	62	2, 32, 62
Small intestinal (pH 7 ± 0.1)	Pancreatin	1:100 pancreatin to meat protein ratio (0.04 USP pancreatin/mg meat protein)	120	182	122, 182

3.2.4.2 Preparation of the digests for further analysis

The digests were centrifuged at 10000 x *g* for 20 min at 2 ℃ using a high speed refrigerated centrifuge (CR 22 GII, Himac, Hitachi Koki Co., Ltd., Tokyo, Japan). The supernatant was filtered through a 0.45 µm polyvinylidene fluoride (PVDF) filter (Millex®-HV, Merck Millipore Ltd., Cork, Ireland) and the filtered samples were used for the analysis of soluble nitrogen, ninhydrin-reactive amino nitrogen and SDS-PAGE.

3.2.4.3 Soluble nitrogen

Soluble nitrogen was analysed using the Kjeldahl method (AOAC, 1981). In short, approximately 3 to 4 g of each filtered sample from **section 3.2.4.2** was weighed into a digestion tube and was digested with the addition of two Kjeltabs (FOSS, Denmark) and 17 mL of concentrated sulphuric acid. A blank digestion tube was prepared with all the reagents except sample. Both blank and sample tubes underwent digestion at 420 ℃ for around 2 h until the solution turned clear completely. After cooling, approximately 70 mL of distilled water was added to each digestion tube and the samples were distilled using a distilling unit (Kjeltec™ 2100, FOSS, Denmark) under excess sodium hydroxide for 4 min. The distillate was collected in a conical flask containing 25 mL of 4 % boric acid with bromocresol green and methyl red indicators, and were titrated with 0.1 M HCl until a grey-mauve end point was observed. The nitrogen and protein content in the digests were calculated using the following equations:

$$\% \text{ Nitrogen} = [(V_{sample} - V_{blank}) \times M_{HCl} \times 14 \times 100] / (Wt \times 1000) \text{ ----------} \textbf{Eq. (3-2)}$$

where V is the volume of HCl used during titration in mL, M is the molarity in M, Wt is the sample weight in g.

3.2.4.4 Tricine SDS-PAGE

Tricine-SDS-PAGE was carried out based on the protocol described by Kaur et al. (2014) with minor modifications. The filtered gastric and small intestinal digests (as prepared in section **3.2.4.2**) were diluted with Milli-Q water at pH 3 and 7 (the pH of gastric and small intestinal fluids), respectively. The diluted digests were then mixed with tricine sample buffer (1:1 ratio) (1610739, Bio-Rad Laboratories, Hercules, CA, USA) containing 5 % β-mercaptoethanol (M6250, Sigma-Aldrich, Saint Louis, MO, USA) to achieve a final protein concentration of 5 mg/mL, based on the protein contents determined in section **3.2.4.3**. The samples were heated at 100 ℃ for 5 min and were cooled to room temperature. After that, the Precision Plus Protein™ Dual Xtra Prestained Protein Standards (Bio-Rad Laboratories, Hercules, CA, USA) as well as the samples (20 µg of protein per well) were loaded to the wells on 10 to 20 % gradient tricine gels. The tricine gels were run using a Criterion™ cell (Bio-Rad Laboratories Pty. Ltd., Hercules, CA, USA) filled with diluted 1x Tris/Tricine/SDS running buffer (Bio-Rad Laboratories, Hercules, CA, USA) at a constant voltage of 125 V, controlled by a power supply (PowerPac™ basic power supply, Bio-Rad Laboratories, Hercules, CA, USA) for 2 h or until the bands reached the bottom of gels. The gels were then treated with fixation solution (40 % methanol and 10 % acetic acid) for 30 min, followed by staining using Bio-Safe™ Coomassie G-250 staining solution (Coomassie Brilliant Blue dye in less than 5 % phosphoric acid and less than 1 % methanol) (Bio-Rad Laboratories, Hercules, CA, USA) for an hour. After that, the gels were washed in Milli-Q water for several times until the backgrounds of the gels were clear. Finally, the gels were scanned using a gel scanning densitometer (Molecular Imager Gel Doc XR, Bio-Rad Laboratories, Hercules, CA, USA) and the images were analysed using the associated software (Image Lab™,

Bio-Rad Laboratories, Hercules, CA, USA). One gel was prepared for each digestion replicate.

3.2.4.5 Ninhydrin-reactive amino nitrogen

Ninhydrin-reactive amino nitrogen (%) was measured as described by Moore (1968) using a ninhydrin reagent (N7285, Sigma-Aldrich, Saint Louis, MO, USA). Briefly, 1 mL of the diluted, filtered digest (as described in **section 3.2.4.2**) was mixed with 0.5 mL of 2 % ninhydrin reagent. The sample-ninhydrin reagent mixture was heated at 100 ℃ for 10 min and were cooled to room temperature before the addition of 2.5 mL of 95 % ethanol. The absorbance of the heated mixture was read at 570 nm using a VIS-spectrophotometer (Helios Epsilon, Thermo Fisher Scientific, Waltham, MA, USA). A stock solution of 50 µM glycine in 0.05 % acetic acid was prepared for the determination of a standard curve. The percentage of ninhydrin-reactive amino nitrogen released at different digestion time points was calculated using equation below:

Ninhydrin-reactive amino nitrogen released (%) = Ninhydrin-reactive amino nitrogen in the digests / total nitrogen present in meat x 100 ----------**Eq. (3-3)**

The ninhydrin analysis was repeated at least three times for each digestion time for each digestion replicate.

3.2.5 Microscopy analysis

Thawed control and PEF-treated samples were cut into rectangular (5 mm x 5 mm x 10 mm) cuboids with the fibre direction parallel to their length. Simulated digestions were performed as described in section **3.2.4.1** in a polyester mesh without the addition of glass balls. Both undigested and digested (cumulative digestion time of 182 min) samples were fixed in 2.5 % glutaraldehyde in 0.1 M sodium cacodylate buffer at pH 5.6. The fixed

samples were cut into 1 to 3 mm^3 and were washed using 0.1 M sodium cacodylate buffer at pH 5.6 for three times, and then post-fixed with 0.04 M Osmium tetroxide in 0.1 M sodium cacodylate buffer for one hour at room temperature. The three buffer washes were repeated, followed by dehydration using an acetone/water series (25 %, 50 %, 75 %, 95 % and 100 %) for 15 min each. The samples were further dehydrated with 100 % acetone for an hour twice. The dehydrated samples were first embedded with an acetone/ resin (Procure 812, ProSciTech, Queensland, Australia) mixture (1: 1 ratio) on a stirrer overnight. Then, the acetone/resin mixture was replaced with 100 % fresh resin, followed by constant stirring for 8 h. The change of 100 % fresh resin was repeated twice, with constant stirring overnight and a further 8h, respectively. The samples were finally moulded in 100 % fresh resin at 60 °C for 48 h. Ultra-thin sections (100 nm) were cut from the resin blocks and were mounted on copper grids. The sections were stained with saturated uranyl acetate in 50 % ethanol for 4 min, washed with 50 % ethanol and Milli-Q water, stained with saturated lead citrate for another 4 min, followed by final wash with Milli-Q water. The stained sections were then viewed under a FEI Tecnai G^2 Spirit BioTWIN transmission electron microscope (FEI Corp., Brno-Černovice, Czech Republic). Sarcomere lengths were measured from the TEM micrograph using ImageJ software version 1.52f (National Institute of Health, Bethesda, MD, USA) (Perkins & Tanentzapf, 2014). The length of 30 sarcomeres were determined for each treatment using the TEM micrographs from one triangular-shaped muscle. Observations were made on TEM sections from one digestion replicate.

3.2.6 Statistical analysis

The pH, moisture content, colour, sarcomere length and DSC results were analysed statistically with one-way analysis of variance (ANOVA) and Tukey's pairwise comparison test (significance level of 0.05) to evaluate the significance of difference

using Minitab Release 17 Statistical Software (Minitab Inc., State College, PA, USA). The ninhydrin-reactive amino nitrogen released at different digestion time points were analysed using a repeated measures one-way ANOVA at significance level of 0.05 by Generalised Linear Model (IBM® SPSS® Statistic version 25, IBM Corporation, Armonk, NY, USA) and no violation of sphericity was detected using Mauchly's Test. Results are expressed as means of at least three replicates ± standard deviation of means from one *Longissimus thoracis* muscle.

3.3 Results and discussion

3.3.1 Effect of PEF on muscle general properties and protein thermal profile

The pH, moisture content and colour of control and PEF-treated samples are summarised in **Table 3-2**. Low-intensity PEF treatment did not affect the pH and colour ($p > 0.05$) of meat, which is in agreement with the available literature (Faridnia et al., 2014; Suwandy et al., 2015d). However, the treatment significantly decreased the moisture content of the treated meat at pulse number 500 ($p < 0.05$) and 2000 ($p < 0.001$), with the moisture loss increasing with elevating treatment intensity. This is possibly due to more severe changes in muscle fibre integrity and membrane disruption in the sample treated with higher PEF intensity, leading to more fluid loss, which has also been previously reported in bovine *Longissimus thoracis* muscles (Faridnia et al., 2014).

Table 3-2. pH, moisture content, colour and sarcomere length of control untreated (C500 and C2000) and PEF-treated samples ((PN500, 48 ± 5 kJ/kg) and (PN2000, 178 ± 11 kJ/kg)) using an electric field strength of 1.00 to 1.25 kV/cm.

Parameters		C500	PN500	C2000	PN2000
pH[#]		5.54 ± 0.02^{A}	5.51 ± 0.00^{A}	5.51 ± 0.02^{A}	5.50 ± 0.04^{A}
Moisture content (%) [#]		72.62 ± 0.00^{A}	71.65 ± 0.00^{B}	72.80 ± 0.00^{A}	69.44 ± 0.01^{C}
Colour[^]	*L**	36.5 ± 0.7^{A}	36.3 ± 0.6^{A}	36.4 ± 0.6^{A}	36.7 ± 0.5^{A}
	*a**	13.0 ± 0.7^{A}	13.0 ± 0.4^{A}	13.5 ± 0.6^{A}	13.6 ± 0.9^{A}
	*b**	4.8 ± 0.4^{A}	5.1 ± 0.2^{A}	4.9 ± 0.3^{A}	5.2 ± 0.4^{A}
Sarcomere length (µm)[~]		1.68 ± 0.04^{a}	1.99 ± 0.06^{b}	1.69 ± 0.03^{a}	2.17 ± 0.11^{c}

Values with different uppercase letters within the same row differ significantly ($p < 0.05$).

Values with different lowercase letters within the same row differ significantly ($p < 0.001$).

$N = 3$ (measurements of three individual muscle pieces obtained from one *Longissimus thoracis* muscle as shown in **Figure 3-1**).

^ $N = 12$ (12 measurements from one muscle piece obtained from one *Longissimus thoracis* muscle as shown in **Figure 3-1**).

~ $N = 30$ (30 measurements from one muscle piece obtained from one *Longissimus thoracis* muscle as shown in **Figure 3-1**).

Colour measurements definition according to León et al. (2006):

- *L**: lightness (0 indicates black while 100 indicates absolute white).
- *a**: redness (positive value)/ greenness (negative value).
- *b**: yellowness (positive value) /blueness (negative value).

The DSC results of the samples are summarised in **Table 3-3**. These results may be useful in determining the optimum cooking temperature of meat, as the thermal denaturation of these proteins is associated with sensory and textural properties of meat (Findlay et al., 1986). Understanding the thermal denaturation properties of proteins enables the selection of the optimal cooking temperatures of meat by setting the temperature high enough to denature collagen in order to decrease the adhesion between muscle fibres, but low enough to prevent excessive denaturation of most myofibrillar proteins to reduce water expulsion from the muscle fibres. The first, second and third peaks of the thermogram represent the thermal denaturation of myosin, collagen and sarcoplasmic proteins, and actin respectively (Bertola et al., 1994). No significant difference in any of the peak temperatures between the PEF-treated samples and their untreated counterparts

was observed ($p > 0.05$). This supports the literature findings that low-intensity PEF treatment results in electroporation of muscle cell membrane but not protein denaturation in muscle-based foods. The protein profiles of the muscles were not modified by the electric pulses applied to the meat, as seen in the gel electrophoresis analysis conducted by Faridnia et al. (2014) on beef (0.2 to 0.6 kV/cm, 0.05 to 30 kJ/kg) and Gudmundsson and Hafsteinsson (2001) on cod muscles (18.6 kV/cm and seven pulses). There are some studies showing protein aggregation and unfolding of lysozyme (35 kV/cm) (Zhao & Yang, 2008) and soy protein isolate (> 30 kV/cm) (Liu et al., 2014) after PEF treatments that were carried out at a much higher treatment intensity than the current study. Hence there is a possibility of protein modification in meat at higher PEF treatment intensities. Alahakoon et al. (2017) found that PEF treatment significantly ($p < 0.05$) decreased the thermal denaturation temperature of the extracted connective tissue from beef *Deep pectoralis* muscle in a model agar system. However, the effect of PEF on connective tissue in a natural meat system would not be expected to be as significant, particularly in *Longissimus thoracis*, as this muscle has only almost half of the connective tissue content compared to *Deep pectoralis* (Keith et al., 1985).

Table 3-3. DSC thermal profiles of control untreated (C500 and C2000) and PEF-treated samples ((PN500, 48 ± 5 kJ/kg) and (PN2000, 178 ± 11 kJ/kg)) using an electric field strength of 1.00 to 1.25 kV/cm. The results showed the thermal denaturation temperature of myosin (first peak), collagen and sarcoplasmic proteins (second peak) and actin (third peak) when heated from 20 ℃ to 100 ℃ at a rate of 2 ℃/min.

	Thermal transition peak	**C500**	**PN500**
Temperature (℃)	First	53.1 ± 0.2^{A}	52.9 ± 0.4^{A}
	Second	61.9 ± 0.4^{A}	62.4 ± 0.3^{A}
	Third	74.2 ± 0.2^{A}	74.4 ± 0.2^{A}
	Thermal transition peak	**C2000**	**PN2000**
Temperature (℃)	First	53.5 ± 0.9^{A}	53.1 ± 0.2^{A}
	Second	62.6 ± 0.7^{A}	61.5 ± 0.8^{A}
	Third	75.1 ± 0.5^{A}	75.1 ± 0.1^{A}

Values with different letters within the same row differ significantly ($p < 0.05$).

$N = 3$ (measurements of three individual muscle pieces obtained from one *Longissimus thoracis* muscle as shown in **Figure 3-1).**

3.3.2 Effect of PEF on muscle ultrastructure

As shown in **Table 3-2**, PEF-treated samples PN500 and PN2000 had significantly longer sarcomere length than their control untreated counterparts ($p < 0.001$, $N = 30$). This indicates that PEF treatment caused physical disruption in the muscle fibres. The extent of sarcomere elongation also increased with increasing treatment intensity. The elongation of sarcomeres might have resulted from the weakening of Z-disk and I-band junctions, as observed in the PEF-treated muscle samples (**Figure 3-2**). Extended sarcomere length has also been observed by Vaskoska et al. (2020) in beef muscles after postmortem ageing, where the endogenous proteases degrade some structural myofibrillar proteins, primarily along the Z-disks. Other structural changes have been described in the literature, with reports on the separation of myofibrils from Z-disks, and the presence of jagged edges in the muscle cells of PEF-treated samples (Faridnia et al., 2016; Faridnia et al., 2015). Physical disruption of muscle structure has a positive correlation with meat tenderisation as it has been reported to reduce the tensile strength of myofibrils (Davey & Gilbert, 1969) and enhance the contact of endogenous proteolytic enzymes during the

postmortem ageing process (Bolumar et al., 2014). Hence, the meat maturation/ageing process might be facilitated by PEF treatment due to the disruption of muscle structure. The electroporation effect of PEF treatment has also been proposed to cause the release of cathepsins from the lysosomes and the activation of calpains by calcium released from the sarcoplasmic reticulum, facilitating meat proteolysis during the ageing process (Alahakoon et al., 2016).

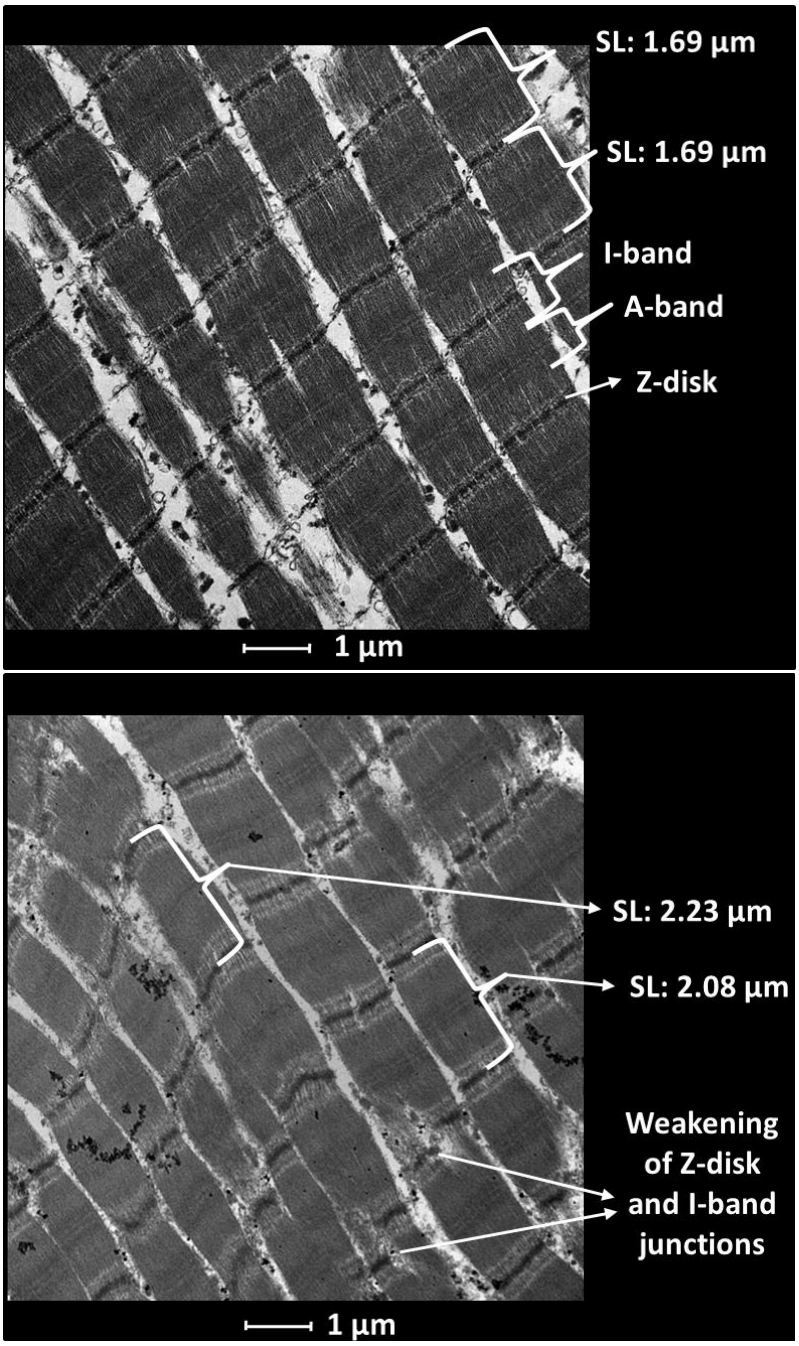

Figure 3-2. Transmission electron micrograph showing elongated sarcomeres and disruption of Z-disk and I-band junctions in the PEF-treated meat sample PN2000 (bottom) (pulse number 2000, 1.00 - 1.25 kV/cm, 178 ± 11 kJ/kg) before *in vitro* digestion. The sarcomere details of the control untreated counterpart (C2000) is presented in the top micrograph.

3.3.3 Effect of PEF on muscle protein digestibility *in vitro*

3.3.3.1 Tricine SDS-PAGE

The enzymatic hydrolysis of meat proteins during *in vitro* digestion was evaluated using SDS-PAGE and the findings are shown in **Figures 3-3** and **Figure 3-4**. As both treatment intensities showed the same trends, only electrophoretograms of C2000 and PN2000 are shown. After 62 min of simulated oral-gastric digestion, new low molecular weight (MW) peptides (< 10 kDa) were generated in both control and PEF-treated samples, indicating protein hydrolysis by pepsin. A new peptide band appeared in both control and treated samples, corresponding to MW 30 kDa, was deduced to be a product of troponin T hydrolysis (Cheftel & Culioli, 1997; Kaur et al., 2014). The bands corresponding to MW 95 kDa (α-actinin) (Obinata et al., 1981) and 34 kDa (β-actinin subunit) (Swartz et al., 2009) in meat digests from PN2000 almost completely disappeared after 62 min of simulated oral-gastric digestion. In contrast, these bands were present, but with decreased intensity in the control untreated sample. This shows that the α-actinin and β-actinin in the PEF-treated samples were broken down more rapidly by pepsin under stimulated gastric digestion condition. As both the α-actinin and β-actinin are the major components of Z-disks, their more rapid disintegration in the PEF-treated samples might be due to the weakening of Z-disk and I-band junctions caused by the treatment, as observed by TEM (**Figure 3-2**) (Strasburg et al., 2008). Patel and Welham (2013) also reported a decrease in the intensity of the band of α-actinin in raw beef digests after 60 min of gastric digestion.

After 122 min of simulated oral-gastro-small intestinal digestion, the MHC (MW 220 kDa) was completely digested in both the PEF-treated and control samples. A new faint band with MW of 58 kDa was observed, only in PN2000 sample, after 60 min of small intestinal digestion. This band was not present in either control or treated samples after

oral-gastric digestion, and hence may be the proteolytic product of a higher MW or insoluble protein. In addition, it was observed that the intensity of the band with MW of 39 kDa of the digest of PEF-treated muscle was higher than the control untreated meat digest at the end of simulated digestion (182 min). The band corresponding to MW 39 kDa has been reported to be a degradation fragment of desmin (Soglia et al., 2018). This showed that desmin was broken down more in the PEF-treated meat at the end of simulated digestion. Overall, the results of SDS-PAGE analysis demonstrate PEF effected the digestion pattern of meat proteins, that may be due to the modification of muscle structure which in turn influences the accessibility of digestive enzymes (Astruc, 2014b).

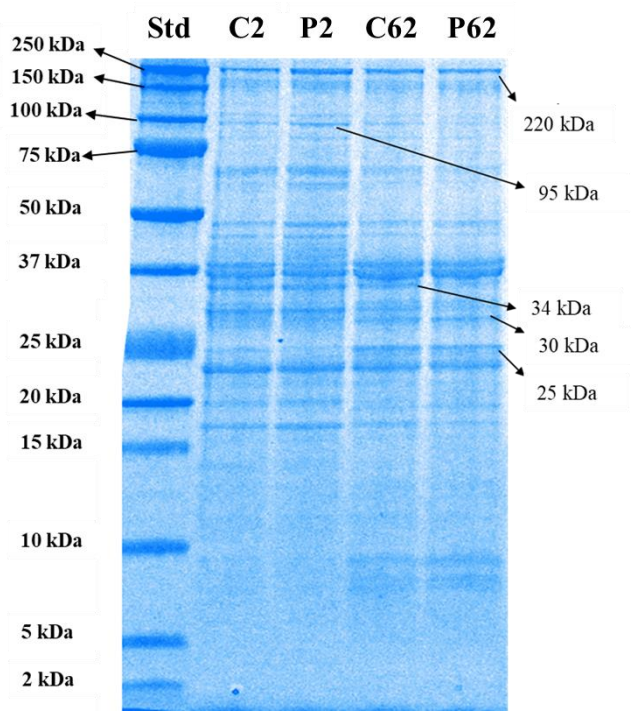

Figure 3-3. Tricine SDS-PAGE electrophoretogram showing protein profiles of the digests of PN2000 (pulse number 2000, 1.00 - 1.25 kV/cm, 178 ± 11 kJ/kg) and its counterpart untreated C2000 during simulated oral-gastric digestion.
C2 and C62 denote C2000 samples at 2 and 62 min of simulated oral-gastric digestion respectively while P2 and P62 denote PN2000 samples at 2 and 62 min of simulated oral-gastric digestion. Std represents the molecular weight standards labelled to the left in kDa.

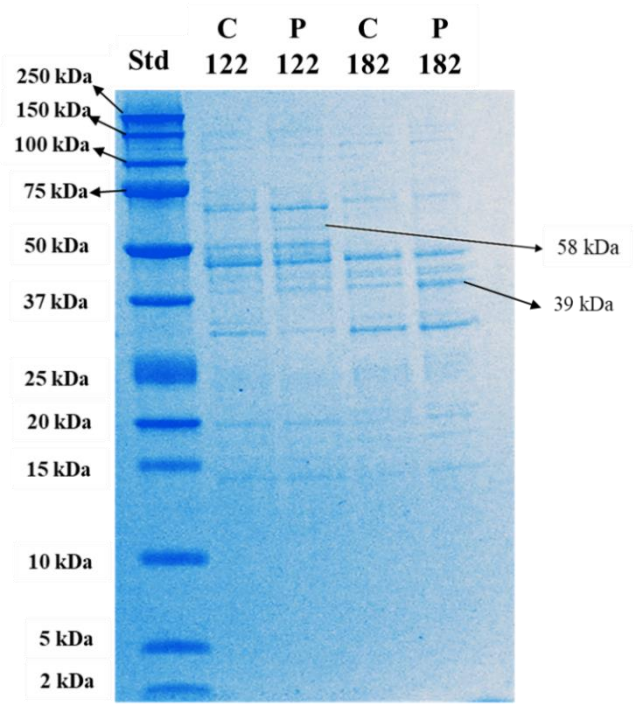

Figure 3-4. Tricine SDS-PAGE electrophoretogram showing proteins profile of the digests of PN2000 (pulse number 2000, 1.00 - 1.25 kV/cm, 178 ± 11 kJ/kg) and its counterpart untreated C2000 during 120 min of *in vitro* small intestinal digestion following 62 min of oral-gastric digestion.
C122 and C182 denote C2000 samples after 122 and 182 min of simulated oral-gastric-small intestinal digestion respectively while P122 and P182 denote PN2000 samples after 122 and 182 min of simulated oral-gastric-small intestinal digestion Std represents the molecular weight standards labelled to the left in kDa.

3.3.3.2 Ninhydrin-reactive amino nitrogen

The protein digestibility of meat was determined in terms of ninhydrin-reactive free amino nitrogen released during simulated oral-gastro-small intestinal digestion, using the ninhydrin assay (**Table 3-4**). Both PN500 and PN2000 released more free amino nitrogen than their respective untreated controls at all the digestion time points. However, this effect was significant ($p < 0.05$) only at the end of 182 min *in vitro* oral gastro-small intestinal digestion. In addition, there was no significant difference in the ninhydrin-reactive amino nitrogen released between various gastric digestion time points among individual control and PEF-treated samples (**Table 3-4**). The pepsin concentration used in this experiment might be too low. Thus, the pepsin concentration is increased slightly for the *in vitro* digestion experiments reported in **Chapter 4** and **Chapter 6**. Overall, PEF

treatment improved the protein digestibility of the muscles by at least 18 % (up to 31 %) after 182 min of simulated oral-gastro-small intestinal digestion, in terms of ninhydrin-reactive amino nitrogen released.

Table 3-4. Ninhydrin-reactive amino nitrogen released from the control untreated (C500 and C2000) and PEF-treated samples ((PN500, 48 ± 5 kJ/kg) and (PN2000, 178 ± 11 kJ/kg)) using an electric field strength of 1.00 to 1.25 kV/cm after *in vitro* oral-gastric (2, 32 and 62 min) and further small intestinal (122 & 182 min) digestion.

Cumulative digestion time (min)	Ninhydrin free amino nitrogen released (%)	
	C500^	PN500^
2	1.8 ± 0.5^{Aa}	2.1 ± 0.5^{Aa}
32	2.1 ± 0.6^{Aa}	2.6 ± 0.7^{Aa}
62	1.9 ± 0.4^{Aa}	2.6 ± 0.6^{Aa}
122	7.4 ± 1.1^{Ab}	8.3 ± 0.4^{Ab}
182	9.0 ± 0.5^{Ac}	11.9 ± 1.5^{Bc}
Cumulative digestion time (min)	**Ninhydrin free amino nitrogen released (%)**	
	C2000*	**PN2000***
2	1.8 ± 0.4^{Aa}	2.1 ± 0.3^{Aa}
32	1.8 ± 0.2^{Aa}	2.4 ± 0.6^{Aa}
62	1.9 ± 0.1^{Aa}	2.3 ± 0.5^{Aa}
122	8.2 ± 0.4^{Ab}	9.3 ± 1.4^{Ab}
182	10.4 ± 0.3^{Ac}	12.2 ± 0.3^{Bc}

Values with different lower-case letters within the same treatment column differ significantly ($p < 0.05$).

Values with different upper-case letters within the same row differ significantly ($p < 0.05$).

^Data are shown as mean ± standard deviation of mean. $N = 4$ (four replicates with 3 measurements from each replicate).

*Data are shown as mean ± standard deviation of mean. $N = 3$ (three replicates with 3 measurements from each replicate).

3.3.4 Ultrastructure of digested meat samples

The effect of PEF on muscle structural changes after 182 min of *in vitro* oral-gastro-small intestinal digestion was observed using TEM (**Figure 3-5**). Small grey spots were observed in the intermyofibrillar spaces, which might be the products of muscle protein degradation, suggesting proteolysis by the digestive enzymes. The Z-disks of both the control and PEF-treated samples were degraded after 182 min of incubation with simulated digestive juices containing digestive proteases (pepsin followed by pancreatin).

However, it was seen that the Z-disk and I-band junctions of the PEF-treated muscle were less dense and more coagulated, with more elongated I-bands than the control untreated muscle (as indicated in the white box drawn in **Figure 3-5**). The disruption of the I-bands might be due to the proteolytic action of the digestive enzymes along the Z-disks, where the thin filaments of I-bands are attached, which corresponds to more rapid degradation of Z-disk components (α-actinin and β-actinin) as discussed in section **3.3.3.1**. Pepsin digestion has been reported to cause Z-disks degradation, and subsequent trypsin and chymotrypsin digestion disrupts the whole sarcomere structure (Astruc, 2014b). The pepsin-catalysed degradation of Z-disks during gastric digestion was also reported by Kaur et al. (2016) and Astruc (2014b). These observations suggested that the PEF-treated muscle was more susceptible to digestive enzyme hydrolysis, which is in agreement with significantly higher ninhydrin-reactive amino nitrogen released than the control, after 182 min of *in vitro* digestion. Myofibrillar disruption, in this case the weakening of the Z-disk and I-band junctions caused by the PEF treatment, might enhance the accessibility of digestive enzymes to their substrates, resulting in improved protein digestion (Astruc, 2014b). Dolatowski (1989) also observed that ruptures in the myofibrils and other structural disruption of the muscle increased the effectiveness of proteolytic enzyme activity in the tissue. The more coagulated I-bands of the PEF-treated sample could be associated with a higher extent of protein denaturation and unfolding by the acidic gastric environment, leading to the exposure of buried peptide bonds, facilitating the enzymatic hydrolysis of the meat proteins during gastric and subsequent small intestinal digestion (McGuire & Beerman, 2012).

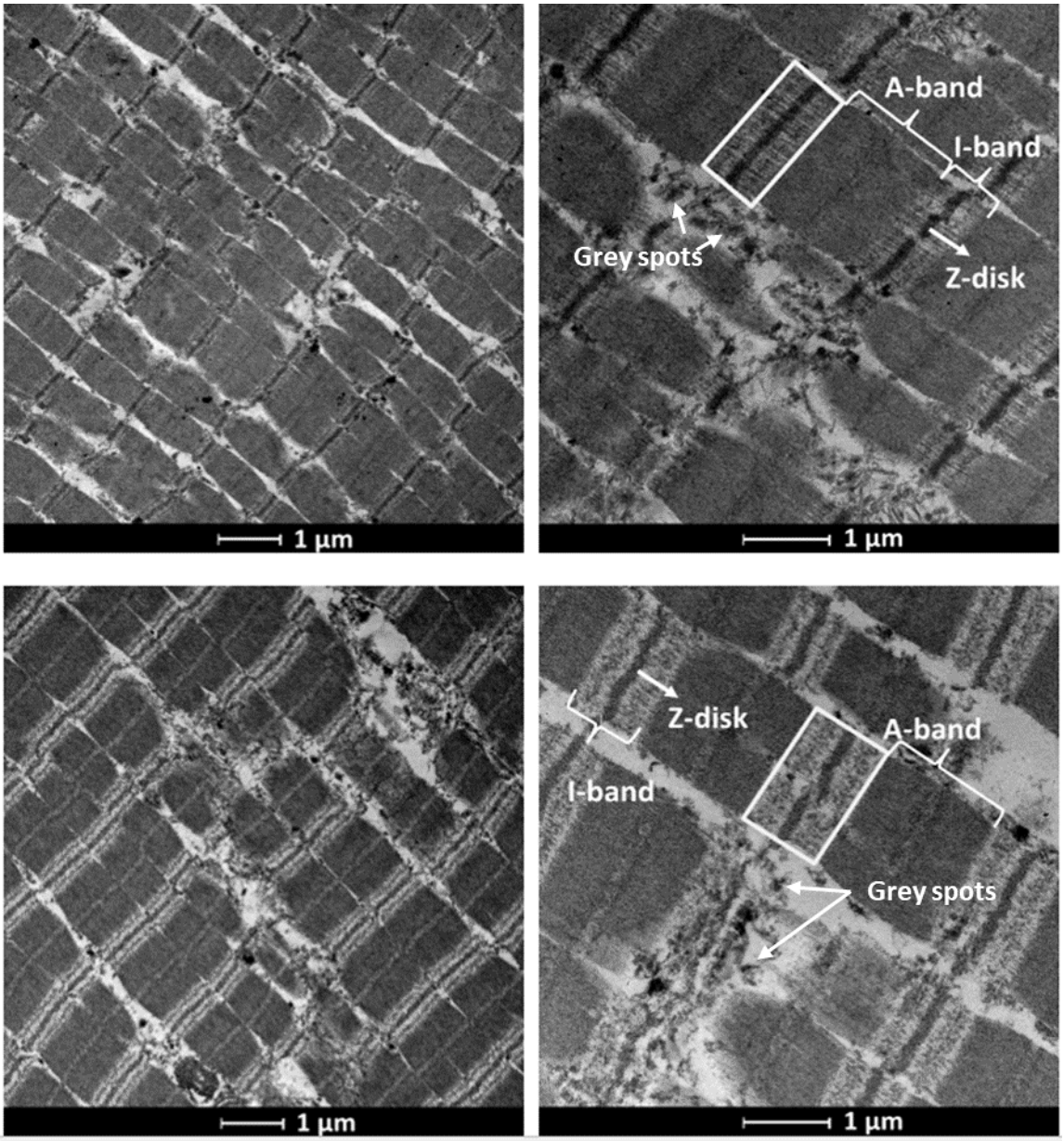

Figure 3-5. Transmission electron micrographs of beef *Longissimus thoracis* muscles showing less dense, more coagulated Z-disk and I-band junctions as well as more elongated I-bands of PEF-treated sample PN2000 (pulse number of 2000, 1.00 - 1.25 kV/cm, 178 ± 11 kJ/kg) (bottom two) than the untreated control C2000 (top two), after 182 min of *in vitro* oral-gastro-small intestinal digestion, at two different magnifications.

3.4 Conclusions

The results of this experiment showed that PEF treatment alone does not affect the appearance and protein thermal profile of bovine *Longissimus thoracis* muscles. The colour and thermal denaturation temperatures of the major meat proteins, such as myosin, collagen and actin, remained unchanged. Moisture loss from the muscle was observed in

treated samples, which was deduced to be due to fluid loss resulting from cell membrane electroporation. The *in vitro* protein digestibility of meat treated with PEF was improved, which might be due to the disruption of myofibrillar structure, enhancing the accessibility of digestive enzymes to their substrates. This chapter showed the positive impacts of PEF treatment on *in vitro* protein digestibility of raw beef ribeye muscles. The effect of PEF in combination with SV cooking on beef brisket, a tough meat cut, will be investigated in **Chapter 4.**

Chapter 4 [3]Effects of pulsed electric fields (PEF) and sous vide (SV) cooking on the lysosomal enzyme activities, muscle structure and *in vitro* protein digestibly of beef brisket

4.1 Introduction

In recent years, low-intensity pulsed electric field, alone or in combination with other processing techniques, has been explored for meat tenderisation. The combined PEF-SV cooking process (Alahakoon et al., 2018a), the combined freezing-PEF process (Faridnia et al., 2015), and the combined PEF-ageing process (Alahakoon et al., 2019; Bhat et al., 2018d) have been reported to promote meat tenderisation. The meat tenderisation mechanisms of PEF are suggested to be due to an earlier activation of the endogenous enzymes, the calpains, by the calcium ions released from the muscle cells, and/or the action of lysosomal enzymes released from the lysosomes, as a result of cell permeabilisation (Alahakoon et al., 2016; Bhat et al., 2018b).

Calpain activation by PEF has been verified by some recent studies. Bhat et al. (2018d) have discovered improved calpain activity in PEF-treated beef *Semimembranosus* (0.36 kV/cm, 90 Hz and 0.60 kV/cm, 20 Hz). Bhat, Morton, Mason, Mungure, et al. (2019) also detected a slight increase in calpain activity in PEF-treated cold-boned venison *Longissimus dorsi* (2.5 kV, 50 Hz and 10 kV, 90 Hz) during ageing. An increased degradation of troponin T, one of the substrates of calpains, was also observed in both studies. However, no study has been conducted to validate the release of lysosomal enzymes due to the permeabilisation of lysosomes by the action of PEF. Lysosomal enzymes, such as cathepsins, are located within lysosomes in the cytoplasm of cell (Geesink & Veiseth, 2008). For meat tenderisation, cathepsins have to be released from the lysosomes into the cytosol to access their substrate, the myofibrillar proteins.

[3]Part of this chapter has been published as **Chian, F. M.**, Kaur, L., Oey, I., Astruc, T., Hodgkinson, S., & Boland, M. (2021). Effects of pulsed electric field processing and sous vide cooking on muscle structure and *in vitro* protein digestibility of beef brisket. *Foods*, *10*(3), 512. https://doi.org/10.3390/foods10030512

Cathepsins are most active in a slightly acidic environment and are more heat-stable than calpains (Dominguez-Hernandez et al., 2018). Cathepsins B and L in porcine *Semitendinosus* and *Longissimus* muscles have been reported to stay active at 58 ℃ for 17 h (Christensen, Ertbjerg, et al., 2011). Kaur et al. (2020) also reported that cathepsins B and L were inactivated after incubating beef brisket at 60 ℃ for 5 h. In contrast, μ-calpain in porcine *Longissimus* muscles lost its activity after incubating at 25 °C for 3 h while m-calpain were inactivated after holding at 40 ℃ for 3 h (Ertbjerg et al., 2012). Both μ- and m-calpains were inactivated after holding at 55 ℃ for 2 min. Due to microbiological safety considerations, it is recommended to cook meat at a minimum temperature of 60 °C by regulatory bodies in some countries (Purslow, 2018). Cathepsins are therefore more likely to contribute to meat tenderisation during low temperature long time cooking processes (Dominguez-Hernandez et al., 2018). If PEF treatment results in the release of cathepsins from the lysosomes by electroporation, as proposed in the literature, the meat tenderisation process could be further promoted during the initial stage of low temperature long time cooking, such as SV cooking. The other mechanism behind the meat tenderisation of a combined PEF-SV process was an increase in collagen solubility during the cooking process, due to the structural disruption of connective tissue by PEF (Alahakoon et al., 2018b).

As consumers are now seeking food products that are tasty and nutritious, it is important to understand the effect of the combined PEF-SV processing on the nutritional value of meat products, in particular the protein digestibility (Hung et al., 2016). Current research to understand the effects of PEF in combination with cooking on meat protein digestibility is limited, particularly in regards to understanding of structural changes occurring during digestion. The *in vitro* protein digestibility of PEF-treated water bath-cooked (core temperature of 75 ℃) bovine *Semimembranosus* muscles has been reported to be higher

than the control untreated cooked meat (Bhat, Morton, Mason, Jayawardena, et al., 2019). Conversely, Alahakoon et al. (2019) did not detect any effect of the combined PEF (0.7 kV/cm, 90 to 100 kJ/kg)-SV (60 ℃ for 24 h) process on the *in vitro* protein digestibility of beef brisket. However, the impact of the structural changes induced by a combined PEF-cooking process on the enzymatic breakdown of meat proteins during digestion has not been explored and requires further research. Thus, this chapter aims to examine the *in vitro* protein digestibility of PEF-treated SV-cooked beef brisket using both biochemical and microscopy approaches. In addition, the effect of PEF on the lysosomal enzymes activity, alone and in combination with SV cooking, is also investigated.

4.2 Materials and methods

4.2.1 Pulsed electric field treatment of beef briskets

Four whole beef briskets (*Deep* and *Superficial pectoral* muscle) from the left and right sides of two Hereford sired heifers (19 months old, mix of Friesian and crossbreed, 195.5 – 270.0 kg carcass weight) were obtained from ANZCO Foods (Eltham, New Zealand). The pre-rigor briskets were stored at 15 ℃ for 48 h until they went into rigor. The briskets were then vacuum-packed, blast-frozen, and kept at -18 ℃ until PEF treatment. The meat was thawed at 4 ℃ for 18 h before PEF treatment. Pulsed electric field treatment was conducted in a pilot-scale batch PEF system (Elcrack-HVP 5, DIL, Quakenbruck, Germany) as described in section **3.2.1** with modifications. After removing the edges of the whole brisket which are too thin for the treatment, the meat was cut into triangular shapes that were 6 cm in height, 4 cm in width and 6 cm in length, with an approximate weight of 70 g (**Figure 4-1**). The treatment was carried out using processing parameters of 0.7 kV/cm electric field strength to achieve a specific energy of 99 ± 5 kJ/kg, at a constant pulse width and frequency of 20 µs and 50 Hz respectively, as optimised by

Alahakoon et al. (2018b). The specific energy was determined using **Eq. (3-1)**. The conductivities of the briskets were measured at more than 25 positions across each per whole brisket, using a handheld meat conductometer (LF-STAR, R. Mathäus, Nobitz, Germany), before and after PEF treatment. The pre- and post-PEF treatment conductivities of the meat were 9 ± 2 mS/cm and 13 ± 1 mS/cm correspondingly. The temperature of the meat had increased by about 14.0 ℃ after PEF treatment to 22.4 ℃.

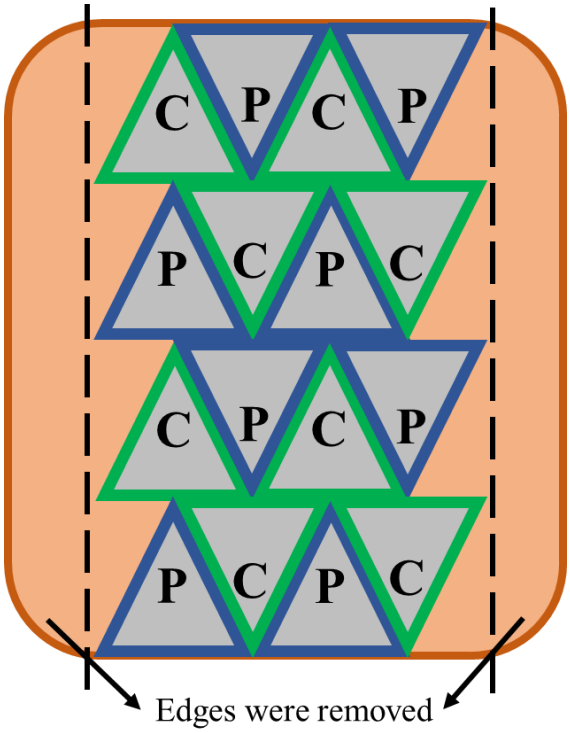

Figure 4-1. Meat sampling position of the control untreated (C) and the PEF-treated (P) samples on each brisket slab.
The edges of the brisket which were too thin for PEF processing were removed. In order to minimise the inconsistency due to inhomogeneity of meat, sampling was performed by assigning the C and P adjacent to each other. The meat was cut into triangular pieces of about 70 g with dimensions of 6 cm in height, 4 cm in width and 6 cm in length for PEF treatment.

4.2.2 Sous vide cooking of beef briskets

After PEF treatment, both control and treated meat samples were vacuum-packed in ‘cook-in’ clear vacuum bags (Cas-Pak Products Ltd, Silverdale, New Zealand) in two different ways. Six triangular pieces, each from the control untreated and PEF-treated samples from the same whole brisket, were used as one replicate for the lysosomal

enzyme activity experiment (total of three replicates from three whole briskets). To minimise the muscle variability in a whole brisket, each of the six triangular pieces was cut and packed in five separate bags for different SV cooking time points (**Figure 4-2**). Each pack contained samples from six triangular pieces of the same whole brisket as one replicate. The vacuum-packed samples were then SV-cooked at 60 °C for 0, 0.5, 2, 5 and 24 h. The individual control untreated and PEF-treated triangular pieces from another brisket were vacuum-packed intact and were SV-cooked at 60 °C for 24 h for protein digestibility analysis. All samples (control raw, PEF-treated raw, Control SV-cooked and PEF-treated SV-cooked samples) were snap-frozen using liquid nitrogen and were stored at -80 °C for further analyses.

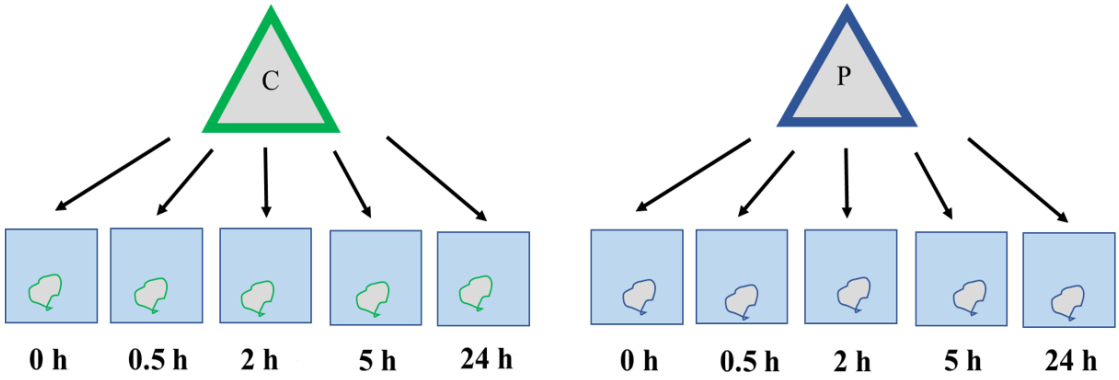

Figure 4-2. Schematic diagram showing the sample allocation for the lysosomal enzyme activity analyses.
In order to minimise muscle variability in a whole brisket, each triangular piece was divided into five individual packages designated for different SV cooking times. Each pack contained samples from six triangular pieces of the same whole brisket as one replicate. The vacuum-sealed packs were then SV-cooked at 60 °C and were sampled at 0, 0.5, 2, 5 and 24 h of cooking.

4.2.3 Endogenous enzyme activities

4.2.3.1 Cytosolic sarcoplasmic protein extraction

The sarcoplasmic protein extract for cytosolic lysosomal enzyme activity assays was prepared as described by Chéret et al. (2007) and Caballero et al. (2007) with modifications. The raw and SV-cooked frozen samples were thawed on ice for 1 h. The samples were then briefly chopped into smaller pieces and were mixed with an extraction

buffer comprising 50 mM Tris–HCl (pH 7.5) (T2319, Sigma-Aldrich, Saint Louis, MO, USA), 10 mM 2-mercaptoethanol (M6250, Sigma-Aldrich, Saint Louis, MO, USA) and 1 mM ethylenediaminetetraacetic acid (EDTA) (EDS, Sigma-Aldrich, Saint Louis, MO, USA) in a ratio of 1:3. The mixtures were then homogenised (5 pulses in total) gently to prevent the disruption of intact cell organelles, in an ice bath using a hand held mixer (BSB310, Breville, Australia). The mixture was then centrifuged at 1000 x *g* for 10 min at 4 ℃ (Heraeus Multifuge 15-R centrifuge, Thermo Fisher Scientific, Waltham, MA, USA) and the pellet containing the myofibrillar fraction was discarded. The supernatant was then centrifuged at 20,000 x *g* (Sorvall Evolution RC centrifuge, Thermo Fisher Scientific, Waltham, MA, USA) for 20 min at 4 ℃ to obtain the cytosolic fraction. After the centrifugation, the supernatant was collected as cytosolic extract and the extract was filtered using 0.45 µm PVDF syringe filter (Millex®-HV, Merck Millipore Ltd., Cork, Ireland), followed by storage in an ice bath. The cytosolic extract was freshly prepared for the assays. The pellets, which contain the large intact organelles including intact lysosomes, were resuspended in 50 mM sodium acetate buffer containing 1 mM EDTA and 0.2 % (v/v) Triton® X-100 (T8787, Sigma-Aldrich, Saint Louis, MO, USA) at pH 5 (Alberts et al., 2002; Mikami et al., 1987). The mixture was then centrifuged at 20,000 x*g* for 20 min and the supernatant was collected as the lysosomal extract. As cellular organelles might be disrupted if homogenisation is not done gently, the activities of the cathepsins in the lysosomal fraction of the control and PEF-treated raw muscles were determined to validate if the extraction process is appropriate (Alberts et al., 2002)

4.2.3.2 Cathepsin B, B+L and H assays

The activities of cathepsins B, B+L and H were determined based on the method from Chéret et al. (2007) with modifications. The assays were carried out in 96-well microplates consisting of 6 µL of 0.08 M CHAPS (3-[(3-Cholamidopropyl)

dimethylammonio]-1-propanesulfonate) (B21927, Alfa Aesar, Lancashire, United Kingdom), 1 µL of 1.4 M 2-mercaptoethanol, 16 µL of 0.04 M Brij® 35 (20150, Thermo Fisher Scientific, Waltham, MA, USA), 5 µL of 20 mM synthetic fluorogenic substrate and 70 µL of 0.4 mM acetate buffer (pH 4) containing 10 mM 2-mercaptoethanol and 1 mM EDTA at 30 ℃. The fluorogenic substrates for cathepsins B, B+L and H were N-benzyloxycarbonyl-arginine-arginine-7-amido-4-methylcoumarin hydrochloride (C5429, Sigma-Aldrich, Saint Louis, MO, USA), N-benzyloxycarbonyl-phenylalanyl-arginine-7-amido-4-methylcoumarin hydrochloride (C9521, Sigma-Aldrich, Saint Louis, MO, USA), and L-Arginine-7-amido-4-methylcoumarin hydrochloride (A2027, Sigma-Aldrich, Saint Louis, MO, USA), respectively, prepared in methanol. The details of the reagents used in the enzyme activity assays for cathepsins B, B+L and H are summarised in **Table 4-1**. The reaction was initiated by the addition of 200 µL of cytosolic sarcoplasmic protein extract with a control run in parallel where the protein extract was replaced by the sarcoplasmic protein extraction buffer. The fluorescence measurement was recorded for 10 min with intervals of 10 s at an excitation and emission wavelength of 355 nm and 460 nm, respectively, using a Varioskan™ LUX multimode microplate reader (Thermo Fisher Scientific, Waltham, MA, USA). The specific activities of the cathepsins B, B+L and H were expressed in FU (fluorescence unit) increase per min per gram of muscle (in triplicate for each whole brisket).

Table 4-1. A summary of the reagents used in the enzyme activity assays for cathepsins B, B+L and H, as described by Chéret et al. (2007).

Reagents		Volume (µL)
0.08 M CHAPS		6
1.4 M 2-mercaptoethanol		1
0.04 M Brij® 35		16
20 mM synthetic fluorogenic substrate in methanol	Cathepsin B: N-benzyloxycarbonyl-arginine-arginine-7-amido-4-methylcoumarin hydrochloride	5
	Cathepsin B+L: N-benzyloxycarbonyl-phenylalanyl-arginine-7-amido-4-methylcoumarin hydrochloride	
	Cathepsin H: L-Arginine-7-amido-4-methylcoumarin hydrochloride	
0.4 mM acetate buffer (pH 4) containing 10 mM 2-mercaptoethanol and 1 mM EDTA		70

4.2.3.3 Cathepsin D assay

The cathepsin D assay was carried out based on the methods of Anson (1938) and Rico et al. (1991) with modifications. The cathepsin D activity was determined by incubating the reaction mixture consisting of 2 mL of 0.6 % (w/v) acid-denatured haemoglobin (H2625, Sigma-Aldrich, Saint Louis, MO, USA) in 0.2 M citrate buffer (pH 3.7) at 45 ˚C for 30 min. The reaction was initiated by the addition of 0.375 mL cytosolic sarcoplasmic protein extract and was terminated by the addition of 0.75 mL of 10 % (w/v) trichloroacetic acid (TCA) (T6399, Sigma-Aldrich, Saint Louis, MO, USA). The mixture was filtered using a 0.45 µm PVDF syringe filter and the TCA-soluble peptides were measured spectrophotometrically at 280 nm using a UV-Visible spectrophotometer (GENESYS 10 UV, Thermo Fisher Scientific, Waltham, MA, USA). A blank was prepared similarly except the TCA was added before the reaction started. The specific activity of cathepsin D was expressed as the absorbance increase at 280 nm per hour per gram of muscle at 45 ℃ (in triplicate for each whole brisket).

4.2.4 Protein digestibility

4.2.4.1 In vitro digestion

The *in vitro* digestion of the meat SV-cooked at 60 °C for 24 h was conducted as described in section **3.2.4.1** with a modification of the pepsin concentration to 8 U/mg meat protein. The digests (20 mL) were sampled at 0, 30 and 60 min of gastric digestion (cumulative digestion time of 2, 32 and 62 min) and 60 and 120 min of small intestinal digestion (cumulative digestion time of 122 and 182 min). In order to stop the activities of the digestive enzymes, 12 µL of pepstatin A (ab141416, Abcam, Cambridge, UK) (0.5 mg/mL methanol) was added to every mL of gastric digest while 0.45 mL of SIGMAFAST™ protease cocktail solution (S8820, Sigma-Aldrich, Saint Louis, MO, USA) (1 tablet/50 mL Milli-Q water) was added to every mL of intestinal digest before storage at -20 °C (Menard et al., 2018). Four digestions were conducted each for the control and PEF-treated SV-cooked samples.

4.2.4.2 Preparation of the digests for further analysis

The digests were processed as described in section **3.2.4.2** for subsequent soluble nitrogen, SDS-PAGE and ninhydrin-reactive free amino nitrogen analyses.

4.2.4.3 Tricine SDS-PAGE and ninhydrin-reactive amino nitrogen analysis

Tricine-SDS-PAGE gel electrophoresis was carried out as described in section **3.2.4.4** on a 16.5 % Criterion™ Tris-tricine gel (3450064, Bio-Rad Laboratories, Hercules, CA, USA). Each lane was loaded with 20 µg of protein after adjusting the protein concentration of the digests-tricine sample buffer mixture (1610739, Bio-Rad Laboratories, Hercules, CA, USA) (1: 1 ratio), based on the nitrogen concentration of the filtered digests determined using the Kjeldahl method, as described in section **3.2.4.3**

(AOAC, 1981). The electrophoresis was then conducted with a Criterion™ Vertical Electrophoresis system (1656001, Bio-Rad Laboratories, Hercules, CA, USA) at a constant voltage of 125 V until the tracking dye front reaches the end of the gel. One gel was prepared for each digestion replicate. Ninhydrin-reactive free amino nitrogen released at different digestion time points was determined using ninhydrin reagent (N7285, Sigma-Aldrich, Saint Louis, MO, USA), as described in section **3.2.4.5.** (Moore, 1968). The ninhydrin analysis was repeated at least three times for each digestion time for each digestion replicate.

4.2.5 Microscopy analysis of digested muscles

The control SV-cooked and the PEF-treated SV-cooked samples were subjected to simulated oral-gastro-small intestinal digestion, as described in section **4.2.4.1**, in a polyester mesh without the addition of glass balls. Samplings were conducted at the end of 62 min and 182 min of oral-gastro-small intestinal digestion. The digested strips (62 and 182 min) were snap-frozen in isopentane (−160 °C) chilled by liquid nitrogen (−196 °C), followed by storage at −80 °C until use for histochemical analysis. The samples digested for 182 min were cut along the direction of the muscle fibre into strips of 10 mm x 3 mm x 3 mm and the pieces were immersed in 2.5 % glutaraldehyde in 0.1 M sodium cacodylate buffer at pH 5.6 overnight at room temperature before storage at 4 °C for TEM analysis. The undigested control cooked and PEF-treated cooked samples were cryofixed and chemically fixed for subsequent comparisons.

4.2.5.1 Histochemical analysis

The cryofixed muscle blocks (as mentioned in section **4.2.5**) were cut into 10 µm thick sections using a cryostat (CM1950, Leica Microsystems GmbH, Wetzlar, Germany) at -20 °C. The sections were mounted on glass slides followed by staining with Picro-Sirius

Red (Flint & Pickering, 1984). In brief, the muscle sections were incubated in acetone for an hour followed by picroformalin (5 % formaldehyde, 90 % ethanol in saturated picric acid) for 10 min. Then, the sections were submerged into 90 % ethanol for 1 min, distilled water for 10 min and Picro-Sirius Red stain (0.1 % Sirius Red in saturated picric acid) for 1 h. After that, the sections were put in a bath of 0.01 M HCl for 5 min and distilled water for 1 min. Finally, the sections were dehydrated by dipping the slides into a bath of 95 % ethanol and two baths of 100 % ethanol, followed by two baths of methylcyclohexane. Observations were conducted using an optical transmission microscope coupled to a digital acquisition kit (Olympus BX61 microscope, Olympus DP 71 digital camera, Olympus France SAS, Rungis, France). Observations were made on histological sections from three digestion replicates.

4.2.5.2 Transmission electron microscopy analysis

The chemically fixed samples (as mentioned in section **4.2.5)** were further processed for TEM analysis, as described in section **3.2.5** with modifications. The samples were post-fixed in 1 % osmium tetroxide in 0.1 M sodium cacodylate buffer (pH 7.2) and were dehydrated through a graded series of ethanol (70 %, 95 % and 100 %). The dehydrated sections were then embedded in epoxy resin (TAAB, Eurobio Scientific, Les Ulis, France), followed by sectioning into 90 nm of ultra-thin sections. The ultra-thin sections were mounted on copper grids, and were stained with saturated uranyl acetate and lead citrate for 30 min each (Reynolds, 1963). The ultrastructure was viewed using a transmission electron microscope (HM 7650, Hitachi, Tokyo, Japan) coupled with a CCD AMT HR digital camera system (Hamamatsu Photonics, Shizuoka, Japan). The reagents used in this section were electron microscopy grade (Electron Microscopy Science, Hatfield, PA, USA). Observations were made on TEM sections from two digestion replicates.

4.2.6 Statistical analysis

The data were reported as means ± standard deviation of means from at least three replications. Statistical analysis was conducted using two-way ANOVA for the cathepsins activity analyses using OriginPro 2018b software (OriginLab Corporation, Northampton, MA, USA). Repeated measures ANOVA by Generalised Linear Model (IBM® SPSS® Statistic version 25, IBM Corporation, Armonk, NY, USA) was performed for protein digestibility analysis and no violation of sphericity was detected using Mauchly's Test. Both analyses were then tested using Tukey's post-hoc analysis to evaluate the significance of difference at a confidence level of 0.05.

4.3 Results and discussion

4.3.1 Effect of PEF on SV cooking on endogenous enzyme activities of beef brisket

In order to validate the proposed mechanism that PEF tenderises meat as a result of the release of lysosomal proteases into the cytosol, the activities of the lysosomal proteases in the cytosolic extract of both control and PEF-treated muscles were quantified. The specific activities of the cathepsins B, B+L, H and D of the control and PEF-treated brisket at different SV cooking times are depicted in **Figure 4-3**. Prior to SV cooking (time = 0 h), there was no significant difference in the specific activities of the cathepsins. Although PEF-treated muscles had higher specific activity of cathepsin B, the difference was insignificant. The specific activities of the cathepsins in the cytosol of PEF-treated samples were not increased by the action of PEF. This could signify that low intensity PEF treatment does not have an electroporation effect on the lysosomal membrane of the samples. As the lysosomes are localised within cytoplasm which is high in electrolytes, higher frequency electric fields have to be used to disrupt the cytosolic contents (Saito et al., 2016). High voltage nano-second electric pulses have been reported to affect cell

organelles, such as lysosomes (Batista Napotnik et al., 2016). However, it is possible that the lysosomes were ruptured during the homogenisation process for cytosolic sarcoplasmic extraction. To verify if the homogenisation process is appropriate, the activity of cathepsin B+L in the lysosomal fraction of the control and PEF-treated raw samples was determined. There was still extractable lysosomal enzymes activity of both control and PEF-treated raw muscles. No significant difference was observed in the activity of the lysosomal cathepsin B+L between the control untreated (1.4 ± 0.1 FU/min/g meat) and PEF-treated samples (1.2 ± 0.4 FU/min/g meat). These findings showed that the homogenisation during the extraction process was appropriate and did not rupture the lysosomes. In addition, the muscles used in this experiment were frozen-thawed before PEF processing and were frozen thawed again after sampling and before extraction. Freezing and thawing might result in the rupture of lysosomes, masking the electroporation effect of PEF on the lysosomes. Rapid freezing and thawing without the use of cryo-protectant has been reported to rupture lysosomes of living cells (Huebinger, 2018). Kaur et al. (2020) also reported an increase in cathepsin B activity in the frozen-thawed beef brisket after storage at -20 ℃ for 4 days when compared to the samples stored at 4 ℃. The increment in cathepsin B activity was suggested to be due to the formation of ice crystals which may have ruptured the lysosomes, resulting in the release of the cathepsins. Thus, in future experiments, fresh samples should be used, and the endogenous enzymes activity should be quantified immediately after PEF treatment, to eliminate the effect of freezing and thawing on the lysosomes.

In addition, PEF treatment might have weakened the lysosomal membrane integrity, causing the membrane to rupture more easily than the untreated membrane at elevated temperatures, such as during low temperature cooking. Higher ageing temperatures (22 ℃ for 4 h followed by 12 ℃ for 8 h) of *Longissimus dorsi* muscles (animal source not

mentioned) resulted in higher free enzyme activities of lysosomal enzymes cathepsin C and β-glucuronidase than the lower ageing temperature (2 ℃ for 12 h), suggesting elevated temperatures facilitate the rupture of the lysosomes (Moeller et al., 1976). An increase in the activity of cathepsin B+L in the soluble fraction and decreased activity in the membrane fraction of the marinated minced bovine *M. sternomandibularis* were observed when the marination temperature increased from 15 ℃ to 30 ℃, suggesting an enhanced release of lysosomal enzymes at a higher temperature (Ertbjerg et al., 1999). As such, the activities of the cathepsins at different time points during low temperature cooking were examined. As shown in **Figure 4-3**, there was no significant difference in the specific activities of the cathepsins between the control and the PEF-treated meat at different cooking time points at 60 ℃.

It was observed that the specific activities of the cathepsins dropped during the first 0.5 h of SV cooking at 60 ℃, especially for cathepsin H. No activity of cathepsin H was detected in both control and PEF-treated muscles after 0.5 h of cooking. Cathepsin H extracted from rabbit *Longissimus dorsi* muscles was reported to be heat-stable up to 50 ℃ and lost its activity completely after 10 min of incubation at 60 ℃ and above (Matsuishi et al., 2003). Kaur et al. (2020) also found that no extractable activity of cathepsin H was detected in the beef brisket after cooking at 55 ℃, 60 ℃, 65 ℃, and 70 ℃ for 1 h. They suggested that cathepsin H is unlikely to contribute to meat tenderisation during SV cooking due to its relatively low heat stability.

In contrast, the initial specific activities of cathepsins B and B+L of both control and treated muscles decreased more gradually after 0.5 h of cooking. The specific activity of cathepsin B of the control and PEF-treated muscled reduced by 41.9 % and 44.8 %, respectively, after 0.5 h of cooking. As for the specific activity of cathepsin B+L, the

initial activity was reduced by 54.0 % and 44.3 % in the control and PEF-treated samples correspondingly. The specific activities of cathepsins B and B+L continued to lose about 99.8 % and 93.7 % of their initial activities respectively in the control samples after 1 h of cooking. Comparable observations were made for the PEF-treated samples where their initial specific activities of cathepsins B and B+L decreased by 98.2 % and 95.7 % respectively after SV cooking for an hour. The activities of cathepsins B and B+L of both samples were completely lost after 5 h of SV cooking at 60 ℃. A similar observation was made by Kaur et al. (2020), where the activities of cathepsins B and B+L of the beef brisket lost significantly after 1 h of SV cooking at 60 ℃, and their activities were completely lost after 5 h of cooking. However, the activities of cathepsin B and L were still measurable in *Semitendinosus* muscles obtained from both cows and young bulls after cooking at 63 ℃ for 19.5 h (Christensen et al., 2013). This difference might be due to the properties of different meat cuts and post-slaughter handling of meat samples.

As for cathepsin D, the initial specific activity of the control and PEF-treated muscles dropped by 43.8 % and 38.0 % respectively after cooking for 0.5 h. No activity was detected after 1 h of cooking. Draper and Zeece (1989) found that Cathepsin D extracted from a bovine heart lost 50 % of its initial activity after incubation at 60 ℃ for 30 min, which is similar to the findings of this experiment. Sous vide cooking time was found to have a significant interaction between the specific activities of the cathepsins ($p < 0.05$), but PEF treatment was not.

As most of the cathepsins were inactivated after SV cooking at 60 ℃ for an hour, multistage SV cooking could be implemented with a lower initial cooking temperature to promote the proteolytic activity of the cathepsins (Ismail et al., 2019; Uttaro et al., 2019). The activities of cathepsins B and L increased in porcine *Semitendinosus* and *Longissimus*

dorsi when incubated at temperatures from 48 to 58 ℃ (Christensen, Ertbjerg, et al., 2011). Increasing activities of cathepsins B, L, and H were also observed in beef brisket cooked at 50 ℃ for the first 5 h (Kaur et al., 2020). Higher temperature cooking could be done at the final stage of multi-stage SV cooking for microbiological safety (Purslow, 2018).

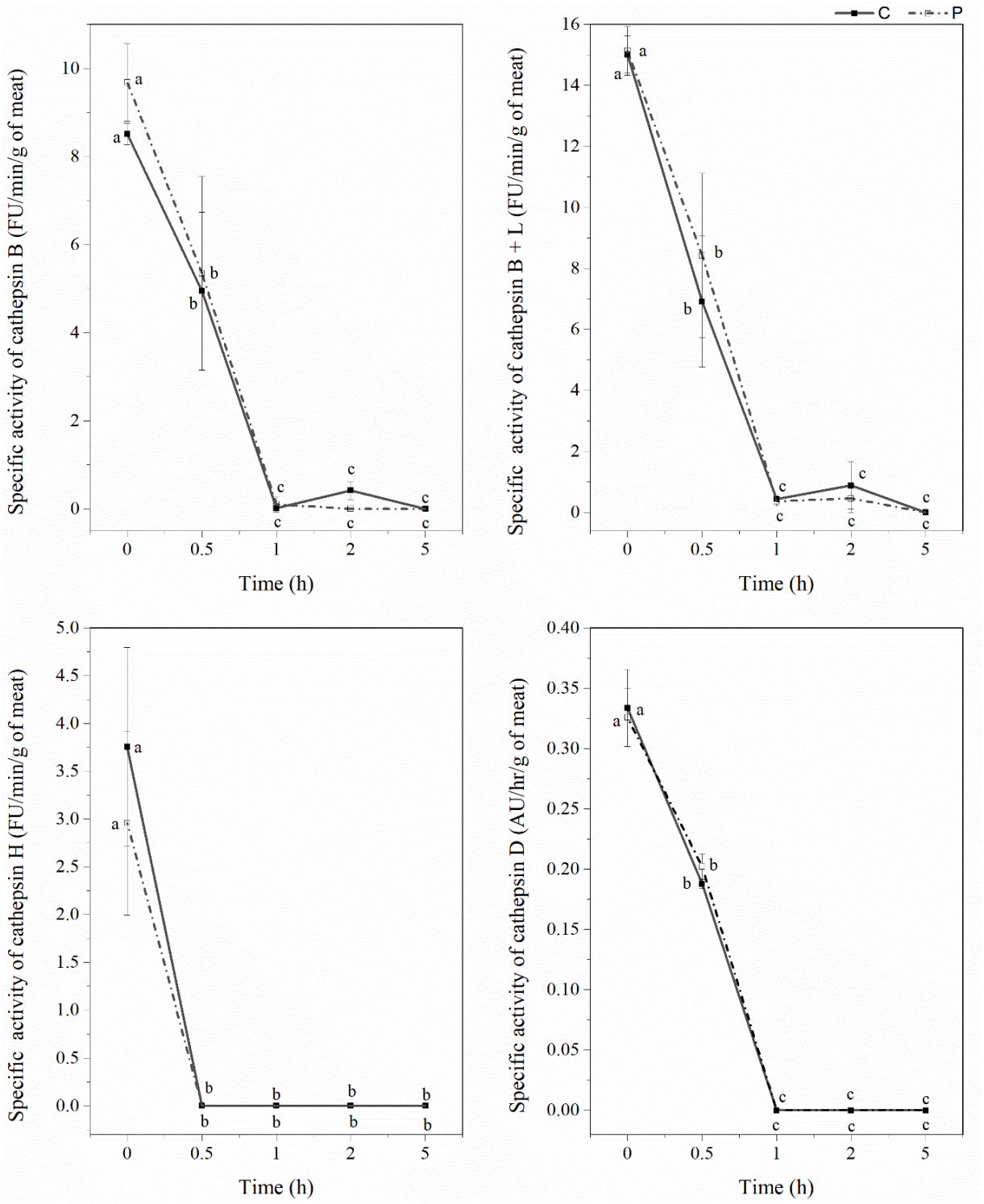

Figure 4-3. The specific activities of cytosolic cathepsins B, B+L, H and D extracted from the control (C) and the PEF-treated (P) meat after SV cooking for 0, 0.5, 2 and 5 h at 60 °C.

There was no significant difference in enzyme activities between treatments, but there were differences in enzyme activities for different SV cooking times ($p < 0.05$). There was no significant interaction between treatment and SV cooking time. Data points with different letters within the same graph differ significantly ($p < 0.05$). Error bars represent the standard deviation. $N = 3$.

4.3.2 Effect of PEF and SV cooking on muscle protein digestibility *in vitro*

4.3.2.1 Tricine SDS-PAGE

The proteolysis of the meat proteins during *in vitro* oral-gastro-small intestinal digestion was studied using tricine SDS-PAGE (**Figure 4-4**). During 62 min of *in vitro* oral-gastric digestion, some differences in the intensities of the protein bands were observed. After 32 min of simulated oral-gastric digestion, the band intensities of the MHC (220 kDa) and C-protein (140 kDa) of the digest of the PEF-treated SV-cooked muscles were lighter than the digest of the control SV-cooked muscles, indicating more breakdown of these proteins in the former. In addition, the intensity of the band with molecular weight (MW) of 36 kDa of the digest of PEF-treated SV-cooked muscles was higher than the control untreated SV-cooked meat digest. A new band with MW 34 kDa was observed in the digest of the treated sample only. Protein bands with molecular weight of 36 kDa and 34 kDa have been reported to be the α- and β-subunit of the β-actinin respectively (Obinata et al., 1981). Similar observations were also made at the end of the simulated oral-gastric digestion (62 min), with the PEF-treated SV-cooked samples displaying improved gastric proteolysis compared to the control SV-cooked samples.

After 122 min of *in vitro* oral-gastro-small intestinal digestion, high MW proteins (MW > 50 kDa) of both control SV-cooked and PEF-treated SV-cooked samples were fully digested by the action of pancreatin. A protein band with a MW of 47 kDa was found in the digest of control SV-cooked meat but not in the digest of the PEF-treated SV-cooked meat. This band has previously been identified as β-enolase (Lindahl et al., 2010) or the degradation product of desmin during aging process (Kaur et al., 2016). An additional hour of digestion resulted in the complete disappearance of this band in the digest of control SV-cooked meat. This observation shows that the protein corresponds to this band

(47 kDa) was digested faster in the PEF-treated SV-cooked meat. Moreover, the bands with MW of 34 kDa, 32 kDa, and 31 kDa were found in both samples at the end of 122 min of simulated digestion, with the intensities of these bands higher in the control SV-cooked meat digests. The protein bands with MW of 34 kDa and 32 kDa (unidentified protein) were not detected in the digest of both the control and the treated samples at the end of 182 min of simulated digestion. At the same time, the intensity of the band with MW of 31 kDa (unidentified protein) was further reduced, with a higher band intensity found in the digest of control SV-cooked samples. Furthermore, a new band with a MW of 26 kDa, which could be the hydrolysis product of higher MW proteins, formed only in the digest of PEF-treated SV-cooked meat (Kaur et al., 2014). These observations demonstrated that the PEF-treated SV-cooked meat was better hydrolysed when compared to the untreated SV-cooked meat during simulated digestion. Bhat, Morton, Mason, Jayawardena, et al. (2019) also observed a greater and faster proteolysis of PEF-treated cooked beef. He proposed that PEF treatment resulted in protein structural changes and improved membrane permeability in meat, increasing the availability of proteolytic sites to digestive enzymes. Overall, the SDS-PAGE analysis demonstrated that PEF treatment influenced the digestive properties of the SV-cooked meat, where the protein and peptide profile of the meat digests was modified.

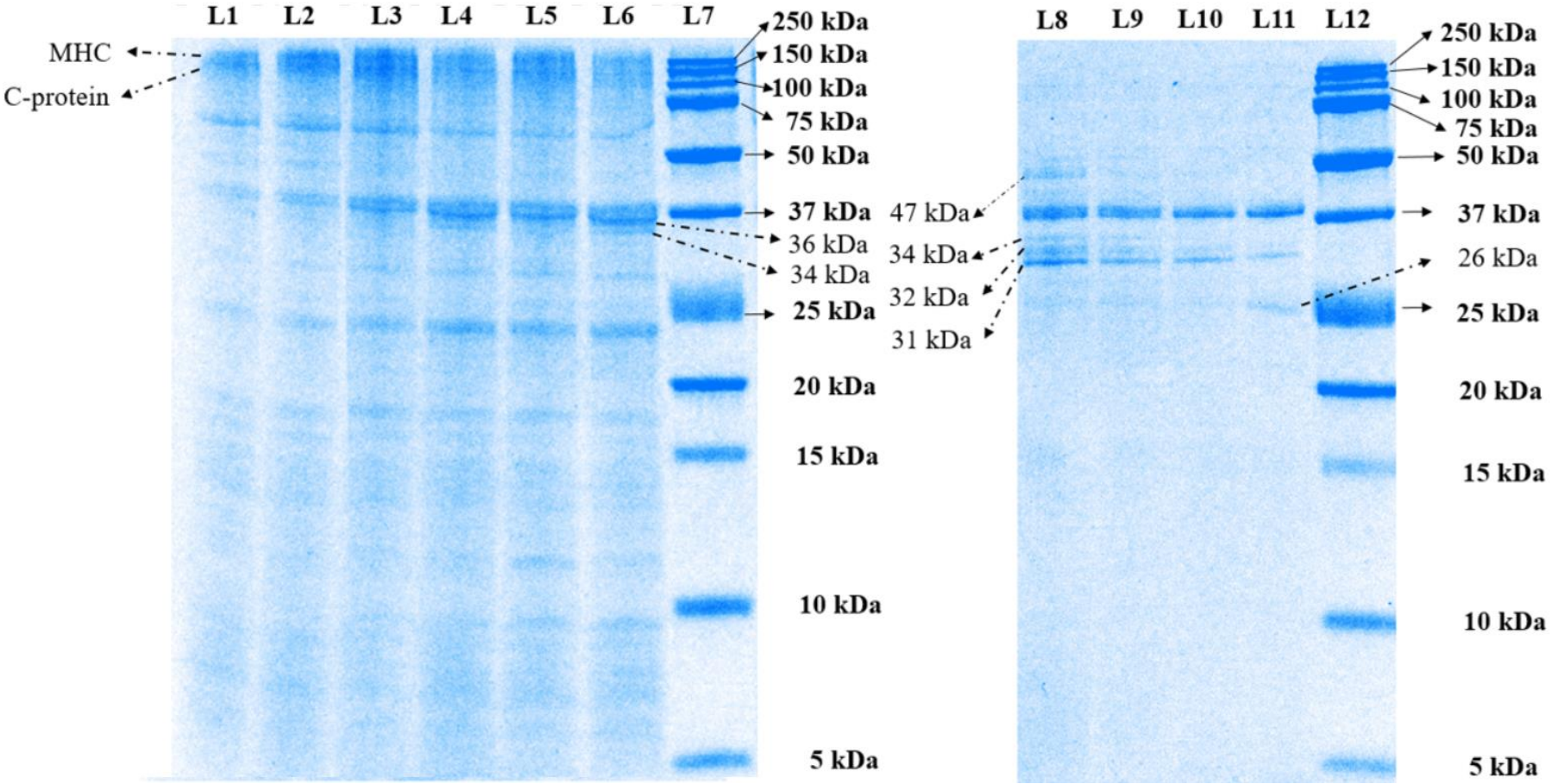

Figure 4-4. Tricine SDS-PAGE electrophoretogram showing the protein profile of the digests of control SV-cooked and PEF-treated SV-cooked meat during simulated digestion.

L7 and L12 are the molecular weight standard, labelled in kDa. L1, L3 and L5 denote control SV-cooked samples at 2, 32 and 62 min of oral-gastric digestion respectively. L2, L4 and L6 denote PEF-treated SV-cooked samples at 2, 32 and 62 min of oral-gastric digestion respectively. L8 and L10 represent control SV-cooked samples at 122 and 182 min of oral-gastric-small intestinal digestion respectively. L9 and L11 represent PEF-treated SV-cooked samples at 122 and 182 min of oral-gastric-small intestinal digestion respectively. The protein were identified on the electrophoretogram as described by Kaur et al. (2014), Kaur et al. (2016), and Boland et al. (2019). MHC stands for myosin heavy chain.

4.3.2.2 Ninhydrin-reactive amino nitrogen

The ninhydrin-reactive amino nitrogen released by meat samples at different digestion time points was determined as a quantitative measure of *in vitro* protein digestibility. A higher percentage of ninhydrin-reactive amino nitrogen indicates a greater extent of protein hydrolysis by the digestive enzymes. As summarised in **Table 4-2**, there was no difference in the percentage of ninhydrin-reactive amino nitrogen released after 122 min of *in vitro* oral-gastro-small intestinal digestion between the control SV-cooked and the PEF-treated SV-cooked meat ($p > 0.05$). However, at the end of 182 min of simulated digestion, there was significantly more ninhydrin-reactive amino nitrogen released from the PEF-treated SV-cooked meat than the control SV-cooked meat. Overall, the combined PEF-SV process increased the *in vitro* oral-gastro-small intestinal protein digestibility by approximately 28.6 %, which is in agreement with the findings of an increased proteolysis of the PEF-treated SV-cooked meat as discussed in section **4.3.2.1**. However, Alahakoon et al. (2019) reported that the *in vitro* protein digestibility of beef brisket was unaffected by the combined PEF-SV cooking process. Although the experiment was conducted with the same meat cut (beef brisket) and processing parameters (0.7 kV/cm, 90 to 100 kJ/kg), the authors reported no significant difference in the trichloroacetic acid (TCA)-soluble peptides concentration between the control SV-cooked and PEF-treated SV-cooked meats at the end of the simulated digestion. This might be due to the difference in the assay used in determining the extent of proteolysis. Measuring the degree of hydrolysis with TCA-soluble peptides concentration assumes that all the intact proteins are precipitated by TCA and only small peptides and amino acids remain in the soluble fraction (Rutherfurd, 2010). However, this assumption might be incorrect as TCA has been reported unable to precipitate up to 70 % of proteins or peptides larger than 10 kDa from ileal digest. Thus, quantifying TCA-soluble peptides might overestimate the degree of proteolysis if the

digest contains more of the larger peptides that cannot be precipitated by TCA. In addition, this method does not quantify the cleavage of peptide bonds (Rutherfurd, 2010). Pulsed electric field treatment (0.6 kV/cm, 73.28 kJ/kg) was found to improve the *in vitro* protein digestibility of water bath-cooked bovine *Semitendinosus* (core temperature of 75°C) by approximately 2 %, based on the protein content left undigested in the samples, quantified using the Kjeldahl method (Bhat, Morton, Mason, Jayawardena, et al., 2019).

Table 4-2. Ninhydrin-reactive amino nitrogen released from the control SV-cooked and the PEF-treated SV-cooked meat after *in vitro* oral-gastric (2, 32 and 62 min) and further small intestinal (122 & 182 min) digestion.

Cumulative digestion time (min)		**2**	**32**	**62**	**122**	**182**
Ninhydrin-reactive amino nitrogen (%)	**Control -SV**	1.9 ± 0.0^{aA}	2.3 ± 0.4^{aA}	2.7 ± 1.0^{aA}	8.1 ± 1.2^{bA}	9.8 ± 0.6^{cA}
	PEF-SV	1.9 ± 0.0^{aA}	2.7 ± 0.6^{abA}	3.4 ± 1.0^{bA}	8.4 ± 0.4^{cA}	12.6 ± 0.7^{dB}

Values with different lower-case letters within the same row differ significantly ($p < 0.05$).

Values with different upper-case letters within the same column differ significantly ($p < 0.05$).

Data are shown as mean ± standard deviation of mean. $N = 4$ (four replicates with 3 measurements from each replicate).

4.3.2.3 Structure of digested meat samples

The microstructure of the control SV-cooked and the PEF-treated SV-cooked meat at different stages of *in vitro* digestion is shown in **Figure 4-5**. Pulsed electric field treatment did not affect the microstructure of the SV-cooked meat. The microstructure of both control and PEF-treated samples appeared to be similar after SV cooking. Although a reduction in muscle cell sizes and the formation of gaps between muscle fibres were observed in PEF-treated raw muscles by Gudmundsson and Hafsteinsson (2001), these observations were not detected in PEF-treated SV-cooked muscles in this experiment. This might be due to the effect of SV cooking on muscle structure being larger and thus masking the effect of PEF on the muscle microstructure. After 62 min of *in vitro* oral-

gastric digestion, the muscle structure of both control SV-cooked and PEF-treated SV-cooked muscles was damaged at the edges of the meat sections. Further *in vitro* digestion with the addition of pancreatin at pH 7.0 ± 0.1 for 2 h resulted in more breakdown of the muscle cells and connective tissue, while the disruption extended towards the core of the samples. The damage to the muscle structure was greater in the PEF-treated SV-cooked samples at the end of both *in vitro* oral-gastric and oral-gastro-small intestinal digestion. This indicates that the PEF-treated SV-cooked brisket was more susceptible to enzymatic hydrolysis by the digestive enzymes, which is in agreement with the outcomes from the SDS-PAGE and ninhydrin-reactive amino nitrogen analysis as mentioned in section **4.3.2.1** and **4.3.2.2**, respectively. Swollen muscle cells were observed in both control SV-cooked and PEF-treated SV-cooked meat after 62 min of simulated oral-gastric digestion, with an enhanced swelling effect observed in the PEF-treated meat. Bordoni et al. (2014) observed the swelling phenomena of muscle cells due to the penetration of the saliva and gastric juices into the meat matrix during simulated digestion. Swelling of muscle cells during gastric digestion has been reported to be due to the effect of acidic gastric juice but not the action of pepsin (Astruc, 2014b). Astruc detected an increment in the muscle cell size in cooked meat samples incubated in simulated gastric juice without the addition of pepsin. Acidic pH (pH < 3.52) resulted in an increment in the net positive charges on the myofibrillar proteins which increased the electrostatic repulsion forces between protein molecules (Ke et al., 2009). This might result in larger spaces between the myofilaments, allowing the penetration of the digestive juice into the meat matrix. In addition, PEF has been reported to lead to the formation of pores in cell membranes due to electroporation (Alahakoon et al., 2016). The formation of pores might enhance the diffusion of digestive juices into the meat matrix. The enhanced penetration of digestive juices facilitates the accessibility of digestive enzymes to their substrates, enabling

enzymatic protein hydrolysis. Thus, the increased enzymatic breakdown of PEF-treated SV-cooked muscle structure could be a consequence of the enhanced diffusion of digestive juices, displaying as more swollen cells of the PEF-treated samples during simulated digestion as observed in **Figure 4-5**, promoting the action of digestive enzymes.

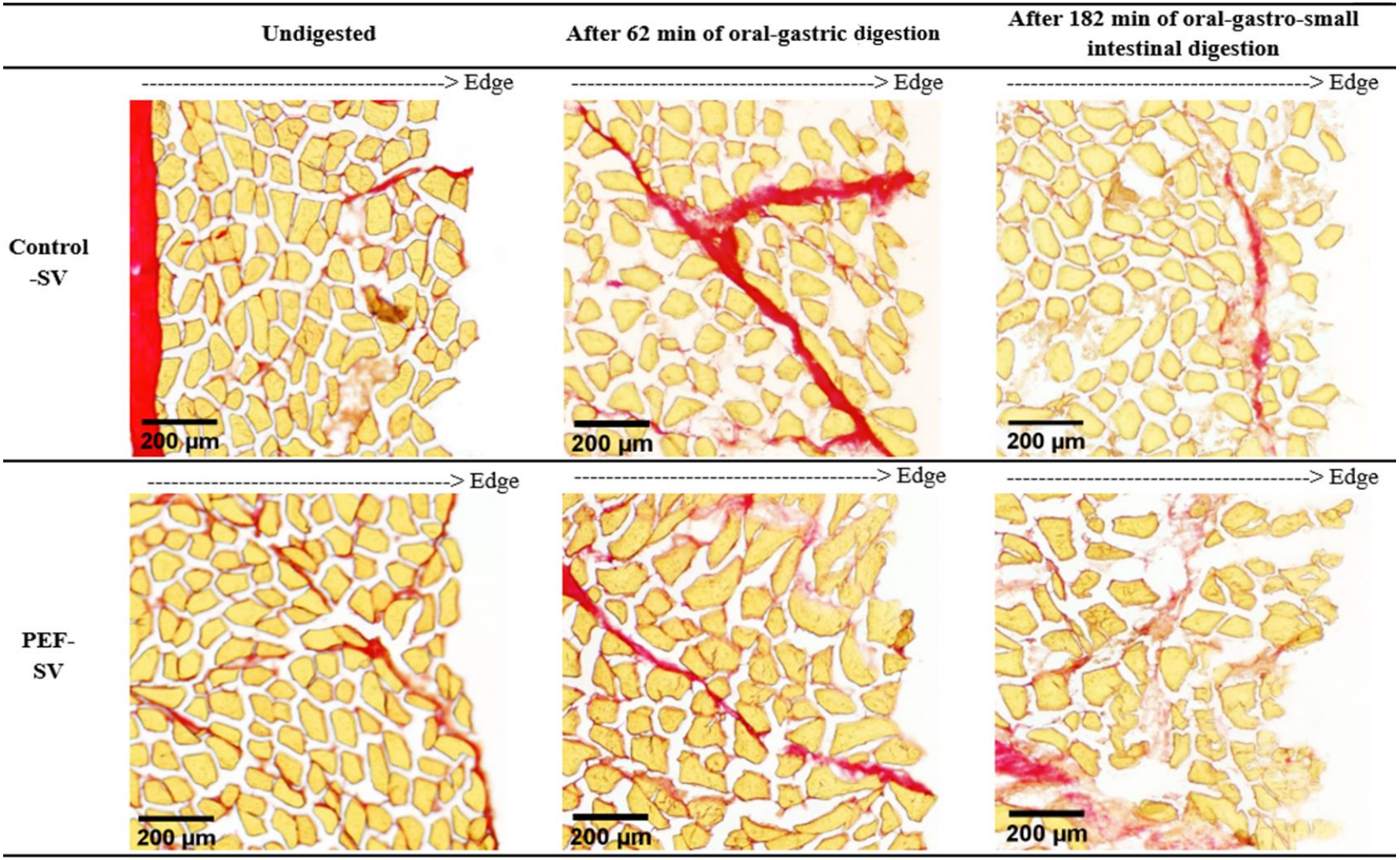

Figure 4-5. Histological sections of the control SV-cooked and the PEF-treated SV-cooked meat at different digestion time points, showing more severe structural degradation of PEF-treated meat by the digestive enzymes at the end of simulated digestion. Connective tissue was stained in red by Sirius Red dye and muscle cells were stained in yellow by picric acid.

As presented in **Figure 4-6**, the ultrastructure of the control SV-cooked and PEF-treated SV-cooked meats was similar. Pulsed electric field treatment did not affect the ultrastructure of the SV-cooked meat. Ultrastructural modification has been reported in PEF-treated raw muscle. Elongated sarcomeres (**Figure 3-2**) and sarcomeres with jagged edges (Faridnia et al., 2015) were found in low intensity PEF-treated uncooked meat. However, these were not observed in the PEF-treated SV-cooked meat. In contrast, both control SV-cooked and PEF-treated SV-cooked meats had coagulated myofibrils accompanied with the formation of granular aggregates, which have previously been detected in thermally treated muscles (Leander et al., 1980; Zhu, Kaur, Staincliffe, et al., 2018). These observations show that SV cooking had a major effect on the muscle ultrastructure when compared to PEF treatment. In addition, degradation of the sarcomeres along the Z-disks was observed in both control and PEF-treated muscles after SV cooking (white arrows in Figure 6A and 6C). The effect of SV cooking on the degradation of sarcomeres along the I-band and Z-disk junctions is considered minor, as the denaturation temperatures of the major I-band and Z-disk associate proteins are mostly higher than the 60 ℃ (SV cooking temperature). For instance, the actin, which is the major component of I-bands and the core of a Z-disk, has maximum thermal denaturation temperatures (Tmax) range from 70 to 80 ℃ (Knoll et al., 2011; Purslow et al., 2016). Nevertheless, prolonged heating of meat might result in a small proportion of actin denaturation at a temperature below its Tmax, but above its denaturation onset temperature (Martens et al., 1982). Disintegration of thin filaments at the I-band and Z-disk junctions were observed in bovine muscles cooked to an internal temperature of 63°C, and the extent of disintegration increased as the final internal temperature raised to 73 ℃ (Leander et al., 1980). The degradation of the sarcomeres along the I-band and Z-disk junctions could also be due to postmortem proteolysis (Astruc, 2014b) and/or protein

hydrolysis during the initial stage of SV cooking by the action of endogenous enzymes. The modification of the I-band and Z-disk junctions has been detected in aged muscles as a result of postmortem proteolysis (Astruc, 2014b; Ouali, 1990). Endogenous enzymes cathepsin H, and cathepsins B, L, and D, were found to be active in the first 30 min and 1 h of SV cooking, respectively (**Figure 4-3**). Structure disruption due to postmortem proteolysis and the action of endogenous enzymes during low temperature long time cooking might promote the action of digestive enzymes during subsequent digestion (Astruc, 2014b).

After 182 min of *in vitro* oral-gastro-small intestinal digestion, the breakdown of the myofibrils was observed in both control SV-cooked and PEF-treated SV-cooked muscles (**Figure 4-7)**. The Z-disks were degraded and the sarcomeres were broken down. More severe Z-disk and sarcomere disruption was observed in the digested PEF-treated SV-cooked muscles than in the digested control SV-cooked muscles. This shows that the PEF-treated SV-cooked muscles were more susceptible to proteolysis by the digestive enzymes, which is consistent with the microstructure analysis as discussed above. In addition, more coagulated and elongated I-bands were found in the digested PEF-treated SV-cooked muscles. This was also observed in the digested raw PEF-treated bovine *Longissimus thoracis* muscles as shown in **Figure 3-5,** where the digested PEF-treated raw muscles had better protein digestibility than the untreated samples. The more coagulated I-bands of the digested PEF-treated muscles might be due to more acid denaturation of the protein by the gastric juices, which exposed buried peptide bonds for the access of digestive enzymes, leading to improved proteolysis (Chian et al., 2019; McGuire & Beerman, 2012).

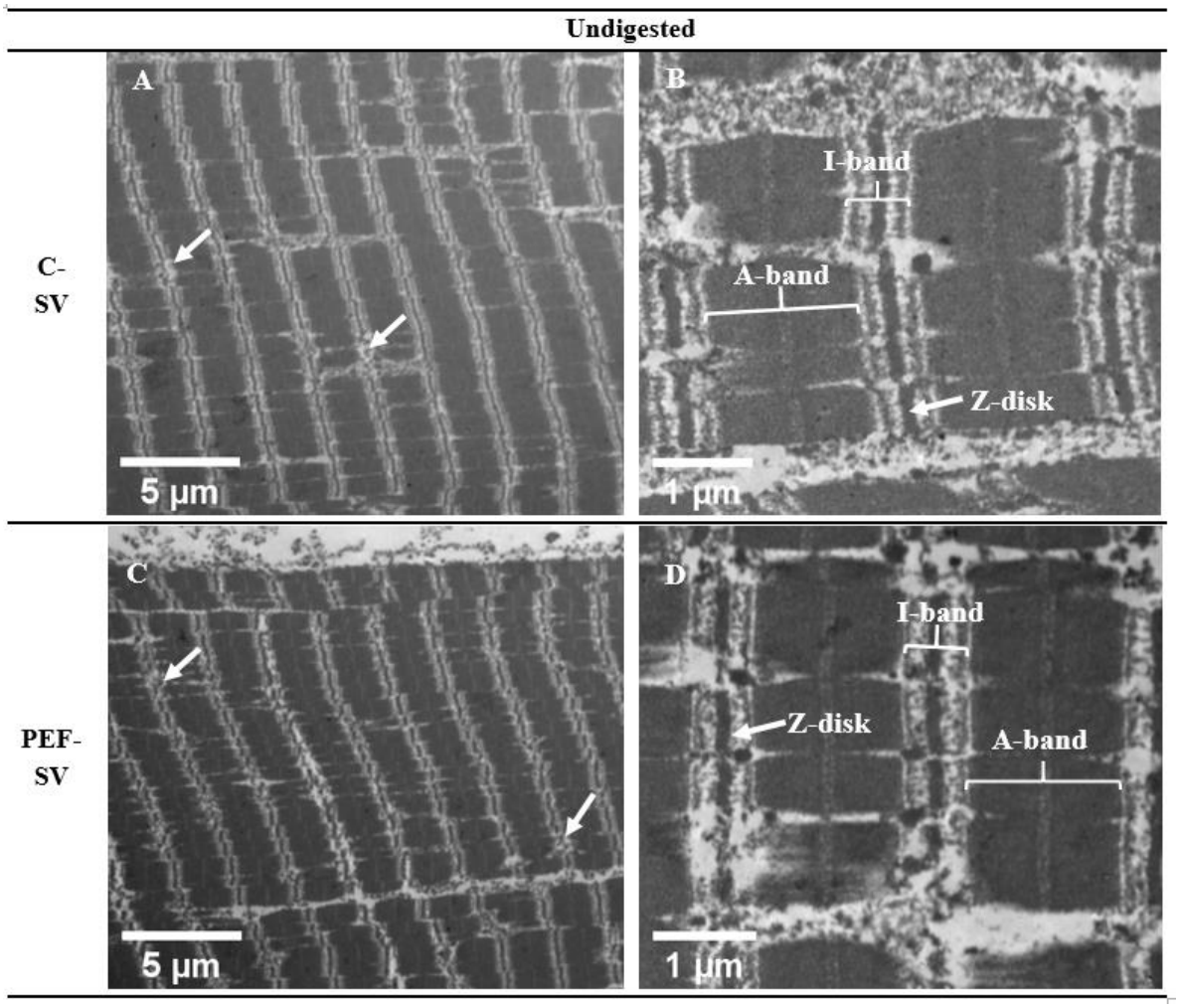

Figure 4-6. Transmission electron micrographs showing the ultrastructure of the control (C) SV-cooked (A, B) and the PEF-treated SV-cooked (C, D) beef brisket before simulated oral-gastro-small intestinal digestion.

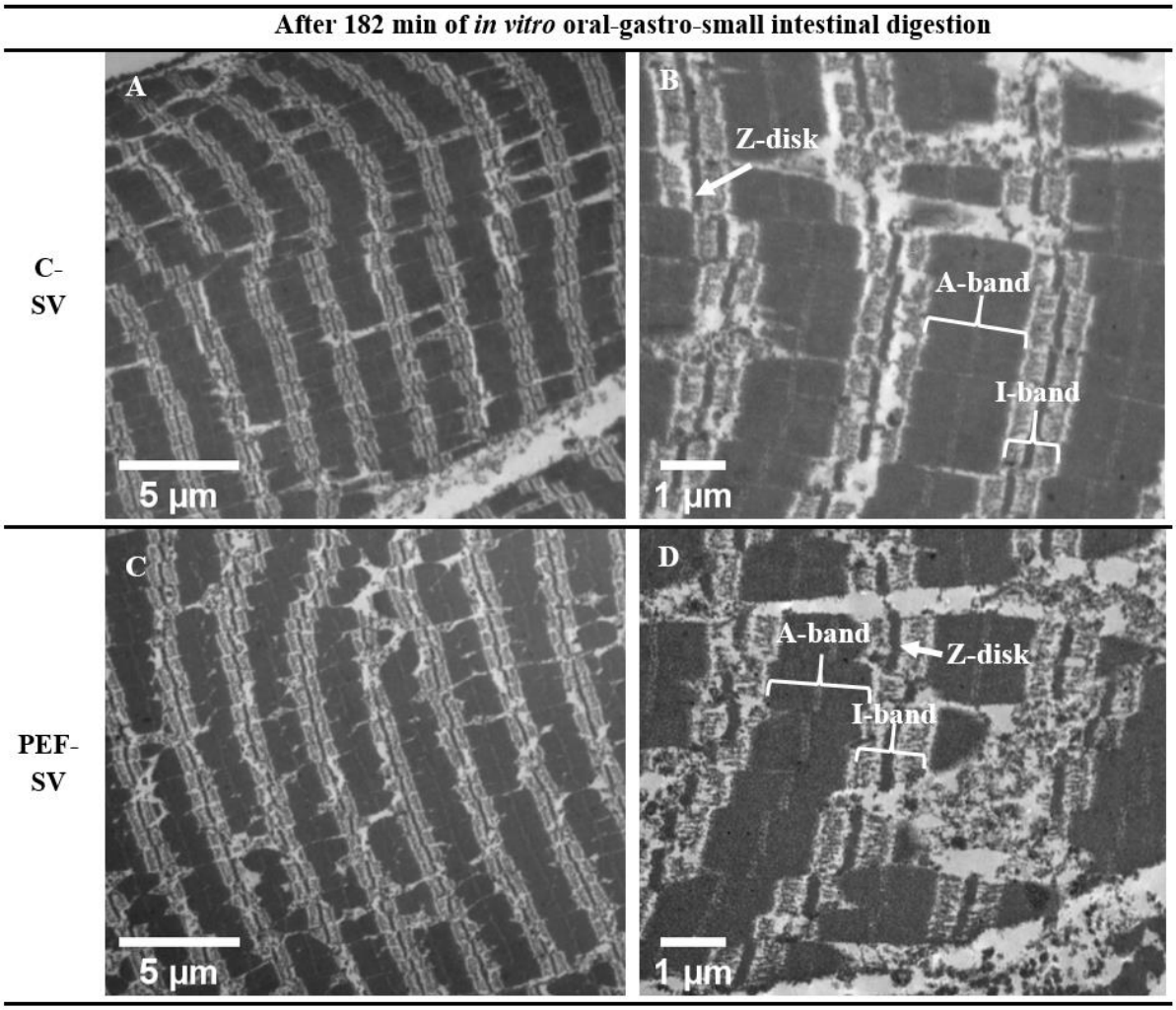

Figure 4-7. Transmission electron micrographs showing the ultrastructure of the control (C) SV-cooked (A, B) and the PEF-treated SV-cooked (C, D) beef brisket after 182 min of simulated oral-gastro-small intestinal digestion.

The digested PEF-treated SV-cooked meat had more damaged sarcomeres and more coagulated and elongated I-bands, indicating more severe proteolysis by the digestive enzymes.

4.4 Conclusions

The results of this experiment provided insights on the effects of low intensity PEF on the activities of the cytosolic cathepsins. There was no significant difference in the specific activities of cathepsins in the cytosolic and lysosomal extracts of both control and PEF-treated raw samples. This indicates that PEF treatment did not promote the release of cathepsins from lysosomes by the electroporation. However, it is possible that the lysosomes were ruptured during the freezing and thawing process of the meat samples. Thus, it is recommended to conduct future studies using unfrozen meat samples to eliminate the effect of freezing and thawing on the lysosomes. Furthermore, the endogenous enzymes activity should be quantified immediately after PEF treatment. There was also no significant difference observed in the specific activities of the cathepsins between the control and PEF-treated samples during subsequent SV cooking at 60 °C. The specific activities of the cathepsins were found to be affected significantly by the SV cooking time at 60 °C but not by PEF treatment. Multistage SV cooking with lower initial and higher final cooking temperature could be adopted to promote the enzymatic hydrolysis by the cathepsins for meat tenderisation, while ensuring microbiological safety of meat.

The *in vitro* protein digestibility of meat was improved by the combined PEF-SV process, where the PEF-treated SV-cooked meat had higher ninhydrin-reactive amino nitrogen ($p < 0.05$) released at the end of the simulated digestion and improved proteolysis observed using tricine-SDS-PAGE, compared to the control SV-cooked meat. The improvement in protein digestibility might be due to the disruption of muscle structure by the combined PEF-SV process. Although the muscle micro- and ultrastructure of the control SV-cooked and PEF-treated SV-cooked meat was similar, their muscle structures changed differently

during simulated digestion. More swollen muscle cells were observed in the PEF-treated SV cooked meat after 62 min of simulated oral-gastric digestion, suggesting an enhanced penetration of digestive juices in the treated samples. The enhanced penetration of digestive juices is postulated be due to the formation of pores in muscle cell membranes as a result of the electroporation effect of PEF, facilitating the accessibility of digestive enzymes to their substrates. More damaged muscle microstructure and ultrastructure was also detected in the PEF-treated SV-cooked muscles at the end of *in vitro* oral-gastro-small intestinal digestion, compared to the control cooked samples. These observations show that a combination of PEF treatment and SV cooking process resulted in muscle structural changes, leading to an improvement in *vitro* protein digestibility of meat.

Chapter 5 [4]Shockwave (SW) processing of beef brisket in conjunction with sous vide (SV) cooking: Effects on protein structural characteristics and muscle microstructure

5.1 Introduction

Emerging technologies for the production of high-quality products are receiving considerable interest from the meat industry. Technologies such as SW processing (Bolumar et al., 2013; Claus, 2017), PEF processing (Faridnia et al., 2014), SV cooking (Roldan et al., 2013) and exogenous enzyme technologies (Zhu, Kaur, Staincliffe, et al., 2018) have been investigated in designing processes that may effectively improve meat quality, especially those low value tougher meat cuts. Low value meat cuts such as brisket (*Superficial* and *Deep pectoral*) usually have a problem of background toughness due to high connective tissue content (Boland et al., 2019). Processing may modify the protein profile and induce structural changes to meat, affecting the organoleptic and nutritional quality of meat (Listrat et al., 2016).

Shockwaves are mechanical high-pressure pulses generated in liquids or gases that can result in underwater pressure of up to 1 GPa (Bolumar et al., 2013). The pressure waves travel through media in fractions of milliseconds. These pressure waves can be generated by using explosive material or conversion of electrical energy into mechanical energy. The SW process can be conducted in either batch or continuous mode. Shockwave processing using underwater electrical discharge in a continuous way has been described as a much safer, cheaper and a more reproducible technique (Bolumar et al., 2013; Bolumar & Toepfl, 2016). Microbial and chemical cross-contamination are prevented as the meat is vacuum-packed before processing, and the use of explosives is avoided. However, there are challenges, such as damage of packaging material during processing,

[4]This chapter has been published as **Chian, F. M.**, Kaur, L., Astruc, T., Vénien, A., Stübler, A.-S., Aganovic, K., Loison, O., Hodgkinson, S., & Boland, M. (2021). Shockwave processing of beef brisket in conjunction with sous vide cooking: Effects on protein structural characteristics and muscle microstructure. *Food Chemistry*, *343*, 128500. https://doi.org/10.1016/j.foodchem.2020.128500

which have to be addressed before application in the meat industry (Bolumar & Toepfl, 2016; Claus, 2017). Shockwave processing causes muscle structure modification, such as myofibrillar fragmentation along the Z-disks (Zuckerman & Solomon, 1998) and disruption of collagen fibrils (Zuckerman et al., 2013). However, the effect of SW on muscle protein molecular structure is unknown. Contrary findings are to be found in the literature about the effect of SW on muscle protein profiles (Bolumar et al., 2014; Bowker, Fahrenholz, Paroczay, Eastridge, et al., 2008).

Sous vide cooking, which is commonly adopted in restaurants, has also gained attention from the meat industry for manufacturing tender and juicy products. Sous vide cooking is a heating process where food is heated at a precisely controlled temperature under vacuum, usually in a water bath for a long time, at temperatures lower than usual cooking methods (Baldwin, 2012; Boland et al., 2019). Unlike other forms of heating such as boiling, grilling and roasting, SV cooking enables mild heating of meat at precise lower temperatures. Sous vide cooking of beef is normally conducted at 58 °C to 63 °C, where the temperature is high enough to solubilise collagen and inactivate microbes, for 10 to 48 h (Roldan et al., 2013), and low enough to avoid excessive denaturation of the muscle protein (Baldwin, 2012). This leads to milder shrinkage of muscle fibres, which results in less water expulsion from the meat. Collagen starts to shrink and is converted to gelatine from 60 °C, which decreases the interfibre adhesion, leading to meat tenderisation.

As both SW processing and SV cooking are found to affect muscle proteins and structure, a combination of these two processes could potentially create new products with enhanced organoleptic and nutritional properties. However, to the best of our knowledge, there is no information available in the literature on how this process combination would affect muscle proteins and structures, which are key determinants in producing quality

meat products. Hence, the objective of this chapter is to study the effect of SW processing alone and subsequent SV cooking on meat proteins and structure of the low value beef brisket. The focus of this chapter is to describe the properties of meat proteins and muscle structures, particularly their SW and heat sensitivity and from this to provide underpinning knowledge that can guide the development of new meat products with enhanced organoleptic and nutritional properties. The textural properties and the *in vitro* protein digestibility of the SW-treated SV-cooked meat will be presented in **chapter 6**.

5.2 Materials and methods

5.2.1 SW processing and SV cooking of beef brisket

Three whole briskets (*Deep* and *Superficial pectoral* muscle, left side) from Simmental beef (21 – 22 months old, 485 ± 48 kg pre-slaughter weight) were obtained from a local slaughterhouse (Birkenfeld, Germany). The average pH of the whole brisket was 5.73 ± 0.15, measured at ten different points per whole brisket using a handheld pH meter (Testo 205, Testo SE & Co. KGaA, Lenzkirch, Germany). After trimming off the visible subcutaneous fat and connective tissue, each brisket was cut perpendicularly to the muscle fibres, into eight steaks which were comparable in size (approximately 35 mm in width x 180 mm in length x 50 mm in height, 400 g in weight). The steaks were vacuum-packed individually in flexible transparent polyamide/polyethylene bags (SAS Boulegon Parry, Clermont Ferrand, France) using a vacuum packer (C200, Multivac, Wolfertschwenden, Germany) (Rohlik et al., 2017). As the muscle was not homogenous throughout each whole brisket, the 1st, 3rd, 5th and 7th steaks were allocated as control and the 2nd, 4th, 6th, and 8th steaks were assigned as SW-treated samples to minimise the effect of sample variation within an animal (**Figure 5-1**). The vacuum-packed steaks were exposed to electro-discharging SW prototype system equipped with a conveyor belt (DIL,

Quakenbrueck, Germany) (**Figure 5-2**). The SW treatment was conducted at a frequency of 0.57 Hz, a voltage of 35 kV and a capacitance of 18 µF, resulting in a SW intensity of 11 kJ/pulse, calculated based on the equation:

$$\text{Energy} = \tfrac{1}{2} \times \text{capacitance} \times \text{voltage}^2 \text{ ----------} \textbf{Eq. (5-1)}$$

(Koita et al., 2017).

The belt speed was set to 50 % (equivalent to 2.22 cm/s) and total of four pulses were received by each piece of brisket steak. The average temperature of the samples before and after the SW treatment was 9.6 ± 0.4 ℃ and 11.8 ± 0.5 ℃ respectively, measured using an infrared thermometer (Testo 831, Testo SE & Co. KGaA, Lenzkirch, Germany). After the SW treatment, half of the control and half of the SW-treated samples from each whole brisket were kept raw at 4 ℃. The remaining half of both control and SW-treated steaks were SV-cooked at 60 ℃ for 12 h in a water bath (**Figure 5-1**). A cooking temperature of 60 ℃ was chosen as this is the minimum allowable meat cooking temperature according to the regulations of some countries (Purslow, 2018). The cooking time was set after conducting an informal sensory evaluation on meat SV-cooked for different times at 60 ℃. No visible packaging failure was detected throughout the SW and SV cooking process. Samples for structural analyses were collected immediately after the treatment. The remaining samples were snap-frozen using liquid nitrogen and were stored at -80 ℃ for other analyses.

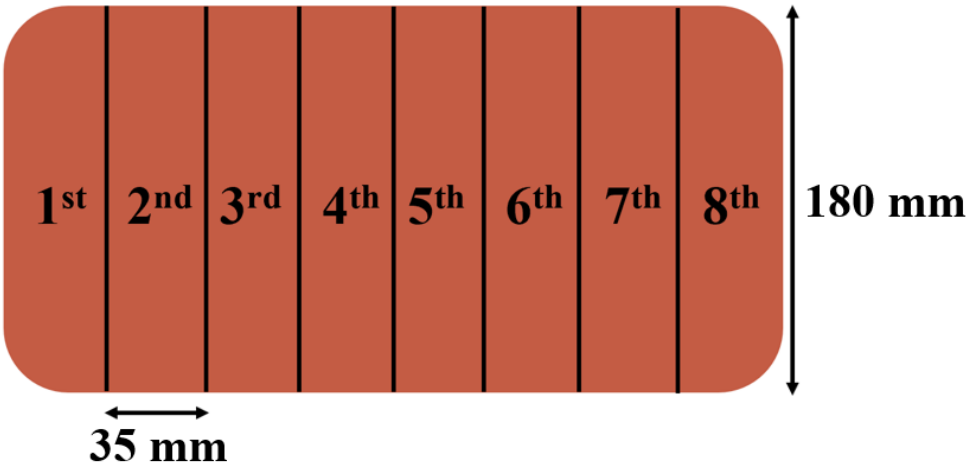

Figure 5-1. Meat sampling position of the control untreated (1st, 3rd, 5th, 7th steaks) and SW-treated (2nd, 4th, 6th, 8th steaks; 35 kV, 11 kJ/pulse) samples on each brisket slab to minimise muscle variation within an animal.
Each steak was cut into 180 mm by length, 35 mm by width and 50 mm by thickness, of approximately 400 g. Subsequent SV cooking was done on the 1st and 5th of control untreated steaks as well as the 2nd and 6th of SW-treated steaks at 60 °C for 12 h while the remaining 3rd, 4th, 7th and 8th steaks were kept raw.

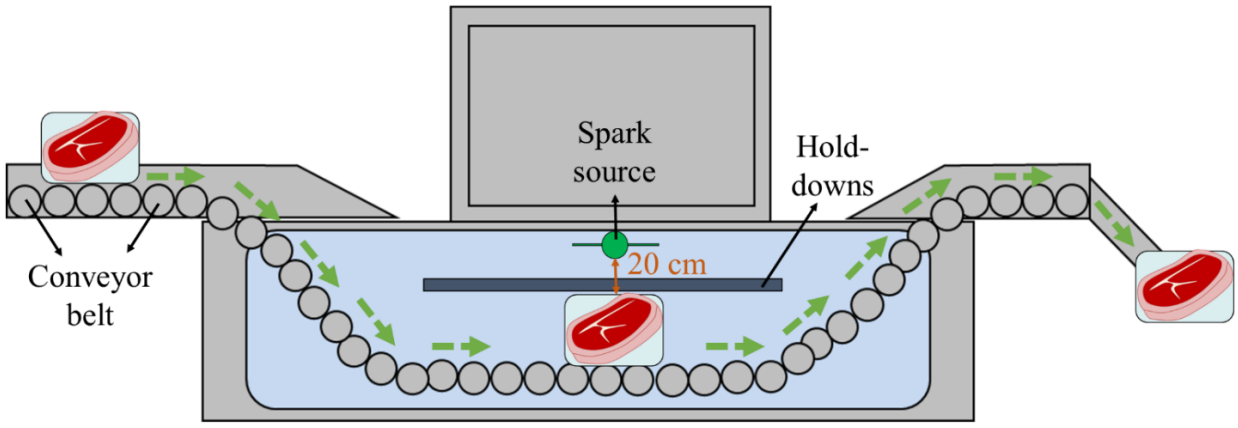

Figure 5-2. A schematic diagram showing the setup of the SW treatment of the beef brisket steaks.
The SW treatment was conducted at a frequency of 0.57 Hz, a voltage of 35 kV and a capacitance of 18 µF, resulting in a SW intensity of 11 kJ/pulse. The vacuum-packed samples were conveyed along the SW prototype at a speed of 2.22 cm/s so that each brisket steak received a total of four SW pulses when the steak travelled under the spark source. The distance between the samples and the spark source was maintained at 20 cm. Hold-downs were installed to ensure the samples were fully submerged during the SW treatment. The SW treatment was performed at room temperature and the average temperature of the samples before and after the treatment was 9.6 ± 0.4 °C and 11.8 ± 0.5 °C respectively.

5.2.2 Differential Scanning Calorimetry (DSC)

The protein thermal profiles of the control and SW-treated raw samples were determined as described in section **3.2.3** at a heating rate of 2 °C/min from 20 to 100 °C (Chian et al., 2019). The DSC measurements were made in triplicate.

5.2.3 Gel electrophoresis

Whole muscle protein extraction for gel electrophoresis was performed as described by Lonergan et al. (2001) with slight modifications. In brief, 0.5 g of frozen muscle was homogenised with 8 mL of extraction buffer consisting 10 mM sodium phosphate and 2 % SDS at pH 7 using an overhead homogeniser (DIAX 600, Heidolph Instrument, Germany) at 13500 rpm for 1 min. The homogenate was centrifuged at 1500 x *g* for 15 min and the protein concentration of the supernatant was quantified using Bio-Rad protein assay dye (5000006, Bio-Rad Laboratories, Hercules, CA, USA) (Bradford, 1976). Briefly, 100 µL of the samples was mixed with 5 mL of the diluted protein assay dye (dye: water = 1: 4), followed by incubation at 20 ℃ for 5 min before measuring the absorbance at 595 nm. The absorbance of bovine serum albumin (A1933, Sigma-Aldrich, Saint Louis, MO, USA) with different concentrations at 595 nm was determined to construct a standard curve.

5.2.3.1 Non-reducing and reducing SDS-PAGE

The extracted proteins were mixed with sample buffer (200 mM Tris-HCl, pH 6.8, 40 % glycerol, 2 % SDS, 0.04 % Coomassie Blue G-250) (1610739, Bio-Rad Laboratories, Hercules, CA, USA), in 1:1 ratio, with (reducing) or without (non-reducing) 5 % β-mercaptoethanol (M6250, Sigma-Aldrich, Saint Louis, MO, USA) (He et al., 2018). The mixtures were then heated at 100 ℃ for 4 min followed by loading onto a polyacrylamide gel (4 % stacking gel and 10 % separating gel) with a final protein concentration of 20 µg

per well. The electrophoresis was executed with a Mini-PROTEAN® electrophoresis system (Bio-Rad Laboratories, Hercules, CA, USA) at a constant voltage of 200 V for an hour or until the tracking dye front was just coming out of the gel. The gel was stained, scanned and analysed as described in section **3.2.4.4**. A total of three gels were prepared for each treatment.

5.2.3.2 Two-dimensional non-reducing/reducing SDS-PAGE (2D-PAGE)

Two-dimensional non-reducing/reducing SDS-PAGE (2D-PAGE) was conducted according to Dave et al. (2013) with some modifications. Whole muscle protein extracts were separated by SDS-PAGE in non-reducing conditions as described in section **5.2.3.1.** The gel strip of approximately 7 mm in width was excised and were reduced using 0.2 M dithiothreitol (DTT) (1610611, Bio-Rad Laboratories, Hercules, CA, USA) solution at 56 °C for 20 min, followed by washing with excess distilled water for 10 min. The reduced gel strip was glued horizontally on the top of a 4 to 20 % Mini-PROTEAN® TGX™ gel (4561103, Bio-Rad Laboratories, Hercules, CA, USA) using molten agarose. The electrophoresis was run and the gel was scanned as described in **5.2.3.1.** A total of three gels were prepared for each treatment.

5.2.4 Structure analysis

After processing, the samples from each animal were cut into small blocks of 5 mm x 5 mm x 5 mm followed by snap freezing in liquid nitrogen (−196 °C) chilled isopentane (−160 °C) (M32631, Sigma-Aldrich, Saint Louis, MO, USA) for at least 30 s. The frozen blocks were kept at −80 °C until use for molecular and microstructure analysis. Other samples were cut along the muscle fibre into strips of 10 mm x 3 mm x 3 mm and were fixed in 2.5 % glutaraldehyde (16210, Electron Microscopy Science, Hatfield, PA, USA)

in 0.1 M sodium cacodylate buffer (12300, Electron Microscopy Science, Hatfield, PA, USA) at pH 5.6 overnight at room temperature before storage at 4 °C for TEM analysis.

5.2.4.1 Fourier-transform infrared (FT-IR) microspectrometry for molecular structure analysis

The cryofixed muscle cubes from each animal were sectioned transversely into 6 µm thick sections using a cryostat (CM1950, Leica Microsystems GmbH, Wetzlar, Germany) at -20 °C. The sections were collected on a BaF_2 window (BAFP13-1, Crystran Ltd, Dorset, United Kingdom) with IR spectroscopy compatibility and were air-dried at room temperature. The FT-IR microspectrometry analysis was performed as described by Motoyama et al. (2017) with modifications. In brief, the infrared spectra were acquired using a FT-IR microspectroscope (Nicolet iN10 MX, Thermo Scientific, Waltham, MA, USA) using a spatial resolution of 15 x 15 µm. For each section, at least 30 sampling sites for both myofibres and connective tissue were scanned with a total of 64 scans accumulated. The accumulated spectra were averaged and subtracted from a background spectrum obtained at the start of the scan, followed by analysis using the Unscrambler software (v9.8, Camo Software AS, Norway). Spectral corrections were performed using extended multiple signal correction (EMSC) to remove the effects of fluctuation in baseline due to light scattering and non-uniformity of sample thickness. The analysis was performed in triplicate (three different animals) for each treatment.

5.2.4.2 Histochemistry for microstructure analysis

The cryosectioning, Picro-Sirius Red staining and imaging process were performed as described in section **4.2.5.1.** Sections were photographed at six different locations per replicate, followed by image analysis with ImageJ (1.52f, National Institute of Health,

Bethesda, MD, USA). The analysis was performed in triplicate (three different animals) for each treatment.

5.2.4.3 Transmission electron microscopy for ultrastructure analysis

Transmission electron microscopy (TEM) analysis was performed according to section **4.2.5.2**. The analysis was performed in triplicate (three different animals) for each treatment.

5.2.5 Statistical analysis

Statistical analysis for the DSC tests and muscle microstructural analysis was performed using one-way and two-way ANOVA respectively to evaluate the significance of difference at a confidence level of 0.05, followed by a post-hoc Tukey test using OriginPro 2018b (OriginLab Corporation, Northampton, MA, USA). Results obtained from the statistical analysis are reported as mean ± standard deviation of mean. The FT-IR spectra obtained were analysed using principal component analysis (PCA), a multivariate statistical analysis, to identify the differences between samples and correlate the differences to spectral bands. The PCA was run using the Unscrambler software (v9.8, Camo Software AS, Oslo, Norway). The computation of PCA was based on Non-linear Iterative Projections by Alternating Least-Squares (NIPALS) algorithm. Correlation loading plots derived from the first (PC1) and second (PC2) principal component X-loading plots were used to reveal and identify characteristic vibrational absorption bands. The spectral domain was focused on the 1500-1800 cm^{-1} range that includes the amide I and amide II band of proteins.

5.3 Results and discussion

5.3.1 Differential Scanning Calorimetry (DSC)

Differential scanning calorimetry provides information on the overall heat conformation stability of proteins, and detects structural modification of proteins due to processing, either via a shift in thermal denaturation temperature and/or a change in the shape of the thermogram (Alsenaidy et al., 2014). Representative DSC thermograms for the samples and the numerical data are presented in **Figure 5-3**. The first, second, and third peaks are considered to signify the thermal denaturation of myosin; collagen and sarcoplasmic proteins; and actin, respectively (Chian et al., 2019). The thermal denaturation temperatures and enthalpy of the second peak of the SW-treated raw samples were lower than those of the untreated samples ($p < 0.05$), indicating the SW-treated samples had lower thermal stability of connective tissue, i.e. collagen, and sarcoplasmic proteins (e.g. myoglobin). Protein that is more thermally unstable is likely to denature at a lower temperature and require less energy to be denatured (Shao et al., 2018). The reduced thermal stability of collagen in the SW-treated samples is speculated to be due to the weakening and disruption of the their quaternary or tertiary structure (collagen triple helices), or both, induced by the extreme pressure changes during SW processing, rendering the muscle protein more liable to heat denaturation (Meyer, 2019). The reduction in the thermal stability enables the collagen of the SW-treated meat to be denatured, shrunk and solubilised more easily during subsequent SV cooking, which could potentially shorten the cooking time of the tough cuts and eventually reduce the production cost (Alahakoon et al., 2017). As collagen starts to shrink at 60 °C, its triple helix tertiary and quaternary structure is destroyed, leading to the formation of random coils and water-soluble gelatine during subsequent heating (Baldwin, 2012; Koide, 2007;

Tornberg, 2005). The degree of this change is dependent on a few factors (e.g. collagen cross-linking), but it is likely that SV heating can decrease the background toughness by reducing the interfibre adhesion (Baldwin, 2012).

There was no difference ($p > 0.05$) in the thermal denaturation temperatures and enthalpies of both myosin and actin between control and SW-treated raw meats. Nonetheless, the total thermal denaturation enthalpy of control untreated raw muscle was about 40 % higher than that of SW-treated raw muscles ($p < 0.05$). This suggests that less energy would be required for SV cooking of SW-treated meat, which could probably reduce the thermal energy and time required for processing. After undergoing SV cooking at 60 °C for 12 h, no peak was observed in the thermograms of both the control and SW-treated samples (**Figure 5-4**), demonstrating that the major muscle proteins were denatured by the SV treatment. The DSC results provide an insight into the thermal stability of proteins in both control and SW-treated raw meats. However, the mechanism of muscle proteins unfolding during heating is very complicated and could not be interpreted just from the DSC results. The thermal denaturation of different muscle proteins occurs over a wide range of temperature and there are other minor muscle proteins (e.g. titin, tropomyosin and others) that may possibly contribute at a lesser extent to the three major peaks appeared on the DSC thermogram (Stabursvik & Martens, 1980).

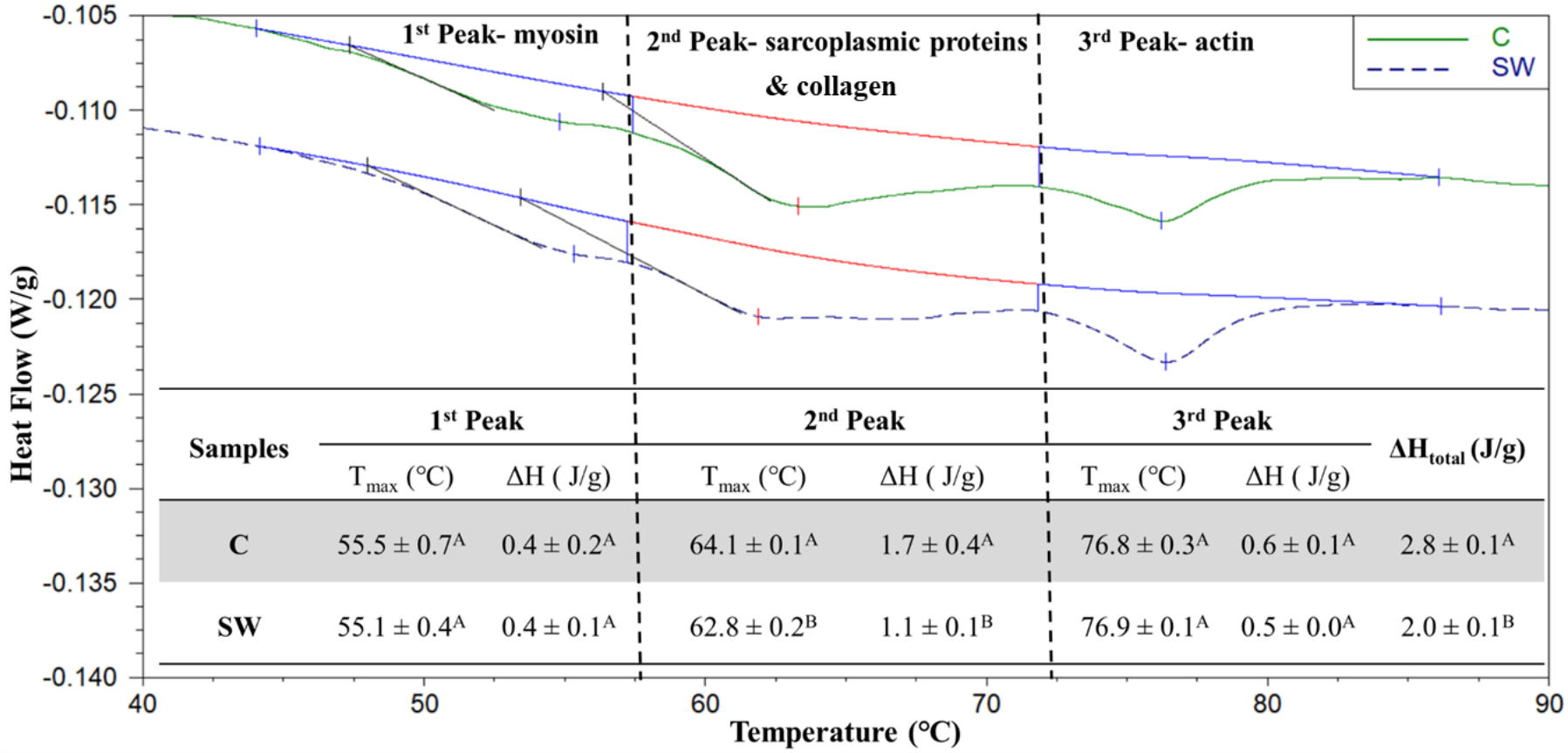

Samples	1st Peak		2nd Peak		3rd Peak		ΔH_{total} (J/g)
	T_{max} (°C)	ΔH (J/g)	T_{max} (°C)	ΔH (J/g)	T_{max} (°C)	ΔH (J/g)	
C	55.5 ± 0.7^{A}	0.4 ± 0.2^{A}	64.1 ± 0.1^{A}	1.7 ± 0.4^{A}	76.8 ± 0.3^{A}	0.6 ± 0.1^{A}	2.8 ± 0.1^{A}
SW	55.1 ± 0.4^{A}	0.4 ± 0.1^{A}	62.8 ± 0.2^{B}	1.1 ± 0.1^{B}	76.9 ± 0.1^{A}	0.5 ± 0.0^{A}	2.0 ± 0.1^{B}

Figure 5-3. Thermal denaturation characteristics of both the control (C) and SW-treated raw beef brisket.
Values with different letters within the same column differ significantly ($p < 0.05$).
Data are shown as mean ± standard deviation of mean. $N = 3$ (3 replicates with 3 measurements from each replicate).

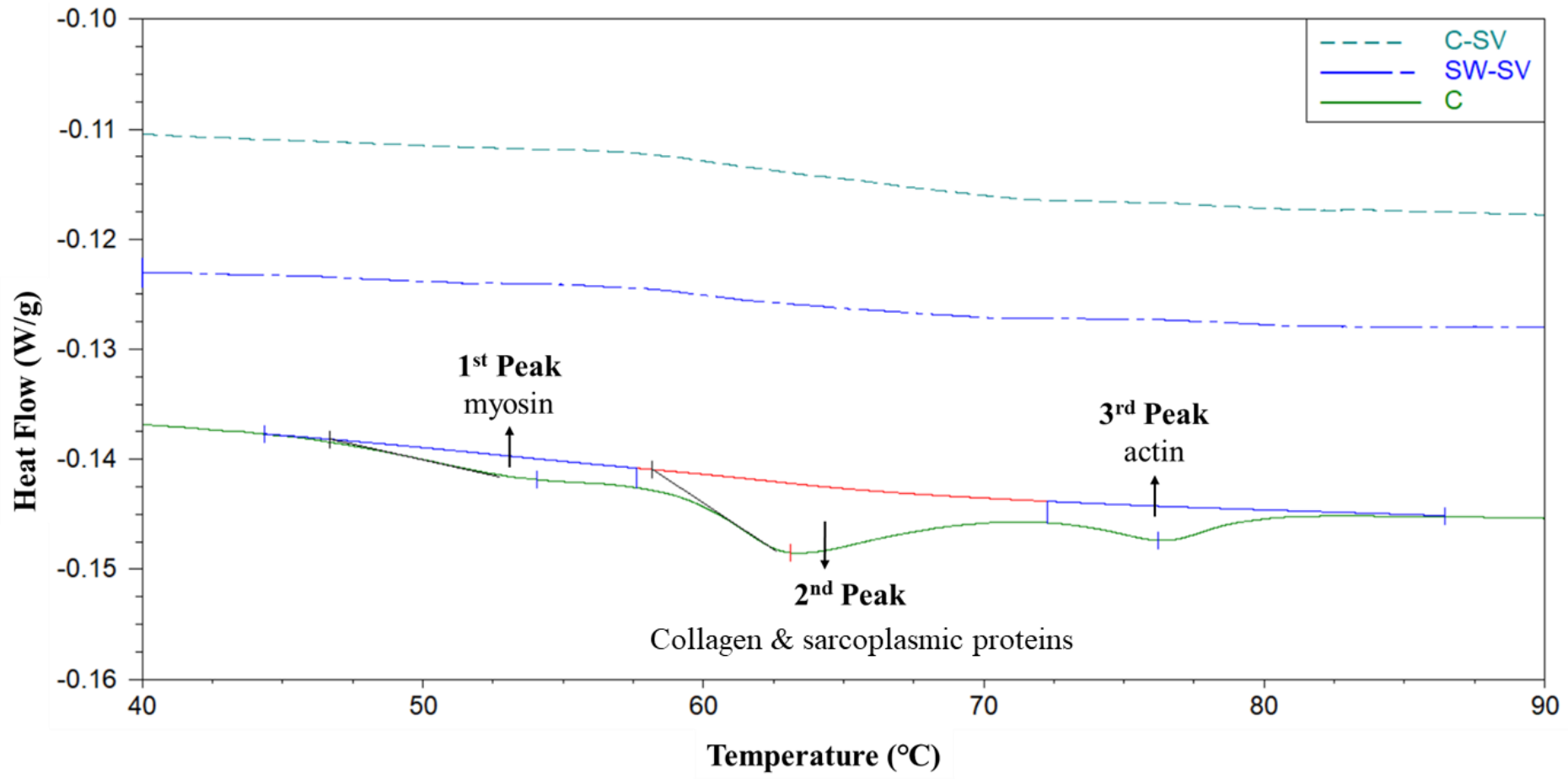

Figure 5-4. Differential scanning calorimetry thermograms showing the 3 peaks (attributed to myosin, collagen and sarcoplasmic proteins, and actin) of raw muscles. These peaks disappeared after 12 h of SV cooking at 60 °C in both the control (C) and SW-treated samples.

5.3.2 Gel electrophoresis

Under non-reducing conditions (**Figure 5-5A**), the profiles of proteins with molecular weight (MW) of equal to and less than 250 kDa of the control and SW-treated raw muscles were similar. Intense protein bands were observed in the sample loading wells of all of the samples, indicating the presence of large proteins and possibly cross-linked proteins, which could not travel through the stacking gel during the electrophoresis process. The intensity of these bands increased after SV cooking, especially in SW-treated SV-cooked sample (solid box in **Figure 5-5A**). The relatively more intense bands at the sample loading wells of SV-cooked samples are presumed to be due to the formation of protein aggregates as a result of protein denaturation, increased protein surface hydrophobicity, and/or through cross-linking such as disulfide bonding, during the cooking (He et al., 2018). The most intense band detected in the SW-treated SV-cooked meat suggests that more protein aggregates were formed compared to the control SV-cooked sample, after the heat treatment.

Under non-reducing conditions, bands with MW above 250 kDa were observed below the sample loading wells (dotted box in **Figure 5-5A**). However, under reducing conditions, these bands were not seen in both the control and SW-treated SV-cooked samples (dotted box in **Figure 5-5B**), demonstrating the reduction of disulfide bonds. Cooking causes the unfolding of the muscle proteins which can lead to protein aggregation promoted by the formation of disulfide bonds from exposed thiol groups (He et al., 2018). Thus, 2D non-reducing/reducing PAGE was performed to further investigate the disulfide bonding formed during the cooking. By reducing the non-reduced first dimension gel before running the second dimension, peptides that are cross-linked with disulfide bonds can be detected as they will not lie on the diagonal (Dave et al., 2013).

The electrophoretic mobilities of peptides cross-linked with disulfide bonds will be higher after reduction. No difference could be observed in the 2D-PAGE between the control and SW-treated SV-cooked samples, showing no new disulfide linkages were formed in SW-treated meat after SV cooking (**Figure 5-6**).

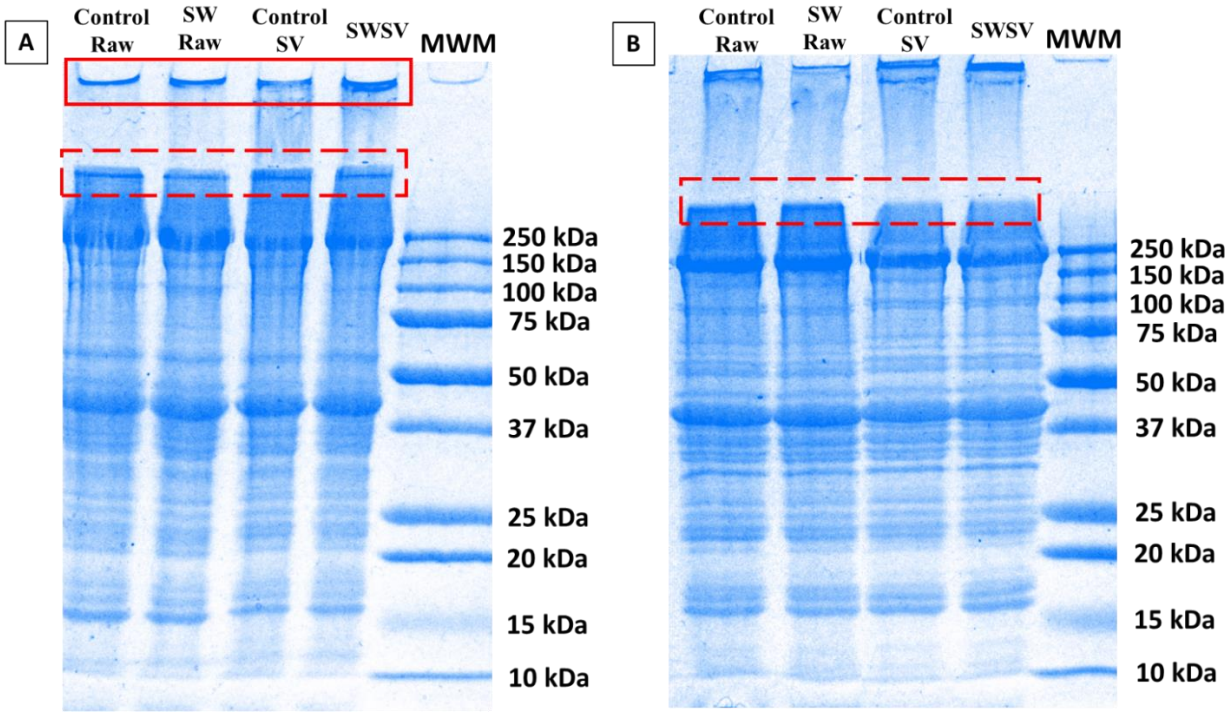

Figure 5-5. Sodium dodecyl sulfate–polyacrylamide gel electrophoretogram showing the profiles of muscle proteins extracted from the control raw muscle, SW-treated raw muscle (SW Raw), control SV-cooked muscle (Control SV) and SW-treated SV-cooked muscle (SWSV) under (A) non-reducing conditions and (B) reducing conditions. MWM represents the molecular weight standards in kDa.

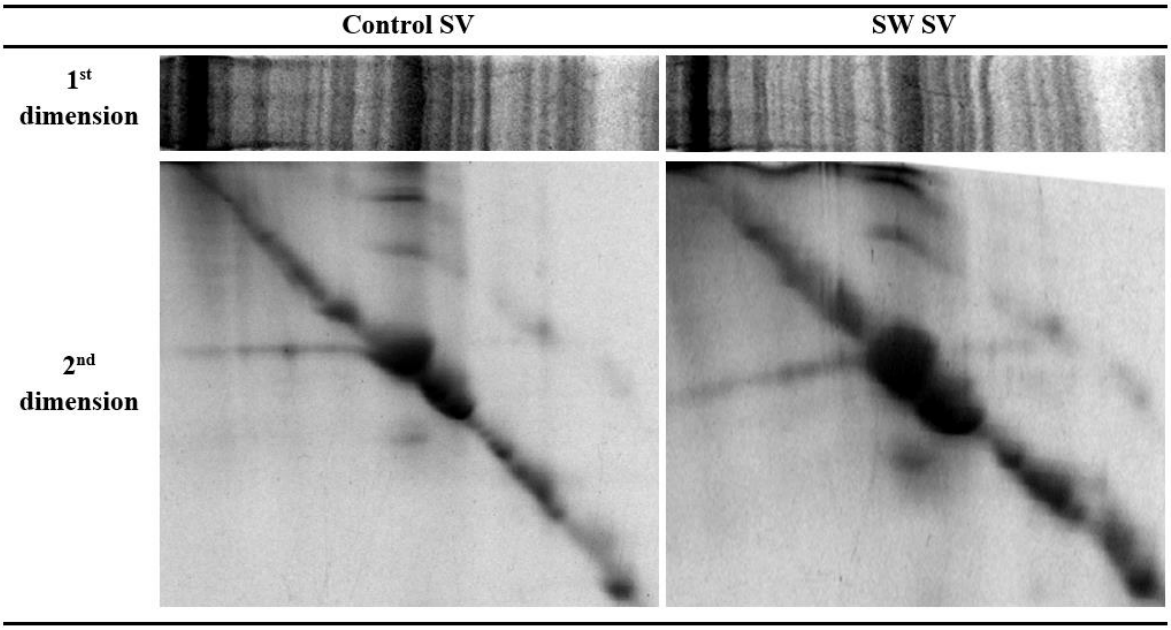

Figure 5-6. Two-dimensional non-reducing/reducing SDS-PAGE electrophoretogram of control and SW-treated SV-cooked muscles showing that no additional disulfide bonds have formed in SW-treated muscles after SV cooking.

5.3.3 Muscle molecular structure

As amide I (1600 to 1700 cm^{-1}) and amide II (1500 to 1600 cm^{-1}) vibrational bands reflect the polypeptide chain structure, the FT-IR spectra range from 1500 to 1800 cm^{-1} was used for the analysis of protein secondary structure of the control and SW-treated meat samples (**Figure 5-7**) (Motoyama et al., 2017). Principal component analysis of the FT-IR spectra of both the myofibres and connective tissue clearly discriminated the raw samples from the cooked ones (results not shown) as a consequence of the thermal protein denaturation (Astruc et al., 2012; Théron, Vénien, et al., 2014). Shockwave treatment did not change the spectral response of the connective tissue both before and after cooking (data not shown). This suggests that SW treatment did not affect the protein secondary structure of the connective tissue. The lowered in thermal stability of connective tissue in SW-treated meat is probably mainly due to the weakening in collagen triple helix tertiary and quaternary structure, as speculated and discussed in section 5.3.1 (Meyer, 2019).

Conversely, SW processing changed the FT-IR response of the myofibres, both with and without SV cooking. The PCA score plot of the raw myofibres highlighted a coarse separation between the control and SW-treated samples mostly in the PC1 (83 % of the overall variation) and marginally in the PC2 (12 % of the overall variation) (**Figure 5-7A**), indicating that SW treatment had altered the protein secondary structure of the myofibres. Subsequent SV cooking resulted in an increased separation between the control and SW-treated muscle mainly in the PC1 (67 % of the overall variation) and slightly in the PC2 (13 % of the overall variation) (**Figure 5-7B**). As the differences between the control and SW-treated samples, with and without SV cooking, were explained majorly in the PC1, the correlation loading plot of PC1 was constructed in order to get further information on the variance.

The correlation loading plot of the raw myofibres (**Figure 5-7C**) reveals that the separation of the control and SW-treated samples in the PC1 are mainly related to the wavenumbers of 1547, 1616 and 1655 cm^{-1}. The wavenumber 1547 cm^{-1} is assigned to the amide II band of alpha helical structures, the wavenumber 1616 cm^{-1} is assigned to the amide I band of intermolecular aggregated beta sheet structures, while the wavenumber 1655 cm^{-1} is assigned to the amide I band of alpha helical structures (Larrea-Wachtendorff et al., 2015; Perisic et al., 2011). As SW-treated samples are concentrated at the positive scale of the PC1 of the PCA score plot, they are highly correlated to alpha helical structures at both the amide I and II band regions (positive peaks showed in the correlation loading plot) and negatively correlated to the intermolecular aggregated beta sheet structures (negative peak showed in the correlation loading plot). This observation was speculated to be due to the reversion of intermolecular aggregated beta sheet in meat into native beta sheet, which are then converted to alpha helices, by the action of SW. The intermolecular aggregated beta sheet of equine serum albumin was dissociated and

refolded to their native structure after the application of high pressure (90 MPa to 740 MPa) at 25 ℃ as higher volume of aggregated beta sheet is unfavourable under high pressure (Okuno et al., 2007). Huang et al. (2016) also observed significantly decreased in beta sheet structure with increasing alpha helical structure in the myofibril isolated from porcine *Longissimus dorsi* treated at 600 MPa at 25 ℃. In contrast, the correlation loading plot of the SV-cooked myofibres (**Figure 5-7D**) shows that the separation of the control and SW-treated samples in the PC1 is largely related to the wavenumbers of 1539, 1628, 1650 and 1701 cm^{-1}. The FT-IR wavenumbers of around 1539 cm^{-1} are possibly aggregated beta sheet or (more likely) denatured random structure of the amide II band of proteins (Carton et al., 2009; Perisic et al., 2011). The wavenumbers of 1628 and 1650 cm^{-1} are assigned to intramolecular aggregated beta sheet structure of the amide I band of proteins and alpha helix structure of the amide I band of proteins respectively (Carton et al., 2009; Larrea-Wachtendorff et al., 2015). The positive peaks of 1539 cm^{-1} and 1628 cm^{-1} signified that the SW-treated meats, which concentrated at the positive scale of the PC 1 of the PCA score plot, formed more aggregated beta sheet structure and/or denatured random structure than the untreated samples after SV cooking, despite retaining more alpha helical structure (positive peak of 1650 cm^{-1}). The negative peak at 1701 cm^{-1} is assigned to the C=O stretching mode, but there is not sufficient evidence to assign it to a specific macromolecular change (Movasaghi et al., 2008).

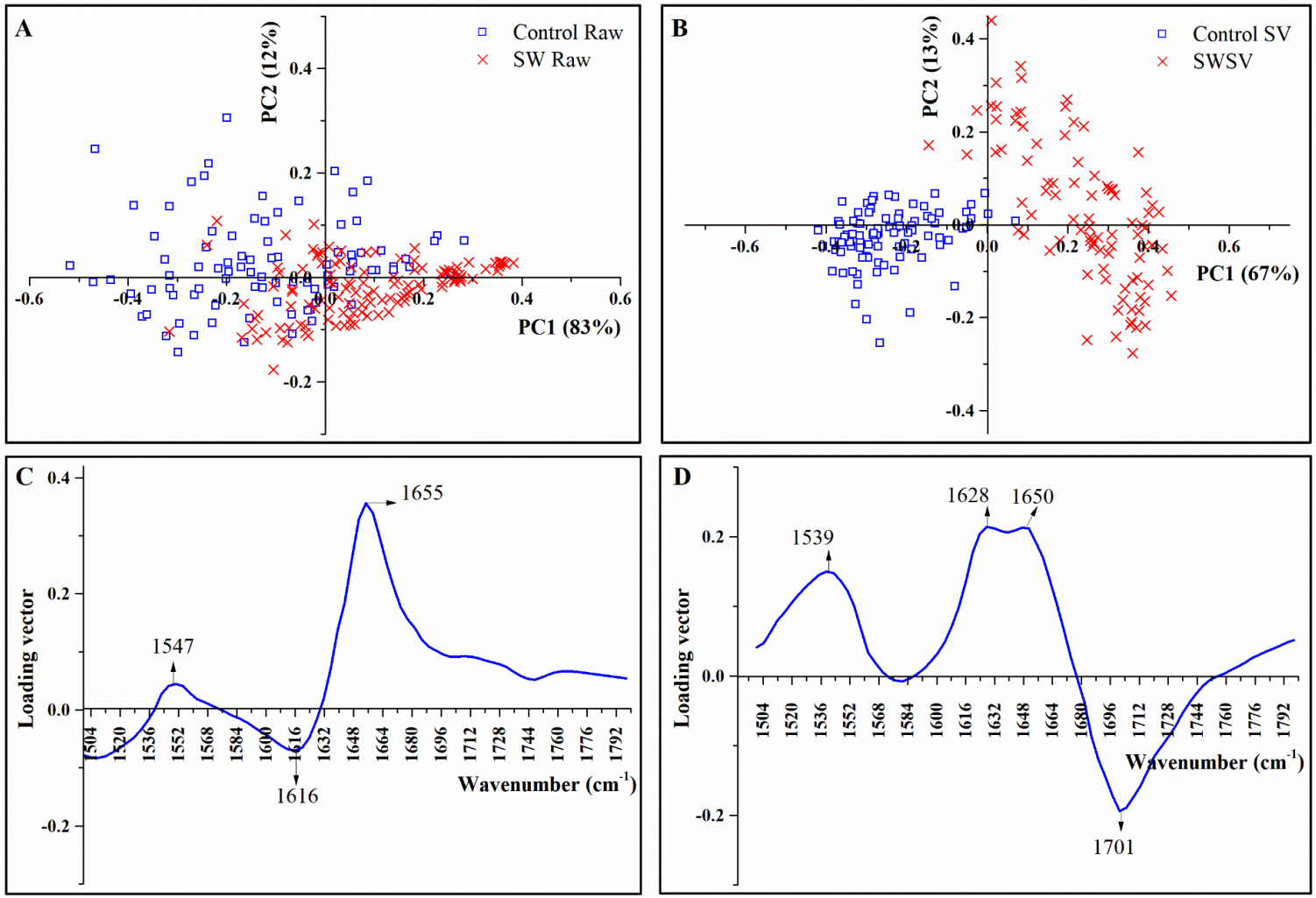

Figure 5-7. The PCA score plots from FT-IR microscopy showing (A) a coarse separation in the PC1 (83 %) of the control and SW-treated raw myofibres and (B) a more distinct separation in the PC1 (67 %) of the control and SW-treated SV-cooked myofibres, in the 1500 to 1800 cm^{-1} region. The correlation loading plots of the (C) control and SW-treated raw myofibres and (D) control and SW-treated SV-cooked myofibres, in the 1500 to 1800 cm^{-1} region, show the major wavenumbers that are responsible for the group separation in PC1.

5.3.4 Muscle microstructure

The histological characteristics of muscle fibres of both the control and SW-treated samples, with and without SV cooking, are tabulated in **Table 5-1**. The histological characteristics studied were the cross-sectional area, perimeter, Feret diameter and extracellular spaces area of the muscle fibres. There were no differences ($p > 0.05$) between the control and SW-treated raw samples in terms of the histological characteristics studied, indicating that SW processing did not significantly affect muscle fibre morphology at the microstructural level (**Figure 5-8**). However, the muscle fibre morphologies of both samples changed ($p < 0.05$) after 12 h of SV cooking at 60 ℃. The muscle fibre cross-sectional area, perimeter and Feret diameter of both control and SW-treated samples significantly decreased, while the area of extracellular spaces increased after SV cooking. These differences were assumed to be due to muscle fibre shrinkage during the heat treatment. Heating has been reported to cause transverse shrinkage of the muscle fibres between 40 ℃ and 60 ℃ (Boland et al., 2019). The shrinkage of the myofibrillar proteins, along with the shrinkage of connective tissue, led to water expulsion from the muscles, contributing to the significantly increased area of the extracellular spaces after SV cooking (Tornberg, 2005). In addition, the SW-treated samples had larger extracellular spaces area than the control samples among the SV-cooked samples ($p < 0.05$). This might be due to the disruption of muscle at the molecular (**Figure 5-7**) and ultrastructural level (**Figure 5-9**) by SW processing, enabling the release of water more easily during muscle shrinkage upon heating (Ha et al., 2017). The lower denaturation temperature of the connective tissue of SW-treated samples also suggests that the shrinkage of the connective tissue had started at lower temperature, which possibly resulted in more water expulsion (**Table 5-1**).

Table 5-1. Histological characteristics of muscle fibres of both the control and SW-treated meat before and after SV cooking: muscle fibres cross-sectional area (CSA), perimeter, Feret diameter and extracellular spaces area (ECSA).

	Control Raw	SW Raw	Control SV	SW SV	Statistical significance		
					SW treatment	SV cooking	SW treatment* SV cooking
CSA x 10^5 (μm^2)	**3.7 ± 0.2^A**	**3.8 ± 0.2^A**	**2.6 ± 0.1^B**	**2.5 ± 0.1^B**	ns	s	ns
Perimeter (µm)	**213 ± 12^A**	**217 ± 8^A**	**165 ± 12^B**	**162 ± 11^B**	ns	s	ns
Feret diameter (µm)	**71 ± 5^A**	**72 ± 3^A**	**53 ± 2^B**	**52 ± 3^B**	ns	s	ns
ECSA x 10^4 (μm^2)	**3 ± 2^A**	**3 ± 1^A**	**15 ± 2^B**	**20 ± 1^C**	ns	s	s

Values with different letters within the same row differ significantly ($p < 0.05$); s: significantly different ($p < 0.05$); ns: not significantly different ($p > 0.05$)

Data are depicted as mean ± standard deviation of mean. $N = 3$ (3 replicates with 6 measurements from each replicate).

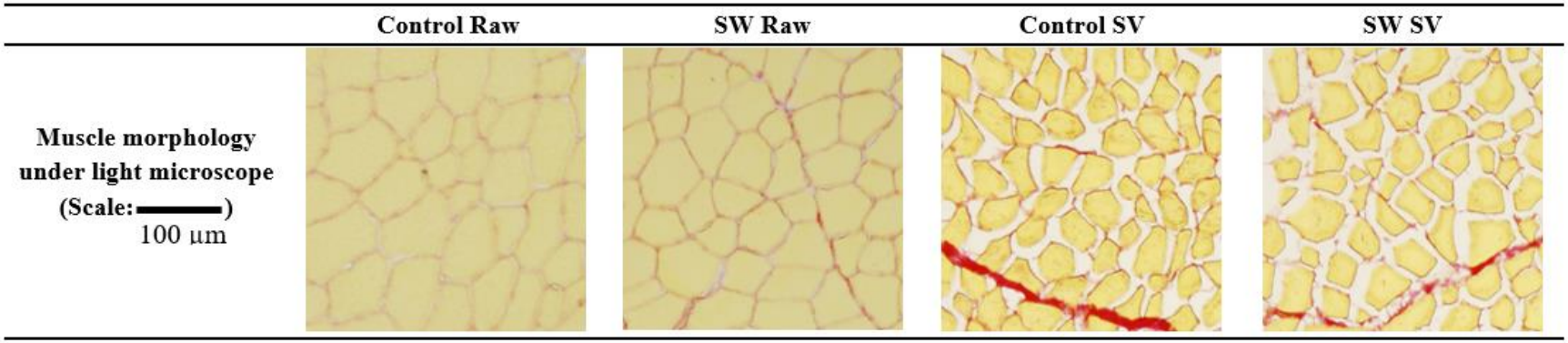

Figure 5-8. The muscle fibre morphology of the samples observed under light microscope, showing an increase in extracellular space area (ECSA) after SV cooking, especially in SW-treated samples. Connective tissue was stained in red by Sirius Red dye while muscle cells were stained in yellow by picric acid.

5.3.5 Muscle ultrastructure

As depicted in **Figure 5-9A** and **Figure 5-9C**, the sarcomeres of the control raw muscle were organised and the Z-disks were well aligned. In contrast, the sarcomeres of the SW-treated raw muscle were disordered. There was the formation of wavy sarcomeres and the Z-disks were disorganised (**Figure 5-9B** and **Figure 5-9D**). The formation of wavy sarcomeres may be due to irreversible changes in the structure of the I-bands after extensive stretching caused by the SW treatment (Zuckerman & Solomon, 1998). Although the titin filaments of I-bands are known to be flexible in their molecular structure, other stretched fibrous proteins of the I-band may not recover when the SW applied to the muscle is released (Tskhovrebova & Trinick, 2010). A-bands, which are relatively more structurally stable, were mostly unaffected.

The ultrastructure of both the control and SW-treated muscles changed after 12 h of SV cooking at 60 ℃. Sous vide cooking resulted in the disintegration of Z-disk structures, coagulation of myofibrils and formation of granular aggregates (**Figure 5-9E** and **Figure 5-9F**) in both samples. The disordered structure along the Z-disks and coagulation of sarcomeres were also observed in the SV-cooked beef brisket at 70 ℃ for 30 min (Zhu, Kaur, Staincliffe, et al., 2018). When meat is heated to between 40 ℃ and 60 ℃, muscle fibres shrink transversely while sarcoplasmic proteins expand, aggregate and form gels (Dominguez-Hernandez et al., 2018; Tornberg, 2005). At temperatures of 60 ℃ and above, both transverse and longitudinal shrinkage of muscle fibres occur. It was observed that the extent of these structural changes was greater in SW-treated SV-cooked samples. More myofibrillar coagulation and aggregation of SW-treated SV-cooked meat indicates more severe protein denaturation by heat, which corresponds to higher correlation to the aggregated beta sheet structure as discussed in section **5.3.3**.

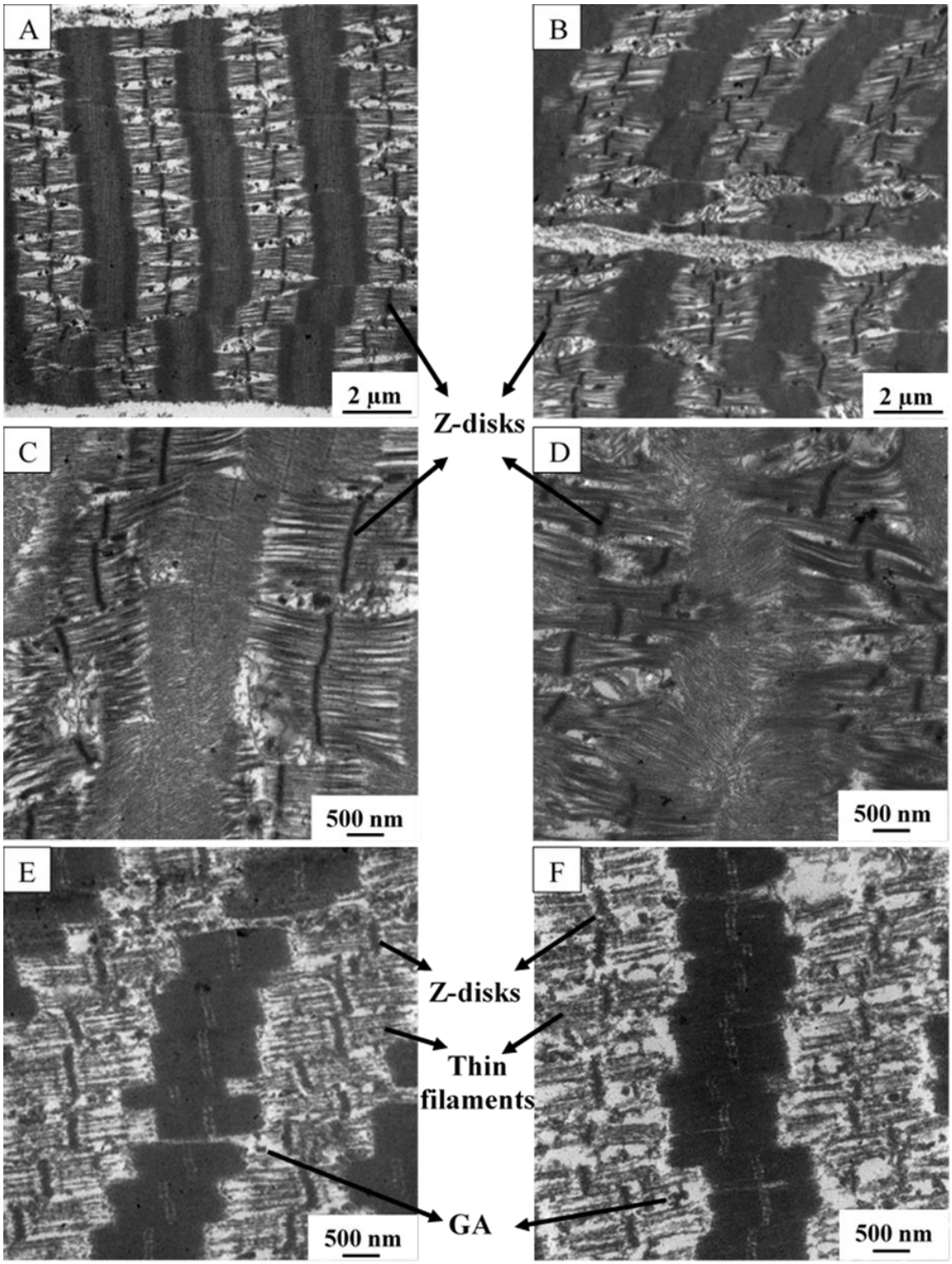

Figure 5-9. Transmission electron micrographs showing the ultrastructure of beef brisket with and without processing.

A and C: control untreated raw muscle; B and D: SW-treated raw muscle; E: control untreated SV-cooked muscle; F: SW-treated SV-cooked muscle. GA: granular aggregate. Shockwave treatment has caused the formation of wavy and disordered sarcomeres. Subsequent SV cooking led to the disintegration of the Z-disk structures and coagulation of the myofibrils to a greater extent when compared to the control untreated SV-cooked meat.

5.4 Conclusions

Shockwave processing lowered the thermal stability but did not affect the protein secondary structure of connective tissue. In contrast, SW affected the protein secondary structure of myofibres and the changes were speculated to be due to the reversion of intermolecular beta sheet structure to native structure and the formation of alpha helices by the application of SW. Shockwave processing disrupted the muscle ultrastructure by the formation of wavy sarcomeres and disorganised Z-disks. Subsequent SV cooking further modified the molecular, micro- and ultrastructures of the SW-treated muscles. More aggregated beta sheet structure and more contracted muscle cells were observed in the SW-treated SV-cooked meat, accompanied with more severe disintegration of Z-disks and coagulated ultrastructure. As the combination of SW processing and SV cooking has a great impact on the muscle structure, it could be a useful approach in adding value to tougher meat cuts by possibly improving meat tenderness. Nevertheless, further research is needed to fully understand the modification in muscle protein and structure of SW-SV-processed meat, such as collagen solubility, which is related to thermal stability of the connective tissue. The effect of the modifications to meat protein and structure caused by SW-SV process on other meat properties such as texture and nutritional qualities will be investigated in **Chapter 6**.

Chapter 6 Shockwave processing and sous vide cooking of beef brisket: Effects on meat physicochemical properties, texture and protein digestibility *in vitro*

6.1 Introduction

Low value meat cuts such as brisket (*Superficial* and *Deep pectorals*) usually have a problem of background toughness due to the presence of a higher amount of connective tissue (Boland et al., 2019). However, their texture can be improved by partial solubilisation of collagen during cooking. The sarcomere structure and postmortem proteolysis of myofibrils are also key determinants of meat tenderness (Boland et al., 2019). It is desirable and beneficial to implement treatments of the tough cuts by targeting both the connective tissue and myofibrillar proteins to create meat products with improved tenderness. A combined SW-SV process has the potential to act on both the connective tissue and myofibrillar proteins for meat tenderisation.

Shockwave processing can be carried out as a pre-treatment, targeting myofibrillar proteins for meat tenderisation and may be followed by subsequent processing such as SV cooking for collagen solubilisation, before distribution to the market or consumer (Bolumar et al., 2013). As discussed in section **2.8.2**, the tenderising effect of SW processing is seen to be largely due to muscle structure modification, such as myofibrillar fragmentation along the Z-disks (Zuckerman & Solomon, 1998) and disruption of collagen fibrils (Zuckerman et al., 2013). These structural disruptions may facilitate the penetration of endogenous meat proteases during maturation (Bolumar et al., 2014). In contrast, SV cooking results in the shrinkage and conversion of connective tissue (such as collagen) to gelatine which decrease the interfibre adhesion, resulting in meat tenderisation. The lower temperatures used in SV cooking also prevent excessive

denaturation of the muscle protein, leading to milder shrinkage of muscle fibres (Baldwin, 2012).

The study described in **Chapter 5** has shown that the combination of these two processes affects the muscle protein molecular, micro- and ultrastructures of beef brisket. These changes may have the potential to improve the textural and nutritional properties of meat. Structural disruption of the muscle has been reported to reduce meat toughness (Boland et al., 2019) and affect the efficiency of the digestive proteases (Astruc, 2014b). Hence, this chapter aims to investigate the effect of SW processing and subsequent SV cooking on the textural properties and *in vitro* protein digestibility of meat.

6.2 Materials and methods

6.2.1 Shockwave processing and SV cooking of beef brisket

The SW processing and SV cooking of beef briskets were conducted as described in section **5.2.1** using the same beef samples. Within 4 h post-treatment, purge loss of the control untreated and SW-treated raw samples as well as cook loss and texture analyses of the control and SW-treated SV-cooked samples, were determined. The remaining samples were snap-frozen using liquid nitrogen and were kept at -80 ℃ for future use.

6.2.2 pH and colour measurements

The pH of the control and SW-treated samples, both raw and SV-cooked, was measured as described in section **3.2.2**. The pH analysis was repeated three times for each replicate for each treatment. The colour measurements of the control and SW-treated raw samples were taken using a handheld Chroma meter (CR400, Konica Minolta, Tokyo, Japan), according to the method mentioned in section **3.2.2**. As for the control and SW-treated SV-cooked samples, the measurements were made on the inner meat surface after cutting

the SV-cooked brisket steak in half across the muscle fibre direction. The measurement was done with a 'D-65' light source and 10 ° observer setting (Brewer et al., 2006). The average value of *L** (black-white), *a** (red-green), *b** (blue-yellow) for each three treatment replicates was determined from 25 individual measurements.

6.2.3 Purge and cook loss

Purge loss was determined after SW processing and cook loss was calculated after the SV-cooked samples were cooled down to room temperature using the following equations (Faridnia et al., 2014):

$$\text{Purge loss (\%)} = (Wt_{\text{after sw processing}} - Wt_{\text{before sw processing}})/\ Wt_{\text{before sw processing}} \times 100 \text{ -------}$$

Eq. (6-1)

$$\text{Cook loss (\%)} = (Wt_{\text{after sv cooking}} - Wt_{\text{before sv cooking}})/\ Wt_{\text{before sv cooking}} \times 100 \text{ ----------}$$

Eq. (6-2)

,where Wt is the weight of the meat samples in g.

Purge loss of the control raw samples was determined by calculating the percentage change in weight of the control untreated sample, measured right before and after the SW processing conducted for the assigned SW-treated samples. In order to prevent the effect of ambient temperature difference on drip loss, the control samples were kept in the same room as the SW prototype for the same duration as for the SW treatment (Hertog-Meischke et al., 1998). Both purge loss and cook loss were determined once for each replicate for each treatment.

6.2.4 Warner-Bratzler (WB) shear force and texture profile analysis (TPA)

Warner-Bratzler shear force and TPA test of SV-cooked meat were performed using a TA.XT2 texture analyser (Stable Micro Systems, Godalming, UK) using a 25 kg load cell. The analysis was repeated six times for each replicate for each treatment. After equilibration to room temperature, SV-cooked samples were cut into strips where the muscle fibre direction is parallel to their length (1 cm in width × 1 cm in height x 4 cm in length), and each strip was sheared perpendicularly to the direction of the muscle fibres with a WB V-slot blade (TA-7) at a constant speed of 1 mms^{-1} (Roldan et al., 2013). Texture profile analysis was conducted using a 40 mm diameter cylindrical probe (TA-40) (2 mms^{-1} test speed, 3 s interval time, 0.1 N trigger force, and 80 % strain), through a 2 cycle sequence of axial compression (Isleroglu et al., 2015) on cooked samples cut into 1 × 1 × 1 cm. The force-time plots obtained were used to determine the TPA attributes.

6.2.5 Protein digestibility

6.2.5.1 In vitro digestion

The *in vitro* digestion of the SV-cooked sample (both control and SW-treated) was conducted as described in section **4.2.4.1.** Three digestions were performed each for the control and SW-treated SV-cooked samples.

6.2.5.2 Preparation of the digests for further analysis

The digests were processed as described in section **3.2.4.2** for subsequent soluble nitrogen, tricine SDS-PAGE and ninhydrin-reactive free amino nitrogen analyses.

6.2.5.3 Tricine SDS-PAGE and ninhydrin-reactive amino nitrogen

Tricine SDS-PAGE was carried out on a tricine gel (acrylamide/bis 40 % = 29:1; 4 % stacking gel and 16 % resolving gel) under reducing conditions. The electrophoresis was run and the gel was scanned as described in section **3.2.4.4**. The protein concentration of the digests was adjusted accordingly, based on the protein concentration of filtered digests quantified using Kjeldahl method (AOAC, 1981), as described in section **3.2.4.3**, so that 20 µg protein was loaded on each lane of the gel. One gel was prepared each for the three individual digestion replicates. Ninhydrin-reactive free amino nitrogen present in the digests was determined using ninhydrin reagent (N7285, Sigma-Aldrich, Saint Louis, MO, USA) as described in section **3.2.4.5**. The analysis was done at least three times for each digestion time for each digestion replicate. The analysis was done at least three times for each digestion time for each digestion replicate.

6.2.6 Microscopy analysis of digested muscles

The SV-cooked samples (both control and SW-treated) were cut into pieces where the muscle fibre direction is parallel to their length (5 mm in width × 5 mm in height x 10 mm in length). Simulated oral-gastro-small intestinal digestions were carried out as described in section **4.2.4.1** in a polyester mesh without the addition of glass balls and samples were taken after 62 and 182 min of simulated oral-gastric-small intestinal digestion. The digested strips (62 and 182 min) were cryofixed in isopentane (−160 °C) chilled by liquid nitrogen (−196 °C), followed by storage at −80 °C until use for histochemical analysis. The samples digested for 182 min were cut along the direction of the muscle fibre into strips of 10 mm x 3 mm x 3 mm and the pieces were immersed in 2.5 % glutaraldehyde in 0.1 M phosphate citrate buffer (pH 7) overnight at room temperature. The fixed samples were washed using 0.1 M sodium cacodylate buffer at pH 7.2 thrice for at least

24 h incubation time each to remove the excess phosphate and prevent granular precipitates during the osmication step (Schiff & Gennaro Jr., 1979). After that, the washed-fixed samples were then stored at 4 °C until subsequent preparation for TEM analysis.

6.2.6.1 Histochemical analysis

The cryosectioning, Picro-Sirius Red staining and imaging process of the cryo-fixed meat samples were performed as described in section **4.2.5.1.** One muscle section was observed per digestion replicate for each treatment.

6.2.6.2 Transmission electron microscopy analysis

Transmission electron microscopy (TEM) analysis was performed according to section **4.2.5.2**. One muscle section was observed per digestion replicate for each treatment.

6.2.7 Statistical analysis

Statistical analyses for the purge loss, cook loss and texture analysis were performed using one-way ANOVA while the statistical analysis for the pH and colour was conducted using two-way ANOVA (Minitab Release 17 Statistical Software, Minitab Inc., State College, PA, USA). Statistical analysis for the ninhydrin analysis of digests at different digestion time points were conducted using a repeated measures one-way ANOVA by Generalised Linear Model (IBM® SPSS® Statistic version 25, IBM Corporation, Armonk, NY, USA) and no violation of sphericity was detected using Mauchly's Test. All the statistical analyses were carried out to using a significance of difference at a confidence level of 0.05, followed by post-hoc Tukey's test. Results obtained from the statistical analysis are reported as means ± standard deviation of means with a least three replications.

6.3 Results and discussion

6.3.1 Effects of SW and SV cooking on pH, colour, purge loss and cook loss

Shockwave processing did not affect the pH value, colour and purge loss of meat samples as tabulated in **Table 6-1**. However, after SV cooking, the pH of both the control and SW-treated meat increased ($p < 0.05$) (**Table 6-1**). Hamm and Deatherage (1960) reported an increment of 0.2 pH unit in meat after cooking at 60 °C, which was deduced to be due to a decrease of carboxyl groups in the meat protein as a result of the conformation change induced by thermal denaturation of the muscle proteins. The results of the current study show that the L^*, a^* and b^* values were different among raw and SV-cooked meats ($p < 0.05$) (**Table 6-1**), both with and without SW pre-treatment. The change in colour after cooking was most likely due to the heat denaturation of muscle proteins, particularly the major colour determinant myoglobin, leading to the formation of a dull brown colour (Bernofsky et al., 1959). The purge losses of both the control and SW-treated raw meat were similar while the cook losses of the SW-SV-cooked meat were higher than those of the control SV-cooked meat ($p < 0.05$) (**Table 6-1**), which is in agreement with the finding of Bowker, Liu, et al. (2010) and the meta-analysis conducted by Ha et al. (2017). This might be due to the disruption of muscle protein structure by the SW, resulting in more water expulsion as the myofibrillar protein system shrunk during the cooking (Palka & Daun, 1999). A significant increment in the extracellular space area denoting shrinkage of muscle proteins was also observed in SW-treated SV-cooked meat as discussed in section **5.3.4** (**Table 5-1** and **Figure 5-8**).

Table 6-1. pH, colour, purge loss and cook loss for control and SW-treated beef brisket, with and without SV cooking.

		Control Raw	SW Raw	Control SV	SW SV	Statistical significance		
						SW treatment	SV cooking	SW treatment x SV cooking
pH^		5.7 ± 0.0^{A}	5.7 ± 0.1^{A}	6.0 ± 0.1^{B}	6.0 ± 0.1^{B}	ns	s	ns
Colour~	*L**	39 ± 0^{A}	39 ± 0^{A}	55 ± 1^{B}	55 ± 1^{B}	ns	s	ns
	*a**	13.5 ± 0.4^{A}	13.5 ± 0.3^{A}	11.8 ± 0.5^{B}	10.8 ± 0.5^{B}	ns	s	ns
	*b**	5.4 ± 0.3^{A}	5.4 ± 0.4^{A}	9.8 ± 0.5^{B}	10.0 ± 0.6^{B}	ns	s	ns
Purge loss (%)#@		0.2 ± 0.1^{A}	0.3 ± 0.1^{A}	N.A		ns	N.A	N.A
Cook loss (%)#		N.A		25 ± 2^{A}	28 ± 1^{B}	s	N.A	N.A

^*N* = 3 (3 replicates with 3 measurements from each replicate).

~*N* = 3 (3 replicates with 25 measurements from each replicate).

#*N* = 3 (3 replicates with 1 measurement from each replicate).

@ Purge loss of the control raw samples was determined by calculating the percentage change in weight of the control untreated sample, measured right before and after the SW processing conducted for the assigned SW-treated samples.

Colour measurements definition according to León et al. (2006):

- *L**: lightness (0 indicates black while 100 indicates absolute white).
- *a**: redness (positive value)/ greenness (negative value).
- *b**: yellowness (positive value) /blueness (negative value).

Values with different letters within the same row differ significantly ($p < 0.05$).

s: significantly different ($p < 0.05$); ns: not significantly different ($p > 0.05$); N.A.: not applicable.

Data are shown as mean ± standard deviation of mean.

6.3.2 Effects of SW and SV cooking on meat texture

The Warner-Bratzler (WB) shear force and TPA of SV-cooked meat (both control and SW-treated) are summarised in **Table 6-2**. A 11 % reduction in WB shear force was observed for the SW-treated SV-cooked meat compared with the cooked control ($p < 0.05$). This observation is consistent with the literature, where the reduction in WB shear force of SW-treated meat has been found to be around 5 to 30 % for electrical discharge SW, depending on the processing conditions and meat cuts (Bolumar & Toepfl, 2016). These texture enhancements were concluded to be due to the physical disruption of muscle fibres and collagen (Solomon et al., 1998; Zuckerman et al., 2013). Disorganisation of the sarcomere structure was also observed in the SW-treated SV-cooked meat as discussed in section **5.3.5** (**Figure 5-9**). However, TPA measurements of both the control and SW-treated SV-cooked samples were not statistically different. The observed differences in measurement of tenderising effect among WB shear force and TPA tests might be due to the inhomogeneity distribution of the connective tissue in the brisket samples. Although visible connective tissue was removed prior to the texture analysis, there is still the possibility of connective tissue embedded in some of the sample. As WB shear force has been reported to be more sensitive to myofibrillar components than the connective tissue, the embedded connective tissue might not affect the WB shear force values when compared to TPA measurements (Møller, 1981). Future work using larger sample sizes (for each replicate) for textural analysis will allow clearer observation of the effect of SW and subsequent SV cooking on meat texture.

Table 6-2. Warner-Bratzler shear force and TPA data for the control and SW-treated SV-cooked beef brisket.

		Control SV			SW SV		
WB shear force (N)		45	±	2^{A}	40	±	1^{B}
TPA	**Hardness (N)**	123	±	12^{A}	113	±	11^{A}
	Chewiness (N)	22	±	3^{A}	19	±	2^{A}
	Cohesiveness	0.45	±	0.03^{A}	0.45	±	0.01^{A}
	Springiness	0.39	±	0.01^{A}	0.37	±	0.00^{A}

Values with different letters within the same row differ significantly ($p < 0.05$).

Data are depicted as depicted as mean ± standard deviation of mean. $N = 3$ (3 replicates with 6 measurements from each replicate).

Measurements definition according to Isleroglu et al. (2015):

- Hardness: the peak force requires during the first compression.
- Chewiness: the product of hardness, cohesiveness and springiness.
- Cohesiveness: the ratio of the positive force area during the second compression to that in the first compression.
- Springiness: the rate at which the sample recovers its original shape after the first compression (the ratio of the time difference of the second to the first compression cycle).

6.3.3 Effect of SW and SV cooking on muscle protein digestibility *in vitro*

6.3.3.1 Tricine SDS-PAGE

The protein profile of the digests from both control and SW-treated SV-cooked meat is shown in **Figure 6-1**. The protein profiles of both the samples are similar after 32 min of oral-gastric digestion. However, after 62 min of simulated oral-gastric digestion, it was observed that the band intensities of MHC (220 kDa) and C-protein (140 kDa) of the SW-treated cooked meat were less intense than those of the control untreated cooked meat, showing the SW treatment improved the peptic hydrolysis of these proteins. The increased protein degradation of SW-treated cooked meat by the digestive enzymes was more obvious in the small intestinal phase. It can be seen that the intensities of bands corresponding to actin (42 kDa) and tropomyosin-α-chain (33 kDa) decreased as the digestion progressed in the small intestinal phase. These bands had nearly disappeared in the digest of SW-treated cooked meat at the end of the simulated digestion. The intensities of bands with molecular weights (MW) of 46 kDa, 30 kDa and 29 kDa in SW-treated

cooked meat were also reduced at the end of digestion. Bands with a MW of 30 kDa were deduced to be the hydrolysis product of troponin T, while bands with MW of 46 kDa and 29 kDa might be the proteolytic products of other high MW myofibrillar proteins (Kaur et al., 2014; Toldrá, 2012). The decrease in their band intensity signifies further break down of these fragments, especially in the SW-treated SV-cooked samples. In addition, the bands with MW of 25 kDa and 18 kDa were also more intense in the SW-treated SV-cooked meat at the end of digestion. These observations demonstrate improved proteolysis of meat protein by the digestive enzymes after SW treatment. Enhanced protein breakdown of high hydrostatic pressure-treated meat during simulated digestion has also been reported by Kaur et al. (2016).

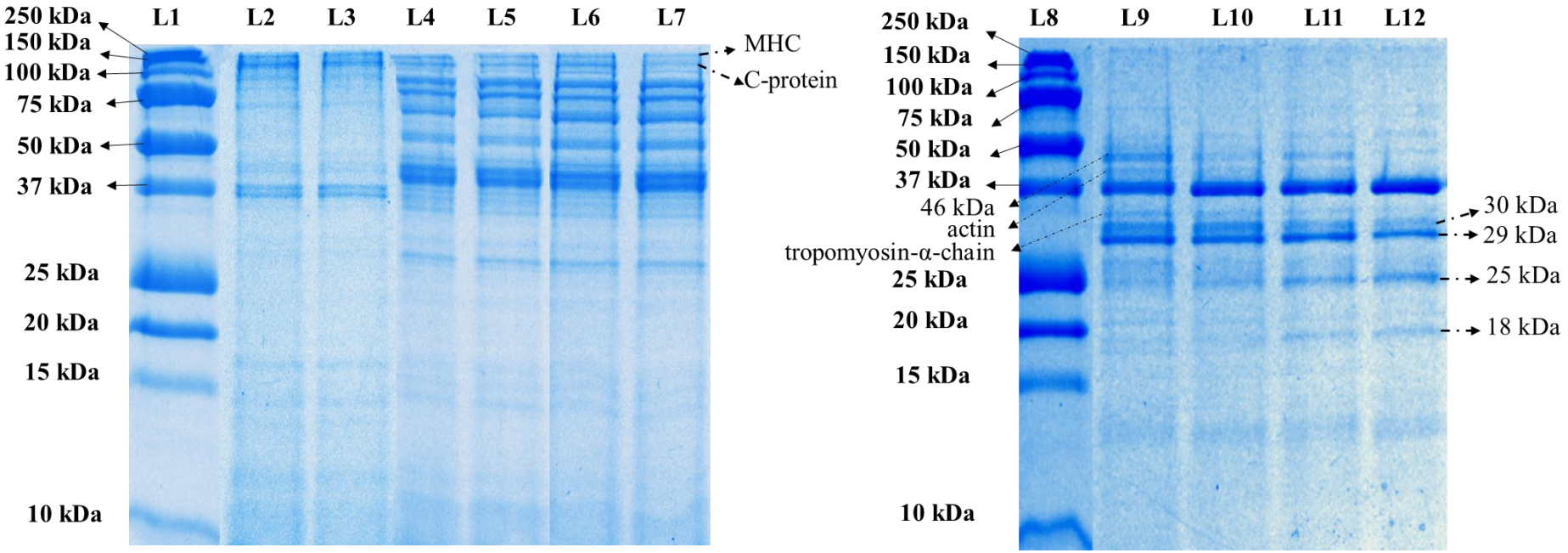

Figure 6-1. Tricine SDS-PAGE electrophoretogram showing protein profiles of the digests of both control and SW-treated SV-cooked meat during simulated digestion.

L1 and L8 are the molecular weight standards labelled in kDa. L2, L4, L6, L9 and L11 denote control SV-cooked samples at 2, 32, 62, 122 and 182 min of oral-gastro-small intestinal digestion respectively. L3, L5, L7, L10 and L12 denote SW-treated SV-cooked samples at 2, 32, 62, 122 and 182 min of oral-gastro-small intestinal respectively. The meat proteins labelled on the electrophoretogram were identified from their apparent MW, according to Kaur et al. (2014) and Boland et al. (2019).

6.3.3.2 Ninhydrin-reactive amino nitrogen

The degree of hydrolysis of the meat samples at different digestion times was determined as ninhydrin-reactive amino nitrogen released during *in vitro* oral-gastro-small intestinal digestion using the ninhydrin assay (**Table 6-3**). The ninhydrin-reactive amino nitrogen released from both control and SW-treated SV-cooked meat were not significantly different after 32 min of oral-gastric digestion. However, at the end of simulated oral-gastric digestion, the ninhydrin-amino nitrogen released from the SW-treated cooked samples was higher than control untreated cooked sample ($p < 0.05$). This trend continued after 122 and 182 min of simulated oral-gastro-small intestinal digestion ($p < 0.05$). Overall, SW processing improved the protein digestibility of the SV-cooked beef by approximately 22 %, in terms of ninhydrin-reactive amino nitrogen released, at the end of *in vitro* oral-gastro-small intestinal digestion.

Table 6-3. Ninhydrin reactive amino nitrogen released from both control and SW-treated SV-cooked meat after *in vitro* oral-gastric (2, 32 and 62 min) and further small intestinal (122 & 182 min) digestion.

Cumulative digestion time (min)		**2**	**32**	**62**	**122**	**182**
Ninhydrin-reactive amino nitrogen (%)	**Control-SV**	1.5 ± 0.4^{aA}	2.0 ± 0.1^{abA}	3.2 ± 0.2^{bA}	9.3 ± 0.7^{cA}	13.1 ± 1.0^{dA}
	SW-SV	1.8 ± 0.3^{aA}	2.1 ± 0.6^{aA}	4.0 ± 0.2^{aB}	12.7 ± 1.9^{bB}	16.0 ± 0.7^{cB}

Values with different lower-case letters within the same row differ significantly ($p < 0.05$).

Values with different upper-case letters within the same column differ significantly ($p < 0.05$).

Data are shown as mean ± standard deviation of mean. $N = 3$ (three replicates with 3 measurements from each replicate).

6.3.3.3 Structure of digested meat samples

The effect of SW on muscle microstructural changes of SV-cooked meat during 182 min of *in vitro* oral-gastro-small intestinal digestion was studied using histochemical analysis (**Figure 6-2**). It was observed that after 62 min of oral-gastric digestion, the muscles at the edge of both the control SV-cooked and SW-treated SV-cooked samples were damaged slightly, probably due to the action of pepsin and the effect of acidic simulated gastric fluid (pH 3 ± 0.1). As the digestion further progressed in the small intestinal phase, the breakdown of the muscle cell was more severe and the digested area had expanded toward the core of the samples, particularly in the SW-treated SV-cooked samples. This observation is consistent with the findings from SDS-PAGE and ninhydrin-reactive amino nitrogen analysis discussed in section **6.3.3.1** and **6.3.3.2** that showed better protein digestibility for the SW-treated SV-cooked samples than the control cooked meat. The muscle cells of both control cooked and SW-treated cooked samples were swollen during the simulated digestion, which is likely to be due to the effect of acidic simulated gastric juices (Astruc, 2014b). The muscle cell swelling was detected when the gastric juice entered the meat matrix, using time domain-nuclear magnetic resonance (TD-NMR) relaxometry (Bordoni et al., 2014). Although muscle cell swelling has been proposed to facilitate the accessibility of the digestive enzymes to their cleavage site, it may lead to a reduction in extracellular spaces, limiting the transfer of the aqueous digestive juices to the core of the samples (Astruc, 2014b; Offer & Knight, 1988). As the muscle cells of the control SV-cooked samples were swollen to a greater extent than the SW-treated cooked samples after both oral-gastric and subsequent small intestinal digestion, delayed penetration of the digestive juices toward the core of the samples might have occurred, resulting in lower digestibility for the control cooked sample.

The ultrastructure of the SV-cooked meat after 182 min of *in vitro* oral-gastro-small intestinal digestion is depicted in **Figure 6-3**. The Z-disks of both control and SW-treated SV-cooked samples were degraded and there was the formation of grey spots in the intermyofibrillar spaces, indicating the breakdown of muscle proteins by digestive enzymes. More elongated I-bands was observed in the SW-treated cooked meat, which might be due to the weakening of the thin filaments in I-bands after excessive enzymatic hydrolysis of the Z-disks (Chian et al., 2019; McGuire & Beerman, 2012). Similar effects were observed in PEF-treated raw bovine *Longissimus thoracis* muscles (**Figure 3-5)** and PEF-treated SV-cooked beef brisket (**Figure 4-7**) with improved protein digestibility. In addition, more coagulated sarcomeres was observed in the SW-treated meat after SV cooking when compared to the control cooked meat (**Figure 5-9**), which might have exposed buried peptide bonds for the access of digestive enzymes, leading to improved proteolysis of the former (McGuire & Beerman, 2012).

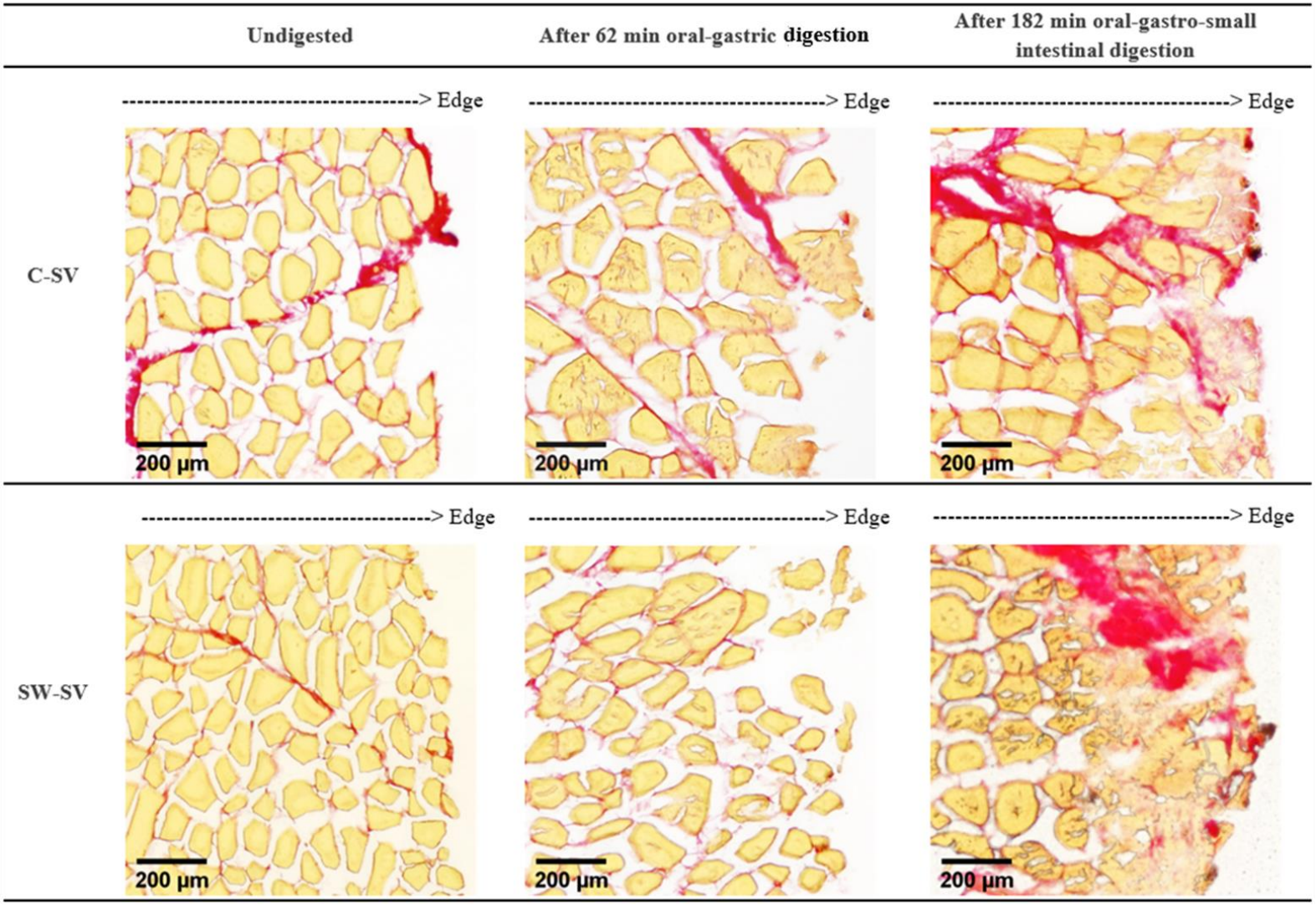

Figure 6-2. Histological sections of both control (C) and SW-treated SV-cooked meat at different digestion time points, showing more severe structural degradation of SW-treated cooked meat by the digestive enzymes at the end of simulated digestion. Connective tissue was stained in red by Sirius Red dye and muscle cells were stained in yellow by picric acid.

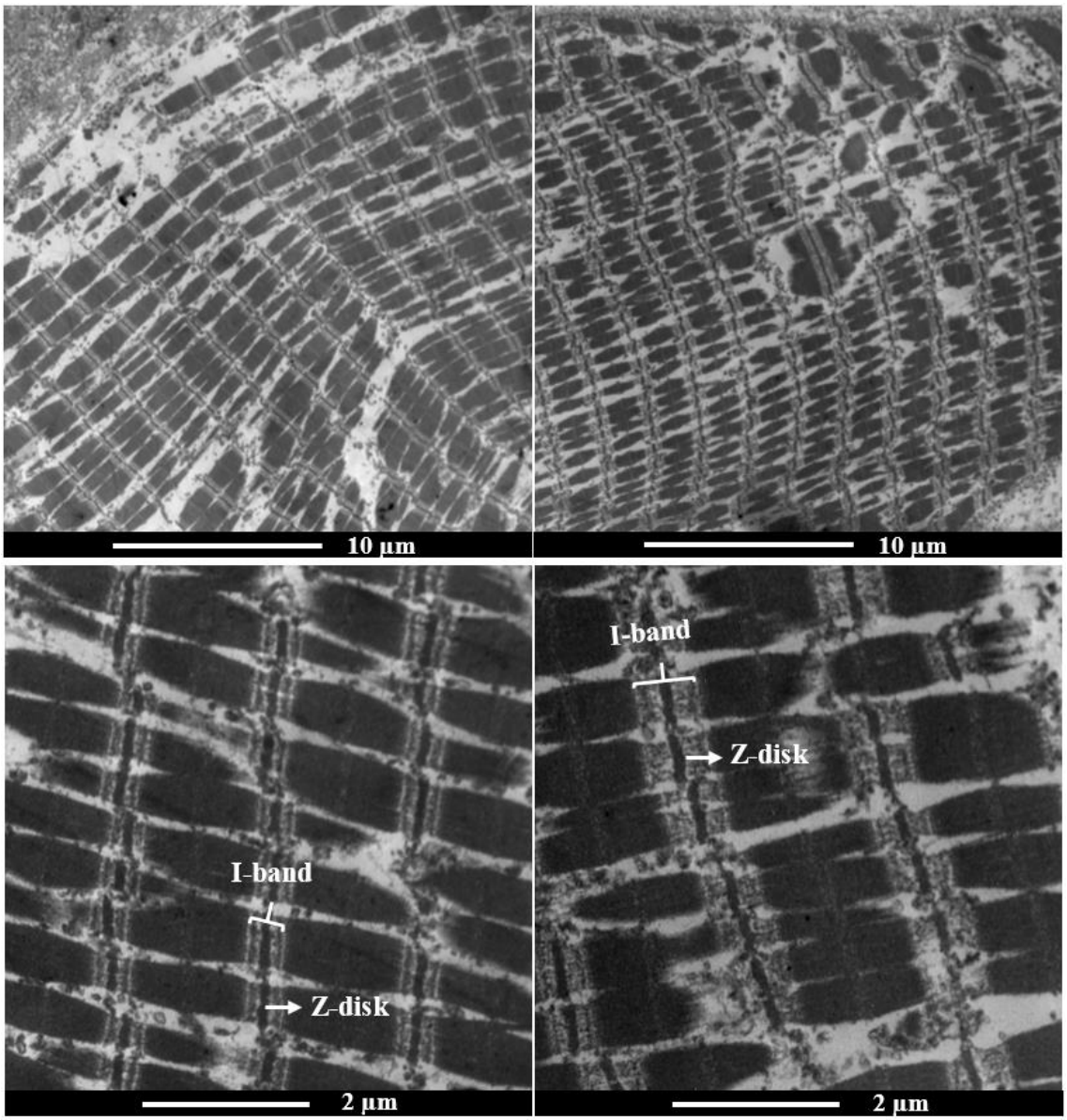

Figure 6-3. Transmission electron micrographs showing the ultrastructure of control SV-cooked (left two) and SW-treated SV-cooked (right two) beef brisket at the end of simulated oral-gastro-small intestinal digestion.

The digested SW-treated SV-cooked meat has more elongated I-bands, indicating more severe proteolysis by the digestive enzymes.

6.4 Conclusion

Shockwave processing did not affect the purge loss, pH and colour of meat. Subsequent SV cooking increased cook loss while decreasing the WB shear force of beef brisket when compared to control SV-cooked meat. Shockwave-treated SV-cooked meat had enhanced protein digestibility after 62 min of simulated oral-gastric digestion and during subsequent 2 h of small intestinal digestion. There was approximately 22 % higher ninhydrin-reactive amino nitrogen released from the SW-treated cooked meat at the end of the *in vitro* oral-gastro-small intestinal digestion, than the control SV-cooked meat. Tricine SDS-PAGE indicates increased proteolysis of the SW-treated SV-cooked meat proteins compared to the control SV-cooked meat by the digestive enzymes. The micro- and ultrastructures of the SW-treated SV-cooked muscle also showed more break down than the control cooked meat, at the end of simulated digestion. These findings suggest combination of SW processing and SV cooking can improve not only tenderness but also enhance nutritional quality of meat. Further research is needed to fully understand SW-SV processing optimisation and to enable a cost-benefit analysis of these processes.

Chapter 7 Effect of kiwifruit extract treatment on muscle microstructure and the localisation of actinidin and pepsin in meat using immunohistofluorescence imaging

7.1 Introduction

Exogenous enzymes, such as papain (from papaya) and bromelain (from pineapple), have been used in meat tenderisation for centuries (Sullivan & Calkins, 2010). These enzymes reportedly reduce the actomyosin toughness and background toughness of meat, by hydrolysing myofibrillar proteins and connective tissue, respectively (Ashie et al., 2002; Ha et al., 2012; Miyada & Tappel, 1956). However, these enzymes have the tendency to create a mushy meat product due to over-tenderisation (Ashie et al., 2002; McKeith et al., 1994; Weir et al., 1958). The kiwifruit enzyme actinidin which has a milder and more controlled meat tenderising ability, is being explored as an alternative to the traditionally used enzymes in order to produce meat products with superior quality (Aminlari et al., 2009; Christensen et al., 2009; Lewis & Luh, 1988; Zhu, Kaur, Staincliffe, et al., 2018).

Actinidin is a cysteine protease which has a wide substrate specificity (Boland, 2013; Boland & Hardman, 1972). It hydrolyses peptide bonds present in proteins, simple esters and amides. Actinidin has a broader active pH range between 3 and 8, and has a lower inactivation temperature of 60 °C (Boland, 2013; Huff-Lonergan, 2014; McDowall, 1970; Payne, 2009; Zhu, Kaur, & Boland, 2018). *Actinidia deliciosa* cv. 'Hayward' (green kiwifruit) and *Actinidia chinenis* cv. 'SunGold' (gold kiwifruit) are two of the main commercial kiwifruit varieties (Chao, 2016). The green kiwifruit has approximately eight times higher actinidin activity than the gold kiwifruit. The application of actinidin on meat causes the degradation of myofibrillar proteins and the solubilisation of connective tissue (Ha et al., 2012; Nishiyama, 2007; Wada et al., 2004). However, Toohey et al.

(2011) have proposed that actinidin prefers to act on myofibrillar proteins rather than connective tissue, as they observed a shear force reduction in the actinidin-treated bovine *Semimembranosus,* but not compression force.

Actinidin treatment has been reported to affect meat ultrastructure, as discussed in section **2.8.4.1**. Muscle destruction along the Z-disks, elongated sarcomeres with extended A-bands, and damaged endomysium were observed in the actinidin-treated muscles (Christensen et al., 2009; Zhu, Kaur, Staincliffe, et al., 2018). Nevertheless, knowledge about the effect of actinidin on meat structure in the current literature is limited, especially with regard to the breakdown of muscle microstructure due to the action of actinidin.

In addition to its meat tenderisation properties, actinidin has been reported to aid in protein digestion, particularly in the gastric phase, both *in vitro* and *in vivo.* Actinidin enhanced the gastric digestion of myofibrillar proteins and improved the small intestinal digestion of collagen slightly, *in vitro* (Kaur et al., 2010a, 2010b). When actinidin was added to the diet of growing pigs, a faster gastric emptying rate (dry matter and nitrogen) and an improvement in gastric digestion of beef muscle proteins were observed (Montoya et al., 2014). However, no study has been conducted to examine the effect of actinidin plus pepsin on food structure during digestion. The mechanism by which the dietary actinidin, when added to the digestive juices, accesses its substrates is also unknown.

Astruc (2014b) examined the accessibility of the digestive enzymes in meat by locating pepsin in peptic digested meat using immunohistofluorescence imaging. These findings would provide some information on the accessibility of pepsin to its substrates during meat proteolysis. During the immunostaining, the peptic digested muscles were treated with a primary antibody, the anti-pepsin, followed by a secondary antibody containing a fluorescent marker, forming an antigen-antibody (Ag/Ab) complex that was able to be

observed under a fluorescence microscope. Hence, immunohistofluorescence imaging could also be adopted to locate actinidin in the actinidin-treated meat by immunostaining with a primary antibody anti-actinidin.

The objective of this experiment is to investigate the effects of actinidin on meat microstructure during marination for meat tenderisation and also during *in vitro* gastric digestion. As beef brisket muscles are rich in connective tissue, they were selected in this experiment so that the effect of actinidin on both connective tissue and muscle cells could be examined. In addition, this experiment aims to locate actinidin in the meat, for the first time in the literature, via immunohistofluorescence imaging. As the anti-actinidin is not commercially available, rabbit anti-actinidin previously raised by our lab is purified for the use in immunohistofluorescence imaging.

7.2 Materials and methods

7.2.1 Study design

Beef briskets (approximately 7 to 14 days postmortem) were purchased from a local supermarket (New Zealand) and were used in two separate experiments. For experiment one, the effect of actinidin on meat microstructure for meat tenderisation was studied. Raw meat samples were incubated in kiwifruit extract at pH 5.6 at 20 ℃ for 30 min to mimic meat marination. A pH of 5.6 was selected to prevent over-tenderisation of meat, as actinidin only hydrolysed MHC but not actin at a pH range of 5.5 to 8.0 (Nishiyama, 2007). In addition, pH 5.6 is also the average pH of raw beef muscles. The incubation time and temperature was chosen after conducting preliminary trials based on the current literature and cooking recipes (Harris & Maxwell, 2009; Lewis & Luh, 1988; Zespri, 2019). In experiment two, the effect of actinidin on meat microstructure during simulated gastric digestion were examined. Sous vide-cooked meat samples were subjected to

simulated gastric digestion at 37 ℃ and pH 3 for 3 h. The incubation conditions for the simulated gastric digestion were chosen according to section **4.2.4.1** and preliminary trials. The details of the incubation are described in section **7.2.4**.

7.2.2 Preparation of kiwifruit extract

Green kiwifruit (*Actinidia deliciosa* cv Hayward) was purchased from a local supermarket (New Zealand) and the kiwifruit extract was prepared according to the method described by Zhu, Kaur and Boland (2018) with modifications. After peeling, the fruit was mixed with 0.1 M ice-cold sodium citrate buffer at pH 3 and pH 5.6 (kiwifruit to buffer ratio = 1: 0.18) for 20 s, using a hand held mixer (BSB310, Breville, Australia). The mixture was then filtered using a cheese cloth followed by centrifugation at 13100 x*g* at 0 ℃ for 30 min (Heraeus™ Fresco™ 17, Thermo Fisher Scientific, Waltham, MA, USA). The supernatant was collected and placed in an ice bath for enzyme activity analysis immediately.

7.2.3 Determination of actinidin activity of the kiwifruit extract

The actinidin activity in the kiwifruit extracts at both pH 3 and pH 5.6 were determined based on the method of Boland and Hardman (1972) and Chao (2016). In brief, 100 µL of the kiwifruit extract was mixed with 100 µL of 0.1 M dithiothreitol (DTT) solution (1610611, Bio-Rad Laboratories, Hercules, CA, USA) for 3 min to activate the enzyme. After that, 100 µL of 2.74 mM actinidin substrate, the N-α-carbobenzoxy-L-lysine-P-nitrophenyl ester (Z-L-Lys-ONp) hydrochloride solution (C3637, Sigma-Aldrich, Saint Louis, MO, USA), was added to 2.85 mL of 0.1 M sodium citrate buffer (pH 3 or pH 5.6, based on the pH of the kiwifruit extract) in a cuvette. After inserting the cuvette into a UV-visible recording spectrophotometer (UV-160A, Shimadzu Corporation, Kyoto, Japan) to measure the rate of spontaneous hydrolysis of the substrate (~10 to 20 s), 50 µL

of the activated kiwifruit extract (25 µL kiwifruit extract and 25 µL of 0.1M DTT solution) was added. The change in absorbance was recorded for 100 s at 348 nm. The enzyme activity of the kiwifruit extract was calculated based on the initial absorbance changing rate (maximum hydrolysis rate), using the **Eq.7-1** (Crowley & Kyte, 2014).

Enzyme activity = (maximum hydrolysis rate) / [(Δε/1000) x l] x (V_R/ V_S) -------**Eq.7-1**

The Δε, l, V_R, and V_S stand for the extinction coefficient (5400 $M^{-1}cm^{-1}$) (Boland, 1973), the optical path length (1 cm), the total volume of the reaction mixture (3 mL) and the volume of kiwifruit extract (0.025 mL), respectively. The actinidin activity was expressed as enzyme activity units per mL of kiwifruit extract (U/mL) at 25 ℃ (*N*=3).

7.2.4 Incubation of beef samples in kiwifruit extracts

For experiment one, raw beef briskets were cut into pieces where the muscle fibre direction is parallel to their length (0.5 cm in width × 0.5 cm in height x 2 cm in length; 0.90 ± 0.10 g in weight) and were incubated in 4.5 mL of the incubation solution (pH 5.6) (**Table 7-1**) at 20 ℃ for 30 min. The actinidin activity of the incubation solutions was set after conducting preliminary trials based on the current meat tenderisation literature (Aminlari et al., 2009; Liu et al., 2011; Pooona et al., 2019; Zhu, 2017).

In the experiment two, beef briskets were SV-cooked at 60 ℃ for 24 h. After cooling to room temperature, the cooked meat was cut into pieces where the muscle fibre direction is parallel to their length (0.5 cm in width × 0.5 cm in height x 2 cm in length; 1.25 ± 0.10 g in weight), followed by immersion in 4.5 mL of the incubation solution (**Table 7-1**) at 37 ℃ for 3 h. The amount of kiwifruit extract added to the incubation solution was adjusted based on the MyPlate dietary guidelines (meat: kiwifruit = 1: 1.85) (U.S. Department of Health and Human Services and U.S. Department of Agriculture, 2015).

According to the MyPlate dietary guidelines, a serving of protein (65 g of meat) and a serving of fruit (120 g of kiwifruit, peeled) has been recommended for inclusion in a meal. The pepsin activity used during the simulated gastric digestion was 8 U/mg meat protein, as described in section **4.2.4.1**.

For both experiments, the meat samples were cut in half across their length using a scalpel and were cryofixed in liquid nitrogen (−196 °C) chilled isopentane (−160 °C) for at least 30 s, at the end of the designated incubation times. The snap-frozen meat samples were then stored at −80 °C for subsequent structural analyses. Both experiments were carried out in triplicate.

Table 7-1. The details of the incubation solutions for the experiments.

Experiments	Samples	Incubation solutions	Actinidin activity (U/g meat)
One- to study the effect of actinidin on meat microstructure during marination	A (Control)	4.5 mL of sodium citrate buffer (100 mM, pH 5.6)	0
	B	60 µL of kiwifruit extract (pH 5.6) and 4.44 mL of sodium citrate buffer (100 mM, pH 5.6)	0.25
	C	416 µL of kiwifruit extract at pH 5.6 and 4.004 mL of sodium citrate buffer (100 mM, pH 5.6)	1.7
Two- to study the effect of actinidin on meat microstructure during simulated gastric digestion	A (Control)	4.5 mL of sodium citrate buffer (100 mM, pH 3)	0
	B	Pepsin (8 U/mg meat protein, based on section **4.2.4.1**) in 4.5 mL of sodium citrate buffer (100 mM, pH 3)	0
	C	416 µL of kiwifruit extract (pH 3) and 4.084 mL of sodium citrate buffer (100 mM, pH 3)	0.4
	D	Pepsin (8 U/mg meat protein, based on section **4.2.4.1**) in 416 µL of kiwifruit extract (pH 3) and 4.084 mL of sodium citrate buffer (100 mM, pH 3)	0.4

7.2.5 Purification of anti-actinidin from rabbit serum

The rabbit serum containing polyclonal anti-actinidin was prepared previously in our lab as per the method described by Chao (2016). In brief, the anti-actinidin antibodies were raised in a rabbit using purified actinidin. 400 µg of the purified actinidin was emulsified with the Freund's Incomplete Adjuvant in 1: 1 ratio followed by injection into a rabbit. 150 µg of the purified actinidin was injected into the rabbit as a booster fortnightly after the first injection. The blood was collected from the euthanased rabbit after the completion of six boosters. After clotting the blood samples for 60 min at room temperature, the samples were centrifuged at 10000 x *g* for 15 min at 4 ℃. The supernatant was collected as the rabbit anti-actinidin serum and was stored at -80 ℃ until further use. Actinidin was detected in a Western blot analysis using the anti-actinidin (raised as mentioned above) as the primary antibody, showing the anti-actinidin was successfully produced. The anti-actinidin was purified from the rabbit serum using a Melon^{TM} Gel IgG (Immunoglobulin G) Spin Purification kit (45206, Thermo Fisher Scientific, Waltham, MA, USA) consisting of an IgG purification support, a purification buffer, and spin columns (with top and bottom caps). First, 500 µL of the purification support was pipetted into a spin column which was placed in a microcentrifuge tube. The spin column was left uncapped and the column-tube assembly was centrifuged at 5000 x *g* for a min. After centrifugation, the flow-through collected in the microcentrifuge tube was discarded. Then, the column was washed by adding 300 µL of the purification buffer to the column, followed by centrifugation at 5000 x *g* for 10 s. The flow-through collected in the microcentrifuge tube was disposed of. The wash step was repeated once. Next, the rabbit serum was diluted with the purification buffer in 1:10 ratio and 500 µL of the diluted rabbit serum was added to the column. The column was then capped and incubated at 20 ℃ for 5 min with end-over-end mixing. After that, the bottom cap was removed and

the top cap was loosened. The column was placed in a new microcentrifuge tube and was centrifuged at 5000 x *g* for a min. After centrifugation, the flow-through accumulated in the microcentrifuge tube was collected as the purified anti-actinidin, which was then stored at -20 ℃ for immunostaining.

7.2.6 Microscopy analysis of treated muscles

7.2.6.1 Histochemical analysis

The effect of kiwifruit extract on muscle microstructure under different incubation conditions was studied by performing Picro-Sirius Red (PSR) staining on the muscle sections. The cryosectioning and the staining of the treated muscles were done as described in section **4.2.5.1.** The observations were made in triplicate for each treatment.

7.2.6.2 Immunohistofluorescence imaging for the localisation of actinidin and pepsin

The cryofixed muscle blocks were cut into 10 µm thick sections using a cryostat (CM1950, Leica Microsystems GmbH, Wetzlar, Germany) at -20 °C, followed by mounting on glass slides and air-drying at room temperature for at least an hour. The localisation of actinidin in the meat sections was done by performing immunohistofluorescence imaging according to the standard protocol (Buchwalow & Böcker, 2010). In brief, the meat sections were covered in 100 µL of 10 % goat serum (G9023, Sigma-Aldrich, Saint Louis, MO, USA) in phosphate buffer saline (P7059, Sigma-Aldrich, Saint Louis, MO, USA) for 10 min to prevent non-specific binding of the antibody. The 10 % goat serum in phosphate buffer saline was then removed gently from the slides before applying the primary antibody solution to the meat sections. The primary antibody solution was prepared by diluting the purified rabbit polyclonal anti-actinidin (produced as mentioned in section **7.2.5**) using phosphate buffer saline solution comprising 1 % goat serum and 0.01 % Tween® 20 (P7949, Sigma-Aldrich, Saint Louis, MO, USA), in a ratio of 1: 5.

The diluted primary antibody was applied to the meat sections and the glass slides were kept in a humidity chamber for 1 h, followed by washing in a washing buffer (phosphate buffer saline containing 0.01 % Tween® 20) thrice. The glass slides were then blot-dried and all of the subsequent procedures were carried in the dark. After blot-drying, the secondary antibody solution was applied to the meat sections and the slides were placed in a humidity chamber for an hour. The secondary antibody solution was prepared by diluting goat anti-rabbit IgG H&L Cyanine (Cy3®) preadsorbed secondary antibody (ab6939, Abcam, Cambridge, UK) using phosphate saline buffer containing 1 % goat serum and 0.01% Tween® 20, in a ratio of 1: 1000. After that, the sections were washed in the washing buffer thrice, followed by blot-drying of the slides. The Fluoromount™ aqueous mounting medium (F4680, Sigma-Aldrich, Saint Louis, MO, USA) was then applied to the sections to preserve the fluorescent dye-stained tissues, before cover-slipping. The slides were allowed to dry for 30 min and the coverslips were sealed with nail polish for long term storage. The imaging was performed using an Olympus BX51 fluorescence light microscope (Olympus Optical, Tokyo, Japan) with a U-61000V2 D/F/R C29141 filter unit (Cy3®, excitation: 552 nm; emission: 570 nm) (Chroma Technology Corp, Bellows Falls, VT, USA). The images were captured via a QImaging MicroPublisher™ 5.0 colour CCD camera using the Q-Capture Pro7 software (QImaging, Surrey, BC, Canada). The localisation of pepsin was conducted as mentioned above with a change of the primary antibodies to the rabbit polyclonal anti-pepsin (ab182945, Abcam, Cambridge, UK) (dilution ratio of 1: 166). The observations were made in triplicate for each treatment.

7.3 Results and discussion

7.3.1 The actinidin activity of the kiwifruit extracts

The actinidin activity of the kiwifruit extracts was quantified for the determination of the amount of kiwifruit extracts required in each incubation solution to achieve a desired actinidin activity. The actinidin activity of kiwifruit extracts at pH 3 and 5.6 were measured during the esterolysis of the actinidin substrate N-α-carbobenzoxy-L-lysine-P-nitrophenyl ester (**Table 7-2)**. The actinidin activity was higher in kiwifruit extract at pH 5.6 than the extract at pH 3. Sugiyama et al. (1997) also found that actinidin had the highest activity at pH 5 to 6 during esterolysis at 37 ℃.

Table 7-2. The actinidin activity of kiwifruit extracts at pH 3 and pH 5.6 at 25 ℃.

	Kiwifruit extract (pH 3)	**Kiwifruit extract (pH 5.6)**
Actinidin activity (U/mL extract)	5.6 ± 0.1	18.7 ± 0.7

N = 3.

7.3.2 Effect of kiwifruit extract on muscle microstructure

As shown in **Figure 7-1** and **Figure 7-2,** the connective tissue was stained in red by the Sirius Red dye and muscle cells were stained in yellow by picric acid. In experiment one, small raw beef brisket muscle pieces were placed in incubation solutions with conditions mimicking marination for meat tenderisation. Differences were observed between meat samples after incubation in different solutions for 30 min. For the control with no kiwifruit extract added, the muscle cells were still intact at the end of incubation. The PSR-stained section of the control showed a uniform mix of redness and yellowness. In contrast, there were structural changes observed at the edges of the meat sections incubated in kiwifruit extract at pH 5.6 for 30 min. In the meat sample incubated in kiwifruit extract with a higher actinidin activity (**Figure 7-1C**, 1.7 U/g meat), the damage to the muscle structure was greater and expanded toward the core. Most of the muscle cells at the edge of the

section were destroyed. In addition, the PSR-stained sections of the meat samples incubated in kiwifruit extract showed a high intensity of redness at the edges of the meat sections, unlike the control sample. The lack of yellowness at the edges of the meat sections incubated in the kiwifruit extract suggests the degradation of the muscle cells by the enzyme actinidin. The area that was high in redness was bigger in the sample incubated in the kiwifruit extract with an actinidin activity of 1.7 U/g meat, showing more muscle cell hydrolysis compared to the sample incubated in the kiwifruit extract with a lower actinidin activity (0.25 U/g meat). Furthermore, as depicted in **Figure 7-1C**, the connective tissue which was stained in red had degraded along with the muscle cells at the end of incubation. These observations demonstrate the ability of actinidin to hydrolyse both the myofibrillar proteins and the connective tissue, particularly the former, at a slightly acidic pH.

The proteolytic activity of actinidin on both myofibrillar proteins and collagen has been reported in several studies. Actinidin has been found to be able to hydrolyse all the myofibrillar proteins at a pH range of 3.0 to 4.5 at 25 ℃ (Nishiyama, 2007). At pH between 5.5 and 8.0, MHC was hydrolysed into smaller fragments by actinidin, but actin remained unaffected. Thus, the meat tenderisation level caused by actinidin could potentially be controlled by manipulating the pH during treatment (Zhu, 2017). Christensen et al. (2009) discovered degradation of desmin, a reduction in myofibrillar particle size and an increment in heat-soluble collagen in porcine *Biceps femoris* muscles injected with neutral marinade containing actinidin, after storage at 2 ℃ for 2 days.

Disruption of type I collagen fibres was detected in raw pork incubated in kiwifruit extract (pH 3.4) at 25 ℃ for 4 h by Nishiyama (2000). Wada et al. (2004) observed the hydrolysis of cattle Achilles tendon treated with actinidin solution at pH 6 and pH 3.3, but not at pH

below 3. The collagen subunits α-chain and β-chain were detected using SDS-PAGE for the tendon samples incubated in actinidin solutions (pH 6 and 3.3) at 20 ℃ for 24 h. These studies showed that actinidin was able to hydrolyse collagen at pH 3 to 6 at room temperature, which was also observed in **Figure 7-1**.

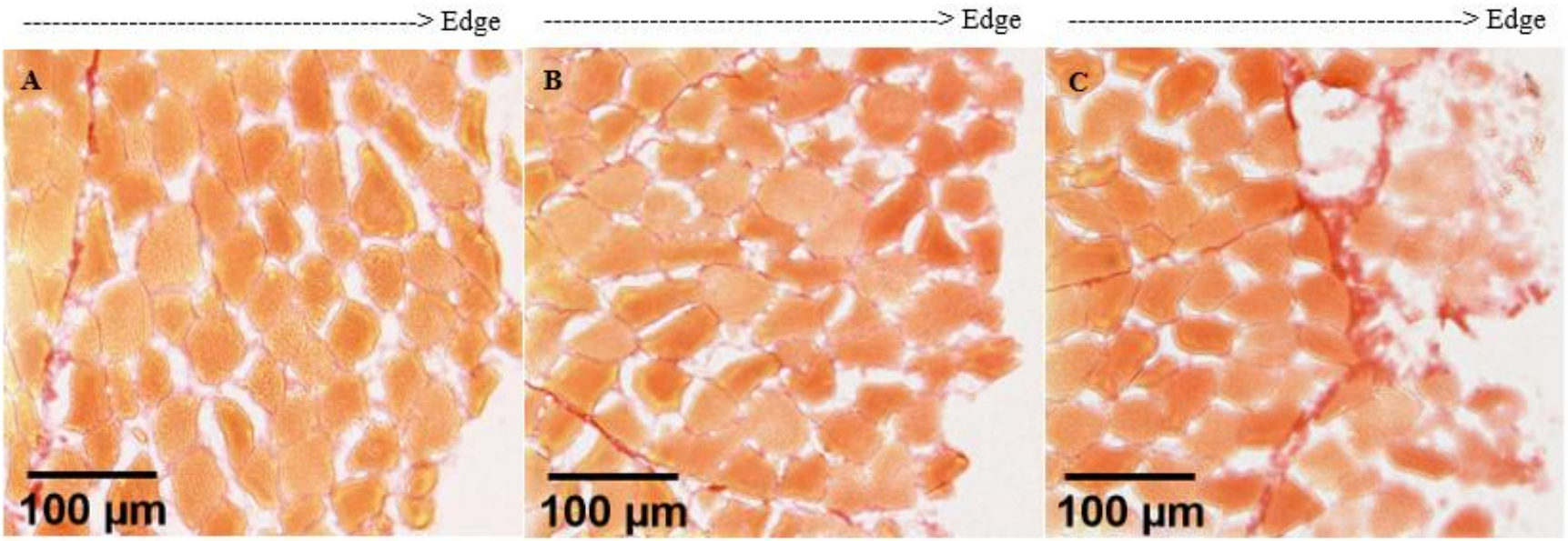

Figure 7-1. Histological sections of meat samples after incubation in (A) sodium citrate buffer at pH 5.6 (control), (B) kiwifruit extract (0.25 U/g meat) at pH 5.6 and (C) kiwifruit extract (1.7 U/g meat) at pH 5.6, at 20 ℃ for 30 min. Connective tissue was stained in red by the Sirius Red dye and muscle cells were stained in yellow by picric acid.

In experiment two, small pieces of SV-cooked beef brisket muscles were placed in incubation solutions with conditions simulating gastric digestion in humans. It was observed that the microstructure of meat incubated in different solutions were dissimilar after 3 h of incubation. For the control with no kiwifruit extract added (**Figure 7-2A**), there was no visible disruption in the meat microstructure. The muscle cells and connective tissue remained intact at the end of incubation. In contrast, the muscle samples placed in incubation solutions containing enzymes had their microstructures damaged in different ways and to different extents. In the samples placed in an incubation solution containing either pepsin (**Figure 7-2B**, 8 U/mg meat protein) or actinidin (**Figure 7-2C**, 0.4 U/g meat), the muscle structures at the edges of the sections were damaged. Both the muscle cells and connective tissue were disintegrated. However, in the sample incubated in the kiwifruit extract, it was observed that the PSR-stained section had relatively higher amounts of redness at the edge of the section than the sample incubated in pepsin solution, showing a high concentration of undegraded connective tissue in the former. These findings showed that actinidin had a greater proteolytic activity on the myofibrillar proteins than on the connective tissue at acidic pH (pH 3) at 37 °C. Pepsin was able to hydrolyse connective tissue more efficiently than actinidin during simulated gastric digestion.

When both pepsin and actinidin were included in the incubation solution (**Figure 7-2D**), the muscle structure of the sample was degraded more and the area of muscle structure destruction was extended towards the core of the section, when compared to meat samples incubated in solutions containing either pepsin or actinidin. Although a large red area was also observed at the edge of the PSR-stained section of the sample incubated in both kiwifruit extract and pepsin, the red area was more damaged than the red area observed in the sample incubated in kiwifruit extract without pepsin. This shows a synergistic

proteolytic effect of both enzymes under simulated gastric conditions, suggesting that co-ingestion of kiwifruit with meat would promote protein digestion in stomach.

Kaur et al. (2010a) reported an improvement in myofibrillar proteins hydrolysis when subjecting myofibrillar proteins to *in vitro* gastric digestion (pH 1.9) in the presence of both pepsin and actinidin. The degradation of the troponin T and other high molecular weights proteins was greater in the presence of both pepsin and actinidin rather than pepsin alone. The combined actinidin and pepsin system did not have any effect on collagen but had a minor effect on gelatine during simulated intestinal digestion (Kaur et al., 2010b). Sugiyama et al. (2005) stated that kiwifruit juice was able to degrade the globular domains of the denatured collagen such as gelatine, but was unable to hydrolyse the collagen triple helical structure. Sous vide cooking results in thermal denaturation of collagen, converting the collagen into random coiled gelatine through triple helical structure destruction (Baldwin, 2012),

Similarly, native collagen which has a rigid supermolecular structure was found to be resistant towards gastrointestinal enzymatic hydrolysis (Harkness et al., 1978; Sugiyama et al., 2005). Limited dialysable material was formed by incubating bovine tendon in human gastric juice (pH 1.5) at 37 ℃ for 2 h. The degree of hydrolysis of collagen was 1.15 % after incubating in simulated gastric juice (pH 2) for 4 h at 37 ℃ (Liang et al., 2014). In contrast, gelatine was partially digested by pepsin, where Giménez et al. (2013) observed a decrease in the intensity of bands corresponding to β-chain (~200 kDa) and α1-chain (~100 kDa) of gelatine after simulated peptic digestion at 37 ℃ for 30 min. This is in agreement with the observation in **Figure 7-2B**, where the connective tissue of the SV-cooked meat was digested along with the muscle cells by pepsin, at the end of incubation.

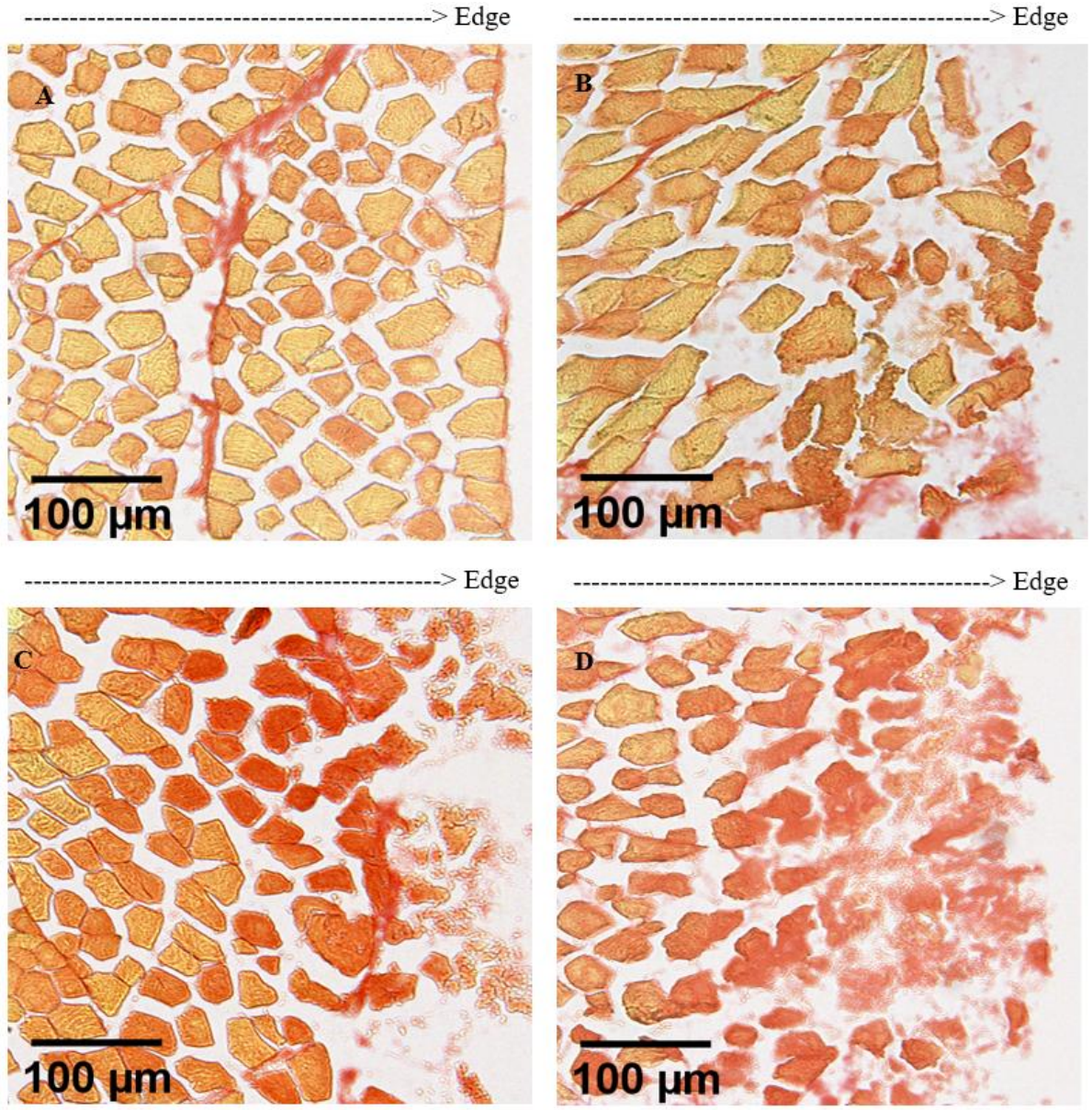

Figure 7-2. Histological sections of meat samples after incubation in (A) sodium citrate buffer at pH 3 (control), (B) sodium citrate buffer at pH 3 containing pepsin (8 U/mg meat protein), (C) kiwifruit extract (0.4 U/g meat) at pH 3, and (D) kiwifruit extract (0.4 U/g meat) at pH 3 containing pepsin (8 U/mg meat protein), at 37 °C for 3h. Connective tissue was stained in red by the Sirius Red dye and muscle cells were stained in yellow by picric acid.

7.3.3 Localisation of actinidin and pepsin using immunohistofluorescence imaging

Both actinidin and pepsin were identified on the meat sections using immunohistofluorescence imaging. During the immunostaining, the antigens, in this experiment the actinidin and pepsin, bound to the primary antibodies followed by forming complexes with the secondary antibodies labelled with fluorescent markers. As the secondary antibody used in this experiment was labelled with a cyanine dye (Cy3)

fluorophore, the antigen-antibody complex glowed red when the fluorophore was excited by the incident light during imaging. For both experiments, actinidin was identified in the meat sections incubated in kiwifruit extracts. In experiment one, no bright dot was observed in the control meat section (**Figure 7-3 A**). Bright red dots were detected in both samples incubated in the kiwifruit extract at pH 5.6, with more bright dots observed in the meat section incubated at a higher actinidin activity (**Figure 7-3 C**, 1.7 U/mg meat).

As for the experiment two, there was no actinidin observed in both the samples incubated in sodium citrate buffer (**Figure 7-4A**) and pepsin solution (**Figure 7-4B**), at pH 3. In contrast, high numbers of bright red dots were identified in both the samples incubated in kiwifruit extract (**Figure 7-4C**) and kiwifruit extract containing pepsin (**Figure 7-4D**). These observations showed that actinidin was successfully located using the purified anti-actinidin via immunohistofluorescence imaging. In addition, it was observed that most of the actinidin was identified at the edges of the muscle cells, and the endomysium which surrounds individual muscle cells. The findings were similar to the observation made by Astruc (2014b), where pepsin was located in the perimysium and endomysium of the peptic digested raw meat. He suggested that digestive juices, which contain the digestive enzymes, travel through the extracellular spaces (connective tissue) to the intracellular spaces (muscle cells), facilitating the accessibility of digestive enzymes to their substrates.

As for the localisation of pepsin, bright red dots were observed only in samples kept in the incubation solutions containing pepsin (**Figure 7-5B** and **Figure 7-5D**). Pepsin was located at the edges of muscle cells and in the extracellular spaces, which was also reported by Astruc (2014b). However, the number of bright red dots detected was very low which might be due to insufficient concentration of the anti-pepsin. Optimal anti-pepsin concentration should be determined in the future to better visualise pepsin in the meat structure.

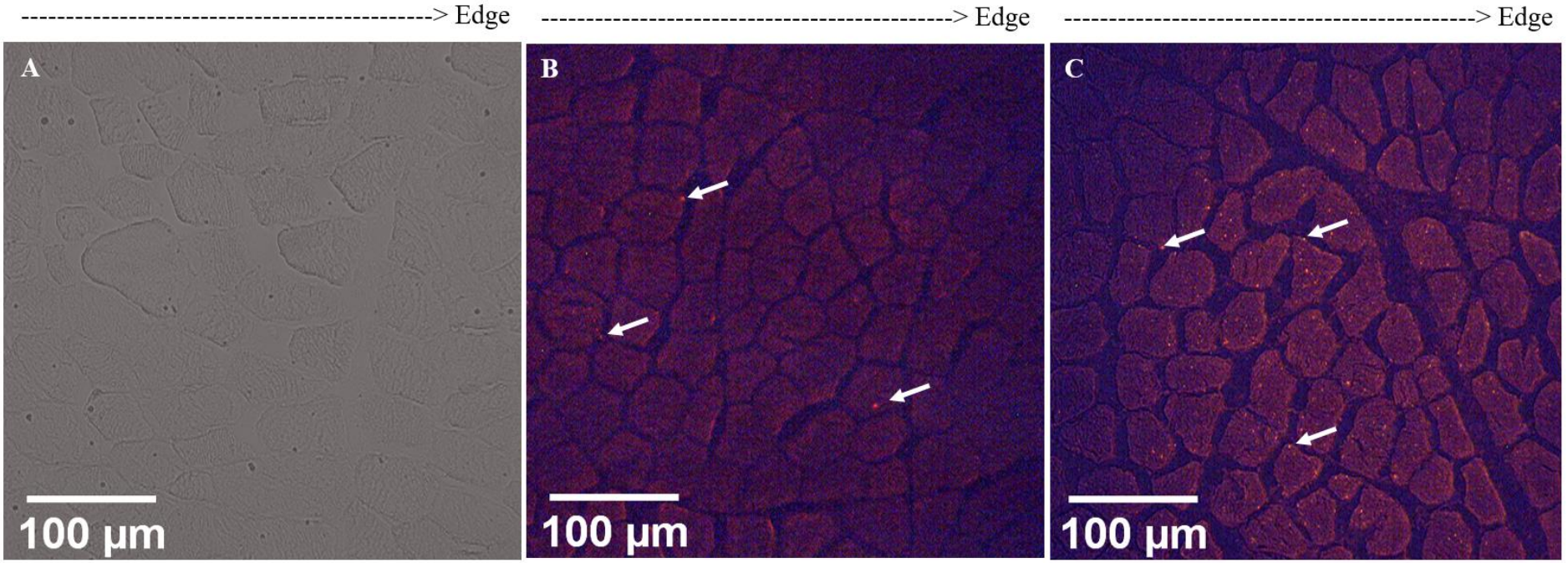

Figure 7-3. Actinidin localisation in the raw beef brisket incubated in (A) sodium citrate buffer at pH 5.6 (control), (B) kiwifruit extract (0.25 U/g meat) at pH 5.6 and (C) kiwifruit extract (1.7 U/g meat) at pH 5.6, at 20 ℃ for 30 min. Actinidin was identified on the muscle sections as bright red dots (white arrows).

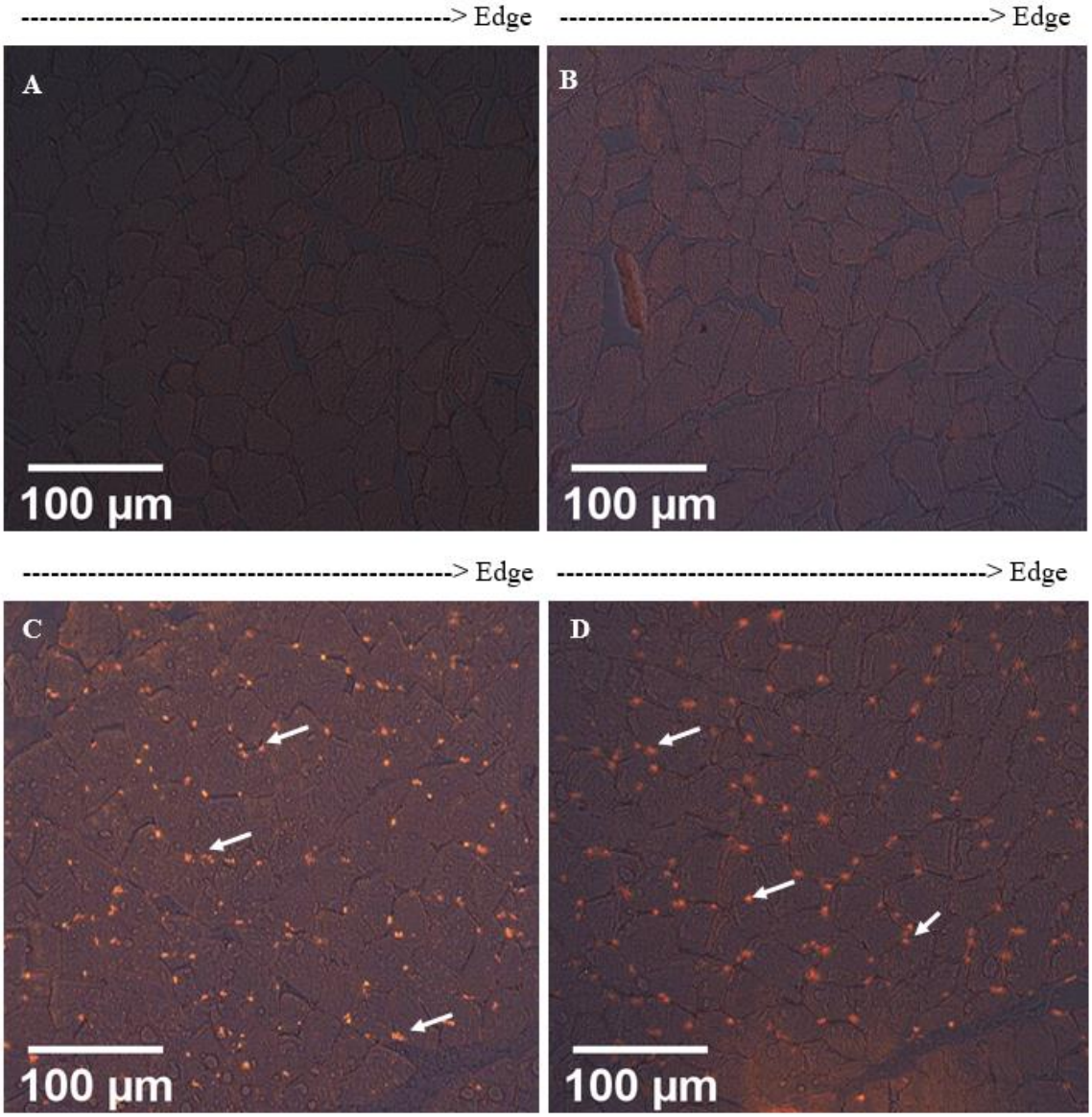

Figure 7-4. Actinidin localisation in the cooked beef brisket incubated in (A) sodium citrate buffer at pH 3 (control), (B) sodium citrate buffer at pH 3 containing pepsin (8 U/mg meat protein), (C) kiwifruit extract (0.4 U/g meat) at pH 3, and (D) kiwifruit extract (0.4 U/g meat) at pH 3 containing pepsin (8 U/mg meat protein), at 37 °C for 3h. Actinidin was identified on the muscle sections as bright red dots (white arrows).

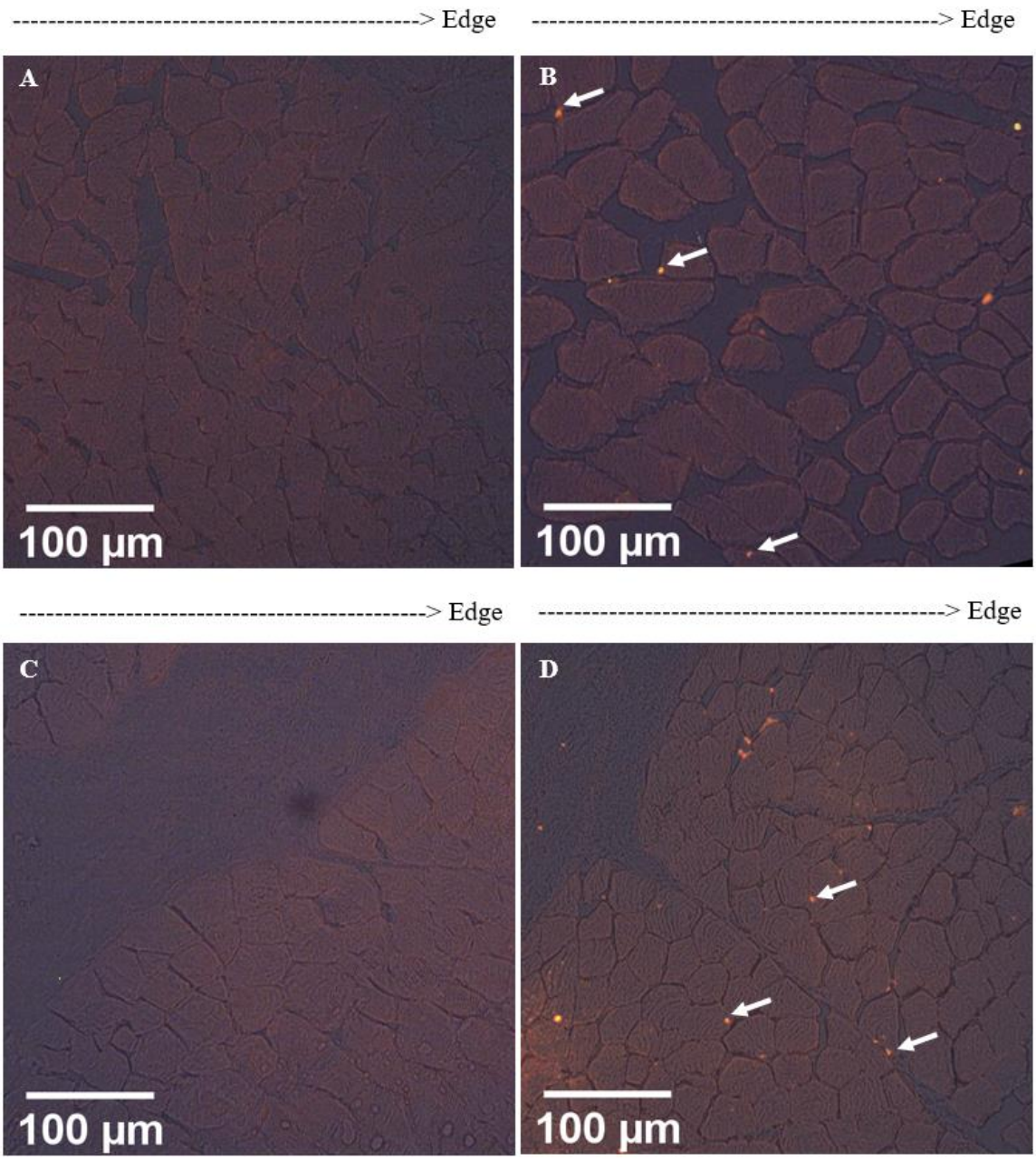

Figure 7-5. Pepsin localisation in the cooked beef brisket incubated in (A) sodium citrate buffer at pH 3 (control), (B) sodium citrate buffer at pH 3 containing pepsin (8 U/mg meat protein), (C) kiwifruit extract (0.4 U/g meat) at pH 3, and (D) kiwifruit extract (0.4 U/g meat) at pH 3 containing pepsin (8 U/mg meat protein), at 37 °C for 3h. Pepsin was identified on the muscle sections as bright red dots (white arrows).

7.4 Conclusions

This experiment revealed the effects of actinidin and pepsin on both myofibrillar proteins and connective tissue under different conditions. It was observed that the kiwifruit enzyme actinidin had a greater proteolytic effect on the myofibrillar proteins than on the connective tissue at both pH 3 and pH 5.6. For the raw samples incubated in kiwifruit extract at pH 5.6, the edges of the PSR-stained sections had a higher intensity in redness (connective tissue) accompanied with a lack of yellowness (muscle cells) at the end of incubation. These observations were also made in SV-cooked meats incubated in kiwifruit extract at pH 3 for 3 h. Pepsin was found to have a greater proteolytic effect on the connective tissue of cooked meats than actinidin, under gastric conditions. When incubating cooked meats with both pepsin and actinidin, more muscle structure breakdown was observed at the end of incubation when compared to meat samples incubated with a single enzyme. This suggested that the co-ingestion of kiwifruit and meat could promote protein digestion in the stomach. Actinidin and pepsin were successfully located via immunohistofluorescence imaging. The findings provide some insights into the penetration of enzymes into meat structure. Both enzymes were identified at the edges of the muscle cells and in the endomysium, suggesting that the incubation solutions diffuse into the muscle through the extracellular matrix to the intracellular area, facilitating the accessibility of enzymes to their substrates. Localisation of the enzymes could be done at different incubation times in the future to have a better understanding on the diffusion path of the enzymes in meat.

Chapter 8 Overall conclusion and recommendations

8.1 Overall conclusion

This thesis studied the impact of different processing technologies on meat protein properties, muscle structure and *in vitro* protein digestibility of beef. In this project, the PEF, SW, and actinidin treatments were applied to beef muscles either alone, or in combination with SV cooking. The effect of different treatments on beef muscle structure was investigated using different imaging techniques. A static *in vitro* digestion model was used to determine the effect of different processing techniques on meat protein digestibility. The impact of processing on meat protein properties, such as the molecular size and thermal stability, was also characterised. The interactions between the processing, muscle protein and structure, and *in vitro* meat protein digestibility were examined. The following research questions were answered in this thesis (**Figure 8-1**):

8.1.1 What is the effect of PEF, SW, and kiwifruit extract treatment alone on beef muscle structure and meat protein?

All of the treatments resulted in muscle structural changes at either molecular, micro- and/or ultrastructural levels. Pulsed electric field treatment on bovine *Longissimus thoracis* muscles caused sarcomere elongation and disruption at the Z-disk and I-band junctions. A sarcomere length increment of approximately 25 to 38 % was detected in the PEF-treated muscles compared to the untreated muscles, depending on the PEF intensities. Shockwave processing of bovine *Deep* and *Superficial pectoral* muscles led to the disorganisation of sarcomere structure and the formation of wavy sarcomeres. The protein secondary structure, as studied by the FT-IR microspectrometry, of the myofibres of the SW-treated muscles was affected. Kiwifruit extract treatment of bovine *Deep* and *Superficial pectoral* muscles resulted in the breakdown of both muscle cells and

connective tissue at the microstructural level, particularly in the muscle cells, due to the proteolytic action of the enzyme actinidin present in the extract.

Meat proteins were affected by SW processing but not by PEF treatment. Based on the differential calorimetric analysis, the thermal denaturation temperature and the enthalpy of collagen were reduced significantly in the SW-treated bovine *Deep* and *Superficial pectoral* muscles, compared to the untreated control muscles. The overall denaturation enthalpy of the former was also significantly lower than the latter, showing that SW treatment reduced the thermal stability of collagen, likely through the disruption of collagen triple helical tertiary or quaternary structure. No difference was observed in the protein profiles, studied using both reducing and non-reducing gel electrophoresis, between the SW-treated and untreated meat.

8.1.2 What is the effect of PEF and SW treatment on beef muscle structure and meat proteins after SV cooking?

No micro- or ultrastructural differences were discovered in both the control SV-cooked and PEF-treated SV-cooked bovine *Deep* and *Superficial pectoral* muscles. Shockwave processing in combination with SV cooking caused a more severe muscle fibre coagulation and denaturation of bovine *Deep* and *Superficial pectoral* muscles, when compared to the untreated SV-cooked muscles. A significant increment in the extracellular space area and more contracted muscle cells of the SW-treated SV-cooked muscles were observed. Differences in the secondary structure of the myofibres were detected between the control SV-cooked and SW-treated SV-cooked meat.

Meat proteins were affected by a SW-SV process but not by a PEF-SV process. Greater numbers of large proteins were observed in the electropherogram of the SW-treated SV-cooked bovine *Deep* and *Superficial pectoral* muscles, compared to the untreated SV-

cooked muscles. This observation shows that SW-SV treatment resulted in more protein aggregation and cross-linking, when compared to SV cooking alone. However, no new disulfide linkages were observed in the SW-SV treated meat, as shown in the 2D non-reducing/reducing PAGE analysis. Although PEF treatment has been reported to facilitate the release of cathepsins from the lysosomes into the cytosol, there was no significant difference in the cytosolic cathepsins activities between the PEF-treated and control untreated bovine *Deep* and *Superficial pectoral* muscles, before and during SV cooking for 0.5, 1, 2, and 5 h. These findings led to a speculation that the intensity of the PEF treatment applied in this experiment might not be high enough to result in the electroporation of the intracellular components such as the lysosomes. Thus, fresh samples should be used, and the endogenous enzymes activity should be quantified immediately after PEF treatment, to eliminate the effect of freezing and thawing on the lysosomes in the future.

8.1.3 Can meat processing improve muscle protein digestibility *in vitro*?

Pulsed electric field processing improved the *in vitro* protein digestibility of raw bovine *Longissimus thoracis* muscles by at least 18 %, in terms of the ninhydrin-reactive amino nitrogen released at the end of simulated digestion. A significantly higher *in vitro* protein digestibility was also observed in the PEF-treated SV-cooked (~29 % higher) and the SW-treated SV-cooked (~22 % higher) bovine *Deep* and *Superficial pectoral* muscles, compared to the untreated SV-cooked meat. The enzymatic hydrolysis of the meat proteins was also investigated using the reducing tricine SDS-PAGE. All of the treated muscles had their SDS-PAGE protein profiles altered, showing that the muscle protein breakdown during digestion was affected by meat processing.

8.1.4 What is the interaction between muscle structure and *in vitro* protein digestibility?

In this project, the muscle structure was closely related to the *in vitro* protein digestibility of meat. Process-induced structural changes were found to enhance the meat protein digestibility. Muscle structure modifications were observed in both PEF-treated bovine *Longissimus thoracis* muscles and SW-treated SV cooked bovine *Deep* and *Superficial pectoral* muscles. Both treatments led to an improvement in *in vitro* protein digestibility of meat. Although PEF-treated SV-cooked bovine *Deep* and *Superficial pectoral* muscles had improved protein digestibility, no muscle structural changes were detected compared with the cooked control after meat processing. However, differences were identified in the muscle micro- and ultrastructures during simulated digestion.

It was observed that the size of the muscle cells of both control and PEF-treated SV-cooked (60 ℃ for 24 h) *Deep* and *Superficial pectoral* muscles increased after 60 min of simulated gastric digestion. The muscle cell swelling was likely due to the absorption of the acidic simulated gastric juice. More severe muscle cell swelling was found in the PEF-treated SV-cooked *pectoral* muscles which had greater protein digestibility, compared to the control untreated SV-cooked muscles. The improved protein digestibility of the PEF-treated SV-cooked meat might be due to the enhanced penetration of gastric juice into meat, which has been reported to facilitate the accessibility of the digestive enzymes to their substrates (Astruc, 2014b; Bordoni et al., 2014). Muscle cell swelling during simulated digestion was also observed in both control and SW-treated SV-cooked *pectoral* muscles (60 ℃ for 12 h). Unlike the observations made in the control and PEF-treated SV-cooked meat samples, the muscle cell swelling in the SW-treated SV-cooked muscles occurred to a smaller extent than the control untreated SV-cooked muscles, despite the fact that the former had a higher protein digestibility. As excessive swelling

of the muscle cells might lead to a reduction in extracellular spaces, the transfer of the aqueous digestive juices to the core of the control untreated SV-cooked samples might be limited, causing the muscles to have a lower protein digestibility than the SW-treated SV-cooked meat (Astruc, 2014; Offer & Knight, 1988). When compared the muscle swelling observations from both experiment, the muscle cell size of meat samples SV-cooked at 60 ℃ for 12 h (both control and SW-treated samples) were larger than the samples SV-cooked for 24 h (both control and PEF-treated samples) after 62 min of simulated oral-gastric digestion. This shows that the muscle cell swelling during simulated digestion was also affected by SV cooking duration. Overall, the muscle microstructure of both PEF/SW-treated SV-cooked *pectoral* muscles was more damaged than the control SV-cooked meat at the end of simulated digestion.

In addition, the ultrastructures of all the treated samples were different from the control untreated samples at the end of simulated digestion. More degraded sarcomeres along with more severely coagulated and elongated I-bands were detected in the digested muscles of all the treated meat when compared to the untreated meat. The more coagulated I-bands might be due to more acid denaturation of the protein by the gastric juices, which exposed buried peptide bonds for the access of digestive enzymes, leading to improved proteolysis (Chian et al., 2019; McGuire & Beerman, 2012). From the observations made in this thesis, it can be concluded that with appropriate processing, meat structure can be modified to improve the accessibility of digestive proteases to their substrates, leading to an improvement in protein digestibility.

8.1.5 How do the enzymes penetrate into the meat?

The study investigated the penetration of enzyme actinidin, for the first time, and pepsin into meat, using immunohistofluorescence imaging. Both the enzyme actinidin and pepsin, were located at the edges of the muscle cells and in the endomysium after incubation. These observations suggest that the incubation solutions diffuse into the muscle through the extracellular matrix (endomysium) to the intracellular area (muscle cells), facilitating the accessibility of enzymes to their substrates.

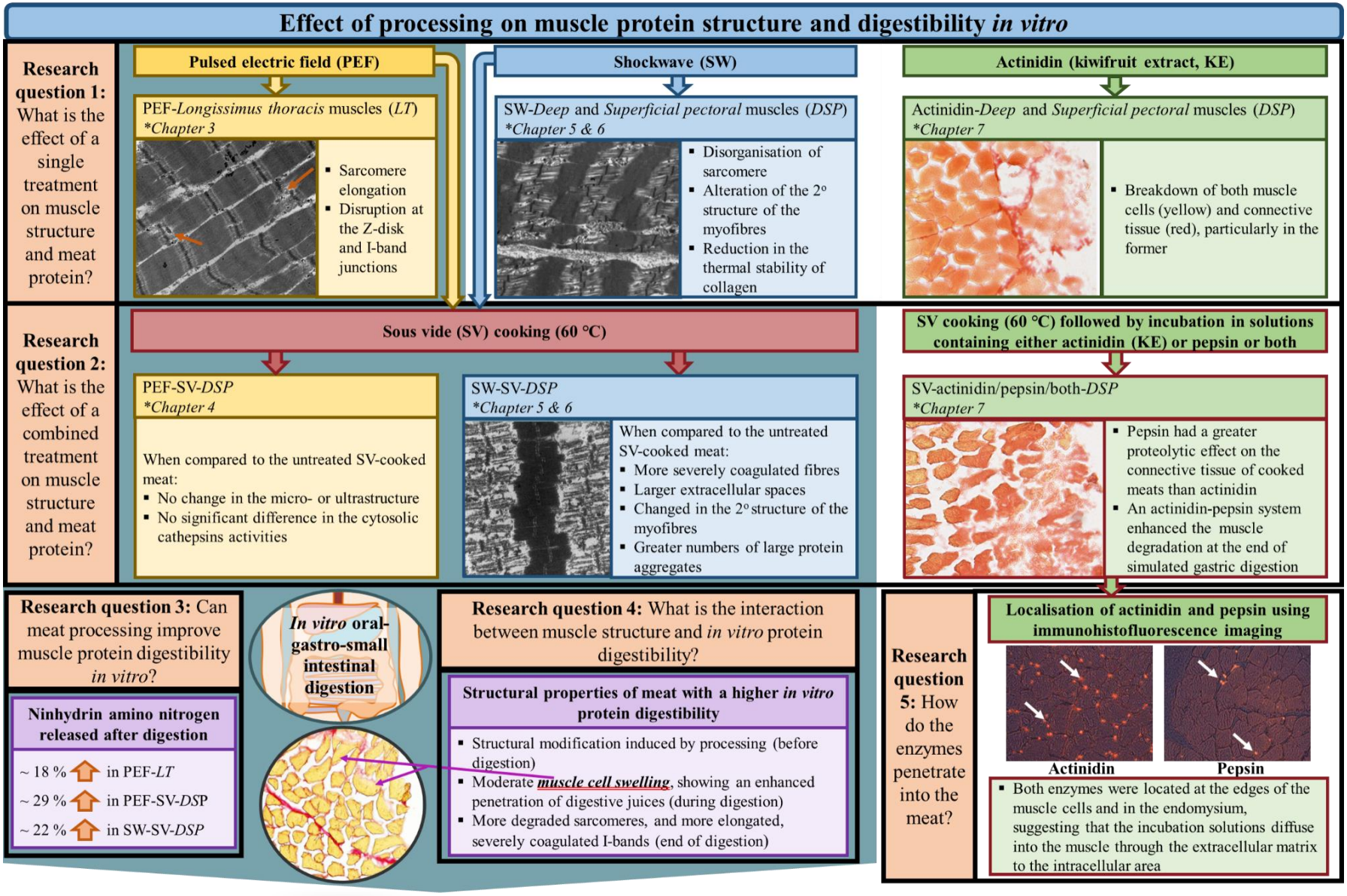

Figure 8-1. A schematic illustration of how the research questions in this thesis were addressed.

8.2 Recommendations

This study has examined different meat processing techniques to discover how effectively they improve the *in vitro* protein digestibility of beef. Future studies could further explore the interaction between the processing methods, meat structure and protein digestibility. Some recommendations for future studies are listed below.

8.2.1 Selection of muscle-based foods

Different meat cuts from different animal sources might respond differently to different processing. The muscle-based foods explored in this thesis were the bovine *Longissimus thoracis* muscles (ribeye) and the bovine *Deep* and *Superficial pectoral* muscles (brisket). Other popular beef cuts such as *Semitendinosus* (eye of round), *Longissimus lumborum* (striploin) and *Semimembranosus* (top round) could be studied in the future. For instance, SW has found to mainly act on the myofibrillar proteins and slightly on the connective tissue. Thus, it might be worth investigating the effect of SW on premium cuts, such as the striploin (lower in connective tissue content), for meat tenderisation and to reduce the ageing time. Moreover, the current application of SW technology is not economically feasible due to the requirement of cost intensive strong and resilient packaging materials (Toepfl et al., 2013). Shockwave processing of premium cuts has the potential to absorb the high production costs incurred which could be beneficial to the industry. Meat cuts from porcine, ovine, and marine sources could also be explored. As meat is a biological tissue which is inherently variable, it is also recommended to conduct future studies using larger sample size to confirm findings of the current study.

8.2.2 Exploration of different processing methods and parameters

Different processing parameters for the PEF processing, SW processing, exogenous enzymes treatment and SV cooking could also be investigated in the future. For instance,

a multistage SV cooking with a lower initial and a higher final cooking temperature could be studied as this process has the potential to promote the enzymatic hydrolysis by the cathepsins for meat tenderisation, while ensuring microbiological safety of meat. It would also be interesting to explore the PEF processing of meat using a continuous PEF system for solid foods, such as the Elea GmBH PEF Advantage^{TM} Belt developed by the German Institute of Food Technology (DIL). The PEF experiments presented in this were done using a batch system which has an approximate processing cost of about NZD 8 cents/kg meat (excluding the costs of meat and packaging materials) due to low product throughputs and relatively high labour costs (Rohlik et al., 2017). Thus, exploring the continuous PEF system might lower the production cost and would be profitable to the industry. However, more trials and process optimisation would be required before commercialisation of this technology.

In addition to the processing techniques studied in this thesis, other processing such as ohmic heating (Hradecky et al., 2017), microwave heating (Wang, Muhoza, et al., 2019), ultrasonic processing (Bagarinao et al., 2020; Barekat & Soltanizadeh, 2017), and fermentation (Charmpi et al., 2020) could be explored in the future. In addition to whole muscles, the impact of different processing methods on comminuted meat products such as burger patties and sausages could be considered.

8.2.3 Characterisation of meat digests

The SDS-PAGE analysis performed in this project was done using the soluble fraction of the meat digests. A homogenised meat digest consisting of both the soluble and insoluble fractions of the digests should be carried out in the future to understand the breakdown of the muscle proteins in both fractions at different digestion time points. More sampling time points could be used to have more detailed information on the digestion kinetic of the samples. In addition to SDS-PAGE analysis and ninhydrin assay, mass spectrometry

such as liquid chromatography–mass spectrometry (LC-MS) and matrix-assisted laser desorption/ionisation time of flight mass spectrometry (MALDI-TOF-MS) could be performed for protein and peptide identification of the digests (Toldra et al., 2008). Furthermore, MALDI-MS imaging could be done to study protein fragments and enzymatic reaction within the muscle structure (Théron, Venien, et al., 2014), along with other histochemical staining analyses. The swelling of the muscle cells at different time points of *in vitro* digestion could also be quantified to establish a correlation between muscle cell swelling and enzymatic degradation of the muscles.

8.2.4 Characterisation of the accessibility of enzymes in meat

In this project, both actinidin and pepsin were successfully located in meat using immunohistofluorescence imaging. However, only a small amount of pepsin was identified which might have been due to insufficient antibody concentration. The optimal concentration of anti-pepsin should be determined in the future. Other than pepsin and actinidin, the accessibility of other digestive enzymes (e.g. trypsin) and food enzymes used as processing aids (e.g. actinidin, papain, bromelain) in meat could be studied using immunohistofluorescence imaging. The localisation of enzymes could also be done at different incubation times to give a better understanding of the diffusion path of the enzymes in meat. More work could also be done to study the relationship between the enzymes diffusion and the extracellular matrix of meat, so that the diffusion rate of the enzymes to the meat could be manipulated, potentially controlling the meat tenderisation process or enhancing the protein digestibility. The diffusion of gastric juice into meat could also be investigated using other methods such as hyperspectral imaging and fluorescence recovery after photobleaching (FRAP) technique. The former was used to map the hydrochloric acid distribution in different foods at different gastric digestion time points (Somaratne et al., 2019). The latter was performed to identify the diffusion

properties of the fluorescein isothiocyanate (FITC)-labelled pepsin in dairy gels using a confocal scanning microscope (Thevenot et al., 2017).

8.2.5 *In vitro* digestion using a dynamic model

In this thesis, the *in vitro* protein digestibility of meat was studied using a static model. Although a static model provided some insights in the protein digestibility, the model does not mimic the actual digestion process in humans. A dynamic model should be used in the future to simulate the dynamic and transient nature of the human digestive system, such as the movement of the stomach wall and gastric emptying. Some of the dynamic models available are the Human Gastric Simulator (HGS) (Kong & Singh, 2010), the Dynamic Gastric Model (DGM) (Thuenemann et al., 2015), the TNO's gastro-intestinal model (TIM) (Minekus, 2015), the DIDGI® (Ménard et al., 2015), the artificial gastric digestive system (AGDS) (Liu et al., 2019) and the new dynamic *in vitro* human stomach system (new DIVHS) (Wang, Wu, et al., 2019). In addition, only porcine pepsin was used in the static simulated gastric digestion in this project. Raw ribeye and cooked brisket tested in this project have approximate fat contents of 8.5 % and 7.1 to 14.4 % respectively (Purchas & Wilkinson, 2013). Although these samples have a reasonably high amount of lipids, no gastric lipase was used in the simulated digestion due to the unavailability of a commercial gastric lipase that has comparable properties to human gastric lipase in the past (Brodkorb et al., 2019). As the rabbit gastric extract, which contains gastric pepsin and gastric lipase in a ratio that resembles human gastric fluid, is now available commercially, it should be used in the simulated gastric digestion instead of porcine pepsin as the only digestive enzyme.

8.2.6 *In vivo* animal and human studies

In vivo models are the gold standard which provide a more precise and accurate systems to study food digestion (Astruc, 2014b). As *in vivo* studies are usually time consuming, expensive, and complex, they could be performed at the final stage of the studies to validate the observations from *in vitro* models. For instance, *in vivo* studies could be conducted to investigate the postprandial plasma amino acid composition in growing pigs or in the elderly to demonstrate if meat processing improves their postprandial protein gains from meat.

References

Agarwal, S. K. (1990). Proteases cathepsins—A view. *Biochemical Education*, *18*(2), 67-72. https://doi.org/10.1016/0307-4412(90)90176-O

Alahakoon, A. U., Faridnia, F., Bremer, P. J., Silcock, P., & Oey, I. (2016). Pulsed electric fields effects on meat tissue quality and functionality. In D. Miklavcic (Ed.), *Handbook of electroporation* (pp. 1-21). Springer International Publishing. https://doi.org/10.1007/978-3-319-26779-1_179-1

Alahakoon, A. U., Oey, I., Bremer, P., & Silcock, P. (2018a). Optimisation of sous vide processing parameters for pulsed electric fields treated beef briskets. *Food and Bioprocess Technology*, *11*(11), 2055-2066. https://doi.org/10.1007/s11947-018-2155-9

Alahakoon, A. U., Oey, I., Bremer, P., & Silcock, P. (2018b). Process optimisation of pulsed electric fields pre-treatment to reduce the sous vide processing time of beef briskets. *International Journal of Food Science & Technology*, *54*(3), 823-834. https://doi.org/10.1111/ijfs.14002

Alahakoon, A. U., Oey, I., Bremer, P., & Silcock, P. (2019). Quality and safety considerations of incorporating post-pef ageing into the pulsed electric fields and sous vide processing chain. *Food and Bioprocess Technology*, *12*(5), 852-864. https://doi.org/10.1007/s11947-019-02254-6

Alahakoon, A. U., Oey, I., Silcock, P., & Bremer, P. (2017). Understanding the effect of pulsed electric fields on thermostability of connective tissue isolated from beef *pectoralis* muscle using a model system. *Food Research International*, *100*(Pt 2), 261-267. https://doi.org/10.1016/j.foodres.2017.08.025

Alberts, B., Johnson, A., Lewis, J., Raff, M., Roberts, K., & Walter, P. (2002). Fractionation of cells. In *Molecular biology of cell* (4th ed.). Garland Science. https://www.ncbi.nlm.nih.gov/books/NBK26936/

Alsenaidy, M. A., Jain, N. K., Kim, J. H., Middaugh, C. R., & Volkin, D. B. (2014). Protein comparability assessments and potential applicability of high throughput biophysical methods and data visualization tools to compare physical stability profiles. *Frontiers in pharmacology*, *5*, 39-39. https://doi.org/10.3389/fphar.2014.00039

Alturkistani, H. A., Tashkandi, F. M., & Mohammedsaleh, Z. M. (2015). Histological stains: a literature review and case study. *Glob J Health Sci*, *8*(3), 72-79. https://doi.org/10.5539/gjhs.v8n3p72

Aminlari, M., Shekarforoush, S. S., Gheisari, H. R., & Golestan, L. (2009). Effect of actinidin on the protein solubility, water holding capacity, texture, electrophoretic pattern of beef, and on the quality attributes of a sausage product. *Journal of Food Science*, *74*(3), C221-C226. https://doi.org/10.1111/j.1750-3841.2009.01087.x

Anson, M. L. (1938). The estimation of pepsin, trypsin, papain, and cathepsin with hemoglobin. *The Journal of general physiology*, *22*(1), 79-89. https://doi.org/10.1085/jgp.22.1.79

Anwar, R. A. (1990). Elastin: A brief review. *Biochemical Education*, *18*(4), 162-166. https://doi.org/10.1016/0307-4412(90)90121-4

AOAC. (1981). Official method 981.10 crude protein in meat: block digestion method. *Official Methods of Analysis of AOAC*, *2*(37), 7-8.

Argyri, K., Birba, A., Miller, D. D., Komaitis, M., & Kapsokefalou, M. (2009). Predicting relative concentrations of bioavailable iron in foods using *in vitro* digestion: New

developments. *Food Chemistry*, *113*(2), 602-607. https://doi.org/10.1016/j.foodchem.2008.07.089

Arroyo, C., Eslami, S., Brunton, N. P., Arimi, J. M., Noci, F., & Lyng, J. G. (2015). An assessment of the impact of pulsed electric fields processing factors on oxidation, color, texture, and sensory attributes of turkey breast meat. *Poultry Science*, *94*(5), 1088-1095. https://doi.org/10.3382/ps/pev097

Arroyo, C., Lascorz, D., O'Dowd, L., Noci, F., Arimi, J., & Lyng, J. G. (2015). Effect of pulsed electric field treatments at various stages during conditioning on quality attributes of beef *longissimus thoracis et lumborum* muscle. *Meat Science*, *99*, 52-59. https://doi.org/10.1016/j.meatsci.2014.08.004

Arroyo, C., & Lyng, J. G. (2017). Electroprocessing of meat and meat products. In *Emerging technologies in meat processing* (pp. 103-130). John Wiley & Sons, Ltd. https://doi.org/10.1002/9781118350676.ch4

Ashie, I. N. A., Sorensen, T. L., & Nielsen, P. M. (2002). Effects of papain and a microbial enzyme on meat proteins and beef tenderness. *Journal of Food Science*, *67*(6), 2138-2142. https://doi.org/10.1111/j.1365-2621.2002.tb09516.x

Astruc, T. (2014a). Connective tissue: structure, function, and influence on meat quality. In M. Dikeman & C. Devine (Eds.), *Encyclopedia of meat science* (2nd ed., pp. 321-328). Academic Press. https://doi.org/10.1016/B978-0-12-384731-7.00186-0

Astruc, T. (2014b). Muscle structure and digestive enzyme bioaccessibility to intracellular compartments. In M. Boland, M. Golding, & H. Singh (Eds.), *Food structures, digestion and health* (pp. 193-222). Academic Press. https://doi.org/10.1016/B978-0-12-404610-8.00007-4

Astruc, T., Gatellier, P., Labas, R., Lhoutellier, V. S., & Marinova, P. (2010). Microstructural changes in *m. rectus abdominis* bovine muscle after heating. *Meat Science*, *85*(4), 743-751. https://doi.org/10.1016/j.meatsci.2010.03.035

Astruc, T., Peyrin, F., Venien, A., Labas, R., Abrantes, M., Dumas, P., & Jamme, F. (2012). In situ thermal denaturation of myofibre sub-type proteins studied by immunohistofluorescence and synchrotron radiation FT-IR microspectroscopy. *Food Chemistry*, *134*(2), 1044-1051. https://doi.org/10.1016/j.foodchem.2012.03.012

Attene-Ramos, M. S., Nava, G. M., Muellner, M. G., Wagner, E. D., Plewa, M. J., & Gaskins, H. R. (2010). DNA damage and toxicogenomic analyses of hydrogen sulfide in human intestinal epithelial FHs 74 Int cells. *Environmental and Molecular Mutagenesis*, *51*(4), 304-314. https://doi.org/10.1002/em.20546

Bagarinao, N. C., Kaur, L., & Boland, M. (2020). Effects of ultrasound treatments on tenderness and *in vitro* protein digestibility of New Zealand abalone, *Haliotis iris*. *Foods*, *9*(8). https://doi.org/10.3390/foods9081122

Bailey, A. J. (1991). The chemistry of natural enzyme-induced cross-links of proteins. *Amino Acids*, *1*(3), 293-306. https://doi.org/10.1007/BF00813999

Bailey, A. J., & Light, N. D. (1989). *Connective tissue in meat and meat products*. Elsevier Science Publishers Ltd. https://doi.org/10.1016/0309-1740%2889%2990016-8

Baker, E. N. (1976). The structure of actinidin at 5.5 Å resolution. *Journal of Molecular Biology*, *101*(2), 185-196. https://doi.org/10.1016/0022-2836(76)90371-5

Baldwin, D. E. (2012). Sous vide cooking: A review. *International Journal of Gastronomy and Food Science*, *1*(1), 15-30. https://doi.org/10.1016/j.ijgfs.2011.11.002

Barekat, S., & Soltanizadeh, N. (2017). Effects of ultrasound on microstructure and enzyme penetration in beef *Longissimus lumborum* muscle. *Food and Bioprocess Technology*. https://doi.org/10.1007/s11947-017-2043-8

Batista Napotnik, T., Rebersek, M., Vernier, P. T., Mali, B., & Miklavcic, D. (2016). Effects of high voltage nanosecond electric pulses on eukaryotic cells (*in vitro):* A systematic review. *Bioelectrochemistry*, *110*, 1-12. https://doi.org/10.1016/j.bioelechem.2016.02.011

Bax, M.-L., Aubry, L., Ferreira, C., Daudin, J.-D., Gatellier, P., Rémond, D., & Santé-Lhoutellier, V. (2012). Cooking temperature is a key determinant of *in vitro* meat protein digestion rate: investigation of underlying mechanisms. *Journal of Agricultural and Food Chemistry*, *60*(10), 2569-2576. https://doi.org/10.1021/jf205280y

Bax, M. L., Buffiere, C., Hafnaoui, N., Gaudichon, C., Savary-Auzeloux, I., Dardevet, D., Sante-Lhoutellier, V., & Remond, D. (2013). Effects of meat cooking, and of ingested amount, on protein digestion speed and entry of residual proteins into the colon: a study in minipigs. *PLoS One*, *8*(4), e61252. https://doi.org/10.1371/journal.pone.0061252

Bax, M. L., Sayd, T., Aubry, L., Ferreira, C., Viala, D., Chambon, C., Remond, D., & Sante-Lhoutellier, V. (2013). Muscle composition slightly affects *in vitro* digestion of aged and cooked meat: identification of associated proteomic markers. *Food Chemistry*, *136*(3-4), 1249-1262. https://doi.org/10.1016/j.foodchem.2012.09.049

Bechet, D., Tassa, A., Taillandier, D., Combaret, L., & Attaix, D. (2005). Lysosomal proteolysis in skeletal muscle. *The International Journal of Biochemistry & Cell Biology*, *37*(10), 2098-2114. https://doi.org/10.1016/j.biocel.2005.02.029

Becila, S., Herrera-Mendez, C. H., Coulis, G., Labas, R., Astruc, T., Picard, B., Boudjellal, A., Pelissier, P., Bremaud, L., & Ouali, A. (2010). Postmortem muscle cells die through apoptosis. *European Food Research and Technology*, *231*(3), 485-493. https://doi.org/10.1007/s00217-010-1296-5

Bejerholm, C., Tørngren, M. A., & Aaslyng, M. D. (2014). Cooking of Meat. In M. Dikeman & C. Devine (Eds.), *Encyclopedia of meat sciences* (2nd ed., pp. 370-376). Academic Press. https://doi.org/10.1016/B978-0-12-384731-7.00187-2

Bekhit, A., Han, J., Morton, J., & Sedcole, R. (2007). Effect of kiwifruit juice and water pre-rigor infusion on lamb quality. Proceedings 53rd International Congress of Meat Science and Technology,

Bekhit, A. E.-D. A., Hopkins, D. L., Geesink, G., Bekhit, A. A., & Franks, P. (2014). Exogenous proteases for meat tenderization. *Critical Reviews in Food Science and Nutrition*, *54*(8), 1012-1031. https://doi.org/10.1080/10408398.2011.623247

Bekhit, A. E.-D. A., van de Ven, R., Suwandy, V., Fahri, F., & Hopkins, D. L. (2014). Effect of pulsed electric field treatment on cold-boned muscles of different potential tenderness [journal article]. *Food and Bioprocess Technology*, *7*(11), 3136-3146. https://doi.org/10.1007/s11947-014-1324-8

Bendall, J. (1973). Postmortem changes in muscle. *The Structure and Function of Muscle*, *2*, 243-309. https://doi.org/10.1016/B978-0-12-119102-3.50012-4

Berlett, B. S., & Stadtman, E. R. (1997). Protein oxidation in aging, disease, and oxidative stress. *Journal of Biological Chemistry*, *272*(33), 20313-20316. https://doi.org/10.1074/jbc.272.33.20313

Bernofsky, C., Fox Jr, J. B., & Schweigert, B. S. (1959). Biochemistry of myoglobin. VII. the effect of cooking on myoglobin in beef muscle. *Journal of Food Science*, *24*(4), 339-343. https://doi.org/10.1111/j.1365-2621.1959.tb17281.x

Bertola, N. C., Bevilacqua, A. E., & Zaritzky, N. E. (1994). Heat treatment effect on texture changes and thermal denaturation of proteins in beef muscle. *Journal of Food Processing and Preservation*, *18*(1), 31-46. https://doi.org/10.1111/j.1745-4549.1994.tb00240.x

Bhat, Z. F., Morton, J. D., Mason, S. L., & Bekhit, A. E.-D. A. (2018a). Applied and emerging methods for meat tenderization: A comparative perspective. *Comprehensive Reviews in Food Science and Food Safety*, *17*(4), 841-859. https://doi.org/10.1111/1541-4337.12356

Bhat, Z. F., Morton, J. D., Mason, S. L., & Bekhit, A. E.-D. A. (2018b). Current and future prospects for the use of pulsed electric field in the meat industry. *Critical Reviews in Food Science and Nutrition*, 1-15. https://doi.org/10.1080/10408398.2018.1425825

Bhat, Z. F., Morton, J. D., Mason, S. L., & Bekhit, A. E.-D. A. (2018c). Pulsed electric field: Role in protein digestion of beef *Biceps femoris*. *Innovative Food Science & Emerging Technologies*, *50*, 132-138. https://doi.org/10.1016/j.ifset.2018.09.006

Bhat, Z. F., Morton, J. D., Mason, S. L., & Bekhit, A. E.-D. A. (2019a). Does pulsed electric field have a potential to improve the quality of beef from older animals and how? *Innovative Food Science & Emerging Technologies*, *56*. https://doi.org/10.1016/j.ifset.2019.102194

Bhat, Z. F., Morton, J. D., Mason, S. L., & Bekhit, A. E.-D. A. (2019b). Pulsed electric field improved protein digestion of beef during *in-vitro* gastrointestinal simulation. *LWT*, *102*, 45-51. https://doi.org/10.1016/j.lwt.2018.12.013

Bhat, Z. F., Morton, J. D., Mason, S. L., Bekhit, A. E.-D. A., & Mungure, T. E. (2019). Pulsed electric field: Effect on *in-vitro* simulated gastrointestinal protein digestion of deer *Longissimus dorsi*. *Food Research International*, *120*, 793-799. https://doi.org/10.1016/j.foodres.2018.11.040

Bhat, Z. F., Morton, J. D., Mason, S. L., & Bekhit, A. E. D. A. (2018d). Calpain activity, myofibrillar protein profile, and physicochemical properties of beef Semimembranosus and Biceps femoris from culled dairy cows during aging. *Journal of Food Processing and Preservation*, *42*(12). https://doi.org/10.1111/jfpp.13835

Bhat, Z. F., Morton, J. D., Mason, S. L., Jayawardena, S. R., & Bekhit, A. E.-D. A. (2019). Pulsed electric field: A new way to improve digestibility of cooked beef. *Meat Science*, *155*, 79-84. https://doi.org/10.1016/j.meatsci.2019.05.005

Bhat, Z. F., Morton, J. D., Mason, S. L., Mungure, T. E., Jayawardena, S. R., & Bekhit, A. E.-D. A. (2019). Effect of pulsed electric field on calpain activity and proteolysis of venison. *Innovative Food Science & Emerging Technologies*, *52*, 131-135. https://doi.org/10.1016/j.ifset.2018.11.006

Bhat, Z. F., Morton, J. D., Zhang, X., Mason, S. L., & Bekhit, A. E.-D. A. (2020). Sous-vide cooking improves the quality and *in-vitro* digestibility of *Semitendinosus* from culled dairy cows. *Food Research International*, *127*, 108708. https://doi.org/10.1016/j.foodres.2019.108708

Biesalski, H. K. (2005). Meat as a component of a healthy diet–Are there any risks or benefits if meat is avoided in the diet? *Meat Science*, *70*(3), 509-524. https://doi.org/10.1016/j.meatsci.2004.07.017

Blanco, A., & Blanco, G. (2017). Digestion - Absorption. In A. Blanco & G. Blanco (Eds.), *Medical biochemistry* (pp. 251-273). Academic Press. https://doi.org/10.1016/B978-0-12-803550-4.00012-4

Böcker, U., Ofstad, R., Wu, Z., Bertram, H. C., Sockalingum, G. D., Manfait, M., Egelandsdal, B., & Kohler, A. (2007). Revealing covariance structures in Fourier transform infrared and Raman microspectroscopy spectra: a study on pork muscle fiber tissue subjected to different processing parameters. *Applied Spectroscopy*, *61*(10), 1032-1039. https://doi.org/10.1366%2F000370207782217707

Bodwell, C., & Anderson, B. (Eds.). (1986). *Nutritional composition and value of meat and meat products*. Academic Press, Inc.

Bohley, P., & Seglen, P. O. (1992). Proteases and proteolysis in the lysosome [journal article]. *Experientia*, *48*(2), 151-157. https://doi.org/10.1007/bf01923508

Boirie, Y., Dangin, M., Gachon, P., Vasson, M.-P., Maubois, J.-L., & Beaufrère, B. (1997). Slow and fast dietary proteins differently modulate postprandial protein accretion. *Proceedings of the National Academy of Sciences of the United States of America*, *94*(26), 14930-14935. https://doi.org/10.1073/pnas.94.26.14930

Boland, M. (1973). *Kinetics and mechanism of proteolytic enzyme catalysed reactions* [Doctoral dissertation, Massey University]. Massey Research Online. http://hdl.handle.net/10179/4575

Boland, M. (2013). Chapter four-Kiwifruit proteins and enzymes: Actinidin and other significant proteins. In B. Mike & J. M. Paul (Eds.), *Advances in food and nutrition research* (Vol. Volume 68, pp. 59-80). Academic Press. https://doi.org/10.1016/B978-0-12-394294-4.00004-3

Boland, M. (2016). Human digestion – A processing perspective. *Journal of the Science of Food and Agriculture*, *96*(7), 2275-2283. https://doi.org/10.1002/jsfa.7601

Boland, M., Kaur, L., Chian, F. M., & Astruc, T. (2019). Muscle proteins. In L. Melton, F. Shahidi, & P. Varelis (Eds.), *Encyclopedia of food chemistry* (pp. 164-179). Academic Press. https://doi.org/10.1016/B978-0-08-100596-5.21602-8

Boland, M. J., & Hardman, M. J. (1972). Kinetic studies on the thiol protease from *Actinidia chinensis*. *FEBS Letters*, *27*(2), 282-284. https://doi.org/10.1016/0014-5793(72)80641-0

Bolumar, T., Bindrich, U., Toepfl, S., Toldra, F., & Heinz, V. (2014). Effect of electrohydraulic shockwave treatment on tenderness, muscle cathepsin and peptidase activities and microstructure of beef loin steaks from Holstein young bulls. *Meat Science*, *98*(4), 759-765. https://doi.org/10.1016/j.meatsci.2014.07.024

Bolumar, T., Enneking, M., Toepfl, S., & Heinz, V. (2013). New developments in shockwave technology intended for meat tenderization: opportunities and challenges. a review. *Meat Science*, *95*(4), 931-939. https://doi.org/10.1016/j.meatsci.2013.04.039

Bolumar, T., & Toepfl, S. (2016). Application of shockwaves for meat tenderization. In K. Knoerzer, P. Juliano, & G. W. Smithers (Eds.), *Innovative food processing technologies: extraction, separation, component modification and process intensification* (pp. 231-258). Woodhead Publishing. https://doi.org/10.1016/b978-0-08-100294-0.00009-2

Bordoni, A., Laghi, L., Babini, E., Di Nunzio, M., Picone, G., Ciampa, A., Valli, V., Danesi, F., & Capozzi, F. (2014). The foodomics approach for the evaluation of protein bioaccessibility in processed meat upon *in vitro* digestion. *Electrophoresis*, *35*(11), 1607-1614. https://doi.org/10.1002/elps.201300579

Bouton, P. E., & Harris, P. V. (1981). Changes in the tenderness of meat cooked at 50–65°c. *Journal of Food Science*, *46*(2), 475-478. https://doi.org/10.1111/j.1365-2621.1981.tb04889.x

Bowker, B. C., Callahan, J. A., & Solomon, M. B. (2010). Effects of hydrodynamic pressure processing on the marination and meat quality of turkey breasts. *Poultry Science*, *89*(8), 1744-1749. https://doi.org/10.3382/ps.2009-00484

Bowker, B. C., Eastridge, J. S., & Solomon, M. B. (2016). Hydrodynamic pressure processing: impact on the quality attributes of fresh and further-processed meat products. In A. K. Jaiswal (Ed.), *Food processing technologies* (pp. 251-270). CRC Press. https://doi.org/10.1201/9781315372365-13

Bowker, B. C., Fahrenholz, T. M., Paroczay, E. W., Eastridge, J. S., & Solomon, M. B. (2008). Effect of hydrodynamic pressure processing and aging on the tenderness and myofibrillar proteins of beef strip loins. *Journal of Muscle Foods*, *19*(1), 74-97. https://doi.org/10.1111/j.1745-4573.2007.00101.x

Bowker, B. C., Fahrenholz, T. M., Paroczay, E. W., & Solomon, M. B. (2008). Effect of hydrodynamic pressure processing and aging on sarcoplasmic proteins of beef strip loins. *Journal of Muscle Foods*, *19*(2), 175-193. https://doi.org/10.1111/j.1745-4573.2007.00104.x

Bowker, B. C., Liu, M., Callahan, J., & Solomon, M. (2010). Effect of hydrodynamic pressure processing on the processing and quality characteristics of moisture-enhanced pork loins. *Journal of Food Science*, *75*(4), S237-S244. https://doi.org/10.1111/j.1750-3841.2010.01581.x

Bradford, M. M. (1976). A rapid and sensitive method for the quantitation of microgram quantities of protein utilizing the principle of protein-dye binding. *Analytical Biochemistry*, *72*(1), 248-254. https://doi.org/10.1016/0003-2697(76)90527-3

Brewer, M. S., Novakofski, J., & Freise, K. (2006). Instrumental evaluation of pH effects on ability of pork chops to bloom. *Meat Science*, *72*(4), 596-602. https://doi.org/10.1016/j.meatsci.2005.09.009

Brodkorb, A., Egger, L., Alminger, M., Alvito, P., Assuncao, R., Ballance, S., Bohn, T., Bourlieu-Lacanal, C., Boutrou, R., Carriere, F., Clemente, A., Corredig, M., Dupont, D., Dufour, C., Edwards, C., Golding, M., Karakaya, S., Kirkhus, B., Le Feunteun, S., Lesmes, U., Macierzanka, A., Mackie, A. R., Martins, C., Marze, S., McClements, D. J., Menard, O., Minekus, M., Portmann, R., Santos, C. N., Souchon, I., Singh, R. P., Vegarud, G. E., Wickham, M. S. J., Weitschies, W., & Recio, I. (2019). INFOGEST static in vitro simulation of gastrointestinal food digestion. *Nature Protocol*, *14*(4), 991-1014. https://doi.org/10.1038/s41596-018-0119-1

Bronfen, E. (2019). *Obsessed: The cultural critic's life in the kitchen*. Rutgers University Press. https://books.google.co.nz/books?id=mvy9DwAAQBAJ

Buchwalow, I. B., & Böcker, W. (2010). *Immunohistochemistry- Basics and methods* (Vol. 1). Springer. https://doi.org/10.1007/978-3-642-04609-4

Buzała, M., Janicki, B., Buzała, M., & Słomka, A. (2015). Heme iron in meat as the main source of iron in the human diet. *Journal of Elementology*(1/2016). https://doi.org/10.5601/jelem.2015.20.1.850

Caballero, B., Sierra, V., Oliván, M., Vega-Naredo, I., Tomás-Zapico, C., Alvarez-García, Ó., Tolivia, D., Hardeland, R., Rodríguez-Colunga, M. J., & Coto-Montes, A. (2007). Activity of cathepsins during beef aging related to mutations in the myostatin gene. *Journal of the Science of Food and Agriculture*, *87*(2), 192-199. https://doi.org/10.1002/jsfa.2683

Camou, J. P., Marchello, J. A., Thompson, V. F., Mares, S. W., & Goll, D. E. (2007). Effect of postmortem storage on activity of μ- and m-calpain in five bovine muscles1. *Journal of Animal Science*, *85*(10), 2670-2681. https://doi.org/10.2527/jas.2007-0164

Capetanaki, Y., Milner, D. J., & Weitzer, G. (1997). Desmin in muscle formation and maintenance: knockouts and consequences. *Cell Structure and Function*, *22*(1), 103-116. https://doi.org/10.1247/csf.22.103

Carmody, R. N., & Wrangham, R. W. (2009). The energetic significance of cooking. *J Hum Evol*, *57*(4), 379-391. https://doi.org/10.1016/j.jhevol.2009.02.011

Carton, I., Böcker, U., Ofstad, R., Sørheim, O., & Kohler, A. (2009). Monitoring Secondary Structural Changes in Salted and Smoked Salmon Muscle Myofiber Proteins by FT-IR Microspectroscopy. *Journal of Agricultural and Food Chemistry*, *57*(9), 3563-3570. https://doi.org/10.1021/jf803668e

Castro, A. J., Barbosa-Cánovas, G. V., & Swanson, B. G. (1993). Microbial inactivation of foods by pulsed electric fields. *Journal of Food Processing and Preservation*, *17*(1), 47-73. https://doi.org/10.1111/j.1745-4549.1993.tb00225.x

Chacko, A., & Cummings, J. (1988). Nitrogen losses from the human small bowel: obligatory losses and the effect of physical form of food. *Gut*, *29*(6), 809-815. https://doi.org/10.1136/gut.29.6.809

Chagnot, C., Listrat, A., Astruc, T., & Desvaux, M. (2012). Bacterial adhesion to animal tissues: protein determinants for recognition of extracellular matrix components. *Cellular Microbiology*, *14*(11), 1687-1696. https://doi.org/10.1111/cmi.12002

Chalabi, M., Khademi, F., Yarani, R., & Mostafaie, A. (2014). Proteolytic activities of kiwifruit actinidin (*Actinidia deliciosa* cv. Hayward) on different fibrous and globular proteins: a comparative study of actinidin with papain [journal article]. *Applied Biochemistry and Biotechnology*, *172*(8), 4025-4037. https://doi.org/10.1007/s12010-014-0812-7

Chao, D. (2016). *Actinidin : The predominant protease in kiwifruit* [Masters dissertation, Massey University]. Massey Research Online. http://hdl.handle.net/10179/10070

Charmpi, C., Van der Veken, D., Van Reckem, E., De Vuyst, L., & Leroy, F. (2020). Raw meat quality and salt levels affect the bacterial species diversity and community dynamics during the fermentation of pork mince. *Food Microbiology*, *89*, 103434. https://doi.org/10.1016/j.fm.2020.103434

Cheftel, J. C., & Culioli, J. (1997). Effects of high pressure on meat: a review. *Meat Science*, *46*(3), 211-236. https://doi.org/10.1016/S0309-1740(97)00017-X

Chen, J. H., Ren, Y., Seow, J., Liu, T., Bang, W. S., & Yuk, H. G. (2012). Intervention technologies for ensuring microbiological safety of meat: Current and future trends. *Comprehensive Reviews in Food Science and Food Safety*, *11*(2), 119-132. https://doi.org/10.1111/j.1541-4337.2011.00177.x

Chéret, R., Delbarre-Ladrat, C., Lamballerie-Anton, M. d., & Verrez-Bagnis, V. (2007). Calpain and cathepsin activities in post mortem fish and meat muscles. *Food Chemistry*, *101*(4), 1474-1479. https://doi.org/10.1016/j.foodchem.2006.04.023

Chian, F. M., Kaur, L., Oey, I., Astruc, T., Hodgkinson, S., & Boland, M. (2019). Effect of Pulsed Electric Fields (PEF) on the ultrastructure and in vitro protein digestibility of bovine longissimus thoracis. *LWT*, *103*, 253-259. https://doi.org/10.1016/j.lwt.2019.01.005

Choi, Y. M., & Kim, B. C. (2009). Muscle fiber characteristics, myofibrillar protein isoforms, and meat quality. *Livestock Science*, *122*(2-3), 105-118. https://doi.org/10.1016/j.livsci.2008.08.015

Christensen, L., Bertram, H. C., Aaslyng, M. D., & Christensen, M. (2011). Protein denaturation and water–protein interactions as affected by low temperature long time treatment of porcine *Longissimus dorsi*. *Meat Science*, *88*(4), 718-722. https://doi.org/10.1016/j.meatsci.2011.03.002

Christensen, L., Ertbjerg, P., Aaslyng, M. D., & Christensen, M. (2011). Effect of prolonged heat treatment from 48°C to 63°C on toughness, cooking loss and color of pork. *Meat Science*, *88*(2), 280-285. https://doi.org/10.1016/j.meatsci.2010.12.035

Christensen, L., Ertbjerg, P., Løje, H., Risbo, J., van den Berg, F. W. J., & Christensen, M. (2013). Relationship between meat toughness and properties of connective tissue from cows and young bulls heat treated at low temperatures for prolonged times. *Meat Science*, *93*(4), 787-795. https://doi.org/10.1016/j.meatsci.2012.12.001

Christensen, L., Gunvig, A., Torngren, M. A., Aaslyng, M. D., Knochel, S., & Christensen, M. (2012). Sensory characteristics of meat cooked for prolonged times at low temperature. *Meat Science*, *90*(2), 485-489. https://doi.org/10.1016/j.meatsci.2011.09.012

Christensen, M., Purslow, P. P., & Larsen, L. M. (2000). The effect of cooking temperature on mechanical properties of whole meat, single muscle fibres and perimysial connective tissue. *Meat Science*, *55*(3), 301-307. https://doi.org/10.1016/S0309-1740(99)00157-6

Christensen, M., Tørngren, M. A., Gunvig, A., Rozlosnik, N., Lametsch, R., Karlsson, A. H., & Ertbjerg, P. (2009). Injection of marinade with actinidin increases tenderness of porcine M. *biceps femoris* and affects myofibrils and connective tissue. *Journal of the Science of Food and Agriculture*, *89*(9), 1607-1614. https://doi.org/10.1002/jsfa.3633

Church, F. C., Porter, D. H., Catignani, G. L., & Swaisgood, H. E. (1985). An o-phthalaldehyde spectrophotometric assay for proteinases. *Analytical Biochemistry*, *146*(2), 343-348. https://doi.org/10.1016/0003-2697(85)90549-4

Clark, K. A., McElhinny, A. S., Beckerle, M. C., & Gregorio, C. C. (2002). Striated muscle cytoarchitecture: An intricate web of form and function. *Annual Review of Cell and Developmental Biology*, *18*(1), 637-706. https://doi.org/10.1146/annurev.cellbio.18.012502.105840

Claus, J. R. (2007). *Color changes in cooked beef*. N. C. B. Association. https://www.beefresearch.org/Media/BeefResearch/Docs/colorchangesincookedbeef_10-26-2020-118.pdf

Claus, J. R. (2017). Application of hydrodynamic shock wave processing associated with meat and processed meat products. In E. J. Cummins & J. G. Lyng (Eds.), *Emerging technologies in meat processing* (pp. 171-210). John Wiley & Sons, Ltd. https://doi.org/10.1002/9781118350676.ch7

Claus, J. R., Schilling, J. K., Marriott, N. G., Duncan, S. E., Solomon, M. B., & Wang, H. (2001a). Hydrodynamic shockwave tenderization effects using a cylinder processor on early deboned broiler breasts. *Meat Science*, *58*(3), 287-292. https://doi.org/10.1016/S0309-1740(01)00028-6

Claus, J. R., Schilling, J. K., Marriott, N. G., Duncan, S. E., Solomon, M. B., & Wang, H. (2001b). Tenderization of chicken and turkey breasts with electrically produced hydrodynamic shockwaves. *Meat Science*, *58*(3), 283-286. https://doi.org/10.1016/S0309-1740(01)00027-4

Combes, S., Lepetit, J., Darche, B., & Lebas, F. (2004). Effect of cooking temperature and cooking time on Warner–Bratzler tenderness measurement and collagen content in rabbit meat. *Meat Science*, *66*(1), 91-96. https://doi.org/10.1016/S0309-1740(03)00019-6

Cramer, T., Penick, M. L., Waddell, J. N., Bidwell, C. A., & Kim, Y. H. B. (2018). A new insight into meat toughness of callipyge lamb loins - The relevance of anti-

apoptotic systems to decreased proteolysis. *Meat Science*, *140*, 66-71. https://doi.org/10.1016/j.meatsci.2018.03.002

Crowley, T. E., & Kyte, J. (2014). Section 1-Purification and characterization of ferredoxin-nadp+ reductase from chloroplasts of *s. Oleracea*. In T. E. Crowley & J. Kyte (Eds.), *Experiments in the purification and characterization of enzymes* (pp. 25-102). Academic Press. https://doi.org/10.1016/B978-0-12-409544-1.00001-1

Cummings, J., & Macfarlane, G. (1991). The control and consequences of bacterial fermentation in the human colon. *Journal of Applied Bacteriology*, *70*(6), 443-459. https://doi.org/10.1111/j.1365-2672.1991.tb02739.x

Cummings, J. H., & Macfarlane, G. T. (1997). Role of intestinal bacteria in nutrient metabolism. *Clinical Nutrition*, *16*(1), 3-11. https://doi.org/10.1016/S0261-5614(97)80252-X

Dangin, M., Boirie, Y., Garcia-Rodenas, C., Gachon, P., Fauquant, J., Callier, P., Ballèvre, O., & Beaufrère, B. (2001). The digestion rate of protein is an independent regulating factor of postprandial protein retention. *American Journal of Physiology - Endocrinology And Metabolism*, *280*(2), E340-E348. https://doi.org/10.1152/ajpendo.2001.280.2.E340

Dangin, M., Guillet, C., Garcia-Rodenas, C., Gachon, P., Bouteloup-Demange, C., Reiffers-Magnani, K., Fauquant, J., Ballèvre, O., & Beaufrère, B. (2003). The rate of protein digestion affects protein gain differently during aging in humans. *The Journal of Physiology*, *549*(Pt 2), 635-644. https://doi.org/10.1113/jphysiol.2002.036897

Dave, A. C., Loveday, S. M., Anema, S. G., Loo, T. S., Norris, G. E., Jameson, G. B., & Singh, H. (2013). β-lactoglobulin self-assembly: structural changes in early stages and disulfide bonding in fibrils. *Journal of Agricultural and Food Chemistry*, *61*(32), 7817-7828. https://doi.org/10.1021/jf401084f

Davey, C. L., & Gilbert, K. V. (1969). Studies in meat tenderness. 7. changes in the fine structure of meat during aging. *Journal of Food Science*, *34*(1), 69-74. https://doi.org/10.1111/j.1365-2621.1969.tb14364.x

Dean, R. T., Fu, S., Stocker, R., & Davies, M. J. (1997). Biochemistry and pathology of radical-mediated protein oxidation. *Biochemical Journal*, *324*(1), 1-18. https://doi.org/10.1042/bj3240001

Debelle, L., & Alix, A. J. P. (1999). The structures of elastins and their function. *Biochimie*, *81*(10), 981-994. https://doi.org/10.1016/S0300-9084(99)00221-7

Del Pulgar, J. S., Gazquez, A., & Ruiz-Carrascal, J. (2012). Physico-chemical, textural and structural characteristics of sous-vide cooked pork cheeks as affected by vacuum, cooking temperature, and cooking time. *Meat Science*, *90*(3), 828-835. https://doi.org/10.1016/j.meatsci.2011.11.024

Dolatowski, Z. J. (1989). Ultraschall. 3. Einfluss von Ultraschall auf die Produktionstechnologie und Qualitaet von Kochschinken. *Die Fleischwirtschaft*, *69*(1), 106-111.

Dominguez-Hernandez, E., Salaseviciene, A., & Ertbjerg, P. (2018). Low-temperature long-time cooking of meat: Eating quality and underlying mechanisms. *Meat Science*. https://doi.org/10.1016/j.meatsci.2018.04.032

Dominguez, R., Gomez, M., Fonseca, S., & Lorenzo, J. M. (2014). Effect of different cooking methods on lipid oxidation and formation of volatile compounds in foal meat. *Meat Science*, *97*(2), 223-230. https://doi.org/10.1016/j.meatsci.2014.01.023

Draper, A. M., & Zeece, M. G. (1989). Thermal stability of cathepsin D. *Journal of Food Science*, *54*(6), 1651-1652. https://doi.org/10.1111/j.1365-2621.1989.tb05181.x

Duance, V. C., Restall, D. J., Beard, H., Bourne, F. J., & Bailey, A. J. (1977). The location of three collagen types in skeletal muscle. *FEBS Letters*, *79*(2), 248-252. https://doi.org/10.1016/0014-5793(77)80797-7

Dubost, A., Micol, D., Meunier, B., Lethias, C., & Listrat, A. (2013). Relationships between structural characteristics of bovine intramuscular connective tissue assessed by image analysis and collagen and proteoglycan content. *Meat Science*, *93*(3), 378-386. https://doi.org/10.1016/j.meatsci.2012.09.020

Dutaud, D., Aubry, L., Sentandreu, M. A., & Ouali, A. (2006). Bovine muscle 20S proteasome: I. Simple purification procedure and enzymatic characterization in relation with postmortem conditions. *Meat Science*, *74*(2), 327-336. https://doi.org/10.1016/j.meatsci.2006.03.027

Dutson, T. R., Smith, G. C., & Carpenter, Z. L. (1980). Lysosomal enzyme distribution in electrically stimulated ovine muscle. *Journal of Food Science*, *45*(4), 1097-1098. https://doi.org/10.1111/j.1365-2621.1980.tb07533.x

Dyer, J. M., & Grosvenor, A. (2014). Chapter 11-novel approaches to tracking the breakdown and modification of food proteins through digestion. In M. Boland, M. Golding, & H. Singh (Eds.), *Food structures, digestion and health* (pp. 303-317). Academic Press. https://doi.org/10.1016/B978-0-12-404610-8.00011-6

Eastridge, J. S., Liu, M. N., Vinyard, B., Solomon, M. B., Kandhari, P., & Callahan, J. A. (2005, July 16–20, 2005). *Effect of hydrodynamic pressure, blade tenderization or their combination on shear force and collagen solubility in top rounds from Brahman cattle* IFT Annual Meeting Book of Abstracts, New Orleans, L.A.

Erickson, R. H., & Kim, Y. S. (1990). Digestion and absorption of dietary protein. *Annual Review of Medicine*, *41*(1), 133-139. https://doi.org/10.1146/annurev.me.41.020190.001025

Ertbjerg, P., Christiansen, L. S., Pedersen, A. B., & Kristensen, L. (2012, 12–17 August). The effect of temperature and time on activity of calpain and lysosomal enzymes and degradation of desmin in porcine *Longissimus* muscle. Proccedings 58th International Congress of Meat Science & Technology, Montreal, Canada.

Ertbjerg, P., Larsen, L. M., & Moøller, A. J. (1999). Effect of prerigor lactic acid treatment on lysosomal enzyme release in bovine muscle. *Journal of the Science of Food and Agriculture*, *79*(1), 95-100. https://doi.org/10.1002/(sici)1097-0010(199901)79:1<95::Aid-jsfa188>3.0.Co;2-f

Escudero, E., Sentandreu, M. Á., & Toldrá, F. (2010). Characterization of peptides released by *in vitro* digestion of pork meat. *Journal of Agricultural and Food Chemistry*, *58*(8), 5160-5165. https://doi.org/10.1021/jf904535m

Faridnia, F., Bekhit, A. E.-D. A., Niven, B., & Oey, I. (2014). Impact of pulsed electric fields and post-mortem vacuum ageing on beef *longissimus thoracis* muscles. *International Journal of Food Science & Technology*, *49*(11), 2339-2347. https://doi.org/10.1111/ijfs.12532

Faridnia, F., Bremer, P., Burritt, D., & Oey, I. (2016). Effects of pulsed electric fields on selected quality attributes of beef outside flat (*biceps femoris*). 1st World Congress on Electroporation and Pulsed Electric Fields in Biology, Medicine and Food & Environmental Technologies, Singapore.

Faridnia, F., Ma, Q. L., Bremer, P. J., Burritt, D. J., Hamid, N., & Oey, I. (2015). Effect of freezing as pre-treatment prior to pulsed electric field processing on quality traits of beef muscles. *Innovative Food Science & Emerging Technologies*, *29*, 31-40. https://doi.org/10.1016/j.ifset.2014.09.007

Filgueras, R. S., Gatellier, P., Ferreira, C., Zambiazi, R. C., & Sante-Lhoutellier, V. (2011). Nutritional value and digestion rate of rhea meat proteins in association with storage and cooking processes. *Meat Science*, *89*(1), 6-12. https://doi.org/10.1016/j.meatsci.2011.02.028

Findlay, C. J., Stanley, D. W., & Gullett, E. A. (1986). Thermomechanical properties of beef muscle. *Meat Science*, *16*(1), 57-70. https://doi.org/10.1016/0309-1740(86)90012-4

Flint, F. O., & Pickering, K. (1984). Demonstration of collagen in meat products by an improved picro-sirius red polarisation method. *Analyst*, *109*(11), 1505-1506. https://doi.org/10.1039/AN9840901505

Foegeding, E., Lanier, T., & Hultin, H. (Eds.). (1996). *Characteristics of edible muscle tissues* (Vol. 3). Marcel Dekker Inc.

Friedman, M. (2004). Applications of the ninhydrin reaction for analysis of amino acids, peptides, and proteins to agricultural and biomedical sciences. *Journal of Agricultural and Food Chemistry*, *52*(3), 385-406. https://doi.org/10.1021/jf030490p

Gachovska, T., Ngadi, M., & Raghavan, G. (2006). Pulsed electric field assisted juice extraction from alfalfa. *Canadian Biosystems Engineering*, *48*, 3. http://citeseerx.ist.psu.edu/viewdoc/download?doi=10.1.1.467.2063&rep=rep1&type=pdf

García-Segovia, P., Andrés-Bello, A., & Martínez-Monzó, J. (2007). Effect of cooking method on mechanical properties, color and structure of beef muscle (*M. pectoralis*). *Journal of Food Engineering*, *80*(3), 813-821. https://doi.org/10.1016/j.jfoodeng.2006.07.010

Gatellier, P., Kondjoyan, A., Portanguen, S., & Sante-Lhoutellier, V. (2010). Effect of cooking on protein oxidation in n-3 polyunsaturated fatty acids enriched beef. Implication on nutritional quality. *Meat Science*, *85*(4), 645-650. https://doi.org/10.1016/j.meatsci.2010.03.018

Gatellier, P., & Sante-Lhoutellier, V. (2009). Digestion study of proteins from cooked meat using an enzymatic microreactor. *Meat Science*, *81*(2), 405-409. https://doi.org/10.1016/j.meatsci.2008.09.002

Gault, N. (1992). Structural aspects of raw meat. *Special Publication-Royal Society of Chemistry*, *106*, 79-79.

Geesink, G., & Veiseth, E. (2008). Muscle enzymes. In L. M. L. Nollet & F. Toldrá (Eds.), *Handbook of muscle foods analysis* (pp. 91-110). CRC Press. https://doi.org/10.1201/9781420045307.ch6

Giménez, B., Moreno, S., López-Caballero, M. E., Montero, P., & Gómez-Guillén, M. C. (2013). Antioxidant properties of green tea extract incorporated to fish gelatin films after simulated gastrointestinal enzymatic digestion. *LWT*, *53*(2), 445-451. https://doi.org/10.1016/j.lwt.2013.03.020

Goll, D. E., Neti, G., Mares, S. W., & Thompson, V. F. (2008). Myofibrillar protein turnover: the proteasome and the calpains 1 2. *Journal of Animal Science*, *86*(14_suppl), E19-E35. https://doi.org/10.2527/jas.2007-0395

Goll, D. E., Thompson, V. F., Li, H., Wei, W., & Cong, J. (2003). The calpain system. *Physiological Reviews*, *83*(3), 731-801. https://doi.org/10.1152/physrev.00029.2002

Gray, G. M., & Cooper, H. L. (1971). Protein digestion and absorption. *Gastroenterology*, *61*(4, Part 1), 535-544. https://doi.org/10.1016/S0016-5085(19)33506-1

Greaser, M. (1986). Conversion of muscle to meat. In P. J. Bechtel (Ed.), *Muscle as food* (pp. 37-102). Academic Press, Inc.

Greaser, M. (2008). Proteins. In L. M. L. Nollet & F. Toldrá (Eds.), *Handbook of muscle foods analysis* (pp. 57-73). CRC Press. https://doi.org/10.1201/9781420045307.ch4

Green, D. R., & Reed, J. C. (1998). Mitochondria and apoptosis. *Science*, *281*(5381), 1309-1312. https://doi.org/10.1126/science.281.5381.1309

Groves, K., & Parker, M. L. (2013). Appendix: Electron microscopy: Principles and applications to food microstructures. In K. Groves & M. L. Parker (Eds.), *Food microstructures-microscopy, measurement and modelling* (pp. 386-428). Woodhead Publishing Limited. https://doi.org/10.1533/9780857098894.2.386

Gudmundsson, M., & Hafsteinsson, H. (2001). Effect of electric field pulses on microstructure of muscle foods and roes. *Trends in Food Science & Technology*, *12*(3–4), 122-128. https://doi.org/10.1016/S0924-2244(01)00068-1

Gunning, P. A. (2013). Light microscopy: principles and applications to food microstructures. In K. Groves & M. L. Parker (Eds.), *Food Microstructures-microscopy, measurement and modelling* (pp. 62-95). Woodhead Publishing Limited. https://doi.org/10.1533/9780857098894.1.62

Ha, M., Bekhit, A. E.-D. A., Carne, A., & Hopkins, D. L. (2012). Characterisation of commercial papain, bromelain, actinidin and zingibain protease preparations and their activities toward meat proteins. *Food Chemistry*, *134*(1), 95-105. https://doi.org/10.1016/j.foodchem.2012.02.071

Ha, M., Bekhit, A. E.-D. A., Carne, A., & Hopkins, D. L. (2013). Characterisation of kiwifruit and asparagus enzyme extracts, and their activities toward meat proteins. *Food Chemistry*, *136*(2), 989-998. https://doi.org/10.1016/j.foodchem.2012.09.034

Ha, M., Dunshea, F. R., & Warner, R. D. (2017). A meta-analysis of the effects of shockwave and high pressure processing on color and cook loss of fresh meat. *Meat Science*, *132*, 107-111. https://doi.org/10.1016/j.meatsci.2017.04.016

Haider, S. R., Reid, H. J., & Sharp, B. L. (2012). Tricine-SDS-PAGE. In B. T. Kurien & R. H. Scofield (Eds.), *Protein electrophoresis* (2012/05/16 ed., Vol. 869, pp. 81-91). https://doi.org/10.1007/978-1-61779-821-4_8

Hamm, R., & Deatherage, F. E. (1960). Changes in hydration, solubility and charges of muscle proteins during heating of meat. *Journal of Food Science*, *25*(5), 587-610. https://doi.org/10.1111/j.1365-2621.1960.tb00004.x

Han, J., Morton, J. D., Bekhit, A. E.-D. A., & Sedcole, J. R. (2009). Pre-rigor infusion with kiwifruit juice improves lamb tenderness. *Meat Science*, *82*(3), 324-330. https://doi.org/10.1016/j.meatsci.2009.02.003

Hansen, T. B., Knøchel, S., Juncher, D., & Bertelsen, G. (1995). Storage characteristics of sous vide cooked roast beef. *International Journal of Food Science & Technology*, *30*(3), 365-378. https://doi.org/10.1111/j.1365-2621.1995.tb01384.x

Harkness, M. L., Harkness, R. D., & Venn, M. F. (1978). Digestion of native collagen in the gut. *Gut*, *19*(3), 240-243. https://doi.org/10.1136/gut.19.3.240

Harris, S., & Maxwell, B. (2009). *On a shoestring: Recipes from the house of the raising sons*. Wakefield Press. https://books.google.co.nz/books?id=Kt16ee9iAIQC

He, J., Zhou, G., Bai, Y., Wang, C., Zhu, S., Xu, X., & Li, C. (2018). The effect of meat processing methods on changes in disulfide bonding and alteration of protein structures: impact on protein digestion products. *RSC Advances*, *8*(31), 17595-17605. https://doi.org/10.1039/c8ra02310g

Hertog-Meischke, M. J. A. d., Smulders, F. J. M., & van Logtestijn, J. G. (1998). The effect of storage temperature on drip loss from fresh beef. *Journal of the Science*

of Food and Agriculture, *78*(4), 522-526. https://doi.org/10.1002/(SICI)1097-0010(199812)78:4<522::AID-JSFA150>3.0.CO;2-F

Hodgkinson, S. M., Montoya, C. A., Scholten, P. T., Rutherfurd, S. M., & Moughan, P. J. (2018). Cooking conditions affect the true ileal digestible amino acid content and digestible indispensable amino acid score (DIAAS) of bovine meat as determined in pigs. *The Journal of Nutrition*, *148*(10), 1564-1569. https://doi.org/10.1093/jn/nxy153

Honikel, K. O. (2014a). Chemical and physical characteristics of meat | pH measurement. In M. Dikeman & C. Devine (Eds.), *Encyclopedia of meat sciences* (2nd ed., pp. 262-266). Academic Press. https://doi.org/10.1016/B978-0-12-384731-7.00086-6

Honikel, K. O. (2014b). Conversion of muscle to meat | glycolysis. In M. Dikeman & C. Devine (Eds.), *Encyclopedia of meat sciences* (2nd ed., pp. 353-357). Academic Press. https://doi.org/10.1016/b978-0-12-384731-7.00095-7

Hopkins, D. L. (2014). Tenderizing mechanisms | mechanical. In M. Dikeman & C. Devine (Eds.), *Encyclopedia of meat sciences* (2nd ed., pp. 443-451). Academic Press. https://doi.org/10.1016/b978-0-12-384731-7.00092-1

Hradecky, J., Kludska, E., Belkova, B., Wagner, M., & Hajslova, J. (2017). Ohmic heating: A promising technology to reduce furan formation in sterilized vegetable and vegetable/meat baby foods. *Innovative Food Science & Emerging Technologies*, *43*, 1-6. https://doi.org/10.1016/j.ifset.2017.07.018

Huang, F., Ding, Z., Zhang, C., Hu, H., Zhang, L., & Zhang, H. (2018). Effects of calcium and zinc ions injection on caspase-3 activation and tenderness in post-mortem beef skeletal muscles. *International Journal of Food Science & Technology*, *53*(3), 582-589. https://doi.org/10.1111/ijfs.13631

Huang, J., & Forsberg, N. E. (1998). Role of calpain in skeletal-muscle protein degradation. *Proceedings of the National Academy of Sciences*, *95*(21), 12100-12105. https://doi.org/10.1073/pnas.95.21.12100

Huang, Y., Guo, L., Xiong, S., & Li, A. (2016). Property and structure changes of myofibril protein in pork treated by high pressure combined with heat. *Food Science And Technology International*, *22*(7), 647-662. https://doi.org/10.1177/1082013216642610

Huang, Y. Y., Liu, G. M., Cai, Q. F., Weng, W. Y., Maleki, S. J., Su, W. J., & Cao, M. J. (2010). Stability of major allergen tropomyosin and other food proteins of mud crab (*Scylla serrata*) by *in vitro* gastrointestinal digestion. *Food and Chemistry Toxicology*, *48*(5), 1196-1201. https://doi.org/10.1016/j.fct.2010.02.010

Huebinger, J. (2018). Modification of cellular membranes conveys cryoprotection to cells during rapid, non-equilibrium cryopreservation. *PLoS One*, *13*(10), e0205520. https://doi.org/10.1371/journal.pone.0205520

Huff-Lonergan, E. (2014). Tenderizing mechanisms | enzymatic. In M. Dikeman & C. Devine (Eds.), *Encyclopedia of meat science* (2nd ed., pp. 438-442). Academic Press. https://doi.org/10.1016/b978-0-12-384731-7.00248-8

Huff-Lonergan, E., & Lonergan, S. M. (2005). Mechanisms of water-holding capacity of meat: the role of postmortem biochemical and structural changes. *Meat Science*, *71*(1), 194-204. https://doi.org/10.1016/j.meatsci.2005.04.022

Huff-Lonergan, E., Mitsuhashi, T., Beekman, D. D., Parrish, F., Olson, D. G., & Robson, R. M. (1996). Proteolysis of specific muscle structural proteins by mu-calpain at low pH and temperature is similar to degradation in postmortem bovine muscle. *Journal of Animal Science*, *74*(5), 993-1008. https://doi.org/10.2527/1996.745993x

Huff-Lonergan, E., Parrish, F. C., Jr., & Robson, R. M. (1995). Effects of postmortem aging time, animal age, and sex on degradation of titin and nebulin in bovine *longissimus* muscle. *Journal of Animal Science*, *73*(4), 1064-1073. https://doi.org/10.2527/1995.7341064x

Hughes, R., Kurth, M. J., McGilligan, V., McGlynn, H., & Rowland, I. (2008). Effect of colonic bacterial metabolites on Caco-2 cell paracellular permeability *in vitro*. *Nutrition and Cancer*, *60*(2), 259-266. https://doi.org/10.1080/01635580701649644

Hung, Y., de Kok, T. M., & Verbeke, W. (2016). Consumer attitude and purchase intention towards processed meat products with natural compounds and a reduced level of nitrite. *Meat Science*, *121*, 119-126. https://doi.org/10.1016/j.meatsci.2016.06.002

Hur, S. J., Lim, B. O., Decker, E. A., & McClements, D. J. (2011). *In vitro* human digestion models for food applications. *Food Chemistry*, *125*(1), 1-12. https://doi.org/10.1016/j.foodchem.2010.08.036

Immonen, K., & Puolanne, E. (2000). Variation of residual glycogen-glucose concentration at ultimate pH values below 5.75. *Meat Science*, *55*(3), 279-283. https://doi.org/10.1016/S0309-1740(99)00152-7

Isleroglu, H., Kemerli, T., & Kaymak-Ertekin, F. (2015). Effect of steam-assisted hybrid cooking on textural quality characteristics, cooking loss, and free moisture content of beef. *International Journal of Food Properties*, *18*(2), 403-414. https://doi.org/10.1080/10942912.2013.833219

Ismail, I., Hwang, Y. H., & Joo, S. T. (2019). Interventions of two-stage thermal sous-vide cooking on the toughness of beef *Semitendinosus*. *Meat Science*, *157*, 107882. https://doi.org/10.1016/j.meatsci.2019.107882

Jalabert-Malbos, M.-L., Mishellany-Dutour, A., Woda, A., & Peyron, M.-A. (2007). Particle size distribution in the food bolus after mastication of natural foods. *Food Quality and Preference*, *18*(5), 803-812. https://doi.org/10.1016/j.foodqual.2007.01.010

Johnston, J., & Coon, C. N. (1979). The use of varying levels of pepsin for pepsin digestion studies with animal proteins. *Poultry Science*, *58*(5), 1271-1273. https://doi.org/10.3382/ps.0581271

Jørgensen, H., Gabert, V. M., Hedemann, M. S., & Jensen, S. K. (2000). Digestion of fat does not differ in growing pigs fed diets containing fish oil, rapeseed oil or coconut oil. *The Journal of Nutrition*, *130*(4), 852-857. https://doi.org/10.1093/jn/130.4.852

Kaláb, M., Allan-Wojtas, P., & Miller, S. S. (1995). Microscopy and other imaging techniques in food structure analysis. *Trends in Food Science & Technology*, *6*(6), 177-186. https://doi.org/10.1016/S0924-2244(00)89052-4

Kapsokefalou, M., & Miller, D. D. (1991). Effects of meat and selected food components on the valence of nonheme iron during *in vitro* digestion. *Journal of Food Science*, *56*(2), 352-355. https://doi.org/10.1111/j.1365-2621.1991.tb05278.x

Kaur, L., Astruc, T., Vénien, A., Loison, O., Cui, J., Irastorza, M., & Boland, M. (2016). High pressure processing of meat: effects on ultrastructure and protein digestibility. *Food & Function*, *7*(5), 2389-2397. https://doi.org/10.1039/C5FO01496D

Kaur, L., Maudens, E., Haisman, D. R., Boland, M. J., & Singh, H. (2014). Microstructure and protein digestibility of beef: the effect of cooking conditions as used in stews and curries. *LWT*, *55*(2), 612-620. https://doi.org/10.1016/j.lwt.2013.09.023

Kaur, L., Rutherfurd, S. M., Moughan, P. J., Drummond, L., & Boland, M. J. (2010a). Actinidin enhances gastric protein digestion as assessed using an in vitro gastric digestion model. *Journal of Agriculture and Food Chemistry*, *58*(8), 5068-5073. https://doi.org/10.1021/jf903332a

Kaur, L., Rutherfurd, S. M., Moughan, P. J., Drummond, L., & Boland, M. J. (2010b). Actinidin enhances protein digestion in the small intestine as assessed using an in vitro digestion model. *Journal of Agriculture and Food Chemistry*, *58*(8), 5074-5080. https://doi.org/10.1021/jf903835g

Kaur, L., Seah, X. H., & Boland, M. (2020). Changes in cathepsin activity during low-temperature storage and sous vide processing of beef brisket. *Food Science of Animal Resources*, *40*(3), 415-425. https://doi.org/10.5851/kosfa.2020.e21

Ke, S., Huang, Y., Decker, E. A., & Hultin, H. O. (2009). Impact of citric acid on the tenderness, microstructure and oxidative stability of beef muscle. *Meat Science*, *82*(1), 113-118. https://doi.org/10.1016/j.meatsci.2008.12.010

Keith, F. K. M., Vol, D. L. D., Miles, R. S., Bechtel, P. J., & Carr, T. R. (1985). Chemical and sensory properties of thirteen major beef muscles. *Journal of Food Science*, *50*(4), 869-872. https://doi.org/10.1111/j.1365-2621.1985.tb12968.x

Kemp, C. M., & Parr, T. (2008). The effect of recombinant caspase 3 on myofibrillar proteins in porcine skeletal muscle. *Animal*, *2*(8), 1254-1264. https://doi.org/10.1017/s1751731108002310

Kemp, C. M., Sensky, P. L., Bardsley, R. G., Buttery, P. J., & Parr, T. (2010). Tenderness-An enzymatic view. *Meat Science*, *84*(2), 248-256. https://doi.org/10.1016/j.meatsci.2009.06.008

Khan, A. A., Randhawa, M. A., Carne, A., Mohamed Ahmed, I. A., Barr, D., Reid, M., & Bekhit, A. E.-D. A. (2017). Effect of low and high pulsed electric field on the quality and nutritional minerals in cold boned beef M. *longissimus et lumborum*. *Innovative Food Science & Emerging Technologies*, *41*, 135-143. https://doi.org/10.1016/j.ifset.2017.03.002

King , N. J., & Whyte, R. (2006). Does it look cooked? A review of factors that influence cooked meat color. *Journal of Food Science*, *71*(4), R31-R40. https://doi.org/10.1111/j.1750-3841.2006.00029.x

Kirschner, C., Ofstad, R., Skarpeid, H. J., Host, V., & Kohler, A. (2004). Monitoring of denaturation processes in aged beef loin by Fourier transform infrared microspectroscopy. *Journal of Agriculture and Food Chemistry*, *52*(12), 3920-3929. https://doi.org/10.1021/jf0306136

Knoll, R., Buyandelger, B., & Lab, M. (2011). The sarcomeric Z-disc and Z-discopathies. *J Biomed Biotechnol*, *2011*, 569628. https://doi.org/10.1155/2011/569628

Koide, T. (2007). Designed triple-helical peptides as tools for collagen biochemistry and matrix engineering. *Philosophical transactions of the Royal Society of London. Series B, Biological Sciences*, *362*(1484), 1281-1291. https://doi.org/10.1098/rstb.2007.2115

Koita, T., Gonai, T., Sun, M., Owada, S., & Nakamura, T. (Eds.). (2017). *The motion of a 2 mm tantalum block induced by underwater explosion* (Vol. 2). Springer International Publishing. https://doi.org/10.1007/978-3-319-44866-4_32.

Kong, F., & Singh, R. P. (2008). Disintegration of solid foods in human stomach. *Journal of Food Science*, *73*(5), R67-80. https://doi.org/10.1111/j.1750-3841.2008.00766.x

Kong, F., & Singh, R. P. (2010). A human gastric simulator (HGS) to study food digestion in human stomach. *Journal of Food Science*, *75*(9), E627-635. https://doi.org/10.1111/j.1750-3841.2010.01856.x

Koohmaraie, M. (1988). The role of endogenous proteases in meat tenderness. Reciprocal Meat Conference Proceedings, Chicago, IL.

Koohmaraie, M. (1992). Ovine skeletal muscle multicatalytic proteinase complex (proteasome): purification, characterization, and comparison of its effects on myofibrils with μ-calpains. *Journal of Animal Science*, *70*(12), 3697-3708. https://doi.org/10.2527/1992.70123697x

Koohmaraie, M. (1994). Muscle proteinases and meat aging. *Meat Science*, *36*(1-2), 93-104. https://doi.org/10.1016/0309-1740(94)90036-1

Koohmaraie, M., & Geesink, G. H. (2006). Contribution of postmortem muscle biochemistry to the delivery of consistent meat quality with particular focus on the calpain system. *Meat Science*, *74*(1), 34-43. https://doi.org/10.1016/j.meatsci.2006.04.025

Koretz, J. F., Irving, T. C., & Wang, K. (1993). Filamentous aggregates of native titin and binding of C-protein and AMP-deaminase. *Arch Biochem Biophys*, *304*(2), 305-309. https://doi.org/10.1006/abbi.1993.1354

Kraus, A. (2015). Development of functional food with the participation of the consumer. Motivators for consumption of functional products. *International Journal of Consumer Studies*, *39*(1), 2-11. https://doi.org/10.1111/ijcs.12144

Laakkonen, E., Sherbon, J. W., & Wellington, G. H. (1970). Low temperature, long time heating of bovine muscle 3. collagenolytic activity. *Journal of Food Science*, *35*(2), 181-184. https://doi.org/10.1111/j.1365-2621.1970.tb12133.x

Laakkonen, E., Wellington, G. H., & Sherbon, J. N. (1970). Low temperature, long time heating of bovine muscle 1. changes in tenderness, water binding capacity, pH and amount of water soluble components. *Journal of Food Science*, *35*(2), 175-177. https://doi.org/10.1111/j.1365-2621.1970.tb12131.x

Labeit, S., & Kolmerer, B. (1995). Titins: giant proteins in charge of muscle ultrastructure and elasticity. *Science*, *270*(5234), 293. https://doi.org/10.1126/science.270.5234.293

Lametsch, R., Knudsen, J. C., Ertbjerg, P., Oksbjerg, N., & Therkildsen, M. (2007). Novel method for determination of myofibril fragmentation post-mortem. *Meat Science*, *75*(4), 719-724. https://doi.org/10.1016/j.meatsci.2006.10.002

Larrea-Wachtendorff, D., Tabilo-Munizaga, G., Moreno-Osorio, L., Villalobos-Carvajal, R., & Pérez-Won, M. (2015). Protein changes caused by high hydrostatic pressure (HHP): A study using differential scanning calorimetry (DSC) and fourier transform infrared (FTIR) spectroscopy. *Food Engineering Reviews*, *7*(2), 222-230. https://doi.org/10.1007/s12393-015-9107-1

Latorre, M. E., Palacio, M. I., Velazquez, D. E., & Purslow, P. P. (2019). Specific effects on strength and heat stability of intramuscular connective tissue during long time low temperature cooking. *Meat Science*, *153*, 109-116. https://doi.org/10.1016/j.meatsci.2019.03.016

Lattouf, R., Younes, R., Lutomski, D., Naaman, N., Godeau, G., Senni, K., & Changotade, S. (2014). Picrosirius red staining: a useful tool to appraise collagen networks in normal and pathological tissues. *Journal of Histochemistry and Cytochemistry*, *62*(10), 751-758. https://doi.org/10.1369/0022155414545787

Lawrence, J. (2010). Meat and meat products. In W. Horwitz & G. W. Lantimer (Eds.), *Official Methods of Analysis of AOAC International* (18th ed., pp. 1-6). AOAC International.

Lawrie, R. A. (1992). Conversion of muscle into meat: biochemistry. *Special Publication-Royal Society of Chemistry*, *106*, 43-43.

Lawrie, R. A. (2006). Chapter 4-Chemical and biochemical constitution of muscle. In *Lawrie's meat science* (7th ed., pp. 75-127). Woodhead Publishing. https://doi.org/10.1533/9781845691615.75

Leadley, C. E., & Williams, A. (2006). Pulsed electric field processing, power ultrasound and other emerging technologies. In J. G. Brennan (Ed.), *Food processing handbook* (pp. 201-235). John Wiley & Sons. https://doi.org/10.1002/3527607579.ch7

Leander, R. C., Hedrick, H. B., Brown, M. F., & White, J. A. (1980). Comparison of structural changes in bovine *longissimus* and *semitendinosus* muscles during cooking. *Journal of Food Science*, *45*(1), 1-6. https://doi.org/10.1111/j.1365-2621.1980.tb03857.x

Lee, S. H., Joo, S. T., & Ryu, Y. C. (2010). Skeletal muscle fiber type and myofibrillar proteins in relation to meat quality. *Meat Science*, *86*(1), 166-170. https://doi.org/10.1016/j.meatsci.2010.04.040

Lehman, W., & Craig, R. (2008). Tropomyosin and the steric mechanism of muscle regulation. In P. Gunning (Ed.), *Tropomyosin* (pp. 95-109). Springer. https://doi.org/10.1007/978-0-387-85766-4_8

León, K., Mery, D., Pedreschi, F., & León, J. (2006). Color measurement in L∗a∗b∗ units from RGB digital images. *Food Research International*, *39*(10), 1084-1091. https://doi.org/10.1016/j.foodres.2006.03.006

Lewis, D. (1992). Structural aspects of processed meat. *Special Publication-Royal Society of Chemistry*, *106*, 203-203.

Lewis, D. A., & Luh, B. (1988). Application of actinidin from kiwifruit to meat tenderization and characterization of beef muscle protein hydrolysis. *Journal of Food Biochemistry*, *12*(3), 147-158. https://doi.org/10.1111/j.1745-4514.1988.tb00368.x

Li, L., Liu, Y., Zou, X., He, J., Xu, X., Zhou, G., & Li, C. (2017). *In vitro* protein digestibility of pork products is affected by the method of processing. *Food Research International*, *92*, 88-94. https://doi.org/10.1016/j.foodres.2016.12.024

Liang, Q., Wang, L., He, Y., Wang, Z., Xu, J., & Ma, H. (2014). Hydrolysis kinetics and antioxidant activity of collagen under simulated gastrointestinal digestion. *Journal of Functional Foods*, *11*, 493-499. https://doi.org/10.1016/j.jff.2014.08.004

Lin, H. C., & Visek, W. J. (1991). Colon mucosal cell damage by ammonia in rats. *The Journal of Nutrition*, *121*(6), 887-893. https://doi.org/10.1093/jn/121.6.887.

Lindahl, G., Lagerstedt, A., Ertbjerg, P., Sampels, S., & Lundstrom, K. (2010). Ageing of large cuts of beef loin in vacuum or high oxygen modified atmosphere--effect on shear force, calpain activity, desmin degradation and protein oxidation. *Meat Science*, *85*(1), 160-166. https://doi.org/10.1016/j.meatsci.2009.12.020

Listrat, A., Lebret, B., Louveau, I., Astruc, T., Bonnet, M., Lefaucheur, L., Picard, B., & Bugeon, J. (2016). How muscle structure and composition influence meat and flesh quality. *The Scientific World Journal*, *2016*. https://doi.org/10.1155/2016/3182746

Liu, C., Xiong, Y. L., & Rentfrow, G. K. (2011). Kiwifruit protease extract injection reduces toughness of pork loin muscle induced by freeze–thaw abuse. *LWT*, *44*(10), 2026-2031. https://doi.org/10.1016/j.lwt.2011.05.019

Liu, G., & Xiong, Y. L. (2000). Electrophoretic pattern, thermal denaturation, and *in vitro* digestibility of oxidized myosin. *Journal of Agricultural and Food Chemistry*, *48*(3), 624-630. https://doi.org/10.1021/jf990520h

Liu, J., Arner, A., Puolanne, E., & Ertbjerg, P. (2016). On the water-holding of myofibrils: Effect of sarcoplasmic protein denaturation. *Meat Science*, *119*, 32-40. https://doi.org/10.1016/j.meatsci.2016.04.020

Liu, W., Fu, D., Zhang, X., Chai, J., Tian, S., & Han, J. (2019). Development and validation of a new artificial gastric digestive system. *Food Research International*, *122*, 183-190. https://doi.org/10.1016/j.foodres.2019.04.015

Liu, Y., & Chen, Y.-R. (2001). Analysis of visible reflectance spectra of stored, cooked and diseased chicken meats. *Meat Science*, *58*(4), 395-401. https://doi.org/10.1016/S0309-1740(01)00041-9

Liu, Y., Du, M., Li, X., Chen, L., Shen, Q., Tian, J., & Zhang, D. (2016). Role of the ubiquitin-proteasome pathway on proteolytic activity in postmortem proteolysis and tenderisation of sheep skeletal muscle. *International Journal of Food Science & Technology*, *51*(11), 2353-2359. https://doi.org/10.1111/ijfs.13214

Liu, Y. Y., Zhang, Y., Zeng, X. A., El Mashad, H., Pan, Z. L., & Wang, Q. J. (2014). Effect of pulsed electric field on microstructure of some amino acid group of soy protein isolates. *International Journal of Food Engineering*, *10*(1), 113-120. https://doi.org/10.1515/ijfe-2013-0033

Lonergan, S. M., Huff-Lonergan, E., Rowe, L. J., Kuhlers, D. L., & Jungst, S. B. (2001). Selection for lean growth efficiency in Duroc pigs influences pork quality. *Journal of Animal Science*, *79*(8), 2075-2085. https://doi.org/10.2527/2001.7982075x

Long, J. B. (1993). *Tenderizing meat* (United State of America Patent No. 5273766). U. S. Patent.

Long, J. B. (2000). *Treatment of meat by capacitor discharge* (United Kingdom Patent No. 0 986 308 B1). E. P. Office.

Lorenzo, J. M., & Domínguez, R. (2014). Cooking losses, lipid oxidation and formation of volatile compounds in foal meat as affected by cooking procedure. *Flavour and Fragrance Journal*, *29*(4), 240-248. https://doi.org/10.1002/ffj.3201

Macfarlane, G. T., Cummings, J. H., & Allison, C. (1986). Protein degradation by human intestinal bacteria. *Journal of General Microbiology*, *132*(6), 1647-1656. https://doi.org/10.1099/00221287-132-6-1647

Macfarlane, J. J., McKenzie, I. J., & Turner, R. H. (1986). Pressure-heat treatment of meat: Changes in myofibrillar proteins and ultrastructure. *Meat Science*, *17*(3), 161-176. https://doi.org/10.1016/0309-1740(86)90001-X

Mackie, A., & Rigby, N. (2015). InfoGest Consensus Method. In K. Verhoeckx, P. Cotter, I. López-Expósito, C. Kleiveland, T. Lea, A. Mackie, T. Requena, D. Swiatecka, & H. Wichers (Eds.), *The impact of food bioactives on health: In vitro and ex vivo models* (pp. 13-22). Springer International Publishing. https://doi.org/10.1007/978-3-319-16104-4_2

Mariotti, F. (2017). Plant Protein, Animal Protein, and Protein Quality. In F. Mariotti (Ed.), *Vegetarian and plant-based diets in health and disease prevention* (pp. 621-642). Academic Press. https://doi.org/10.1016/b978-0-12-803968-7.00035-6

Marriott, N. G., Wang, H., Solomon, M. B., & Moody, W. G. (2001). Studies of cow beef tenderness enhancement through supersonic-hydrodynamic shock wave treatment. *Journal of Muscle Foods*, *12*(3), 207-218. https://doi.org/10.1111/j.1745-4573.2001.tb00689.x

Martens, H., Stabursvik, E., & Martens, M. (1982). Texture and colour changes in meat during cooking related to thermal denaturation of muscle proteins. *Journal of Texture Studies*, *13*(3), 291-309. https://doi.org/10.1111/j.1745-4603.1982.tb00885.x

Matsuishi, M., Saito, G., Okitani, A., & Kato, H. (2003). Purification and some properties of cathepsin H from rabbit skeletal muscle. *The International Journal of Biochemistry & Cell Biology*, *35*(4), 474-485. https://doi.org/10.1016/S1357-2725(02)00279-0

Matsukura, U., Okitani, A., Nishimuro, T., & Kato, H. (1981). Mode of degradation of myofibrillar proteins by an endogenous protease, cathepsin L. *Biochimica et Biophysica Acta (BBA) - Enzymology*, *662*(1), 41-47. https://doi.org/10.1016/0005-2744(81)90221-7

McCormick, R. J. (1999). Extracellular modifications to muscle collagen: Implications for meat quality. *Poultry Science*, *78*(5), 785-791. https://doi.org/10.1093/ps/78.5.785

McDonnell, C. K., Allen, P., Chardonnereau, F. S., Arimi, J. M., & Lyng, J. G. (2014). The use of pulsed electric fields for accelerating the salting of pork. *LWT*, *59*(2), 1054-1060. https://doi.org/10.1016/j.lwt.2014.05.053

McDowall, M. A. (1970). Anionic proteinase from *Actinidia chinensis*. *European Journal of Biochemistry*, *14*(2), 214-221. https://doi.org/10.1111/j.1432-1033.1970.tb00280.x

McElhinny, A. S., Kazmierski, S. T., Labeit, S., & Gregorio, C. C. (2003). Nebulin: The nebulous, multifunctional giant of striated muscle. *Trends in Cardiovascular Medicine*, *13*(5), 195-201. https://doi.org/10.1016/S1050-1738(03)00076-8

McGuire, M., & Beerman, K. A. (2012). Protein. In *Nutritional sciences: From fundamentals to food* (3rd ed., pp. 161-216). Cengage Learning. https://books.google.co.nz/books?id=bYAJAAAAQBAJ

McKeith, F. K., Brewer, M. S., & Bruggen, K. A. (1994). Effects of enzyme applications on sensory, chemical and processing characteristics of beef steaks and roasts. *Journal of Muscle Foods*, *5*(2), 149-164. https://doi.org/10.1111/j.1745-4573.1994.tb00527.x

Meat Industry Association. (2020, 6 August). Red meat exports record seven per cent increase year on year. https://mia.co.nz/news-and-views/red-meat-exports-record-seven-per-cent-increase-year-on-year/

Menard, O., Bourlieu, C., De Oliveira, S. C., Dellarosa, N., Laghi, L., Carriere, F., Capozzi, F., Dupont, D., & Deglaire, A. (2018). A first step towards a consensus static *in vitro* model for simulating full-term infant digestion. *Food Chemistry*, *240*, 338-345. https://doi.org/10.1016/j.foodchem.2017.07.145

Ménard, O., Picque, D., & Dupont, D. (2015). The DIDGI® system. In K. Verhoeckx, P. Cotter, I. López-Expósito, C. Kleiveland, T. Lea, A. Mackie, T. Requena, D. Swiatecka, & H. Wichers (Eds.), *The impact of food bioactives on health: In vitro and ex vivo models* (pp. 73-81). Springer International Publishing. https://doi.org/10.1007/978-3-319-16104-4_8

Meyer, M. (2019). Processing of collagen based biomaterials and the resulting materials properties. *Biomedical Engineering Online*, *18*(1), 24. https://doi.org/10.1186/s12938-019-0647-0

Mhemdi, H., Bals, O., Grimi, N., & Vorobiev, E. (2012). Filtration diffusivity and expression behaviour of thermally and electrically pretreated sugar beet tissue and press-cake. *Separation and Purification Technology*, *95*, 118-125. https://doi.org/10.1016/j.seppur.2012.04.031

Mikami, M., Whiting, A. H., Taylor, M. A. J., Maciewicz, R. A., & Etherington, D. J. (1987). Degradation of myofibrils from rabbit, chicken and beef by cathepsin L and lysosomal lysates. *Meat Science*, *21*(2), 81-97. https://doi.org/10.1016/0309-1740(87)90022-2

Minekus, M. (2015). The TNO gastro-intestinal model (TIM). In K. Verhoeckx, P. Cotter, I. López-Expósito, C. Kleiveland, T. Lea, A. Mackie, T. Requena, D. Swiatecka, & H. Wichers (Eds.), *The impact of food bioactive on health: In vivo and ex vivo models* (pp. 37-46). Springer International Publishing. https://doi.org/10.1007/978-3-319-16104-4_5

Minekus, M., Alminger, M., Alvito, P., Ballance, S., Bohn, T., Bourlieu, C., Carriere, F., Boutrou, R., Corredig, M., Dupont, D., Dufour, C., Egger, L., Golding, M., Karakaya, S., Kirkhus, B., Le Feunteun, S., Lesmes, U., Macierzanka, A., Mackie, A., Marze, S., McClements, D. J., Menard, O., Recio, I., Santos, C. N., Singh, R. P., Vegarud, G. E., Wickham, M. S., Weitschies, W., & Brodkorb, A. (2014). A standardised static in vitro digestion method suitable for food - an international consensus. *Food & Function*, *5*(6), 1113-1124. https://doi.org/10.1039/c3fo60702j

Mitra, B., Lametsch, R., Akcan, T., & Ruiz-Carrascal, J. (2018). Pork proteins oxidative modifications under the influence of varied time-temperature thermal treatments: A chemical and redox proteomics assessment. *Meat Science*, *140*, 134-144. https://doi.org/10.1016/j.meatsci.2018.03.011

Miyada, D. S., & Tappel, A. L. (1956). The hydrolysis of beef proteins by various proteolytic enzymes. *Journal of Food Science*, *21*(2), 217-225. https://doi.org/10.1111/j.1365-2621.1956.tb16913.x

Moeller, P. W., Fields, P. A., Dutson, T. R., Landmann, W. A., & Carpenter, Z. L. (1976). Effect of high temperature conditioning on subcellular distribution and levels of lysosomal enzymes. *Journal of Food Science*, *41*(1), 216-217. https://doi.org/10.1111/j.1365-2621.1976.tb01143.x

Moeller, P. W., Fields, P. A., Dutson, T. R., Landmann, W. A., & Carpenter, Z. L. (1977). High temperature effects on lysosomal enzyme distribution and fragmentation of bovine muscle. *Journal of Food Science*, *42*(2), 510-512. https://doi.org/10.1111/j.1365-2621.1977.tb01534.x

Moeller, S., Wulf, D., Meeker, D., Ndife, M., Sundararajan, N., & Solomon, M. B. (1999). Impact of the hydrodyne process on tenderness, microbial load, and sensory characteristics of pork *longissimus* muscle. *Journal of Animal Science*, *77*(8), 2119-2123. https://doi.org/10.2527/1999.7782119x

Møller, A. J. (1981). Analysis of Warner-Bratzler shear pattern with regard to myofibrillar and connective tissue components of tenderness. *Meat Science*, *5*(4), 247-260. https://doi.org/10.1016/0309-1740(81)90015-2

Montoya, C. A., Rutherfurd, S. M., Olson, T. D., Purba, A. S., Drummond, L. N., Boland, M. J., & Moughan, P. J. (2014). Actinidin from kiwifruit (*Actinidia deliciosa cv. Hayward*) increases the digestion and rate of gastric emptying of meat proteins in the growing pig. *British Journal of Nutrition*, *111*(6), 957-967. https://doi.org/10.1017/S0007114513003401

Moore, S. (1968). Amino acid analysis: aqueous dimethyl sulfoxide as solvent for the ninhydrin reaction. *Journal of Biological Chemistry*, *243*(23), 6281-6283.

Mostafaie, A., Bidmeshkipour, A., Shirvani, Z., Mansouri, K., & Chalabi, M. (2008). Kiwifruit actinidin: a proper new collagenase for isolation of cells from different tissues. *Applied Biochemistry and Biotechnology*, *144*(2), 123-131. https://doi.org/10.1007/S12010-007-8106-Y

Motoyama, M., Vénien, A., Loison, O., Sandt, C., Watanabe, G., Sicard, J., Sasaki, K., & Astruc, T. (2017). In situ characterization of acidic and thermal protein denaturation by infrared microspectroscopy. *Food Chemistry*. https://doi.org/10.1016/j.foodchem.2017.11.031

Movasaghi, Z., Rehman, S., & Rehman, I. U. (2008). Fourier Transform Infrared (FTIR) Spectroscopy of Biological Tissues. *Applied Spectroscopy Reviews*, *43*(2), 134-179. https://doi.org/10.1080/05704920701829043

Muir, J., & Yeow, E. (2000). Importance of combining indigestible carbohydrate with protein sources in the diet: implications for reducing colorectal cancer risk. *Proceedings of the Nutrition Society of Australia*, *24*, 196-204. http://apjcn.nhri.org.tw/server/APJCN/ProcNutSoc/2000+/2000/Muir196.pdf

Nishimura, T., Hattori, A., & Takahashi, K. (1995). Structural weakening of intramuscular connective tissue during conditioning of beef. *Meat Science*, *39*(1), 127-133. https://doi.org/10.1016/0309-1740(95)80014-X

Nishiyama, I. (2000). Comparison of the proteolytic effects of hayward and hort16a kiwifruit juice. *Journal of Home Economics of Japan*, *51*(7), 621-626. https://doi.org/10.11428/jhej1987.51.621

Nishiyama, I. (2007). Fruits of the *Actinidia* genus. In S. L. Taylor (Ed.), *Advances in food and nutrition research* (Vol. 52, pp. 293-324). Academic Press. https://doi.org/10.1016/S1043-4526(06)52006-6

O'Dowd, L. P., Arimi, J. M., Noci, F., Cronin, D. A., & Lyng, J. G. (2013). An assessment of the effect of pulsed electrical fields on tenderness and selected quality attributes of post rigor beef muscle. *Meat Science*, *93*(2), 303-309. https://doi.org/10.1016/j.meatsci.2012.09.010

Oberli, M., Marsset-Baglieri, A., Airinei, G., Sante-Lhoutellier, V., Khodorova, N., Remond, D., Foucault-Simonin, A., Piedcoq, J., Tome, D., Fromentin, G., Benamouzig, R., & Gaudichon, C. (2015). High true ileal digestibility but not postprandial utilization of nitrogen from bovine meat protein in humans is moderately decreased by high-temperature, long-duration cooking. *The Journal of Nutrition*, *145*(10), 2221-2228. https://doi.org/10.3945/jn.115.216838

Obinata, T., Maruyama, K., Sugita, H., Kohama, K., & Ebashi, S. (1981). Dynamic aspects of structural proteins in vertebrate skeletal muscle. *Muscle & Nerve*, *4*(6), 456-488. https://doi.org/10.1002/mus.880040604

Offer, G., & Knight, P. (1988). The structural basis of water-holding in meat. Part 1: General principles and water uptake in processing. In R. A. Lawrie (Ed.), *Developments in meat science* (pp. 63-171). Elsevier Science

Offer, G., & Trinick, J. (1983). On the mechanism of water holding in meat: the swelling and shrinking of myofibrils. *Meat Science*, *8*(4), 245-281. https://doi.org/10.1016/0309-1740(83)90013-X

Okuno, A., Kato, M., & Taniguchi, Y. (2007). Pressure effects on the heat-induced aggregation of equine serum albumin by FT-IR spectroscopic study: Secondary structure, kinetic and thermodynamic properties. *Biochim Biophys Acta*, *1774*(5), 652-660. https://doi.org/10.1016/j.bbapap.2007.03.003

Ouali, A. (1990). Meat tenderization: possible causes and mechanisms. A review. *Journal of Muscle Foods*, *1*(2), 129-165.

Ouali, A., Gagaoua, M., Boudida, Y., Becila, S., Boudjellal, A., Herrera-Mendez, C. H., & Sentandreu, M. A. (2013). Biomarkers of meat tenderness: present knowledge and perspectives in regards to our current understanding of the mechanisms involved. *Meat Science*, *95*(4), 854-870. https://doi.org/10.1016/j.meatsci.2013.05.010

Ouali, A., Garrel, N., Obled, A., Deval, C., Valin, C., & Penny, I. F. (1987). Comparative action of cathepsins D, B, H, L and of a new lysosomal cysteine proteinase on rabbit myofibrils. *Meat Science*, *19*(2), 83-100. https://doi.org/10.1016/0309-1740(87)90014-3

Ouali, A., Herrera-Mendez, C. H., Coulis, G., Becila, S., Boudjellal, A., Aubry, L., & Sentandreu, M. A. (2006). Revisiting the conversion of muscle into meat and the underlying mechanisms. *Meat Science*, *74*(1), 44-58. https://doi.org/10.1016/j.meatsci.2006.05.010

Palka, K. (1999). Changes in intramuscular connective tissue and collagen solubility of bovine *M. semitendinosus* during retorting. *Meat Science*, *53*(3), 189-194. https://doi.org/10.1016/S0309-1740(99)00047-9

Palka, K., & Daun, H. (1999). Changes in texture, cooking losses, and myofibrillar structure of bovine *M. semitendinosus* during heating. *Meat Science*, *51*(3), 237-243. https://doi.org/10.1016/S0309-1740(98)00119-3

Patel, N., & Welham, S. J. (2013). Peptic digestion of beef myofibrils is modified by prior marination. *Food Nutrition Research*, *57*, 20294. https://doi.org/10.3402/fnr.v57i0.20294

Payne, C. T. (2009). Enzymes. In R. Tarté (Ed.), *Ingredients in meat products: Properties, functionality and applications* (pp. 173-198). Springer New York. https://doi.org/10.1007/978-0-387-71327-4_8

Pearce, K. L., Rosenvold, K., Andersen, H. J., & Hopkins, D. L. (2011). Water distribution and mobility in meat during the conversion of muscle to meat and ageing and the impacts on fresh meat quality attributes-A review. *Meat Science*, *89*(2), 111-124. https://doi.org/10.1016/j.meatsci.2011.04.007

Pearson, A. M., & Gillett, T. A. (2012). *Composition and nutritive value of raw materials and processed meats*. Springer https://doi.org/10.1007/978-1-4615-7685-3_2

Pearson, A. M., & Young, R. B. (1989). 11-Sarcoplasmic proteins. In *Muscle and meat biochemistry* (pp. 296-337). Academic Press. https://doi.org/10.1016/B978-0-12-548055-0.50015-5

Perisic, N., Afseth, N. K., Ofstad, R., & Kohler, A. (2011). Monitoring protein structural changes and hydration in bovine meat tissue due to salt substitutes by fourier transform infrared (FTIR) microspectroscopy. *Journal of Agricultural and Food Chemistry*, *59*(18), 10052-10061. https://doi.org/10.1021/jf201578b

Perkins, A. D., & Tanentzapf, G. (2014). An ongoing role for structural sarcomeric components in maintaining drosophila melanogaster muscle function and structure. *PLoS One*, *9*(6), e99362. https://doi.org/10.1371/journal.pone.0099362

Piper, D., & Fenton, B. H. (1965). pH stability and activity curves of pepsin with special reference to their clinical importance. *Gut*, *6*(5), 506. https://doi.org/10.1136/gut.6.5.506

Pooona, J., Singh, P., & P, P. (2019). Effect of kiwifruit juice and tumbling on tenderness and lipid oxidation in chicken nuggets. *Nutrition & Food Science*, *50*(1), 74-83. https://doi.org/10.1108/nfs-12-2018-0352

Pospiech, M., Rezacova-Lukaskova, Z., Tremlová, B., Randulová, Z., & Bartl, P. (2011). Microscopic methods in food analysis. *Maso International*, *1*, 27-34. https://doi.org/10.2754/avb201101010027

Prodhan, U. K., Pundir, S., Chiang, V. S., Milan, A. M., Barnett, M. P. G., Smith, G. C., Markworth, J. F., Knowles, S. O., & Cameron-Smith, D. (2020). Comparable postprandial amino acid and gastrointestinal hormone responses to beef steak cooked using different methods: A randomised crossover trial. *Nutrients*, *12*(2). https://doi.org/10.3390/nu12020380

Puértolas, E., Luengo, E., Álvarez, I., & Raso, J. (2012). Improving mass transfer to soften tissues by pulsed electric fields: fundamentals and applications. *Annual Review of Food Science and Technology*, *3*, 263-282. https://doi.org/10.1146/annurev-food-022811-101208

Purchas, R. W., & Wilkinson, B. (2013). *The concentration of selected nutrients in New Zealand beef and lamb cuts and offal items: A report to beef + lamb New Zealand limited* (9780473229412). https://books.google.co.nz/books?id=XoITnwEACAAJ

Purslow, P. P. (2005). Intramuscular connective tissue and its role in meat quality. *Meat Science*, *70*(3), 435-447. https://doi.org/10.1016/j.meatsci.2004.06.028

Purslow, P. P. (2018). Contribution of collagen and connective tissue to cooked meat toughness; some paradigms reviewed. *Meat Science*. https://doi.org/10.1016/j.meatsci.2018.03.026

Purslow, P. P., Oiseth, S., Hughes, J., & Warner, R. D. (2016). The structural basis of cooking loss in beef: Variations with temperature and ageing. *Food Res Int*, *89*(Pt 1), 739-748. https://doi.org/10.1016/j.foodres.2016.09.010

Quiles, A., Perez-Munuera, I., Larrea, V., & Lluch, M. A. (2008). Microstructure of muscle foods. In L. M. L. Nollet & F. Toldrá (Eds.), *Handbook of muscle foods analysis* (pp. 335-352). CRC Press. https://doi.org/10.1201/9781420045307.ch19

Rao, M., Gault, N., & Kennedy, S. (1989). Changes in the ultrastructure of beef muscle as influenced by acidic conditions below the ultimate pH. *Food Structure*, *8*(1), 14.

Raynaud, F., Fernandez, E., Coulis, G., Aubry, L., Vignon, X., Bleimling, N., Gautel, M., Benyamin, Y., & Ouali, A. (2005). Calpain 1–titin interactions concentrate calpain 1 in the Z-band edges and in the N2-line region within the skeletal myofibril. *The Febs Journal*, *272*(10), 2578-2590. https://doi.org/10.1111/j.1742-4658.2005.04683.x

Realini, C. E., Venien, A., Gou, P., Gatellier, P., Perez-Juan, M., Danon, J., & Astruc, T. (2013). Characterization of *longissimus thoracis*, *semitendinosus* and *masseter* muscles and relationships with technological quality in pigs. 1. microscopic analysis of muscles. *Meat Science*, *94*(3), 408-416. https://doi.org/10.1016/j.meatsci.2013.03.009

Rémond, D., Machebeuf, M., Yven, C., Buffière, C., Mioche, L., Mosoni, L., & Mirand, P. P. (2007). Postprandial whole-body protein metabolism after a meat meal is influenced by chewing efficiency in elderly subjects. *The American Journal of Clinical Nutrition*, *85*(5), 1286-1292. https://doi.org/10.1093/ajcn/85.5.1286

Reynolds, E. S. (1963). The use of lead citrate at high pH as an electron-opaque stain in electron microscopy. *The Journal of Cell Biology*, *17*(1), 208-212. https://doi.org/10.1083/jcb.17.1.208

Rico, E., Toldrá, F., & Flores, J. (1991). Problems associated with the assay of cathepsin D in meat and meat products. *Food Chemistry*, *40*(1), 87-91. https://doi.org/https://doi.org/10.1016/0308-8146(91)90021-F

Rohlik, B.-A., Bolumar, T., Sikes, A., Broch, M., Øiseth, S., Watkins, P., & Buckow, R. (2017). *Optimising meat quality and functionality through novel processing interventions–final report*. http://www.ampc.com.au/uploads/pdf/Processing-Hygiene-Quality-and-Meat-Science/2013-5040%20-%20TMS%202%20-%20Final%20report.pdf

Roldan, M., Antequera, T., Martin, A., Mayoral, A. I., & Ruiz, J. (2013). Effect of different temperature-time combinations on physicochemical, microbiological, textural and structural features of sous-vide cooked lamb loins. *Meat Science*, *93*(3), 572-578. https://doi.org/10.1016/j.meatsci.2012.11.014

Ruiz, J., Calvarro, J., Sánchez del Pulgar, J., & Roldán, M. (2013). Science and technology for new culinary techniques. *Journal of Culinary Science & Technology*, *11*(1), 66-79. https://doi.org/10.1080/15428052.2013.755422

Rutherfurd, S. (2010). Methodology for determining degree of hydrolysis of proteins in hydrolysates: A review. *Journal of AOAC International*, *93 5*, 1515-1522. https://doi.org/10.1093/JAOAC/93.5.1515

Rutherfurd, S. M., Montoya, C. A., Zou, M. L., Moughan, P. J., Drummond, L. N., & Boland, M. J. (2011). Effect of actinidin from kiwifruit (*Actinidia deliciosa* cv. Hayward) on the digestion of food proteins determined in the growing rat. *Food Chemistry*, *129*(4), 1681-1689. https://doi.org/10.1016/j.foodchem.2011.06.031

Sa, A. G. A., Moreno, Y. M. F., & Carciofi, B. A. M. (2019). Food processing for the improvement of plant proteins digestibility. *Critical Reviews in Food Science and Nutrition*, 1-20. https://doi.org/10.1080/10408398.2019.1688249

Saito, K., Hoki, K., & Minamitani, Y. (2016, 6-9 July 2016). Effect of brine and temperature in sterilization using nanosecond pulsed electric fields for packaged fresh foods. 2016 IEEE International Power Modulator and High Voltage Conference (IPMHVC), San Francisco, CA.

Sanchez-Sabate, R., & Sabate, J. (2019). Consumer Attitudes Towards Environmental Concerns of Meat Consumption: A Systematic Review. *Int J Environ Res Public Health*, *16*(7). https://doi.org/10.3390/ijerph16071220

Santé-Lhoutellier, V., Astruc, T., Marinova, P., Greve, E., & Gatellier, P. (2008). Effect of meat cooking on physicochemical state and *in vitro* digestibility of myofibrillar proteins. *Journal of Agricultural and Food Chemistry*, *56*(4), 1488-1494. https://doi.org/10.1021/jf072999g

Schellekens, M. (1996). New research issues in sous-vide cooking. *Trends in Food Science & Technology*, *7*(8), 256-262. https://doi.org/10.1016/0924-2244(96)10027-3

Schiff, R. I., & Gennaro Jr., J. F. (1979). The role of the buffer in the fixation of biological specimens for transmission and scanning electron microscopy. *Scanning*, *2*(3), 135-148. https://doi.org/10.1002/sca.4950020304

Schilling, M. W., Claus, J. R., Marriott, N. G., Solomon, M. B., Eigel, W. N., & Wang, H. (2002). No effect of hydrodynamic shock wave on protein functionality of beef muscle. *Journal of Food Science*, *67*(1), 335-340. https://doi.org/10.1111/j.1365-2621.2002.tb11406.x

Sensoy, I. (2014). A review on the relationship between food structure, processing, and bioavailability. *Critical Reviews in Food Science and Nutrition*, *54*(7), 902-909. https://doi.org/10.1080/10408398.2011.619016

Sentandreu, M. A., Coulis, G., & Ouali, A. (2002). Role of muscle endopeptidases and their inhibitors in meat tenderness. *Trends in Food Science & Technology*, *13*(12), 400-421. https://doi.org/10.1016/S0924-2244(02)00188-7

Shao, Y., Xiong, G., Ling, J., Hu, Y., Shi, L., Qiao, Y., Yu, J., Cui, Y., Liao, L., Wu, W., Li, X., Ding, A., & Wang, L. (2018). Effect of ultra-high pressure treatment on shucking and meat properties of red swamp crayfish (Procambarus clarkia). *LWT*, *87*, 234-240. https://doi.org/10.1016/j.lwt.2017.07.062

Sifre, L., Coton, J. P., Andre, B., & Rezacova-Lukaskova, Z. (2013). Optimization of a quantitative method for muscle histology assessment. *J Microsc*, *250*(1), 50-56. https://doi.org/10.1111/jmi.12016

Singh, H., Ye, A., & Ferrua, M. J. (2015). Aspects of food structures in the digestive tract. *Current Opinion in Food Science*, *3*, 85-93. https://doi.org/10.1016/j.cofs.2015.06.007

Smith, D. M. (2000). Chapter eleven-functional properties of muscle proteins in processed poultry products. In C. M. Owens, C. Alvarado, & A. R. Sams (Eds.),

Poultry meat processing (2nd ed., pp. 231-244). CRC Press. https://books.google.co.nz/books?id=2ILLBQAAQBAJ

Smith, M. E., & Morton, D. G. (2010). Digestion and absorption. In M. E. Smith & D. G. Morton (Eds.), *The digestive system* (2nd ed., pp. 129-152). Churchill Livingstone. https://doi.org/10.1016/B978-0-7020-3367-4.00008-6

Soglia, F., Zeng, Z., Gao, J., Puolanne, E., Cavani, C., Petracci, M., & Ertbjerg, P. (2018). Evolution of proteolytic indicators during storage of broiler wooden breast meat. *Poultry Science*, *97*(4), 1448-1455. https://doi.org/10.3382/ps/pex398

Soladoye, O. P., Juárez, M. L., Aalhus, J. L., Shand, P., & Estévez, M. (2015). Protein Oxidation in Processed Meat: Mechanisms and Potential Implications on Human Health. *Comprehensive Reviews in Food Science and Food Safety*, *14*(2), 106-122. https://doi.org/10.1111/1541-4337.12127

Solomon, M., Long, J., & Eastridge, J. (1997). The hydrodyne: a new process to improve beef tenderness. *Journal of Animal Science*, *75*(6), 1534-1537. https://doi.org/10.2527/1997.7561534x

Solomon, M. B., Carpenter, C. E., Snowder, G. D., & Cockett, N. E. (1998). A research note tenderizing callipyge lamb with the hydrodyne process and electrical stimulation. *Journal of Muscle Foods*, *9*(3), 305-311. https://doi.org/10.1111/j.1745-4573.1998.tb00663.x

Somaratne, G., Reis, M. M., Ferrua, M. J., Ye, A., Nau, F., Floury, J., Dupont, D., Singh, R. P., & Singh, J. (2019). Mapping the spatiotemporal distribution of acid and moisture in food structures during gastric juice diffusion using hyperspectral imaging. *Journal of Agricultural and Food Chemistry*, *67*(33), 9399-9410. https://doi.org/10.1021/acs.jafc.9b02430

Spanier, A. M., & Fahrenholz, T. M. (2005). Hydrodynamic pressure (HDP)-treatment: Influence on beef striploin proteins. In A. M. Spanier, F. Shahidi, T. H. Parliment, C. Mussinan, C. T. Ho, & E. T. Contis (Eds.), *Food flavor and chemistry: explorations into the 21st century* (pp. 391-404). Royal Society of Chemistry.

Spanier, A. M., Fahrenholz, T. M., Paoczay, E. W., & Schmukler, R. (2005). Comparison of the influence of hydrodynamic pressure (HDP)-treatment and aging on beef striploin proteins. In A. M. Spanier, F. Shahidi, T. H. Parliment, C. Mussinan, C. T. Ho, & E. T. Contis (Eds.), *Food Flavor and Chemistry: Explorations into the 21st Century* (pp. 375-390). Royal Society of Chemistry.

Spanier, A. M., & Romanowski, R. D. (2000). A potential index for assessing the tenderness of hydrodynamic pressure (HDP)-treated beef strip loins. *Meat Science*, *56*(2), 193-202. https://doi.org/10.1016/S0309-1740(00)00042-5

Stabursvik, E., & Martens, H. (1980). Thermal denaturation of proteins in Post rigor muscle tissue as studied by differential scanning calorimetry. *Journal of the Science of Food and Agriculture*, *31*(10), 1034-1042. https://doi.org/10.1002/jsfa.2740311010

Straadt, I. K., Rasmussen, M., Andersen, H. J., & Bertram, H. C. (2007). Aging-induced changes in microstructure and water distribution in fresh and cooked pork in relation to water-holding capacity and cooking loss - A combined confocal laser scanning microscopy (CLSM) and low-field nuclear magnetic resonance relaxation study. *Meat Science*, *75*(4), 687-695. https://doi.org/10.1016/j.meatsci.2006.09.019

Strasburg, G., Xiong, Y. L., & Chiang, W. (2008). Physiology and chemistry of edible muscle tissues. In S. Damodaran, K. L. Parkin, & O. R. Fennema (Eds.), *Fennema's food chemistry* (4th ed., pp. 923-973). CRC Press.

Sugiyama, S., Hirota, A., Okada, C., Yorita, T., & Ohtsuki, K. (2005). Effect of kiwifruit juice on beef collagen. *Journal of Nutritional Science and Vitaminology*, *51*(1), 27-33. https://doi.org/10.3177/jnsv.51.27

Sugiyama, S., Ohtsuki, K., Sato, K., & Kawabata, M. (1997). Enzymatic properties, substrate specificities and pH-activity profiles of two kiwifruit proteases. *Journal of Nutritional Science and Vitaminology*, *43*(5), 581-589. https://doi.org/10.3177/jnsv.43.581

Sullivan, G. A., & Calkins, C. R. (2010). Application of exogenous enzymes to beef muscle of high and low-connective tissue. *Meat Science*, *85*(4), 730-734. https://doi.org/10.1016/j.meatsci.2010.03.033

Suman, S. P., & Joseph, P. (2013). Myoglobin chemistry and meat color. *Annual Review of Food Science and Technology*, *4*, 79-99. https://doi.org/10.1146/annurev-food-030212-182623

Suman, S. P., & Joseph, P. (Eds.). (2014). *Chemical and physical characteristics of meat | color and pigment* (2nd ed.). Academic Press. https://doi.org/10.1016/b978-0-12-384731-7.00084-2.

Sun, W., Zhou, F., Zhao, M., Yang, B., & Cui, C. (2011). Physicochemical changes of myofibrillar proteins during processing of Cantonese sausage in relation to their aggregation behaviour and *in vitro* digestibility. *Food Chemistry*, *129*(2), 472-478. https://doi.org/10.1016/j.foodchem.2011.04.101

Suriaatmaja, D. (2013). *Mechanism of meat tenderization by long-time low-temperature heating* [Doctoral dissertation, North Carolina State University]. Raleigh, NC.

Suwandy, V., Carne, A., van de Ven, R., Bekhit, A. E.-D. A., & Hopkins, D. L. (2015a). Effect of pulsed electric field on the proteolysis of cold boned beef m. l*ongissimus lumborum* and *m. semimembranosus*. *Meat Science*, *100*, 222-226. https://doi.org/10.1016/j.meatsci.2014.10.011

Suwandy, V., Carne, A., van de Ven, R., Bekhit, A. E.-D. A., & Hopkins, D. L. (2015b). Effect of pulsed electric field treatment on hot-boned muscles of different potential tenderness. *Meat Science*, *105*, 25-31. https://doi.org/10.1016/j.meatsci.2015.02.009

Suwandy, V., Carne, A., van de Ven, R., Bekhit, A. E.-D. A., & Hopkins, D. L. (2015c). Effect of pulsed electric field treatment on the eating and keeping qualities of cold-boned beef loins: impact of initial pH and fibre orientation. *Food and Bioprocess Technology*, *8*(6), 1355-1365. https://doi.org/10.1007/s11947-015-1498-8

Suwandy, V., Carne, A., van de Ven, R., Bekhit, A. E. D., & Hopkins, D. L. (2015d). Effect of repeated pulsed electric field treatment on the quality of cold-boned beef loins and topsides. *Food and Bioprocess Technology*, *8*(6), 1218-1228. https://doi.org/10.1007/s11947-015-1485-0

Suzuki, A., Matsumoto, Y., Sato, T., Nonami, Y., & Saito, M. (1982). Ca2+-activated protease in stored muscle. *Meat Science*, *7*(4), 269-278. https://doi.org/10.1016/0309-1740(82)90055-9

Swartz, D., Greaser, M., & Cantino, M. (2009). Muscle structure and function. In M. Du & R. J. McCormick (Eds.), *Applied muscle biology and meat science* (pp. 1-45). CRC Press. https://doi.org/10.1201/b15797-210.1201/b15797-2

Taylor, R. G. (2004). Connective tissue structure, function and influence on meat quality. In W. K. Jensen (Ed.), *Encyclopedia of meat sciences* (1st ed., pp. 306-314). Academic Press. https://doi.org/10.1016/B0-12-464970-X/00255-5

Taylor, R. G., Geesink, G., Thompson, V., Koohmaraie, M., & Goll, D. (1995). Is Z-disk degradation responsible for postmortem tenderization? *Journal of Animal Science*, *73*(5), 1351-1367. https://doi.org/10.2527/1995.7351351x

Taylor, R. G., Tassy, C., Briand, M., Robert, N., Briand, Y., & Ouali, A. (1995). Proteolytic activity of proteasome on myofibrillar structures. *Molecular Biology Reports*, *21*(1), 71-73. https://doi.org/10.1007/BF00990974

Théron, L., Venien, A., Boland, M., Kaur, L., Loison, O., Chambon, C., Sante-Lhoutellier, V., & Astruc, T. (2014, 17-22nd August). Meat proteolysis by pepsin highlighted by MALDI imaging mass spectrometry. 60th International Congress of Meat Science and Technology, Punta del Este, Uruguay.

Théron, L., Vénien, A., Jamme, F., Fernandez, X., Peyrin, F., Molette, C., Dumas, P., Réfrégiers, M., & Astruc, T. (2014). Protein matrix involved in the lipid retention of foie gras during cooking: A multimodal hyperspectral imaging study. *Journal of Agricultural and Food Chemistry*, *62*(25), 5954-5962. https://doi.org/10.1021/jf5009605

Thevenot, J., Cauty, C., Legland, D., Dupont, D., & Floury, J. (2017). Pepsin diffusion in dairy gels depends on casein concentration and microstructure. *Food Chemistry*, *223*, 54-61. https://doi.org/10.1016/j.foodchem.2016.12.014

Thuenemann, E. C., Mandalari, G., Rich, G. T., & Faulks, R. M. (2015). Dynamic gastric model (DGM). In K. Verhoeckx, P. Cotter, I. López-Expósito, C. Kleiveland, T. Lea, A. Mackie, T. Requena, D. Swiatecka, & H. Wichers (Eds.), *The impact of food bioactives on health: In vitro and ex vivo models* (pp. 47-59). Springer International Publishing. https://doi.org/10.1007/978-3-319-16104-4_6

Toepfl, S., Bolumar, T., & Heinz, V. (2013). *Development of shock wave technology for packed meat*. https://cordis.europa.eu/docs/results/287/287034/final1-final-publishable-summary-report-shockmeat.pdf

Toepfl, S., Heinz, V., & Knorr, D. (2007a). 2-History of pulsed electric field treatment. In H. L. M. Lelieveld, S. Notermans, & S. W. H. de Haan (Eds.), *Food preservation by pulsed electric fields* (pp. 9-39). Woodhead Publishing. https://doi.org/10.1533/9781845693831.9

Toepfl, S., Heinz, V., & Knorr, D. (2007b). High intensity pulsed electric fields applied for food preservation. *Chemical Engineering and Processing: Process Intensification*, *46*(6), 537-546. https://doi.org/10.1016/j.cep.2006.07.011

Toldrá, F. (2012). Biochemistry of processing meat and poultry. In B. K. Simpson, L. M. L. Nollet, F. Toldrá, G. Paliyath, S. Benjakul, & Y. H. Hui (Eds.), *Food biochemistry and food processing* (pp. 303-316). John Wiley & Sons. https://doi.org/10.1002/9781118308035.ch16

Toldra, F., & Reig, M. (2004). Analysis of meat-containing food. In L. M. L. Nollet (Ed.), *Handbook of food analysis: Methods and instruments in applied food analysis* (2nd ed., Vol. 3, pp. 1941-1959). Marcel Dekker, Inc. http://dx.doi.org/10.1201/b11081-53

Toldra, F., Sentandreu, M. A., & Aristoy, M.-C. (2008). Peptides. In L. M. L. Nollet & F. Toldrá (Eds.), *Handbook of muscle foods analysis* (pp. 41-55). CRC Press. https://doi.org/10.1201/9781420045307.ch3

Tomé, D. (2013). Digestibility issues of vegetable versus animal proteins: Protein and amino acid requirements—Functional aspects. *Food and Nutrition Bulletin*, *34*(2), 272-274. https://doi.org/10.1177%2F156482651303400225

Toohey, E. S., Kerr, M. J., van de Ven, R., & Hopkins, D. L. (2011). The effect of a kiwi fruit based solution on meat traits in beef *m. semimembranosus* (topside). *Meat Science*, *88*(3), 468-471. https://doi.org/10.1016/j.meatsci.2011.01.028

Tornberg, E. (2005). Effects of heat on meat proteins - Implications on structure and quality of meat products. *Meat Science*, *70*(3), 493-508. https://doi.org/10.1016/j.meatsci.2004.11.021

Torrescano, G., Sánchez-Escalante, A., Giménez, B., Roncalés, P., & Beltrán, J. A. (2003). Shear values of raw samples of 14 bovine muscles and their relation to muscle collagen characteristics. *Meat Science*, *64*(1), 85-91. https://doi.org/10.1016/S0309-1740(02)00165-1

Tortora, G. J., & Derrickson, B. H. (2013). Principles of anatomy and physiology. In *Chapter 10 muscular tissue* (14th ed.). Wiley Global Education. https://books.google.co.nz/books?id=boNbAgAAQBAJ

Troy, D. J., & Kerry, J. P. (2010). Consumer perception and the role of science in the meat industry. *Meat Science*, *86*(1), 214-226. https://doi.org/10.1016/j.meatsci.2010.05.009

Troy, D. J., Ojha, K. S., Kerry, J. P., & Tiwari, B. K. (2016). Sustainable and consumer-friendly emerging technologies for application within the meat industry: an overview. *Meat Science*, *120*, 2-9. https://doi.org/10.1016/j.meatsci.2016.04.002

Tskhovrebova, L., & Trinick, J. (2003). Titin: properties and family relationships [https://doi.org/10.1038/nrm1198]. *Nature Reviews Molecular Cell Biology*, *4*(9), 679-689. https://doi.org/10.1038/nrm1198

Tskhovrebova, L., & Trinick, J. (2010). Roles of titin in the structure and elasticity of the sarcomere. *J Biomed Biotechnol*, *2010*(article ID 612482), 7pp. https://doi.org/10.1155/2010/612482

U.S. Department of Health and Human Services and U.S. Department of Agriculture. (2015). *2015-2020 Dietary guidelines for Americans*. http://health.gov/dietaryguidelines/2015/guidelines/.

Uttaro, B., Zawadski, S., & McLeod, B. (2019). Efficacy of multi-stage sous-vide cooking on tenderness of low value beef muscles. *Meat Science*, *149*, 40-46. https://doi.org/10.1016/j.meatsci.2018.11.008

van Lieshout, G. A. A., Lambers, T. T., Bragt, M. C. E., & Hettinga, K. A. (2020). How processing may affect milk protein digestion and overall physiological outcomes: A systematic review. *Critical Reviews in Food Science and Nutrition*, *60*(14), 2422-2445. https://doi.org/10.1080/10408398.2019.1646703

vanderVen, P. F., Obermann, W., Lemke, B., Gautel, M., Weber, K., & Fürst, D. O. (2000). Characterization of muscle filamin isoforms suggests a possible role of γ-filamin/ABP-L in sarcomeric Z-disc formation. *Cell Motility and the Cytoskeleton*, *45*, 149-162. https://doi.org/10.1002/(SICI)1097-0169(200002)45:2<149::AID-CM6>3.0.CO;2-G

Vaskoska, R., Ha, M., Naqvi, Z. B., White, J. D., & Warner, R. D. (2020). Muscle, Ageing and Temperature Influence the Changes in Texture, Cooking Loss and Shrinkage of Cooked Beef. *Foods*, *9*(9). https://doi.org/10.3390/foods9091289

Vaudagna, S. R., Sánchez, G., Neira, M. S., Insani, E. M., Picallo, A. B., Gallinger, M. M., & Lasta, J. A. (2002). Sous vide cooked beef muscles: effects of low temperature–long time (LT–LT) treatments on their quality characteristics and storage stability. *International Journal of Food Science & Technology*, *37*(4), 425-441. https://doi.org/10.1046/j.1365-2621.2002.00581.x

Voermans, N. C., Bonnemann, C. G., Huijing, P. A., Hamel, B. C., van Kuppevelt, T. H., de Haan, A., Schalkwijk, J., van Engelen, B. G., & Jenniskens, G. J. (2008). Clinical and molecular overlap between myopathies and inherited connective tissue diseases. *Neuromuscular Disorders*, *18*(11), 843-856. https://doi.org/10.1016/j.nmd.2008.05.017

Wada, M., Hosaka, M., Nakazawa, R., Kobayashi, Y., & Hasegawa, T. (2004). The solubilization of unheated cattle achilles tendon with actinidin under neutral and

acidic conditions. *Food Science and Technology Research*, *10*(1), 35-37. https://doi.org/10.3136/fstr.10.35

Wang, J., Wu, P., Liu, M., Liao, Z., Wang, Y., Dong, Z., & Chen, X. D. (2019). An advanced near real dynamic in vitro human stomach system to study gastric digestion and emptying of beef stew and cooked rice. *Food & Function*, *10*(5), 2914-2925. https://doi.org/10.1039/c8fo02586j

Wang, X., Muhoza, B., Wang, X., Feng, T., Xia, S., & Zhang, X. (2019). Comparison between microwave and traditional water bath cooking on saltiness perception, water distribution and microstructure of grass crap meat. *Food Research International*, *125*, 108521. https://doi.org/10.1016/j.foodres.2019.108521

Warner, R., Ha, M., Sikes, A., & Vaskoska, R. (2017). Chapter 15-Cooking and novel postmortem treatments to improve meat texture. In P. P. Purslow (Ed.), *New aspects of meat quality - From genes to ethic* (pp. 387-423). Woodhead Publishing. https://doi.org/10.1016/b978-0-08-100593-4.00016-3

Weir, C. E., Wang, H., Birkner, M. L., Parsons, J., & Ginger, B. (1958). Studies on enzymatic tenderisation of meat. II Panel and histological analyses of meat treated with liquid tenderising containing papain. *Journal of Food Science*, *23*(5), 411-422. https://doi.org/10.1111/j.1365-2621.1958.tb17589.x

Wellner, N. (Ed.). (2013). *Fourier transform infrared (FTIR) and Raman microscopy: Principles and applications to food microstructures*. Woodhead Publishing. https://doi.org/10.1533/9780857098894.1.163.

Wen, S., Zhou, G., Li, L., Xu, X., Yu, X., Bai, Y., & Li, C. (2015). Effect of cooking on in vitro digestion of pork proteins: A peptidomic perspective. *Journal of Agriculture and Food Chemistry*, *63*(1), 250-261. https://doi.org/10.1021/jf505323g

Wen, S., Zhou, G., Song, S., Xu, X., Voglmeir, J., Liu, L., Zhao, F., Li, M., Li, L., Yu, X., Bai, Y., & Li, C. (2015). Discrimination of *in vitro* and *in vivo* digestion products of meat proteins from pork, beef, chicken, and fish. *Proteomics*, *15*(21), 3688-3698. https://doi.org/10.1002/pmic.201500179

Wheeler, T., & Koohmaraie, M. (1994). Prerigor and postrigor changes in tenderness of ovine *longissimus* muscle. *Journal of Animal Science*, *72*(5), 1232-1238. https://doi.org/10.2527/1994.7251232x

Whitnall, T., & Pitts, N. (2019). Global trends in meat consumption. In ABARES (Ed.), *Agricultural commodities: March quarter 2019* (pp. 95-98). Australian Bureau of Agricultural and Resource Economics and Sciences. https://www.agriculture.gov.au/sites/default/files/sitecollectiondocuments/abares/agriculture-commodities/AgCommodities201903_MeatConsumptionOutlook_v1.0.0.pdf

Williams, J. L. (2008). Genetic control of meat quality traits. In F. Toldrá (Ed.), *Meat biotechnology* (pp. 21-60). Springer.

Williams, P. (2007). Nutritional composition of red meat. *Nutrition & Dietetics*, *64*, S113-S119. https://doi.org/10.1111/j.1747-0080.2007.00197.x

Work, T. S., & Rurdon, R. H. (Eds.). (1981). *Chapter 5-Methods for the detection of peptides* (Vol. 9). North-Holland Biomedical Press. https://doi.org/10.1016/S0075-7535(08)70244-4.

Xiong, Y. (1997). Structure-function relationships of muscle proteins. In S. Damodaran (Ed.), *Food proteins and their applications* (pp. 341-392). Marcel Dekker, Inc.

Yao, C. K., Muir, J. G., & Gibson, P. R. (2016). Review article: insights into colonic protein fermentation, its modulation and potential health implications. *Aliment Pharmacol Ther*, *43*(2), 181-196. https://doi.org/10.1111/apt.13456

Yi, L., Van Boekel, M. A. J. S., Boeren, S., & Lakemond, C. M. M. (2016). Protein identification and in vitro digestion of fractions from *Tenebrio molitor*. *European Food Research and Technology*, *242*(8), 1285-1297. https://doi.org/10.1007/s00217-015-2632-6

You, Z., & Cheng, F. (2014). The development of infrared microspectroscopy (IMS) and its applications in agricultural and aquatic products. *Applied Spectroscopy Reviews*, *49*(1), 83-96. https://doi.org/10.1080/05704928.2013.798803

Zespri. (2019). *Quick and easy kiwi recipes from sunrise to sunset*. Zespri Group Limited. Retrieved November 18, 2019 from https://www.zespri.com/en-US/blogdetail/quick-kiwi-recipes

Zhang, B., Sun, Q., Liu, H.-J., Li, S.-Z., & Jiang, Z.-Q. (2017). Characterization of actinidin from Chinese kiwifruit cultivars and its applications in meat tenderization and production of angiotensin I-converting enzyme (ACE) inhibitory peptides. *LWT*, *78*, 1-7. https://doi.org/10.1016/j.lwt.2016.12.012

Zhao, W., & Yang, R. (2008). Comparative study of inactivation and conformational change of lysozyme induced by pulsed electric fields and heat. *European Food Research and Technology*, *228*(1), 47-54. https://doi.org/10.1007/s00217-008-0905-z

Zhu, X. (2017). *Actinidin treatment and sous vide cooking : effects on tenderness and in vitro protein digestibility of beef brisket* [Masters Dissertation, Massey University]. Massey Research Online. http://hdl.handle.net/10179/12752

Zhu, X., Kaur, L., & Boland, M. (2018). Thermal inactivation of actinidin as affected by meat matrix. *Meat Science*, *145*, 238-244. https://doi.org/10.1016/j.meatsci.2018.06.027

Zhu, X., Kaur, L., Staincliffe, M., & Boland, M. (2018). Actinidin pretreatment and sous vide cooking of beef brisket: Effects on meat microstructure, texture and *in vitro* protein digestibility. *Meat Science*, *145*, 256-265. https://doi.org/10.1016/j.meatsci.2018.06.029

Zielbauer, B. I., Franz, J., Viezens, B., & Vilgis, T. A. (2016). Physical aspects of meat cooking: Time dependent thermal protein denaturation and water loss [journal article]. *Food Biophysics*, *11*(1), 34-42. https://doi.org/10.1007/s11483-015-9410-7

Zot, A. S., & Potter, J. D. (1987). Structural aspects of troponin-tropomyosin regulation of skeletal muscle contraction. *Annual Review of Biophysics and Biophysical Chemistry*, *16*(1), 535-559. https://doi.org/10.1146/annurev.bb.16.060187.002535

Zuckerman, H., Bowker, B. C., Eastridge, J. S., & Solomon, M. B. (2013). Microstructure alterations in beef intramuscular connective tissue caused by hydrodynamic pressure processing. *Meat Science*, *95*(3), 603-607. https://doi.org/10.1016/j.meatsci.2013.05.041

Zuckerman, H., & Solomon, M. B. (1998). Ultrastructural changes in bovine longissimus muscle caused by the hydrodyne process. *Journal of Muscle Foods*, *9*(4), 419-426. https://doi.org/10.1111/j.1745-4573.1998.tb00745.x

Appendices

Appendix A- Copyright permission from John Wiley & Sons, Inc. (for Figure 2-1)

RE: Request permission to re-use figures

Wiley Global Permissions <permissions@wiley.com>
Thu 6/04/2017 8:29 AM
To: Chian, Feng Ming <F.Chian@massey.ac.nz>

Dear Feng Chian:

Thank you for your email.

Permission is hereby granted for the use requested subject to the usual acknowledgements (author, title of material, title of book, ourselves as publisher). You should also duplicate the copyright notice that appears in the Wiley publication; this can be found on the copyright page in the book.

Any third party material is expressly excluded from this permission. If any of the material you wish to use appears within our work with credit to another source, authorization from that source must be obtained.

This permission does not include the right to grant others permission to photocopy or otherwise reproduce this material except for accessible versions made by non-profit organizations serving the blind, visually impaired and other persons with print disabilities (VIPs).

Sincerely,

Sheik Safdar
Permissions Coordinator II/Sr.
Copyright & Permissions
Wiley

ssafdar@wiley.com
T +1 201-748-6512
F +1 201-748-6008

111 River Street
Hoboken, NJ 07030-5774
U.S.
permissions@wiley.com

WILEY

From: Chian, Feng Ming [mailto:F.Chian@massey.ac.nz]
Sent: Sunday, March 26, 2017 7:18 PM
To: Wiley Global Permissions
Subject: Request permission to re-use figures

Dear Sir/Mdm,

I am writing to seek for permission to re-use Figure 10.1 and Figure 10.3 from *Principles of Anatomy and Physiology, 14th Edition: 14th Edition* written by Tortora, G. J., & Derrickson, B. H. (2013).

I am a PhD student studying in Massey University, New Zealand and would like to include both figures mentioned in the literature review of my PhD thesis.

Thank you and I look forward to hearing from you soon.

Regards,
Feng Ming, Chian

Appendix B- Copyright permission from Elsevier (for Figure 2-2, Figure 2-3, Figure 2-4, Table 2-2)

ELSEVIER LICENSE
TERMS AND CONDITIONS

Sep 23, 2020

This Agreement between Ms. Feng Ming Chian ("You") and Elsevier ("Elsevier") consists of your license details and the terms and conditions provided by Elsevier and Copyright Clearance Center.

License Number	4890050065240
License date	Aug 15, 2020
Licensed Content Publisher	Elsevier
Licensed Content Publication	Elsevier Books
Licensed Content Title	Encyclopedia of Food Chemistry
Licensed Content Author	Mike Boland,Lovedeep Kaur,Feng Ming Chian,Thierry Astruc
Licensed Content Date	Jan 1, 2019
Licensed Content Pages	16
Start Page	164
End Page	179
Type of Use	reuse in a thesis/dissertation
Portion	figures/tables/illustrations
Number of figures/tables/illustrations	4

Format	both print and electronic
Are you the author of this Elsevier chapter?	Yes
Will you be translating?	No
Title	PhD student
Institution name	Massey University
Expected presentation date	Sep 2020
Portions	Figure 3, Figure 5, Figure 6 and Table 3
Requestor Location	Ms. Feng Ming Chian 8 Chelwood Street, Takaro Palmerston North, Manawatu 4412 New Zealand Attn: Ms. Feng Ming Chian
Publisher Tax ID	GB 494 6272 12
Total	0.00 AUD

Terms and Conditions

INTRODUCTION

1. The publisher for this copyrighted material is Elsevier. By clicking "accept" in connection with completing this licensing transaction, you agree that the following terms and conditions apply to this transaction (along with the Billing and Payment terms and conditions established by Copyright Clearance Center, Inc. ("CCC"), at the time that you opened your Rightslink account and that are available at any time at http://myaccount.copyright.com).

GENERAL TERMS

2. Elsevier hereby grants you permission to reproduce the aforementioned material subject to the terms and conditions indicated.

3. Acknowledgement: If any part of the material to be used (for example, figures) has appeared in our publication with credit or acknowledgement to another source, permission must also be sought from that source. If such permission is not obtained then that material may not be included in your publication/copies. Suitable acknowledgement to the source must be made, either as a footnote or in a reference list at the end of your publication, as follows:

"Reprinted from Publication title, Vol /edition number, Author(s), Title of article / title of chapter, Pages No., Copyright (Year), with permission from Elsevier [OR APPLICABLE SOCIETY COPYRIGHT OWNER]." Also Lancet special credit - "Reprinted from The Lancet, Vol. number, Author(s), Title of article, Pages No., Copyright (Year), with permission from Elsevier."

4. Reproduction of this material is confined to the purpose and/or media for which permission is hereby given.

5. Altering/Modifying Material: Not Permitted. However figures and illustrations may be altered/adapted minimally to serve your work. Any other abbreviations, additions, deletions and/or any other alterations shall be made only with prior written authorization of Elsevier Ltd. (Please contact Elsevier's permissions helpdesk here). No modifications can be made to any Lancet figures/tables and they must be reproduced in full.

6. If the permission fee for the requested use of our material is waived in this instance, please be advised that your future requests for Elsevier materials may attract a fee.

7. Reservation of Rights: Publisher reserves all rights not specifically granted in the combination of (i) the license details provided by you and accepted in the course of this licensing transaction, (ii) these terms and conditions and (iii) CCC's Billing and Payment terms and conditions.

8. License Contingent Upon Payment: While you may exercise the rights licensed immediately upon issuance of the license at the end of the licensing process for the transaction, provided that you have disclosed complete and accurate details of your proposed use, no license is finally effective unless and until full payment is received from you (either by publisher or by CCC) as provided in CCC's Billing and Payment terms and conditions. If full payment is not received on a timely basis, then any license preliminarily granted shall be deemed automatically revoked and shall be void as if never granted. Further, in the event that you breach any of these terms and conditions or any of CCC's Billing and Payment terms and conditions, the license is automatically revoked and shall be void as if never granted. Use of materials as described in a revoked license, as well as any use of the materials beyond the scope of an unrevoked license, may constitute copyright infringement and publisher reserves the right to take any and all action to protect its copyright in the materials.

9. Warranties: Publisher makes no representations or warranties with respect to the licensed material.

10. Indemnity: You hereby indemnify and agree to hold harmless publisher and CCC, and their respective officers, directors, employees and agents, from and against any and all claims arising out of your use of the licensed material other than as specifically authorized pursuant to this license.

11. No Transfer of License: This license is personal to you and may not be sublicensed, assigned, or transferred by you to any other person without publisher's written permission.

12. No Amendment Except in Writing: This license may not be amended except in a writing signed by both parties (or, in the case of publisher, by CCC on publisher's behalf).

13. Objection to Contrary Terms: Publisher hereby objects to any terms contained in any purchase order, acknowledgment, check endorsement or other writing prepared by you, which terms are inconsistent with these terms and conditions or CCC's Billing and Payment terms and conditions. These terms and conditions, together with CCC's Billing and Payment terms and conditions (which are incorporated herein), comprise the entire agreement between you and publisher (and CCC) concerning this licensing transaction. In the event of any conflict between your obligations established by these terms and conditions and those established by CCC's Billing and Payment terms and conditions, these terms and conditions shall control.

14. Revocation: Elsevier or Copyright Clearance Center may deny the permissions described in this License at their sole discretion, for any reason or no reason, with a full refund payable to you. Notice of such denial will be made using the contact information provided by you. Failure to receive such notice will not alter or invalidate the denial. In no event will Elsevier or Copyright Clearance Center be responsible or liable for any costs, expenses or damage incurred by you as a result of a denial of your permission request, other than a refund of the amount(s) paid by you to Elsevier and/or Copyright Clearance Center for denied permissions.

LIMITED LICENSE

The following terms and conditions apply only to specific license types:

15. **Translation**: This permission is granted for non-exclusive world **English** rights only unless your license was granted for translation rights. If you licensed translation rights you may only translate this content into the languages you requested. A professional translator must perform all translations and reproduce the content word for word preserving the integrity of the article.

16. **Posting licensed content on any Website**: The following terms and conditions apply as follows: Licensing material from an Elsevier journal: All content posted to the web site must maintain the copyright information line on the bottom of each image; A hyper-text must be included to the Homepage of the journal from which you are licensing at http://www.sciencedirect.com/science/journal/xxxxx or the Elsevier homepage for books at http://www.elsevier.com; Central Storage: This license does not include permission for a scanned version of the material to be stored in a central repository such as that provided by Heron/XanEdu.

Licensing material from an Elsevier book: A hyper-text link must be included to the Elsevier homepage at http://www.elsevier.com . All content posted to the web site must maintain the copyright information line on the bottom of each image.

Posting licensed content on Electronic reserve: In addition to the above the following clauses are applicable: The web site must be password-protected and made available only to bona fide students registered on a relevant course. This permission is granted for 1 year only. You may obtain a new license for future website posting.

17. **For journal authors:** the following clauses are applicable in addition to the above:

Preprints:

A preprint is an author's own write-up of research results and analysis, it has not been peer-reviewed, nor has it had any other value added to it by a publisher (such as formatting, copyright, technical enhancement etc.).

Authors can share their preprints anywhere at any time. Preprints should not be added to or enhanced in any way in order to appear more like, or to substitute for, the final versions of articles however authors can update their preprints on arXiv or RePEc with their Accepted Author Manuscript (see below).

If accepted for publication, we encourage authors to link from the preprint to their formal publication via its DOI. Millions of researchers have access to the formal publications on ScienceDirect, and so links will help users to find, access, cite and use the best available version. Please note that Cell Press, The Lancet and some society-owned have different preprint policies. Information on these policies is available on the journal homepage.

Accepted Author Manuscripts: An accepted author manuscript is the manuscript of an article that has been accepted for publication and which typically includes author-incorporated changes suggested during submission, peer review and editor-author communications.

Authors can share their accepted author manuscript:

- immediately
  - via their non-commercial person homepage or blog
  - by updating a preprint in arXiv or RePEc with the accepted manuscript
  - via their research institute or institutional repository for internal institutional uses or as part of an invitation-only research collaboration work-group
  - directly by providing copies to their students or to research collaborators for their personal use
  - for private scholarly sharing as part of an invitation-only work group on commercial sites with which Elsevier has an agreement
- After the embargo period
  - via non-commercial hosting platforms such as their institutional repository
  - via commercial sites with which Elsevier has an agreement

In all cases accepted manuscripts should:

- link to the formal publication via its DOI
- bear a CC-BY-NC-ND license - this is easy to do
- if aggregated with other manuscripts, for example in a repository or other site, be shared in alignment with our hosting policy not be added to or enhanced in any way to appear more like, or to substitute for, the published journal article.

Published journal article (JPA): A published journal article (PJA) is the definitive final record of published research that appears or will appear in the journal and embodies all value-adding publishing activities including peer review co-ordination, copy-editing, formatting, (if relevant) pagination and online enrichment.

Policies for sharing publishing journal articles differ for subscription and gold open access articles:

Subscription Articles: If you are an author, please share a link to your article rather than the full-text. Millions of researchers have access to the formal publications on ScienceDirect, and so links will help your users to find, access, cite, and use the best available version.

Theses and dissertations which contain embedded PJAs as part of the formal submission can be posted publicly by the awarding institution with DOI links back to the formal publications on ScienceDirect.

If you are affiliated with a library that subscribes to ScienceDirect you have additional private sharing rights for others' research accessed under that agreement. This includes use for classroom teaching and internal training at the institution (including use in course packs and courseware programs), and inclusion of the article for grant funding purposes.

Gold Open Access Articles: May be shared according to the author-selected end-user license and should contain a CrossMark logo, the end user license, and a DOI link to the formal publication on ScienceDirect.

Please refer to Elsevier's posting policy for further information.

18. **For book authors** the following clauses are applicable in addition to the above: Authors are permitted to place a brief summary of their work online only. You are not allowed to download and post the published electronic version of your chapter, nor may you scan the printed edition to create an electronic version. **Posting to a repository:** Authors are permitted to post a summary of their chapter only in their institution's repository.

19. **Thesis/Dissertation**: If your license is for use in a thesis/dissertation your thesis may be submitted to your institution in either print or electronic form. Should your thesis be published commercially, please reapply for permission. These requirements include permission for the Library and Archives of Canada to supply single copies, on demand, of the complete thesis and include permission for Proquest/UMI to supply single copies, on demand, of the complete thesis. Should your thesis be published commercially, please reapply for permission. Theses and dissertations which contain embedded PJAs as part of the formal submission can be posted publicly by the awarding institution with DOI links back to the formal publications on ScienceDirect.

Elsevier Open Access Terms and Conditions

You can publish open access with Elsevier in hundreds of open access journals or in nearly 2000 established subscription journals that support open access publishing. Permitted third party re-use of these open access articles is defined by the author's choice of Creative Commons user license. See our open access license policy for more information.

Terms & Conditions applicable to all Open Access articles published with Elsevier:

Any reuse of the article must not represent the author as endorsing the adaptation of the article nor should the article be modified in such a way as to damage the author's honour or reputation. If any changes have been made, such changes must be clearly indicated.

The author(s) must be appropriately credited and we ask that you include the end user license and a DOI link to the formal publication on ScienceDirect.

If any part of the material to be used (for example, figures) has appeared in our publication with credit or acknowledgement to another source it is the responsibility of the user to ensure their reuse complies with the terms and conditions determined by the rights holder.

Appendix C- Statement of contribution

DRC 16

MASSEY UNIVERSITY
TE KUNENGA KI PŪREHUROA
UNIVERSITY OF NEW ZEALAND

GRADUATE RESEARCH SCHOOL

STATEMENT OF CONTRIBUTION
DOCTORATE WITH PUBLICATIONS/MANUSCRIPTS

We, the candidate and the candidate's Primary Supervisor, certify that all co-authors have consented to their work being included in the thesis and they have accepted the candidate's contribution as indicated below in the *Statement of Originality*.

Name of candidate:	Feng Ming Chian
Name/title of Primary Supervisor:	Dr. Lovedeep Kaur
In which chapter is the manuscript /published work:	Chapter 2

Please select one of the following three options:

(●) The manuscript/published work is published or in press

- Please provide the full reference of the Research Output:

Boland, M., Kaur, L., Chian, F. M., & Astruc, T. (2019). Muscle proteins. In L. Melton, F. Shahidi, & P. Varelis (Eds.), Encyclopedia of food chemistry (pp. 164-179). Academic Press. https://doi.org/10.1016/B978-0-08-100596-5.21602-8

( ) The manuscript is currently under review for publication – please indicate:

- The name of the journal:
- The percentage of the manuscript/published work that was contributed by the candidate:
- Describe the contribution that the candidate has made to the manuscript/published work:

( ) It is intended that the manuscript will be published, but it has not yet been submitted to a journal

Candidate's Signature:	Feng Ming Chian Digitally signed by Feng Ming Chian Date: 2020.09.21 16:41:32 +12'00'
Date:	21-Sep-2020
Primary Supervisor's Signature:	Lovedeep Kaur Digitally signed by Lovedeep Kaur Date: 2020.09.22 13:34:49 +12'00'
Date:	22-Sep-2020

This form should appear at the end of each thesis chapter/section/appendix submitted as a manuscript/ publication or collected as an appendix at the end of the thesis.

GRS Version 5 – 13 December 2019
DRC 19/09/10

DRC 16

MASSEY UNIVERSITY
TE KUNENGA KI PŪREHUROA
UNIVERSITY OF NEW ZEALAND

GRADUATE RESEARCH SCHOOL

STATEMENT OF CONTRIBUTION
DOCTORATE WITH PUBLICATIONS/MANUSCRIPTS

We, the candidate and the candidate's Primary Supervisor, certify that all co-authors have consented to their work being included in the thesis and they have accepted the candidate's contribution as indicated below in the *Statement of Originality*.

Name of candidate:	Feng Ming Chian
Name/title of Primary Supervisor:	Dr. Lovedeep Kaur
In which chapter is the manuscript /published work:	Chapter 3

Please select one of the following three options:

(●) The manuscript/published work is published or in press

- Please provide the full reference of the Research Output:

Chian, F. M., Kaur, L., Oey, I., Astruc, T., Hodgkinson, S., & Boland, M. (2019). Effect of Pulsed Electric Fields (PEF) on the ultrastructure and in vitro protein digestibility of bovine longissimus thoracis. LWT, 103, 253-259. https://doi.org/10.1016/j.lwt.2019.01.005

( ) The manuscript is currently under review for publication – please indicate:

- The name of the journal:
- The percentage of the manuscript/published work that was contributed by the candidate:
- Describe the contribution that the candidate has made to the manuscript/published work:

( ) It is intended that the manuscript will be published, but it has not yet been submitted to a journal

Candidate's Signature:	Feng Ming Chian Digitally signed by Feng Ming Chian Date: 2020.09.21 16:29:23 +12'00'
Date:	21-Sep-2020
Primary Supervisor's Signature:	Lovedeep Kaur Digitally signed by Lovedeep Kaur Date: 2020.09.22 13:38:42 +12'00'
Date:	22-Sep-2020

This form should appear at the end of each thesis chapter/section/appendix submitted as a manuscript/ publication or collected as an appendix at the end of the thesis.

DRC 16

MASSEY UNIVERSITY
TE KUNENGA KI PŪREHUROA
UNIVERSITY OF NEW ZEALAND

GRADUATE RESEARCH SCHOOL

STATEMENT OF CONTRIBUTION
DOCTORATE WITH PUBLICATIONS/MANUSCRIPTS

We, the candidate and the candidate's Primary Supervisor, certify that all co-authors have consented to their work being included in the thesis and they have accepted the candidate's contribution as indicated below in the *Statement of Originality*.

Name of candidate:	Feng Ming Chian
Name/title of Primary Supervisor:	Dr. Lovedeep Kaur
In which chapter is the manuscript /published work:	Chapter 4

Please select one of the following three options:

(●) The manuscript/published work is published or in press

- Please provide the full reference of the Research Output:

Chian, F. M., Kaur, L., Oey, I., Astruc, T., Hodgkinson, S., & Boland, M. (2021). Effects of pulsed electric field processing and sous vide cooking on muscle structure and in vitro protein digestibility of beef brisket. Foods, 10(3), 512. https://doi.org/10.3390/foods10030512

( ) The manuscript is currently under review for publication – please indicate:

- The name of the journal:
- The percentage of the manuscript/published work that was contributed by the candidate:
- Describe the contribution that the candidate has made to the manuscript/published work:

( ) It is intended that the manuscript will be published, but it has not yet been submitted to a journal

Candidate's Signature:	Chian Feng Ming Digitally signed by Chian Feng Ming Date: 2021.03.02 09:22:24 +13'00'
Date:	02-Mar-2021
Primary Supervisor's Signature:	Lovedeep Kaur Digitally signed by Lovedeep Kaur Date: 2021.03.02 09:28:09 +13'00'
Date:	2-Mar-2021

This form should appear at the end of each thesis chapter/section/appendix submitted as a manuscript/ publication or collected as an appendix at the end of the thesis.

DRC 16

MASSEY UNIVERSITY
TE KUNENGA KI PŪREHUROA
UNIVERSITY OF NEW ZEALAND

GRADUATE RESEARCH SCHOOL

STATEMENT OF CONTRIBUTION
DOCTORATE WITH PUBLICATIONS/MANUSCRIPTS

We, the candidate and the candidate's Primary Supervisor, certify that all co-authors have consented to their work being included in the thesis and they have accepted the candidate's contribution as indicated below in the *Statement of Originality*.

Name of candidate:	Feng Ming Chian
Name/title of Primary Supervisor:	Dr. Lovedeep Kaur
In which chapter is the manuscript /published work:	Chapter 5

Please select one of the following three options:

(●) The manuscript/published work is published or in press

- Please provide the full reference of the Research Output:

Chian, F. M., Kaur, L., Astruc, T., Vénien, A., Stübler, A.-S., Aganovic, K., Loison, O., Hodgkinson, S., & Boland, M. (2021). Shockwave processing of beef brisket in conjunction with sous vide cooking: Effects on protein structural characteristics and muscle microstructure. Food Chemistry, 343, 128500. https://doi.org/10.1016/j.foodchem.2020.128500

( ) The manuscript is currently under review for publication – please indicate:

- The name of the journal:
- The percentage of the manuscript/published work that was contributed by the candidate:
- Describe the contribution that the candidate has made to the manuscript/published work:

( ) It is intended that the manuscript will be published, but it has not yet been submitted to a journal

Candidate's Signature:	Chian Feng Ming Digitally signed by Chian Feng Ming Date: 2021.03.02 09:24:09 +13'00'
Date:	02-Mar-2021
Primary Supervisor's Signature:	Lovedeep Kaur Digitally signed by Lovedeep Kaur Date: 2021.03.02 09:29:05 +13'00'
Date:	2-Mar-2021

This form should appear at the end of each thesis chapter/section/appendix submitted as a manuscript/ publication or collected as an appendix at the end of the thesis.

DRC 16

MASSEY UNIVERSITY
TE KUNENGA KI PŪREHUROA
UNIVERSITY OF NEW ZEALAND

GRADUATE RESEARCH SCHOOL

STATEMENT OF CONTRIBUTION
DOCTORATE WITH PUBLICATIONS/MANUSCRIPTS

We, the candidate and the candidate's Primary Supervisor, certify that all co-authors have consented to their work being included in the thesis and they have accepted the candidate's contribution as indicated below in the *Statement of Originality*.

Name of candidate:	Feng Ming Chian
Name/title of Primary Supervisor:	Dr. Lovedeep Kaur
In which chapter is the manuscript /published work:	Chapter 6

Please select one of the following three options:

○ The manuscript/published work is published or in press

- Please provide the full reference of the Research Output:

○ The manuscript is currently under review for publication – please indicate:

- The name of the journal:
- The percentage of the manuscript/published work that was contributed by the candidate:
- Describe the contribution that the candidate has made to the manuscript/published work:

◉ It is intended that the manuscript will be published, but it has not yet been submitted to a journal

Candidate's Signature:	Feng Ming Chian Digitally signed by Feng Ming Chian Date: 2020.09.21 16:58:17 +12'00'
Date:	21-Sep-2020
Primary Supervisor's Signature:	Lovedeep Kaur Digitally signed by Lovedeep Kaur Date: 2020.09.22 13:40:47 +12'00'
Date:	22-Sep-2020

This form should appear at the end of each thesis chapter/section/appendix submitted as a manuscript/ publication or collected as an appendix at the end of the thesis.